Investigating neutrophil phenotype and migration mechanisms in the tissue draining lymph node during acute pulmonary infection with *Streptococcus pneumoniae*

Amy Kathleen Sawtell

PhD

University of York
Biology

January 2015

Abstract

Neutrophils are innate immune cells that form part of the first line of defense against pathogens. These cells are rapidly mobilised in response to infection and inflammation and are equipped with a range of pathogen destruction mechanisms. In recent years it has been demonstrated that neutrophils can also modulate innate and adaptive immune responses. Neutrophils have been found to enter secondary lymphoid organs including lymph nodes, however the phenotype and function of neutrophils in lymph nodes is not well understood. Work in this thesis utilised an acute pulmonary infection model with the lung pathogen *Streptococcus pneumoniae*, to investigate neutrophil recruitment, phenotype and function in the lung draining (mediastinal) lymph node. It was hypothesised that neutrophil phenotype and behaviours are not cell intrinsic, rather dictated by the localised microenvironment of the cell. To investigate this hypothesis a combination of flow cytometry, immunohistochemistry, quantitative PCR and four dimensional multiphoton explant imaging was used.

Neutrophil recruitment to the lung draining lymph node was rapid, peaking at 6 - 12 hours post infection. Neutrophils were localised in the lymphatic sinus, specifically in areas with medullary macrophages. Neutrophil migration in this region was highly dynamic, with swarms of neutrophils observed. When compared to blood, lung and airway neutrophils, lymph node neutrophils showed an intermediate activation profile, similar to lung tissue neutrophils. Interestingly a small population of lymph node neutrophils expressed markers of antigen presenting cells. Neutrophils in the lymph node utilised mainly chemotactic migration mechanisms involving phosphatidylinositde 3-kinase signalling and leukotriene B4, however migration was not completely integrin independent. Thus the results support the hypothesis that neutrophil phenotype and behaviours are environment dependent as opposed to cell-intrinsic, also they demonstrate and support the evolving view of the neutrophil as a complex cell type that has multiple functional profiles and mechanisms of migration.

List of Contents

Abstract **2**

List of Contents **3**

List of Tables **9**

List of Figures **10**

Acknowledgments **12**

Declaration **13**

Chapter 1: Introduction **14**

1.1 Role of neutrophils in host defense **14**

1.2 Neutrophil homeostasis **15**

1.2.1 Neutrophil retention in the bone marrow 15

1.2.2 Neutrophil release from the bone marrow 15

1.2.3 Neutrophil margination 16

1.2.4 Neutrophil clearance 16

1.2.5 Neutrophil circadian rhythm and regulation of the hematopoietic niche 17

1.2.6 Neutrophil homeostasis regulation 18

1.3 The neutrophil recruitment cascade **19**

1.3.1 Capture and rolling 19

1.3.2 Slow rolling and arrest 19

1.3.3 Crawling and transendothelial migration 20

1.3.4 Abluminal crawling 21

1.3.5 Interstitial neutrophil migration 22

1.3.6 Neutrophil recruitment in the lung 23

1.4 Neutrophil activation and pathogen clearance **24**

1.4.1 Pathogen recognition by innate immune cells 24

1.4.2 Pathogen killing by neutrophils 25

1.4.3 Neutrophil extracellular traps 27

1.5 Neutrophils in innate and adaptive immunity **28**

1.5.1 Neutrophil-macrophage interactions 28

1.5.2 Modulation of DC activation and function 28

1.5.3 Neutrophil mediated T cell modulation 29

1.5.4 Neutrophil modulation of NK cell homeostasis 29

1.6 *Streptococcus pneumonaie* **30**

1.6.1 Bacterial pneumonia 30

1.6.2 *Streptococcus pneumonaie* colonization and treatment....30
1.6.3 The immune response to *Streptococcus pneumonaie*....31
1.6.4 Animal models of pneumonia....32
1.7 Structure and function of the lung....32
1.7.1 Lung defenses....33
1.7.2 Immune defenses in the lung....33
1.8 Lymph node structure....33
1.9 Lymph node stromal cells....35
1.9.1 Fibroblastic reticular cells....35
1.9.2 Fibroblastic dendritic cells....36
1.9.3 Marginal zone reticular cells....37
1.10 Lymph node macrophages....37
1.11 Medulla function....39
1.12 Lymph node entry and exit....39
1.12.1 High-endothelial venules....39
1.12.2 Lymphatic vessels....40
1.13 Early events in immune response generation in the lymph node....41
1.13.1 T cell activation....42
1.13.2 B cell activation....43
1.14 Lymph node function during inflammation....44
1.14.1 HEV network expansion....44
1.14.2 Lymphangiogenesis in the draining lymph node....45
1.15 Innate immune defenses in the lymph node....46
1.16 *In vivo* live cell imaging....47
1.16.1 Visualising cells....47
1.16.2 Live cell imaging techniques....48
1.16.3 One and two-photon microscopy....48
1.17 Summary and aims....49
1.18 Hypothesis....50
1.19 Specific aims....50
Chapter 2: Materials and Methods....51
2.1 Reagents....51
2.2 Mice....54
2.3 Bacteria....55
2.3.1 *Streptococcus pneumoniae* culture....55
2.3.2 CFU calculation....56
2.3.3 Heat-killed *S. pneumoniae*....56
2.3.4 *S. pneumoniae* validation....56

2.3.5 Fluorescent labeling of *S. pneumoniae* 58
2.3.6 Intranasal administration of *S. pneumoniae* 58
2.4 Tissue and Sample collection 58
2.5 Flow Cytometry 59
2.5.1 Sample preparation 59
2.5.2 Reactive oxygen species detection 60
2.5.3 Surface marker antibody staining for flow cytometry 60
2.5.4 Live cell/dead cell discrimination 61
2.5.5 Calculating total cellularity using flow cytometry 61
2.6 Cell sorting 63
2.6.1 Giemsa staining 65
2.7 Quantitative PCR 65
2.7.1 RNA extraction 65
2.7.2 Complementary DNA synthesis 65
2.7.3 Primer design 66
2.7.4 Primer testing 66
2.7.5 Q-PCR reaction 66
2.7.6 Q-PCR data analysis 67
2.8 Immunohistochemistry 67
2.8.1 Tissue preparation and frozen sectioning 67
2.8.2 Immunofluorescent staining of frozen tissue 67
2.8.3 Confocal microscopy 68
2.9 Multiphoton explant imaging 68
2.9.1 Explant tissue preparation 68
2.9.2 Multiphoton microscopy 69
2.9.3 Investigating signalling pathways involved in neutrophil dynamics 71
2.9.4 Image analysis 71
2.10 Cell culture 72
2.11 $CD11c^+$ cell depletion using diphtheria toxin 72
2.12 Antibody mediated neutrophil depletion 73
2.13 Statistics 75
Chapter 3: Characterisation of neutrophils in the lung draining lymph node following acute pulmonary infection with *Streptococcus pneumoniae* 76
3.1 Neutrophils in secondary lymphoid organs 76
3.1.1 B-helper neutrophils in the spleen 76
3.1.2 Bacterial infection induced neutrophil recruitment to the tissue draining lymph node 76

3.1.3 Parasitic infection induced neutrophil recruitment to the tissue draining lymph node 77
3.1.4 Chronic inflammation induced neutrophil recruitment to the tissue draining lymph node 77
3.1.5 Vaccine and adjuvant induced neutrophil recruitment to the tissue draining lymph node 78
3.1.6 Neutrophil function in the tissue draining lymph node 79
3.1.7 Neutrophil heterogeneity 79
3.2 Summary 80
3.3 Aims 81
3.4 Results 82
3.4.1 Pulmonary infection with *S. pneumoniae* induced neutrophil recruitment to the LdLN 82
3.4.2 Formation of neutrophil:monocyte pairs 84
3.4.3 Pulmonary infection with *S. pneumoniae* induced early neutrophil recruitment to the LdLN 87
3.4.4 Investigating neutrophil localisation within the LdLN following pulmonary infection with *S. pneumoniae* 89
3.4.5 Neutrophils in the circulation, lung, alveolar space and LdLN had different activation states during pulmonary infection with *S. pneumoniae* 93
3.4.6 Gene transcription analysis of neutrophils in the circulation, lung tissue, alveolar space and LdLN during infection with *S. pneumoniae* 96
3.4.7 Neutrophil antigen presenting cell marker expression in the LdLN during pulmonary infection with *S. pneumoniae* 98
3.4.8 Neutrophils in the LdLN were not specialised for B helper functions during infection with *S. pneumoniae* 100
3.5 Summary of results 101
3.6 Discussion 101
3.6.1 Neutrophil involvement in early immune response events in the lung draining lymph node following pulmonary *S. pneumoniae* infection 101
3.6.2 Neutrophils in the circulation, lung, airways and LdLN have different activation states 102
3.6.3 ICAM-1 expression on neutrophils 105
3.6.4 Clues to neutrophil function in the LdLN following acute pulmonary *S. pneumoniae* infection 106
3.6.5 Investigating neutrophil function in the lymph node 107
3.7 Conclusion 108

Chapter 4: Investigating neutrophil dynamics and migration mechanisms in the lung draining lymph node 109

4.1 Molecular mechanisms of leukocyte migration 109

4.2 Leukocyte migration is environment dependent 111

4.3 Investigating leukocyte migration 112

4.4 Summary 113

4.5 Aims 113

4.6 Results 114

4.6.1 Tracking neutrophils using GFP B6.LysM Cre x B6.Rosa26 mT/mG F1 mice 114

4.6.2 Visualising neutrophil dynamics in the lung draining lymph node using *ex vivo* explant imaging 116

4.6.3 Dynamic neutrophil migration in the lung draining lymph node following pulmonary *S. pneumoniae* infection 119

4.6.4 Role of phosphoinositide 3-kinase γ in neutrophil migration in the lung draining lymph node 124

4.6.5 Role of phosphoinositide 3-kinase δ in neutrophil migration in the lung draining lymph node 126

4.6.6 Role of leukotriene B4 in neutrophil migration in the lung draining lymph node 128

4.6.7 Role of sphingosine-1-phosphate in neutrophil migration in the lung draining lymph node 130

4.6.8 Role of spleen tyrosine kinase in neutrophil migration in the lung draining lymph node 133

4.6.9 Role of CD11b in neutrophil migration in the lung draining lymph node 135

4.7 Summary of results 138

4.8 Discussion 138

4.8.1 Dynamic neutrophil migration in the lung draining lymph node 138

4.8.2 *Ex vivo* explant imaging 139

4.8.3 Molecular mechanisms involved in neutrophil dynamics in the lung draining lymph node: Phosphoinositide 3-kinase γ 140

4.8.4 Molecular mechanisms involved in neutrophil dynamics in the lung draining lymph node: Phosphoinositide 3-kinase δ 140

4.8.5 Molecular mechanisms involved in neutrophil dynamics in the lung draining lymph node: Leukotriene B4 141

4.8.6 Molecular mechanisms involved in neutrophil dynamics in the lung draining lymph node: Sphingosine-1-phosphate 141

4.8.7 Molecular mechanisms involved in neutrophil dynamics in the lung draining lymph node: Spleen tyrosine kinase and CD11b 142

4.8.8 Neutrophil migration within the lung draining lymph node is dependent on chemokines and integrins 143
4.9 Conclusion 143
Chapter 5: Investigating neutrophil recruitment to the lung draining lymph node 144
5.1 Neutrophil recruitment to tissue draining lymph nodes 144
5.2 Summary 144
5.3 Aims 144
5.4 Results 145
5.4.1 Investigating the role of subcapsular macrophages on neutrophil recruitment to the lung draining lymph node following pulmonary *S. pneumoniae* infection 145
5.4.2 Investigating the role of S1P signalling in neutrophil recruitment to, and retention in the lung draining lymph node 153
5.4.3 Summary of results: 155
5.5 Discussion 155
5.5.1 CD11c cell mediated recruitment of neutrophils to the lung *during S. pneumoniae* infection 155
5.5.2 Sphingosine-1-phosphate receptor signalling and neutrophil recruitment to the LdLN 156
5.6 Conclusion 157
Chapter 6: Discussion 158
6.1 Summary of findings 158
6.1.1 Early recruitment to the lung draining lymph node following pulmonary *S. pneumoniae* infection 158
6.1.2 Lung draining lymph node neutrophils resembled lung tissue neutrophils 159
6.1.3 Both phosphoinositide 3-kinase and integrin signalling control neutrophil migration in the lung draining lymph node 159
6.1.4 Mechanism of neutrophil trafficking to the lung draining lymph node following pulmonary *S. pneumoniae* infection 160
6.2 Conclusion 161
6.3 Outstanding questions and future directions 161
6.3.1 Neutrophils in the lung draining lymph node at 24 to 72 hours following pulmonary *S. pneumoniae* infection 161
6.3.2 Neutrophil function in the lung draining lymph node following pulmonary *S. pneumoniae* 162
Definitions 163
Bibliography 168

List of Tables

Table 2.1: General reagents. 51
Table 2.2: Primary antibodies. 53
Table 2.3: Secondary antibodies. 53
Table 2.4: *In vivo* and *ex vivo* use antibodies. 54
Table 2.5: Primers for quantitative PCR. 54
Table 2.6: Purities of sorted neutrophils. 63
Table 2.7: List of explant imaging videos 70
Table 2.8: Chemical compounds. 71
Table 2.9: Liquid chromatography-tandem mass spectrometry (LC-MS/MS) results. 71
Table 4.1 Analysis of mechanisms involved in neutrophil migration within the LdLN 138

List of Figures

Figure 1.1: The neutrophil recruitment cascade....22
Figure 1.2: Lymph node basic structure and cellularity....35
Figure 2.1: *Streptococcus pneumoniae* culture and verification....57
Figure 2.2: AccuCheck counting beads were used to calculate absolute cell number by flow cytometry....62
Figure 2.3: Cell sorting neutrophils using flow cytometry....64
Figure 2.4: Neutrophil depletion was not achieved using the Ly6G specific 1A8 clone monoclonal antibody....74
Figure 3.1: Pulmonary infection with *S. pneumoniae* induced neutrophil recruitment to the LdLN....83
Figure 3.2: $CD11b^{+}$ $Ly6C^{hi}$ $Ly6G^{+}$ cells in the LdLN following pulmonary *S. pneumoniae* infection....85
Figure 3.3: $CD11b^{+}$ $Ly6C^{hi}$ $Ly6G^{+}$ cells were neutrophil-monocyte doublets....86
Figure 3.4: Pulmonary infection with *S. pneumonie* induced early neutrophil recruitment to the LdLN....88
Figure 3.5: Neutrophils localised to the lymphatic sinus in the LdLN following pulmonary infection with *S. pneumoniae*....90
Figure 3.6: Neutrophils localised to the lymphatic sinus and not the T cell zone in the LdLN following pulmonary infection with *S. pneumoniae*....91
Figure 3.7: Neutrophils in the LdLN were located in close vicinity to medullary sinus macrophages following pulmonary infection with *S. pneumoniae*....92
Figure 3.8: Neutrophils in the circulation, lung and LdLN had different activation states during pulmonary infection with *S. pneumoniae*....94
Figure 3.9: Gene transcription analysis of neutrophils in the circulation, lung tissue, alveolar space and LdLN during infection with *S. pneumoniae*....97
Figure 3.10: A subset of neutrophils in the LdLN express antigen presenting cell markers during pulmonary infection with *S. pneumoniae*....99
Figure 3.11: Neutrophils in the LdLN were not specialised for B helper function during infection with *S. pneumoniae*....100
Figure 4.1: Amoeboid cell polarisation and migration....109
Figure 4.2: Neutrophils were distinguished from monocytes in B6.LysM Cre x B6.Rosa26 mT/mG F1 mice by GFP expression....115
Figure 4.3: Explant imaging was used to visualise neutrophil dynamics in the LdLN in 3D, in real time....117
Figure 4.4: Neutrophil cell shape was highly dynamic during migration in the LdLN....118

Figure 4.5: Neutrophil migration was dynamic in the LdLN following pulmonary *S. pneumoniae* infection. 120
Figure 4.6: Neutrophils in the LdLN were highly dynamic following pulmonary *S. pneumoniae* infection. 121
Figure 4.7: Neutrophils formed swarms in the LdLN following pulmonary *S. pneumoniae* infection. 122
Figure 4.8: The effect of swarming on neutrophil migration. 123
Figure 4.9: Investigating the effect of PI3 Kinase γ inhibition on neutrophil migration in the LdLN following pulmonary *S. pneumoniae* infection. 125
Figure 4.10: Investigating the effect of PI3 Kinase δ inhibition on neutrophil migration in the LdLN following pulmonary *S. pneumoniae* infection. 127
Figure 4.11: Investigating the effect of LTB4 receptor BLT1 inhibition on neutrophil migration in the LdLN following pulmonary *S. pneumoniae* infection. 129
Figure 4.12: 10 μM FTY720 induced S1P receptor internalisation. 131
Figure 4.13: Investigating the effect of S1P receptor inhibition on neutrophil migration in the LdLN following pulmonary *S. pneumoniae* infection. 132
Figure 4.14: Investigating the effect of Syk inhibition on neutrophil migration in the LdLN following pulmonary *S. pneumoniae* infection. 134
Figure 4.15: Confirmation of *ex vivo* anti-CD11b monoclonal antibody clone M1/70 binding. 136
Figure 4.16: Investigating the effect of CD11b blockade on neutrophil migration in the LdLN following pulmonary *S. pneumoniae* infection. 137
Figure 5.1: Subcapsular macrophage depletion following DT treatment of B6.CD11c Cre x B6.Rosa26 iDTR F1 mice. 147
Figure 5.2: CD11c depletion resulted in a reduction of the number of neutrophils migrating to the LdLN. 148
Figure 5.3: CD11c depletion resulted in a reduction in the number of neutrophils recruited to the lung. 149
Figure 5.4: GFP expression on neutrophils in B6.CD11c Cre x B6.Rosa26 mT/mG F1 mice. 150
Figure 5.5: MHC II expression on neutrophils from B6.CD11c Cre x B6.Rosa26 mT/mG F1 mice. 151
Figure 5.6: CD11c expression in the LdLN following pulmonary infection with *S. pneumoniae.* 152
Figure 5.7: FTY720 treatment had no effect on neutrophil recruitment to the LdLN following pulmonary infection with *S. pneumoniae.* 154

Acknowledgments

I would like to thank my supervisor Dr Mark Coles for giving me the chance to complete a PhD, and for introducing me to the wonderful world of imaging and my favorite cell type, the neutrophil. Thanks also for all the guidance, help and advice. I have loved being a part of the Coles lab. I would also like to thank my second supervisor Dr Robert Henderson for his advice, support and for organising access to novel GlaxoSmithKline compounds that have been essential tools in my thesis. Thanks also to my thesis advisory panel members, Prof Paul Kaye and Dr Allison Green, for the guidance and support they gave me.

Thanks to all members of the Coles lab, past and present, for all the support they gave me. Specifically I would like to thank Anne Thuery for helping me in particularly large experiments, and my summer student in 2013 Rebecca Dookie who tracked cells in some of the videos that contributed to Figures 4.9 and 4.14. Additionally thanks to all those in the Centre for Immunology and Infection that gave me advice or lent me reagents, in particular Dr Lynette Beattie, Dr Jane Dalton and Dr Naj Brown. The help and advice (and antibodies) I received from these people got me through my PhD! Thanks to all the members of the Imaging and Cytometry Department in the Technology Facility at York, the support and training I received enabled me to complete this thesis to a high standard.

Thanks to the BBSRC and my CASE partner GlaxoSmithKline for funding this work. Thanks to Dr Augustin Amour and Dr Marion Dickson at GlaxoSmithKline who provided, and gave advice on inhibitor compounds Shionogi-12 and GSK143, and Dr Klaus Okkenhaug at the Babraham Institute who provided compound IC87114. These compounds formed a major part of my thesis. Thanks also to Dr Cesar Ramirez-Molina and Dr Edward Hooper-Greenhill at GlaxoSmithKline who were involved in organising sample collection from York, and performed the liquid chromatography-tandem mass spectrometry in Chapter 2.9.3, Table 2.9.

Finally thank you to my family who have always supported me in everything I have done. Thanks to my friends, especially friends also completing PhDs who have given me advice and put up with my moaning. Thank you also to Simon for your support and importantly patience during completion of this PhD.

Declaration

This thesis has not previously been accepted in substance for any degree and is not being concurrently submitted in candidature for any degree other than Doctor of Philosophy of the University of York. This thesis is the result of my own investigations, except where stated in the acknowledgments.

Chapter 1: Introduction

Immune responses to pathogen infection are initiated in peripheral tissues through the activation of innate immune cells that migrate to tissue draining lymph nodes, where they prime adaptive immune responses. The structural organization of both peripheral tissues and the secondary lymphoid tissues is required for efficient immune responses. An intricate set of interactions of different cell types, in the right time and space is required in order for the immune system to respond effectively to the pathogen infection. In peripheral tissues (e.g. lung, skin, intestines) multiple innate immune cells are activated through a range of pathogen and damage recognition receptors. These include dendritic cells (DC), macrophages, monocytes and neutrophils. The role of dendritic cells in the initiation of T cell mediated immune responses is a paradigm of modern immunology, however the role of other cells including neutrophils and tissue resident macrophages, in both the site of infection and the tissue draining lymph node are less clear.

1.1 Role of neutrophils in host defense

Neutrophils form the first line of defense for the immune system against infection, thus rapid neutrophil mobilisation, recruitment and activation is essential in early response to infection. Neutrophils were first discovered by Paul Ehrlich in the 19th century and classified by their distinct 'polymorphous nucleus'. Ilya Ilyich Metchnikoff demonstrated in starfish larvae that neutrophils are recruited to sites of injury; Metchnikoff also correctly theorized that these cells were important for clearing bacteria. In 1908 Ehrlich and Metchnikoff shared the Nobel prize in physiology or medicine for their discoveries and work on immunity[1]. Neutrophils are the most abundant white leukocyte in human blood making up 50-70% of the white blood cell population, however in specific pathogen free mice this percentage is lower; 15-20%[2]. Neutrophils are highly granulocytic, terminally differentiated cells that are specalised in pathogen destruction. These cells have a characteristic lobular nucleus and thus are easily phenotypically identifiable. Neutrophils circulate in the blood where they have a short half-life in circulation; 8-12 hours, however in tissues they can last for 1-2 days[1].

In adult mice and humans neutrophils are produced in the bone marrow with nearly two-thirds of hematopoiesis dedicated to neutrophil and monocyte production. In humans during homeostasis $1\text{-}2\times10^{11}$ neutrophils are generated per day, with this rate increasing during infection[3]. Mature neutrophils are stored in this niche, with only 1-2% found in the circulation[4]. Thus there are large numbers of mature neutrophils ready to be released in response to infection. The formation of mature neutrophils through the process of terminal granulopoiesis is dependent on granulocyte colony stimulating factor (G-CSF). Terminal granulopoiesis involves the sequential differentiation of common myeloid progenitors into myeloblasts, promyelocytes,

myelocytes, metamyelocytes, band cells and finally functional polymorphonuclear cells. G-CSF regulates this process by regulating the transit time through the granulocytic compartment and release of mature cells from the bone marrow[5]. Granulopoiesis is also reliant on a set of transcription factors, the balance between C/EBPα, Gfi-1 and PU.1 expression is key to regulating neutrophil differentiation[3].

1.2 Neutrophil homeostasis

1.2.1 Neutrophil retention in the bone marrow

Under homeostatic conditions, a balance between chemokine receptor CXCR4 and CXCR2 signalling controls release of mature neutrophils from the bone marrow[4]. Bone marrow stromal cells produce CXCL12 (SDF-1α), which binds CXCR4 chemokine receptor on neutrophils, maintaining their retention in specialised bone marrow niches. Deficiency in CXCL12 or CXCR4 results in blood neutrophilia, treatment of both humans and mice with a CXCR4 antagonist (AMD 3100/Plerixafor) mobilises haematopoietic stem cells, inducing a rapid rise of neutrophil numbers in the blood[4]. The rise in neutrophil numbers in the blood following AMD3100 treatment was initially attributed to mobilisation from the bone marrow; however more recently it has been demonstrated that demarginiation from the lung vasculature is the mechanism of AMD3100 induced blood neutrophilia. This is discussed further in Chapter 1.2.3. A congenital disease myelokathexis (WHIM syndrome) results from a gain-of-function mutation in CXCR4. Patients with this disease have severe neutropenia, but normal or increased numbers of neutrophils in the bone marrow[4]. Neutropenia is likely the result of sustained activation of neutrophil CXCR4 and inability to desensitize to CXCL12[6]. Integrin signalling also has a role in bone marrow retention, neutrophils express the integrin very late antigen-4 (VLA-4) that can bind vascular cell adhesion protein 1 (VCAM-1) on bone marrow stromal cells[4]. However unlike CXCL12-CXCR4 signalling, adhesion is not essential in regulating neutrophil retention in the bone marrow.

1.2.2 Neutrophil release from the bone marrow

Upon maturation neutrophils down-regulate CXCR4 and up-regulate CXCR2. CXCR2 binds chemokines CXCL1 (KC) and CXCL2 (MIP-2) produced by bone marrow endothelial cells and megakaryocytes, permitting efficient mature neutrophil egress into circulation. G-CSF also contributes to this process through down-regulating VLA4 expression by neutrophils and CXCL12 production by bone marrow stromal cells, aiding neutrophil egress from the bone marrow. CXCR2 deficiency results in neutrophil retention in the bone marrow[5]. Under homeostatic conditions CXCL12 chemokine production by stromal cells, biases towards

neutrophil retention. In contrast, during inflammation the chemokine balance is tipped in favor of neutrophil egress. During acute infection macrophage derived cytokines interleukin (IL)-1β and IL-23 induce IL-17 production by Th17 cells, innate lymphoid cells (ILC), natural killer T (NKT) cells and γδT cells. IL-17 stimulates both systemic and bone marrow G-CSF levels. G-CSF promotes granulopoiesis, production of CXCR2 ligands in the bone marrow and decreases expression of CXCL12 in the bone marrow, further promoting neutrophil release[5].

1.2.3 Neutrophil margination

Under homeostatic conditions mature neutrophils circulate in the blood for roughly 6-8 hours, however *in vivo* studies have found neutrophils can circulate for up to 18 hours in the mouse, and 5 days in human. Approximately 50% of the circulating neutrophils are adhered to blood vascular walls in a process termed margination[5]. Marginated neutrophils form intravascular pools of neutrophils in organs such as the spleen, liver, bone marrow and lungs. Marginated neutrophils may be remobilized from these sites, for example in exercise the size of the marginated pool of neutrophils decreases and the circulating pool size increases[5]. Inhibition of CXCR4 by the antagonist AMD 3100/Plerixafor induces blood neutrophilia, a process thought to result from bone marrow egress. Using intravital microscopy of bone marrow this hypothesis has been challenged, in contrast to what was expected imaging demonstrated that CXCR4 antagonism did not induce neutrophil egress from the bone marrow, unlike G-CSF, which readily induced fast neutrophil egress and increased numbers in the blood[7]. Rather neutrophilia by CXCR4 antagonism was due to rapid neutrophil release from the marginated pool in the lungs that, in combination with an inhibition of neutrophil homing to the bone marrow, lead to neutrophilia[7]. It was postulated that the release of neutrophils from the lung vasculature could have been due to altered integrin expression; CXCL12 signalling has been shown to regulate lymphocyte function-associated antigen 1 (LFA-1; CD11a) and VLA-4 expression in haematopoietic stem cells[7]. Thus the process of margination is key to regulating neutrophil homeostasis.

1.2.4 Neutrophil clearance

Upon priming neutrophils enter the site of infection where they fully activate, clear pathogens and undergo apoptosis. Tissue macrophages clear apoptotic neutrophils in a process called efferocytosis. Stimulation of tissue localised DCs and macrophages by apoptotic neutrophils inhibits IL-23 production leading to reduced IL-17 production by Th17 cells, ILCs, NKT cells and γδT cells. This leads to reduced G-CSF production, decreased granulopoiesis and the balance of CXCR4-CXCR2 signalling is tipped back in favor of CXCR4 signalling, and thus neutrophil retention in the bone marrow[8]. Thus the uptake of apoptotic neutrophils is key in

initiating inflammation resolution. In humans with leukocyte adhesion deficiency type I (LAD-1), a condition where there is loss of CD18 expression, and in CD18 deficient mice, severe periodontal disease occurs. Neutrophils are unable to enter the tissue, therefore there is no uptake of apoptotic neutrophils by macrophages. As a result IL-23 levels are not down regulated, localised IL-17 levels become pathological, inflammation doesn't resolve, bacteria grow uncontrolled, all leading to inflammatory bone loss[9]. This process may be important in a number of pathological conditions.

In homeostatic and inflammatory conditions clearance of neutrophils also occurs in the spleen, liver and bone marrow, in a process mediated by macrophages[5]. Uptake of apoptotic neutrophils activates the Liver X receptors (LXRs) inhibiting inflammatory gene transcription. LXR signalling in splenic macrophages reduces IL-23 transcription and G-CSF systemic production. In the absence of LXRs, splenic IL-17A^{+} T helper 17 lymphocytes are increased[10]. Thus LXR signalling in tissue macrophages, upon uptake of apoptotic neutrophils, modulates G-CSF production in the bone marrow, and thus neutrophil production and release[11].

1.2.5 Neutrophil circadian rhythm and regulation of the hematopoietic niche

Clearance of apoptotic neutrophils during infection is essential to controlling rates of neutrophil production and bone marrow release. Additionally, removal of aged neutrophils is important, as these cells have a more activated phenotype and could potentially cause pathology including small-vessel vasculitis[12]. This removal of aged neutrophils by bone marrow macrophages, also modulates the entire hematopoietic niche. Neutrophil numbers in the blood follow a circadian rhythm with clear periods of clearance and release. Neutrophil numbers are highest at Zeitgeber time 5 (Z5; 6 hours after the induction of the 12 hour light and dark cycle), and lowest at Z13 (1 hour into the dark cycle). The numbers of hematopoietic stem and precursor cells (HSPC) in the blood follow the same pattern as neutrophil numbers. Experimental elevation of neutrophil numbers in the blood promotes HSPC release from the bone marrow[13]. Depletion of neutrophils promotes HSPC retention in the bone marrow, and an increase in bone marrow stromal cells and CXCL12 expression[13]. Macrophages are essential for this bone marrow niche modulation by neutrophils. Aged neutrophils (CD62L^{lo} CXCR4^{hi}) home to the bone marrow where they are phagocytosed by macrophages, inducing a reduction in CXCL12 production by bone marrow stromal cells, and thus HSPCs are release into the blood[13]. LXR is also essential in regulating this process, and it is proposed that uptake of aged neutrophils activates LXR in macrophages, inducing the modulatory effect on the bone marrow niche[13].

1.2.6 Neutrophil homeostasis regulation

The homeostatic regulation of granulopoiesis and neutrophil release is essential to maintain an optimal number of neutrophils in circulation. Likewise, sensing of a need for increased neutrophils numbers during infection, 'emergence granulopoiesis'[14], is also an essential function of the homeostatic loop of chemokines (CXCL1, CXCL2, CXCL12), cytokines (IL-23, IL-17 and G-CSF) and stromal cells, macrophages and DCs, controlling granulopoiesis and neutrophil homeostasis. Recently it has been found that microbiota in the gut also has a key role in neutrophil homeostasis. A feedback circuit involving CXCR2, its ligand CXCL5, gut microbiota, IL-17A and G-CSF has been proposed. *Cxcr2*$^{-/-}$ mice have high plasma IL-17A and G-CSF resulting in blood and bone marrow neutrophilia. Transfer of CXCR2^{+} neutrophils into these mice leads to basal IL-17A and G-CSF levels. Under homeostatic conditions, CXCL5 is primarily produced by enterocytes in the intestine making up the lamina propria. In response to gut microbiota resident intestinal cells recruit neutrophils in a CXCL5 dependent process. Localised neutrophil apoptosis leads to down regulation of intestinal IL-23 production, modulating local IL-17A production and regulating systemic G-CSF levels. When neutrophils are unable to migrate into the intestine there is no regulation on IL-17A induction. It was found that microbiota in the gut, in particular segmented filamentous bacteria, induce IL-17A and thus G-CSF production. Therefore there is a complex relationship between different microbiota, localised inflammation and global immune responses[15].

The IL-23-IL-17 axis is not solely responsible for controlling rates of granulopoiesis. In neutropenic conditions steady-state G-CSF concentration in plasma is increased, resulting in an expansion of neutrophil progenitor cells in the bone marrow. In NOD SCID gamma (NSG) mice lacking that lack T, B and natural killer (NK) cells, in response to neutropenia there is no increase in IL-17 or IL-23 levels. However there is still an increase in G-CSF levels, this is in response to Toll-like Receptor 4 (TLR4) signalling resulting from stimulation by LPS[16], however there is some evidence for endogenous TLR ligands. Thus under homeostatic conditions in addition to IL-17 and IL-23, TLR4 signalling stimulated by microbiota can modulate plasma G-CSF and thus granulopoiesis[16]. Multiple feedback circuits exist to control granulopoiesis, indeed, *gcsf*$^{-/-}$ or *gcsfr*$^{-/-}$ mice still have 20-30% of basal neutrophil numbers, and thus other mechanisms also modulate emergency granulopoiesis[5]. IL-6 is secreted in response to TRL4 stimulation by a number of cell types including lymphocytes, macrophages and stromal cells. In the absence of G-CSF IL-6 can induce granulopoiesis. This redundancy is a common theme in both the regulation of haematopoiesis and immune system function.

1.3 The neutrophil recruitment cascade

Neutrophils in the blood are in a quiescent state, under homeostatic conditions they patrol the circulatory system and do not enter tissues. Upon inflammatory stimulation they become primed, inducing a cascade of events leading to their migration into inflamed tissue, full activation, pathogen clearance and finally cell death. Neutrophil recruitment from the blood follows a series of events that occur mainly in post-capillary venules; capture, rolling, slow rolling, arrest, crawling, transendothelial migration (TEM) and abluminal crawling summarised in Figure 1.1.

1.3.1 Capture and rolling

In order for neutrophils to enter the site of inflammation, endothelial cell activation must occur to allow neutrophil attachment to the endothelium. Tissue resident sentinel cells, including macrophages and mast cells, bind pathogen-associated molecular patterns (PAMPs) and danger-associated molecular patterns (DAMPs) via pattern recognition receptors (PRRs), PRR signalling induces the production of pro-inflammatory mediators such as tumor necrosis factor α (TNFα) and IL-1β[17]. These cytokines cause endothelial cell activation, which results in up regulation of selectins; E- and P-selectin, P-selectin glycoprotein ligand 1 (PSGL1) and adhesion molecules; intercellular adhesion molecule 1 (ICAM-1) and VCAM-1[18]. P-selectin is pre-stored within Weibel-Palade bodies thus appears on the cell surface within minutes, however E-selectin is synthesized *de novo*, thus up regulation is slower, taking up to 90 minutes[19].

Neutrophils in the blood express L-selectin and PSGL1, these selectins are crucial for neutrophil capture by the endothelium. Endothelial cell PSGL1 binds L-selectin, 'catching' the neutrophil, like-wise, endothelial cell P-selectin binds neutrophil PSGL1, catching the neutrophil. Selectin binding has a fast on and off rate, thus adhesive bonds are quickly made and broken. This permits neutrophil rolling along the endothelium through breaking and forming new bonds[20]. Sheer stress generated by blood flow is important for selectin binding, in the absence of sheer stress the bond between selectin and PSGL1 does not form. This type of bond is known as a catch bond, the bond becomes stronger when a force is applied[20].

1.3.2 Slow rolling and arrest

Integrins are αβ heterodimers with three confirmations; inactive (bent), primed (intermediate extended) and ligand bound (extended). In the bent confirmation integrin proteins cannot bind their ligands, however in the primed confirmation the ligand binding site is exposed. Upon

ligand binding the integrin fully extends and inside-out signalling occurs[18]. L-selectin - PSGL1 binding induces signalling in both the neutrophil and endothelium, this induces integrin extension on the neutrophil and up regulation of ICAM-1 on vascular endothelium. LFA-1 (CD11a, $\alpha_L\beta_2$ integrin) and macrophage-1 antigen (MAC-1; CD11b, $\alpha_M\beta_2$ integrin) on neutrophils extend and bind ICAM-1 on the endothelial surface. This binding decreases neutrophil speed and slow rolling occurs, it is also essential for firm adhesion[18].

Activation of the endothelium also induces expression of chemokines on the endothelial luminal surface. These cells are also able to transport chemokines from the tissue (on their abluminal side) to their luminal cell surface. This process is called transcytosis, and is mediated by the Duffy antigen receptor (DARC) which is abundantly expressed by venular endothelial cells [19,21]. DARC is an atypical chemokine receptor that does not couple to G-protein proteins and thus does not signal. It can bind multiple inflammatory CC and CXC chemokines, internalising and transcytosing them to the luminal surface[21]. Chemokine is immobilized on the endothelium by negatively charged heparin sulfate that permits decoration of the vessel wall with chemokines that are positively charged[19]. Neutrophils express G protein coupled receptors (GPCR) that bind chemoattractants. During slow rolling neutrophil GPCRs bind chemokine on the endothelium[18]. Chemokine signalling inside the neutrophil induces full integrin activation, thus increasing neutrophil adhesion to the endothelium causing their arrest in movement[3]. GPCR activation of integrin proteins regulates the process of neutrophil transmigration through outside-in signalling. Chemokine signalling also induces the release of pre-stored CD11b to the neutrophil surface, increasing adhesion[19].

1.3.3 Crawling and transendothelial migration

Once attached to the endothelium neutrophils do not transmigrate at the point of arrest, instead they proceed to crawl along the endothelium to find a suitable point of exit. This process is dependent on CD11b - ICAM-1 interactions[22]. Neutrophils then undergo TEM either through the paracellular route, where neutrophils squeeze through the junction between adjacent endothelial cells, or the less well understood transcellular route, where neutrophils move through an endothelial cell[23]. Paracellular migration involves endothelial cell expression of; ICAM-1, ICAM-2, platelet endothelial cell adhesion molecule 1 (PECAM-1), junctional adhesion molecule (JAM)-A, -B and –C, endothelial cell-selective adhesion molecule (ESAM), CD99, CD99L2 and VE-cadherin[3]. PECAM-1, JAM A, -B and -C, ESAM, CD99 and VE-cadherin make homotypic bonds with molecules on adjacent endothelial cells forming a tight endothelial cell junction. These interactions are important for endothelium integrity and barrier function. Ligation of ICAM-1 on vascular endothelium by neutrophils induces cytoskeletal rearrangements that cause cell contractility and release of VE-cadherin interactions, thus

making the junctions accessible to neutrophils. ICAM-2 signalling leads neutrophils towards the endothelial cell junctions, JAM-A guides the neutrophil through the endothelial cell junction. PECAM-1 stimulates neutrophil expression of integrin $\alpha_6\beta_1$ on neutrophils that binds laminin and allows them to migrate through the basement membrane[23]. JAM C is a ligand of CD11b and has an important role in supporting the luminal-to-abluminal migration of neutrophils. In a model of ischemia-reperfusion (I-R) injury, reverse TEM (rTEM) was observed whereby neutrophils that had already transmigrated moved in an abluminal-to-luminal direction. This rTEM was caused by loss of JAM-C at endothelial cell junctions as a result of I-R and could be enhanced by blockade or deletion of JAM-C. These rTEM neutrophils expressed ICAM-1 and have also been shown to be associated with injury in the lung[24], underlining the importance of proper control of neutrophil TEM in normal immune responses.

1.3.4 Abluminal crawling

The venule wall consists of endothelial cells, pericytes and non-cellular basement membrane (BM). Both endothelial cells and pericytes secrete BM; a matrix structure containing laminin and collagen proteins. Pericytes ensheath capillaries and venules and are embedded within the BM[25]. Once through the endothelial layer neutrophils crawl along the pericyte layer to find suitable gaps through which they can exit into tissue parenchyma, through interactions with Pericyte ICAM-1 which interacts with neutrophil CD11a and CD11b. Inflammatory mediators such as TNFα and IL-1β act on pericytes to induce larger gaps, aiding neutrophil exit[25]. Pericyte gaps align with areas of the BM with low density of matrix deposition through which neutrophils preferentially migrate[26]. Neutrophils make and store in granules large quantities of proteases such as elastase and matrix metalloproteinase (MMP) 8 and 9 that can lead to BM degradation potentialy aiding in their interstitial migration, however the evidence that this process occurs is not clear[18,23].

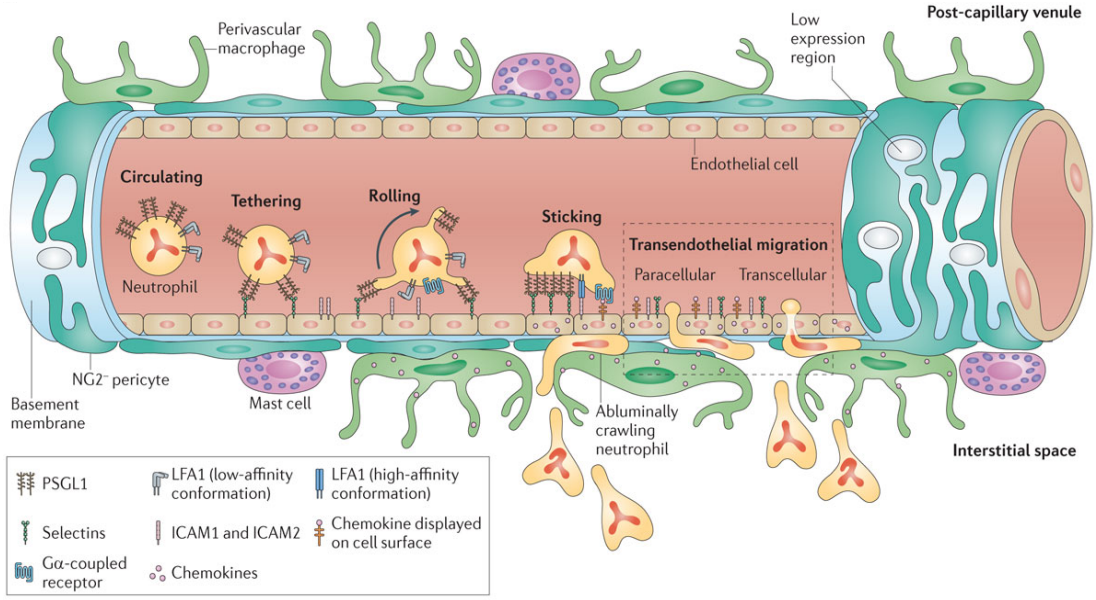

Figure 1.1: The neutrophil recruitment cascade.

A diagram of the steps involved in the neutrophil recruitment cascade, leading to neutrophil extravasation and subsequent tissue infiltration. From Weninger, Biro and Jain, 2014[27].

1.3.5 Interstitial neutrophil migration

Neutrophils express multiple different chemokine receptors, and thus migrate towards various chemoattractants. Following extravasation, once in the tissue they respond to numerous chemokine gradients. To ensure they migrate to the site of infection or injury they respond preferentially to primary, or end-target chemoattractants, including bacterial products such as N-formyl-l-methionyl-l-leucyl-phenylalanine (fMLP) and the complement component 5a (C5a) fragment. Secondary, or intermediate chemoattractants include leukotriene B4 (LTB4) and chemokines such as CXCL1[5]. This prioritisation allows neutrophils to move away from secondary chemokine gradients at the endothelium and travel into the tissue to locate the infection site where there is high concentration of end-target chemoattractant. This is achieved by activation of different downstream signalling molecules. Secondary chemoattractant GPCRs such as CXCR2 activate phosphoinositide 3-kinase γ (PI3Kγ) to induce cell migration, however the formyl peptide receptor 1 (FPR1) GPCR also activates p38 mitogen-activated protein kinase (MAPK)[28]. Indeed PI3Kγ only accelerates migration towards fMLP, but is not required for migration towards fMLP[29]. *In vitro* it was shown that when neutrophils are faced with two opposing chemokine gradients; CXCL8 versus fMLP, they preferentially migrate towards fMLP, even if the concentration of fMLP is a 1/10000th of the concentration of CXCL8. When p38 MAPK is inhibited neutrophils are found to move out of the fMLP gradient and towards CXCL8. Thus neutrophils prioritise end-target chemoattractants by utilizing different signalling pathways; this potentially involves inhibition of PI3Kγ signalling by p38 MAPK[30].

Intravital microscopy studies imaging neutrophil interstitial migration in real time have shown that the collective migration of these cells is highly coordinated. In response to sterile injury (laser induced tissue damage), or intradermal *Leishmania major* infection, neutrophil recruitment is observed to happen in phases[31-33]. First, small numbers of 'scout' neutrophils arrive at the injury site, presumably responding to PAMP or DAMP release[31]. These initial cells then amplify the recruitment of further neutrophils by releasing LTB4[33]. Paracrine LTB4 acts as a relay molecule, signalling from cell to cell over long distances. It also amplifies neutrophil migration towards fMLP[34]. Recruited neutrophils move in a highly directed manner away from the blood vessel towards the site of inflammation[31]. Neutrophil interstitial migration is also facilitated by $NG2^+$ pericytes that express macrophage migration inhibitory factor (MIF) on their surface in response to DAMPs and PAMPS[35]. These cells attach to the outside of capillaries and arterioles, thus after TEM neutrophils may migrate along them, aiding their guidance to the site of inflammation. After the period of amplification stabilization occurs where further neutrophil infiltration stops. The recruited neutrophils form a cluster that seals off the injury site. Neutrophil clusters can be stable as seen in laser induced tissue injury, where neutrophil migration arrests[32,33]. However they can also be highly dynamic as seen in neutrophil 'swarms' induced in response to *L. major*[31], *Toxoplasma gondii*[36], *Listeria monocytogenes, Escherichia coli, Pseudomonas aeruginosa*[33] and ischemia-reperfusion injury[37].

1.3.6 Neutrophil recruitment in the lung

The process of neutrophil recruitment from the blood to tissues has been well studied and characterized by intravital microscopy studies, particularly in tissues such as the mesentery and cremaster muscle, where the tissue is thin and easily accessible to microscopy. However, in some tissues the recruitment cascade does not follow the same classical steps, in liver sinusoids neutrophils do not roll, they directly adhere to the endothelium. In sterile liver inflammation neutrophil adherence is integrin dependent, involving CD11b and ICAM-1 interaction[19]. In contrast during inflammation induced by systemic endotoxemia, sinusoid adherence is integrin independent, involving neutrophil CD44 binding endothelial cell hyaluronan[38]. Likewise in the lung, neutrophils do not follow the classical recruitment cascade. First, neutrophil TEM occurs mainly in the capillaries of the lung, not post capillary venules. The lung is made up of a vast network of very thin capillaries (mean diameter 5.5 μm); to migrate through these capillaries neutrophils (mean diameter 8 μm) must dramatically change their shape. Blood flow velocity is also low in the lungs, these two factors combined together lead to a slower neutrophil transit time through the lungs, and thus neutrophil margination under homeostatic conditions[39]. Upon activation neutrophils become rigid due to actin cytoskeletal rearrangements, they can no-longer deform their shape and become stuck[40], thus arrest in the capillaries. There is no rolling step due to the size of the capillaries.

Depending on the stimulus, neutrophil migration from the blood into the alveolar space can be selectin and integrin dependent or independent. In E- and P-selectin, and β_2 integrin (CD18) deficient mice, neutrophil migration into the alveolar space in response to gram-positive *Streptococcus pneumoniae*, Group B *Streptococcus* and *Staphylococcus aureus* bacterial infection is not hindered[41-43]. However in bacterial pneumonia induced by gram-negative *E. coli* lipopolysaccharide (LPS) or *P. aeruginosa* infection, β_2 integrin and E-selectin deficiency reduced neutrophil extravasation into the alveolar space[42]. However it is not only bacterial strains that cause opposing requirements for neutrophil recruitment; IL-1 induced neutrophil influx is integrin dependent, whereas C5a induced influx is integrin independent[40]. Thus, although the rolling and firm adhesion steps do not appear to occur in the lung, selectins and integrins still have a role in neutrophil extravasation. None of these studies involved intravital microscopy, thus the role of physical neutrophil trapping or adhesion molecules in neutrophil pulmonary extravasation *in vivo* has not been directly demonstated. Like in the classical neutrophil recruitment cascade, chemokines on the pulmonary endothelial cell surface have an essential role in neutrophil recruitment[40].

1.4 Neutrophil activation and pathogen clearance

Neutrophils have the potential to cause tissue damage due to the contents of their granules. To avoid unwanted activation of neutrophils and thus tissue destruction, neutrophils must first be primed before they can fully activate. Priming involves exposure to activating stimuli, including TNFα, LPS, chemokines and adhesion molecules. A single stimuli will not fully activate neutrophils, however enhances their ability to activate in response to a second stimuli[2]. Un-primed neutrophils stimulated with fMLP alone produce minimal reactive oxygen species (ROS), however stimulation of un-primed neutrophils with fMLP and TNFα induces priming, leading to production of large amounts of ROS[44]. Priming is initiated during the neutrophil recruitment cascade by interaction with activated endothelial cells[5]. Once in the tissue neutrophils become fully activated. Activation results in the enhancement of phagocytic capability, release of granular proteins (degranulation) and neutrophil extracellular trap (NET) release.

1.4.1 Pathogen recognition by innate immune cells

Neutrophils, like other innate immune cells, possess a number of PRRs on their surface enabling them to detect a wide range of different pathogenic stimuli. These include TLRs, C-type lectin receptors (CLRs) and nucleotide-binding oligomerisation domain (NOD)-like receptors (NLRs). Pattern recognition receptors allow neutrophils to distinguish gram-positive and -negative

bacteria, fungi, protozoan parasites and viruses, thus enabling the correct response to the pathogen to be generated[45]. Neutrophils express many TLRs including TLR1, -2, -4, -5, -6, -7, -8, -9 and -10. Thus they can recognize lipids, carbohydrates, peptides, DNA and single- and double- stranded RNA. Ligation of neutrophil TLRs modulates many aspects of their function including migration, phagocytosis, degranulation, ROS production, NETosis and cytokine production[45]. It also regulates their life span, both directly and indirectly; in human neutrophils TLR4 ligation activates NF-κB and MAPK cascades inhibiting their apoptosis. Indirectly, TLR4 activation of monocytes induces their production of neutrophil pro-survival factors, prolonging neutrophil life span[46]. This may help ensure efficient pathogen clearance, thus both direct and indirect TLR signalling is highly important for neutrophil function, in addition to its role in regulating granulopoiesis and neutrophil egress from the bone marrow.

C-type lectin receptors recognize carbohydrate moieties, neutrophil CLR PRRs include Dectin-1, Mincle, and C-type lectin domain family 2 (CLEC2). These CLRs are particularly important in fungal infections; Dectin-1 and Mincle recognize carbohydrates found in the fungal cell wall, their ligation induces phagocytosis, respiratory burst, degranulation and pro-inflammatory cytokine production[45]. Unlike in macrophages, the anti-fungal response induced by Dectin-1 requires co-binding of the ligand by CD11b. Dectin-1 and CD11b both bind fungal β-glucan, Dectin-1-β-glucan ligation induces inside-out signalling, activating CD11b, thus allowing it to bind β-glucan, this results in phagocytosis and ROS production[47].

Other neutrophil PRRs include the FPR1 and FPR2 that bind bacterial and mitochondrial formyl peptides, including fMLP. Ligation of FPRs not only induces potent activation of neutrophil migration, but also degranulation, ROS production and up regulation of adhesion molecules[45]. Intracellular PRRs include NOD1 and NOD2 recognise structures in the bacterial cell wall component peptidoglycan. In contrast to human neutrophils, mouse neutrophils express NOD1. Systemic peptidoglycan derived from gut microbiota acts on NOD1 in bone marrow neutrophils, priming them for killing of pathogens by phagocytosis and respiratory burst *ex vivo*[45]. Both human and murine neutrophils express NOD2, its ligation results in up regulation of CD11b, chemokine production and migration[45]. Collectively PRRs allow neutrophils to detect bacterial, fungal, viral and protozoan pathogens, leading to activation of signalling cascades involving NF-κB and MAPK, to initiate their functional immune response to pathogen infection, resulting in pathogen clearance.

1.4.2 Pathogen killing by neutrophils

Neutrophils are specialised in pathogen killing. They possess a number of mechanisms to carry out this function. Mature neutrophils express Fcγ receptors that allow binding of opsonized

pathogens, also endocytic PRRs such as Dectin-1 and triggering receptor expressed on myeloid cells 1 (TREM-1) that assist in the phagocytic process. Binding of these receptors induces very rapid pathogen phagocytosis, leading to formation of a phagosome inside the neutrophil containing the pathogen. Unlike macrophage phagosomes, that acidify; neutrophil phagosomes maintain a neutral pH 7[48]. Granules then rapidly fuse with the phogosome. Granules are exocytic vesicles formed by budding off from the golgi[49]; they start to form during granulopoiesis at the promyelocyte stage up to the band cell stage[3]. Neutrophils contain three different types of granules; primary (azurophil), secondary (specific) and tertiary (gelatinase) granules. Neutrophils also contain secretory vesicles that are seen at the final polymorphonuclear stage in neutrophil development, and are thought to form by endocytosis. Primary granules contain various lytic enzymes and anti-microbial proteins such as defensins that are essential to neutrophil function. Primary granules are not exocytosed upon neutrophil stimulation, but targeted to the phagosome, and are key in destruction of pathogens[49]. A key primary granule marker is myeloperoxidase (MPO); it makes up to 5% of the neutrophil protein content and is responsible for the catalysis of hypochlorous acid (HOCl), a potent oxidant that is bactericidal[50]. Secondary granules contain primarily anti-microbial substances, for example lactoferrin, whereas tertiary granules contain mainly matrix-degrading enzymes, for example MMP-8 and -9. Secondary granules are mainly targeted to the phagosome to aid in bacterial killing whereas tertiary granules are exocytosed to aid in neutrophil extravasation and digestion of extracellular matrix. Tertiary granules and secretory vesicles also contain β_2 integrins that are rapidly exocytosed, particularly secretory vesicles, in response to stimulation to allow adherence of the neutrophil to the endothelium[49].

The anti-microbial granules released into the phagosome lead to pathogen killing through a number of different chemical pathways. In addition to granule content ROS are generated by respiratory burst within the phagosome to aid in killing. In response to pathogen binding and phagocytosis the NADPH oxidase assembles at the phagosome membrane. Cytosolic components $p47^{phox}$, $p67^{phox}$ and $p40^{phox}$ associate with membrane bound $gp91^{phox}$ and $p22^{phox}$ to form the NADPH oxidase complex. Fully functioning GTP-bound Rac1 or -2 also needs to be associated with the complex[48]. NADPH oxidase converts oxygen into superoxide, $O_2^{-}\bullet$, this readily converts to hydrogen peroxide, H_20_2[51] and other reactive intermediates. Reactive nitrogen species (RNS) are also produced in the phagosome by inducible nitric oxide synthase (iNOS) generating nitric oxide (•NO). Superoxide and nitric oxide combine to form peroxynitrite ($ONOO^-$). ROS and RNS together target various microbial molecules and components; ROS are key in DNA damage and RNS inhibit respiration and interfere with DNA replication[52]. Together granules, ROS and RNS kill intracellular pathogens, however if a pathogen is too large to be phagocytosed, or it is extracellular, then degranulation occurs inducing release of granule contents into the extracellular milieu[19]. NADPH oxidase forms on

the cell plasma membrane generating extracellular ROS. Neutrophils also make NETs to capture and kill extracellular bacteria[53], fungi, viruses[54] and parasites[55].

1.4.3 Neutrophil extracellular traps

Neutrophil extracellular traps are formed during a unique process of cell death termed NETosis. Following phagocytosis and ROS production, H_20_2 causes the dissociation of neutrophil elastase (NE) from the primary granule membrane into the cytoplasm where it binds the actin cytoskeleton and is sequestered. Neutrophil elastase degrades intracellular filamentous actin, thus liberating itself, permitting nuclear entry. In the nucleus NE degrades and processes histones[56], inducing chromatin decondensation, followed by the detachment of the nuclear membranes. At the same time the granules disintegrate. After an hour the nuclear membrane breaks down into vesicles and the nuclear and cytoplasmic contents mix. The cell then rounds up and contracts before the membrane ruptures releasing the cell contents into the extracellular matrix, forming a net-like structure. This entire process takes one and a half hours[57]. The NADPH oxidase and ROS production are essential for NET formation. Patients with chronic granulomatous disease (CGD) have mutations in the NADPH oxidase and thus cannot make NETs, leading to granulomatous pathology[57]. Additionally mice lacking NE or patents lacking MPO are also unable to make NETs, however the function of MPO in NET formation is not clear[58]. Not all neutrophils form NETs, however all neutrophils have the capacity to undergo this process, therefor this process must be regulated either by neutrophil activation or by localized environmental cues[58]. Neutrophil extracellular traps can contribute to neutrophil defense against viruses. Human neutrophils detect human immunodeficiency virus -1 (HIV-1) through endocytic TLR7 and 8. *In vitro,* activation of these PRRs triggers ROS production and subsequent NET formation that can trap HIV-1. When neutrophils are co-cultured with T cells, neutrophils reduce the infection efficiency of HIV-1 through NET production. However, HIV-1 is capable of counteracting this process by activating the C-type lectin dendritic cell-specific intercellular adhesion molecule (DC-SIGN) on DCs, causing their production of IL-10. IL-10 inhibits TLR7 and 8 signalling thus inhibits NETosis[54]. There is no evidence that this process occurs *in vivo*.

The net-like structures formed by chromatin are decorated with granular proteins, particularly NE, and also histones. Histones themselves have bactericidal activity. In the resolution of inflammation DNase1 that is produced in the pancreas breaks down NETs. Additionally pathogenic bacteria use a similar method to evade killing by NETs; they produce extracellular DNase[59]. Indeed, one of the virulence factors of *Streptococcus pneumoniae* is an endonuclease EndA that degrades NETs, thus preventing their killing by these structures[60]. Neutrophil extracellular traps may have a beneficial role in pathogen clearance, however they are also

implicated in pathologies including vasculitis, sepsis and systemic lupus erythematosus (SLE) nephritis[2]. NETs are capable of trapping platelets and RBCs, and have shown to be key in the development of thrombus in deep vein thrombosis and implicated in the formation of atherosclerotic plaques. In autoimmunity, the production of pathological autoantibodies against neutrophil cytoplasmic components is thought to be a result of excessive NET formation[19].

Following pathogen killing neutrophils that have not undergone NETosis undergo apoptosis and are phagocytosed by macrophages. This avoids excessive release of ROS and granular contents that mediate tissue damage, and helps promote inflammation resolution through inhibiting secretion of pro-inflammatory mediators such as TNFα[61] and modulation of granulopoiesis[8]. *In vitro* it has been demonstrated that activated neutrophils can also participate in apoptotic neutrophil clearance, and that this uptake inhibits pro-inflammatory function, including ROS production and TNFα release. This is consistent with the paradigm that clearance of apoptotic neutrophils is a key initiation event in inflammation resolution[62].

1.5 Neutrophils in innate and adaptive immunity

Further to host protection through rapid pathogen detection and clearance, neutrophils are also capable of interacting with, and modulating the function of, other innate and adaptive immune cells. The outcomes of these interactions are both stimulus and environment dependent.

1.5.1 Neutrophil-macrophage interactions

During helminth infections a type 2 innate and adaptive immune response is required, characterised by Type 2 T helper cell (T_H2) induction and production of IL-4, -5, -9 and -13. Following primary infection with the helminth *Nippostrongylus brasiliensis* mice are protected from secondary infection and worms are rapidly expelled. This protection is conferred by primed macrophages that are alternatively activated (M2 phenotype). Alternative macrophage activation and anti-helminth function is mediated by polarised neutrophils that produce IL-13, amongst other soluble inflammatory factors[63].

1.5.2 Modulation of DC activation and function

In models of lung inflammation neutrophils are key for DC maturation and function. During pulmonary *Mycobacterium tuberculosis* infection, uptake of apoptotic neutrophils that contain *M. tuberculosis* is necessary for myeloid $CD11b^+$ DC migration to the draining lymph node (dLN) and their ability to stimulate early $CD4^+$ T cell activation[64]. Delaying neutrophil apoptosis is an *M. tuberculosis* virulence mechanism to prevent the induction of T cell

responses[65]. Pulmonary challenge with *Aspergillus fumigatus* germ tubes reveals a similar result; neutrophils are required for $CD11b^+$ DC migration to the dLN and neutrophil mediated maturation inducing CD40, CD86, and major histocompatibility complex class II (MHC II) up-regulation. *In vitro* it was found that neutrophil mediated DC maturation is dependent on the presence of *A. fumigatus* and also DC-SIGN binding on the DC. It is not clear however if it is DC-SIGN binding by the neutrophil or *A. fumigatus* or binding on both cell types that is key[66].

1.5.3 Neutrophil mediated T cell modulation

There are a number of studies that find a role for neutrophils in directly modulating T cell functions; however the results vary, with some studies finding activating roles and other inhibitory roles. This complexity could be due to the variation in experimental models employed and endogenous microbiota. In several different system neutrophils have been shown to express MHC II *in vivo* and are able to directly activate T cells *in vitro*, however the significance of these interactions *in vivo* is less clear. During chronic colitis there is a large influx of neutrophils in the colon, these neutrophils express MHC II and the co-stimulatory molecule CD86. *In vitro* these cells can activate antigen specific (ovalbumin; OVA) $CD4^+$ T cell proliferation[67]. Similarly, thioglycollate elicited neutrophils co-cultured *in vitro* with T cells could also induce OVA specific $CD4^+$ T cell proliferation and skew the induction of T_H1 and T_H17 cells[68]. Neutrophils are also able to cross-present antigens (OVA) to $CD8^+$ T cells, inducing their proliferation *in vitro* and differentiation into effector cells *in vivo*[69]. Conversely, neutrophils may inhibit T cell responses through ROS and RNS production that can inhibit T cell activation. In addition, activated neutrophils produce high levels of arginase I, which when released causes depletion of localised extracellular L-arginine, and can thus inhibit T cell activation, as L-arginine is essential for T cell function and cell cycle progression[70].

1.5.4 Neutrophil modulation of NK cell homeostasis

Neutrophils have a role in modulating both NK cell activation and functional capacity. The full activation of NK cell effector function requires priming by cytokines such as IL-12, IL-15 and IL-18. To control *Legionella pneumophila* infection neutrophils are required, however *L. pneumophila* is resistant to neutrophil antimicrobial mechanisms. Instead the mechanism of bacterial killing is through the activation of NK cells. Neutrophils, along with DCs, form a tripartite complex with NK cells, where neutrophil derived IL-18 stimulates NK cell interferon γ (IFNγ). IL-12 produced by DCs is also important for NK cell IFNγ production stimulation[71]. It is the localised IFNγ production that drives macrophages to clear the infection.

Further to effector function activation neutrophils regulate NK cell maturation and homeostasis. In a random chemical mutagenesis screen, *Gentista* mice were generated that had a mutation in the growth factor independent-1 (Gfi-1) transcription factor, which resulted in a defect in terminal differentiation of neutrophils. These mice therefore lacked mature functional neutrophils. In these mice, NK cells were hyporesponsive, blocked in an immature stage of development and showed poor survival. In humans who lack mature neutrophils; severe congenital neutropenia (SCN) patients, NK cells were also found to have the same hyporesponsive, immature phenotype. Thus neutrophils, both in humans and mice are required for full NK cell maturation and function. This process may be a contact dependent process due to the co-localisation of neutrophils and NK cells in mouse lymphoid organs and human tissues[72]. Further evidence of how neutrophils are capable of modulating immune responses, particularly adaptive immune responses in secondary lymphoid organs is discussed in Chapter three.

1.6 *Streptococcus pneumonaie*

1.6.1 Bacterial pneumonia

The main cause of bacterial pneumonia infection is *Streptococcus pneumoniae*. Invasive pneumococcal disease (IPD) is a major cause of morbidity and mortality in the young (under five years old), elderly and immunocompromised[73]. It is the leading cause of death for children worldwide; 18% of deaths of children under-five worldwide are due to pneumonia. Pneumonia kills on average 1.1 million children per year and is particularly prevalent in South Asia and sub-Saharan Africa. Bacterial pneumonia can be treated by antibiotics, however only 30% of children worldwide receive antibiotics[74] and it is a major causative agent in antibiotic resistance.

1.6.2 *Streptococcus pneumonaie* colonization and treatment

S. pneumoniae is a gram positive encapsulated cocci that grows in pairs or short chains. There have been ninety different capsule types identified that differ in polysaccharide chemical structure[75]. The capsule polysaccharide is used to define *S. pneumoniae* serotypes[76]. A small number of *S. pneumoniae* serotypes are associated with IPD[75]. *S. pneumoniae* asymptomatically colonises mucosal surfaces in the upper respiratory tract; 8-20% of healthy individuals are carriers, however local infection can cause sinusitis and otitis media (inflammation of the middle ear)[77]. If the bacteria reach the sterile lower respiratory tract, this can result in robust bacterial growth, causing pneumonia and a massive inflammatory neutrophil influx into the lung. Should *S. pneumoniae* cross into the blood sepsis ensues which can be fatal[78]. To colonise the human respiratory tract and spread to the lower respiratory tract *S. pneumoniae* has many

virulence factors. The main virulence factor is the capsule, this provides resistance to phagocytosis, complement binding and entrapment in NETs[79]. Another major virulence factor is pneumolysin, which forms pores in mammalian cells directly killing them and is critical in pneumonia and lung pathology[79]. Pneumococcal disease is treated with antibiotics including; β -lactams (penicillin G, amoxicillin, cephalosporins), respiratory fluoroquinolones, macrolides, and vancomycin, often requiring hospitalization and intravenous antibiotics. However there is increasing antibiotic resistance, 69.4% of pneumonia isolates are resistant to one or more antibiotics[80]. This is strongly associated with particular pathogenic serotypes, thus making treatment of some cases, particularly in the young and elderly, challenging.

Pneumococcal vaccines are available against select serotypes. Early antibody has a key role in reducing colonization of the lower lung and thus reduces the incidence of invasive disease particularly in the young, however overall death rates particularly in the elderly have not changed[81]. All vaccines are designed to target the capsule polysaccharide which is serotype specific, however no current vaccine covers all serotypes and most vaccines have poor immunogenicity in children and the elderly[81]. The current licensed vaccine PCV13 (Prevnar, Pfizer) is a pneumonococcal-protein conjugate, 13-valent vaccine and is immunogenic in children[82]. It covers 13 serotypes including serotype 19A, the most common cause of IPD. This vaccine is mainly used in children under two years of age. In adults the vaccine PPV23 (Pneumovax II, Sanofi Pasteur MSD) is commonly used to prevent IPD. This is a 23-valent pneumococcal polysaccharide vaccine that protects against 23 serotypes that are responsible for more than 95% of IPD[83]. However studies have found that although vaccination has dramatically reduced the incidence of IPD caused by the serotypes targeted by vaccines, colonization by non-targeted serotypes is occurring as a result, causing the incidence of IPD by non-targeted serotypes to increase, particularly in adults[84]. Thus efforts are being made to design vaccines against other virulence factors that are more widely conserved[81].

1.6.3 The immune response to *Streptococcus pneumonaie*

One to three days after the initial colonization by *S. pneumoniae*, neutrophils migrate to the nasal passage, phagocytose and directly kill the bacteria. Clearance is not complete though and some bacteria remain once the inflammation has subsided[81]. *S. pneumoniae* is recognized by PRRs including TLR2, which binds lipoteichoic acid (LTA) and lipoproteins in the bacterial cell wall, TLR4 that interacts with pneumolysin and TLR9 that recognises unmethylated CpG motifs in the bacterial DNA. Toll-like receptor signalling induces inflammatory cytokine and chemokine production, triggering the activation of multiple immune and non-immune cells in the tissue and tissue draining lymphoid organs. Toll-like receptor 2 and TLR9 signalling enhances phagocytosis and intracellular killing of the bateria[79], this is key to the innate defense

against *S. pneumoniae*. Mice lacking the TLR signalling adaptor molecule MyD88, and humans with defects in TLR signalling are highly susceptible to *S. pneumoniae* invasive infection[79,85].

1.6.4 Animal models of pneumonia

S. pneumoniae pneumonia has been widely studied in numerous animal models to investigate disease pathogenesis, to understand host immune response to infection, and to test vaccines and anti-microbials to treat pneumonia and sepsis. Mice are the most frequently used infection model; the main routes of infection employed to induce pneumonia are intratracheal (i.t.) and intranasal (i.n.). The i.t. route is most invasive but achieves the best delivery of bacteria to the lower lungs. The i.n. route is easier to perform and more commonly used, it closer resembles the natural human route of infection, however it is unclear how the dosing of bacteria correlates to human lungs[77]. Various serotypes of *S. pneumoniae* have been investigated; virulent serotypes in mice are 2-6. Classic strains, for example strain D39, serotype 2, have been widely used because they produce consistent features of disease, and thus results can be compared between research groups, however significant variation in pathogenesis can occur due to culturing and handling conditions[77]. Most mouse models of pneumonia also result in sepsis. Bacteremia is not common in human pneumonia, thus these mouse models are less helpful investigating disease pathogenesis exclusively in the lung[77].

1.7 Structure and function of the lung

The function of the lung is to ensure that blood is oxygenated by absorbing oxygen from breathed in air, while allowing release of carbon dioxide (CO_2) from the blood, into the air. Thus its structure is designed to maximize the surface area available for this exchange process, and additionally to minimize the distance through which the gases diffuse. The trachea divides into two bronchi that enter the lungs. The bronchi then further divide and branch off to form many smaller airways that narrow into terminal bronchioles. At the end of the bronchioles are acini that are made up of multiple alveoli. Alveoli are covered with a network of fine capillaries that carry oxygenated and oxygen poor blood. The alveoli are the site of respiratory gas exchange and thus the distance between the capillaries and the alveolar airspace is never more than 1μm. To create this microenvironment type I alveolar epithelial cells spread out to make a very thin respiratory surface, in contrast type II alveolar cells have a rounder structure. Type II cells function to produce surfactant that is a mixture of lipids (90%) and protein (10%). Surfactant reduces the surface tension of alveoli to prevent their collapse[86].

1.7.1 Lung defenses

In serving its function the lungs take in large amounts of air that contains particular matter, pollen and airborne pathogens. Thus the lungs are designed to trap and clear particulate matter and pathogens to maintain sterility. In the lung airways, specialized epithelial cells have ciliated surfaces. Mucus produced by sub-mucosal tracheobronchial glands and epithelial goblet cells traps particles, then the beating of the cilia moves them up and out of the airways. Additionally airway epithelial cells form a continuous layer, joined by tight junctions, thus providing a barrier to the airspace. In the alveoli these mechanisms do not exist and would impede gaseous exchange, however inhaled pathogens such as *S. pneumoniae* cocci or *A. fumigatus* fungal spores are able to get into the alveoli, thus alternative protection is required[86].

Surfactant produced by type II alveolar epithelial cells forms a thin layer over the alveolar surface. Surfactant also functions to trap particles, however further to this it contains surfactant proteins (SP) A, -B, -C and -D. Surfactant proteins A and D are C-type lectins that bind carbohydrate moieties on pathogens, they cause pathogen agglutination, enhancing phagocytosis and killing by macrophages and neutrophils[87]. In addition, SPs can modulate immune cell function, including inhibiting DC maturation and T cell proliferation[87].

1.7.2 Immune defenses in the lung

The airways, alveoli and interstitial space contain a number of prepositioned immune cells. Alveolar macrophages (AM) are tissue resident, non-motile cells that lay flat to the alveolar surface. They phagocytose and clear any particulate antigen or pathogen that has not been caught by mucus. Dendritic cells are also resident in the lung, they project their dendrites into alveoli to capture antigen. They then move to the larger airways and LNs where they activate T cells[88]. Neutrophils are also present in the lung under homeostatic conditions due to their margination within the narrow capillaries. Thus they are prepositioned and rapidly infiltrate, in large numbers, in response to an inflammatory insult where they then patrol the interstitium. This has been imaged *in vivo* and it is found that infiltrating neutrophils follow a leading monocyte. Neutrophils were observed to form large dynamic clusters around these cells, and clodronate liposome mediated monocyte depletion resulted in inhibition of neutrophil TEM and cluster formation[37].

1.8 Lymph node structure

Lymph nodes function to filter antigen and pathogens from the lymph fluid and support formation of high affinity adaptive immune responses proximal to tissues. Under homeostatic

conditions they provide a microenvironment for rare naïve lymphocytes to survey and respond to cognate antigen. T lymphocytes undergo a process of recirculation; exiting the blood vessels, surveying LNs, and then re-entering the blood, spending on average four days with the parenchyma of the LN. Pathogen or adjuvant activated DCs drain from peripheral tissues to LNs to present antigens to T cells. This process permits the efficient detection of infection, tissue damage and cellular stress.

Lymph nodes are highly organized complex structures containing a plethora of different cell types, enabling the effective induction of immune responses (Figure 1.2). Lymph nodes have three main regions; the cortex, paracortex and the medulla. Within the cortex are the B cell follicles, these are the sites of high affinity antibody production. In the paracortex is the T cell zone, this is where interactions between DCs and T cells occur, leading to T cell activation. The medulla is made up of the medullary sinus, where cells exit the LN and particulate antigen is cleared from the lymph. The medullary cords are a niche for antibody secreting plasma B cells. Blood vessels in the medulla branch into post-capillary high endothelial venules (HEV) that run throughout the paracortex and are the main route of entry for lymphocytes into the LN and provide oxygen and nutrients to the LN parenchyma. Lymphatic vessels make up a network in the LN that can be divided into the subcapsular sinus (SCS), paracortical sinus and medullary sinus (MS)[89]. Encasing the LN is a collagen rich capsule, below this is the SCS where cells and antigen enter the LN. Lymph fluid enters the LN through afferent lymphatic vessels, into the subcapsular space, it then flows through the sinuses and out into efferent lymphatics draining the LN. Particles of 20-200 nm in size may enter the LN passively through the lymphatics, this size range includes some viruses. Large particles, greater than 500nm in size, are not able to enter the unless actively transported by antigen presenting cells (APC)[90]. However during an inflammatory immune responses an increase in interstitial fluid flow is observed allowing entry of larger particles[90]. This change in lymphatic flow has been shown to assist *T. gondii* parasite access to the tissue draining LN[36]. During bacterial infection, degradation by immune cell derived proteases, or secretion of antigenic material permits access of bacterial antigens to the lymphatics to initiate adaptive immune responses[90].

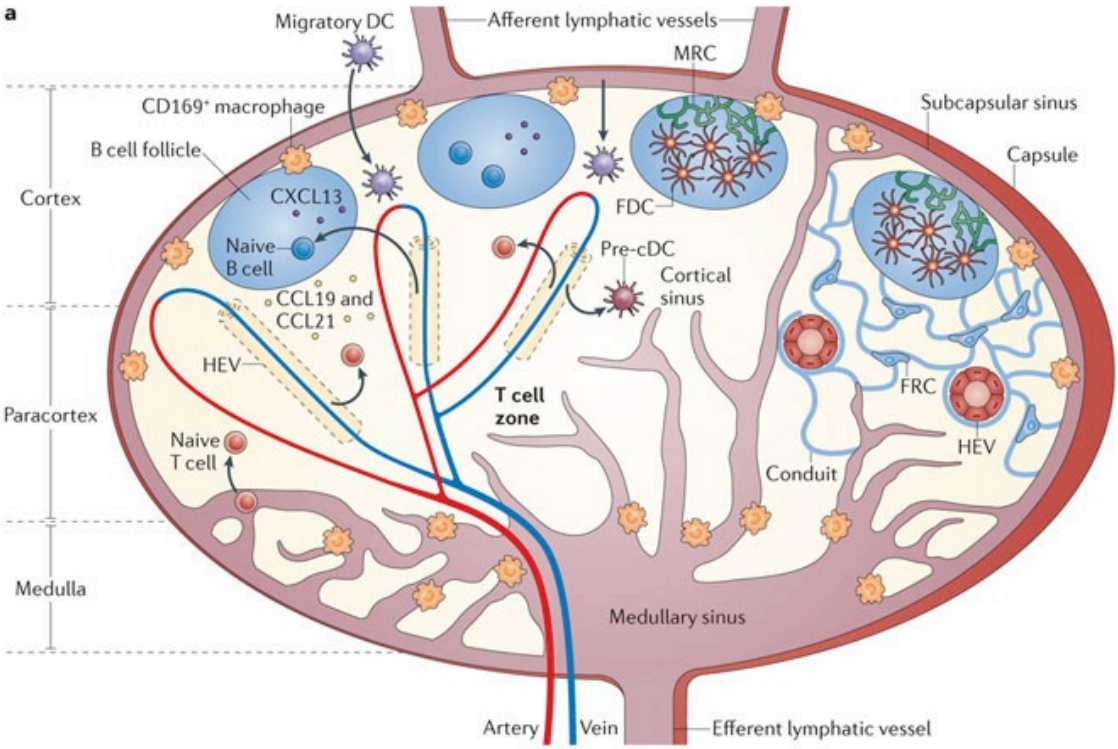

Figure 1.2: Lymph node basic structure and cellularity.

A diagram of the basic structure of a lymph node, including key cell populations and their location. From Girard, Moussion and Forster, 2012[91].

1.9 Lymph node stromal cells

Mesenchymal stromal cells form the ultrastructure of the LN and are required for productive immune responses making sure the right cells come together at the right time and place[92].

1.9.1 Fibroblastic reticular cells

Fibroblastic reticular cells (FRCs) are specialized stromal cells of the T cell zone. They ensheath pericytes that surround the HEVs and form a lattice like cellular frame work within the paracortex[92]. Fibroblastic reticular cells express the T cell and DC chemoattractants CCL19 and CCL21, and a subpopulation expresses CXCL12. CCL21 is immobilized on the FRC surface by heparin sulfate residues, thus the chemokine receptor CCR7 on DCs and T cells binds immobilized CCL21 guiding migration along the FRCs. This migration is termed haptotaxis; cell migration along an adhesive gradient[92,93]. Fibroblastic reticular cells are also characterised by expression of the glycoprotein gp38 (podoplanin). Dendritic cells express the C-type lectin receptor CLEC-2, binding of gp38 by this receptor activates DC migration on FRCs[94]. Thus FRCs are able to guide T cells from the HEVs to the paracortex where they survey antigen loaded DCs for cognate antigen. Fibroblastic reticular cell guidance of both T cells and DCs

increases the chance of these cells finding each other, thus aiding productive immune response generation[95].

Additional to migration cues, FRCs produce the T cell survival factor IL-7, that regulates T cell homeostasis[95]. In the steady state they express TLR4, and in response to LPS induced inflammation they are found to up-regulate MHC II expression and also mRNA encoding molecules involved in the acute-phase response, inflammatory cytokines and interferon and TLR4 inducible genes[96]. Depletion of FRCs, either resulting from lymphatic choriomeningitis virus (LCMV) infection where the FRC network is killed by virus specific CTLs, or by conditional ablation of CCL19 expressing cells using CCL19-Cre x Rosa26-DTR mice, demonstrates the essential role of these cells in LN function. Following LCMV infection of stromal cells, loss of the FRC network occurs rendering the host unable to respond to secondary antigens[97]. Conditional depletion of FRCs results in a reduction in T cell viability, numbers and aberrant T cell positioning in the cortex. In the absence of FRCs, in response to ovalbumin-expressing, inactivated influenza virus, there is a major defect in T cell activation and responses, and a significant reduction in immunoglobulin (Ig) M and IgG2b influenza-specific antibody production resulting in part from small disorganized germinal centers (GC) likely due to a loss of T helper and follicular helper cells[98]. There is no apparent defect in FDC function, thus this effect is due to loss of FRCs. Thus FRCs are able to promote hematopoietic cell survival, interaction, and activation, whilst regulating their recruitment and localisation emphasising the critical role of stromal cells in the organization and proper functioning of the LN.

The FRC network is also responsible for permitting access of low molecular weight (less than 70kDa) lymph borne molecules such as chemokines, cytokines, small molecules and soluble antigen into the lymph node parenchyma. Fibroblastic reticular cells ensheath and form conduits that are comprised of extracellular matrix surrounding a collagen I core that connect the lymphatic vessels with the HEVs. Small soluble molecules can enter these conduits, thus delivering proteins to T cells and dendritic cells deep in the paracortex[99]. Resident DCs attached to the conduits are able to take up soluble antigens from these and preset them to T cells[100]. This process represents an early ‘wave’ of antigen presentation in the lymph node as it has been demonstrated that soluble antigen can arrive in lymph node conduits within minutes of injection[100]. These conduits can also deliver chemokines to HEVs aiding lymphocyte entry into the lymph node[99].

1.9.2 Fibroblastic dendritic cells

Fibroblastic dendritic cells (FDCs) are a specialised stromal cell type found in adult B cell follicles that develop post-natal in a TNFα and lymphotoxin (LT) β dependent process. These

cells make the B cell attractant chemokine CXCL13 and B cell activating factor (BAFF), which is required for B cell recruitment and survival[101]. Thus the FDC network attracts and maintains B cells within the follicle in a TNFα/CXCL13 dependent process. B cells have been found to migrate along FDC processes, thus FDCs act like FRCs to aid rapid B cell migration and survey for antigen[90]. Fibroblastic dendritic cells express high levels of complement receptor (CR) -1 and -2, and capture and display opsonized antigen on their surface to cognate B cells in the form of immune complexes (IC) that compete for antigen driving high affinity immune responses. They can also acquire complement ICs from non-cognate B cells through CR2[102]. These IC are then processed in an endocytic pathway that does not degrade the IC, but recycles them to the surface for recognition by cognate B cells[90].

Fibroblastic dendritic cells have an essential role in the formation of the GC reaction where B cells undergo rounds of selection, proliferation and apoptosis to select for high affinity class switched antibody responses[103]. Germinal centers contain a light zone, which contains FDCs, that is located near the SCS and a dark zone where B cells undergo rapid proliferation that extends towards the T cell zone containing a CXCL12 producing stromal cells[90]. Fibroblastic dendritic cells retain B cells within the GC by promoting their survival and through providing antigen complexes. If FDCs are depleted during the GC reaction then GC B cells disperse and die[101].

1.9.3 Marginal zone reticular cells

Marginal zone reticular cells (MRCs) are the stromal cells found beneath the SS floor, on the edge of the B cell follicles, and also in inter-follicular regions. Within the MRC zone small numbers of NK cells, ILC type 1 and 3 (ILC1, ILC3), and invariant NKT cells are found and have roles in the initiation of antibody responses. They form reticular fibers, like FRCs, and express CCL19, CCL21, CXCL13, IL-7 and mucosal vascular addressin cell adhesion molecule 1 (MAdCAM-1), and have a role in regulating antigen delivery to the B cell follicles[104]. Marginal zone reticular cells have been shown to act as a pool of precursor cells that can differentiate into FDCs during an immune response[105]. They are involved in B cell migration and entry of DCs and memory T cells into the LN[104].

1.10 Lymph node macrophages

Lymph nodes also contain resident macrophage populations; subcapsular sinus and medullary sinus macrophages (SSM and MSM) that are strategically located within the LN. Subcapsular sinus macrophages line the bottom of the SS and they have dendrite-like protrusions that extend into B cell follicles. Intravital microscopy studies have shown that these cells, including their

protrusions, are immobile[90]. Subcapsular sinus macrophages are characterised by expression of CD11b and CD169 (sialoadhesin), they also express low levels of CD11c and are negative for F4/80[106]. Subcapsular sinus macrophages are poorly endocytic and have low degradative capacity[102]. The SSMs function to remove any particulate antigen in the lymph fluid by capture on their surface[99]. This includes capture of viral particles[90,107]. Upon capturing antigen on their surface in the SS they then move these antigens along their protrusions into the B cell follicle for recognition by cognate B cells via their B cell receptor (BCR)[106]. Subcapsular sinus macrophages also capture opsonized antigen and translocate it to the B cell follicle. In the follicle non-cognate B cells take up the antigen by CR1 and 2 and transport the antigen complexes to FDCs in the germinal center, where it has an essential role in driving affinity maturation and development of memory B cells[102]. Intravital imaging studies have visualized this transfer of particles along the SSM surface, however, due to the resolution of multiphoton microscopy it can't be eliminated that these cells may take up particles into non-degradative early endosomes and recycle them to the surface[90]. The interaction between SSM and B cells is bidirectional, the development and maintenance of SSM is dependent on B cell derived $LT\alpha_1\beta_2$ [102,107]. Without B cells, or when B cells specifically lack $LT\alpha_1\beta_2$, SSM numbers are reduced, and in contrast when $LT\alpha_1\beta_2$ is overexpressed SSM numbers increase, the SSM layer becomes thicker[102]. Unpublished results from the Coles laboratory indicate that MRCs and ILC3s also have an important role in maintenance of the SSM positioning and function.

Subcapsular sinus macrophages have several key roles in immunity including prevention of systemic spread of viruses by clearing them from the draining lymph fluid; this is mediated by capture of viruses from the lymph, and is important in induction of antiviral antibody responses. During a subcutaneous vesicular stomatitis virus (VSV) infection SSM prevent VSV spread to peripheral nerves that are situated in the LN. Selective depletion of SSM results in spread of VSV to the central nervous system and paralysis of the mice. Type I interferon (IFN-α) production by SSM is essential for prevention of VSV spread and replication within nerves[108]. Replication of VSV within the SSM is required for induction of Type I IFN production. Anti-viral antibodies are important for protection from VSV, however even with high antibody titers approximately 60% of mice lacking SSM die. Even though antibody was not, B cell $LT\alpha_1\beta_2$ was essential for survival. In the absence of B cells or when B cells lacked $LT\alpha_1\beta_2$, SSM did not develop properly and thus VSV was able to spread to the central nervous system[107]. Subcapsular sinus macrophages are not only permissive to VSV infection, they are also permissive to dengue virus, vaccinia virus, cow pox, murine cytomegalovirus[106] and the parasite *T. gondii*[36].

Medullary sinus macrophages (MSM), are highly phagocytic macrophages that express CD169 and CD11b, additionally they are also characterized by F4/80, SIGN-R1, macrophage receptor with collagenous structure (MARCO), mannose receptor (MR) and lymphatic vessel endothelial

hyaluronan receptor 1 (Lyve-1) expression[106]. SIGN-R1 is a C-type lectin and is a receptor for bacterial dextrans, including the polysaccharide capsule from *S. pneumoniae*. MARCO is a scavenger receptor that binds unopsonised bacteria and particles. Thus due to the location in the lymph and the expression of PRR and scavenging receptors on the MSM surface it is unsurprising that the main function of MSM is clearance of particulate antigen in the lymph, thus preventing spread of pathogens beyond the dLN. Injection of labeled antigen in peripheral tissues is observed in MSM phagosomes within minutes of injection[106].

1.11 Medulla function

The medulla of the LN is a region that is less well understood, its main functions are to clear particulate antigen from the lymph by MSMs, support cellular egress from the LN and provide a niche for long lived plasma cells. An extensive lymphatic sinus network connects to the efferent lymphatic vessels and is the site of lymphocyte exit from the LN back into circulation. The localised production of sphingosphine-1-phosphate (S1P) by lymphatic endothelial cells is essential in enabling lymphocyte egress from the LN. An additional role for the medulla is as a niche for plasmablasts and mature plasma cells. During B cell activation a proportion of activated B cells differentiate into plasmablasts. These cells down-regulate chemokine receptors CXCR5 and CCR7, and thus they are no longer retained in the B cell follicles. Instead they up-regulate CXCR4 and migrate to CXCL12 rich areas; these include the lymph node medulla, splenic red pulp and bone marrow[109]. Here they differentiate into long-lived plasma cells. In the medulla plasma cells are non-migratory [110] and produce large amounts of antibody that is transported out of the LN in the lymph. These cells die in the medulla and are cleared by medullary cord macrophages[106]. Long lived plasma cells reside in the bone marrow which provides a niche for their long term survival.

1.12 Lymph node entry and exit

1.12.1 High-endothelial venules

Entry to the lymph node occurs through the blood, through specialized post-capillary venules; HEVs or from the lymphatic system through afferent lymphatic vessels. Naïve lymphocytes enter through HEVs that run through the LN. Crossing the HEV endothelium involves a similar cascade of events as seen in neutrophil TEM. First, lymphocytes tether to the endothelium through L-selectin (CD62L) binding to HEV mucin-like glycoproteins, these are highly sulfated, fucosylated and sialylated. These sialomucins are also known as peripheral node addressins (PNAd)[111]. PNAd binding causes lymphocytes to begin to roll on the endothelial surface. Critical for CD62L binding is the recognition of 6-sulpho sialyl Lewis X which is

found specifically in HEV sialomucins[91]. Once rolling lymphocytes are in close proximity to the HEV endothelium, chemokine receptors can bind heparin sulfate immobilized chemokine. CCL21, CXCL12 and CXCL13 are the key chemokines involved in lymphocyte extravasation. High endothelial venules and pericytes produce CCL21, however CXCL12 and CXCL13 are made by FRCs and FDCs respectively, and are transcytosed to the endothelial surface [112]. Endothelial cell heparin sulfate has been shown to bind CCL21 and immobilise it on the cell surface. T cells express chemokine receptors CCR7 and CXCR4 that bind CCL21 and CXCL12, B cell express CXCR5 that binds CXCL13, but also CCR7 and CXCR4. Chemokine receptor signalling, in addition to sheer stress from blood flow, induces inside-out signalling, resulting in integrin activation, allowing the extension of CD11a and binding to ICAM-1 or 2 on the endothelium, this process causes lymphocyte arrest, B and T cells then crawl along the HEV lumen[91]. This process is thought to lead to the lymphocyte finding a suitable exit point through which it can transmigrate through the vessel wall, other lymphocytes follow and use the same route. Lymphocytes then move in perivascular channels to find a location to enter the lymph node parenchyma.

High endothelial venules also have a key role in controlling the rate of lymphocyte entry into the parenchyma of the LN. Lymphocytes were found to be held in HEV pockets formed between endothelial cells. When lymphocyte egress was blocked the number of lymphocytes held in these pockets increased. It was hypothesized that due to the close proximity of HEV and paracortical lymphatic sinuses (where lymphocytes exit the lymph node parenchyma), during homeostasis when lymphocytes enter the lymphatic sinuses lymphocytes are released from these pockets to balance the loss[113]. Central memory and $FOXP3^+$ regulatory T cells also enter the lymph node via HEVs, in the same way as naïve T cells. Plasmacytoid DCs and precursors to conventional DC also enter LNs through HEVs, as do a small number of NK cells, thus HEV are important for the entry of other immune cells, not exclusively B and T cells[91].

1.12.2 Lymphatic vessels

Immune cells migrating from peripheral tissue sites enter the lymph node through the afferent lymphatics. This process has been most widely studied in dermal DCs[93,114]. In tissues resident DC enter terminal lymphatic vessels in a mechanism dependent on CCR7 expressed by DCs and CCL21 made by lymphatic endothelial cells. CCL21 is located in distinct pockets; immobilized on the abluminal side of lymphatic vessels by heparin sulfate. CCL21 is also found immobilized in the interstitium, either on cell surfaces or matrix components, immobilization is mediated by heparin sulfate binding[93]. The interstitial CCL21 forms a gradient by which DCs can migrate along to reach the lymphatic vessels. Dendritic cells dock to the lymphatics by binding CCL21, they then move through gaps in the basement membrane and cross the lymphatic endothelium,

entering the lymph vessel. Lymphatic endothelial cells in initial lymphatics are oak leaf shaped and overlapping, unlike blood vascular endothelium they are not tightly joined together by conventional zipper-like junctions; rather they are joined by discontinuous button junctions. Thus DCs can squeeze through valves between button junctions to access the vessel lumen[115]. Once inside initial lymphatics *in vivo* imaging studies revealed that DCs crawl along the luminal lymphatic endothelium in the direction of lymph flow. Once in collecting lymphatics DCs drifted freely with lymph flow[114] towards the LN.

Dendritic cells enter the LN through afferent lymphatic vessels, into the SCS. They then move through the SCS floor into inter-follicular regions, then to the CCL19 and CCL21 rich areas of the T cell zone. This directed migration is dependent on sensing of a CCL21 gradient through CCR7 on the DC; there is little CCL21 in the SCS lumen, however from the SCS floor into the paracortex there is an increase in CCL21. This gradient is maintained by the atypical chemokine receptor CCRL1 expressed specifically on the lymphatic endothelial cells lining the ceiling of the SCS. CCRL1 binds CCL21, internalizing it and degrading it, maintaining low CCL21 concentration in the SCS lumen. In mice deficient of CCRL1 this gradient is lost and DC migration across the SCS floor into the paracortex is inhibited[116].

All cells exiting the LN leave through the medullary sinus into efferent lymphatic vessels. Cells then rejoin the circulation through the thoracic duct. Egress from the parenchyma of the LN occurs predominantly in blind ended paracortical lymphatic sinuses in the paracortex, fluid in these vessels flows to the medullary sinus. The process of lymphocyte egress from LNs is dependent on the phospholipid S1P. Naïve T cells express the GPCR S1P receptor 1 (S1PR1) on their surface. Lymphatic endothelial cells express high levels of S1P kinase and thus make S1P that is released into the lymph[117]. T cells probe paracortical sinuses, upon binding S1P G protein signalling is activated driving the cell to enter the sinus. T cells then flow to the medullary sinus where they are released into the subcapsular space and egress through efferent lymphatic vessels[118]. Lack of S1PR1 expression blocks entry into the paracortical sinuses and thus lymphocyte egress from the LN, resulting in blood lymphopenia. B cell and plasma cell egress is also dependent in S1P-S1PR1 signalling[119].

1.13 Early events in immune response generation in the lymph node

Soluble antigen rapidly drains to the LN within minutes, however APC that have phagocytosed antigen take a considerably longer period of time to migrate to the LN. This is due to a requirement for DCs to mature and up-regulate CCR7, required for entry into the lymphatics. The presence of antigen in the LN can lead to T and B lymphocyte activation, inducing the first steps in the adaptive immune response. T and B cell activation takes several days and requires

multiple signals and different cell types to ensure that the response is robust, goes on to develop memory and that inappropriate activation that could lead to autoimmune disease does not occur.

1.13.1 T cell activation

Upon exposure to inflammatory stimuli, or microbial products DCs change from immature, antigen-capturing cells, to mature, antigen presenting cells. This maturation includes up-regulation of antigen processing machinery, MHC II, T cell stimulation molecules CD80/86 and chemokine receptors that allow them to migrate to the draining LN[120]. Migratory and resident mature DCs in the LN present MHC II restricted antigens or MHC I restricted antigens to naïve T cells. $CD4^+$ T cells recognize MHC II via their T cell receptor (TCR). The CD4 co-receptor was thought to stabilise the interaction, however studies have found this is not the case, the co-receptor functions to bring the src family kinase p56(lck) to the TCR[121], this is an essential molecule for TCR signalling. This interaction is signal-1, the first signal required for T cell activation, however to fully activate T cells further stimulation is required. Dendritic cell CD80/86 molecules bind T cell CD28 thus co-stimulating the T cell and providing signal-2. Signals 1 and 2 trigger CD40 ligand (CD40L) expression on T cells, which binds CD40 on DCs promoting cytokine release, the third signal in T cell activation. The cytokine produced by the activating DC can determine which subset of T_H cell the naïve cell differentiates into; T_H1, T_H2, T_H17, regulatory T cell (T_{reg}), follicular T helper (T_{FH}) or regulatory T_{FH} cell (T_{FR}). The type of PAMP and tissue factors released by resident cells such as mast cells, epithelial cells and macrophages, determines DC polarisation and patterns of cytokines production[122].

Following activation, T cells undergo multiple rounds of cell division termed clonal expansion. During clonal expansion T cells differentiate into effector cells that migrate to the infection site and memory cells that protect against any future infection by the same pathogen[123]. Memory cells are divided into central memory (T_{CM}) or effector memory (T_{EM}) subsets, central memory T cells are in a quiescent state and are able to enter and patrol LNs through CD62L and CCR7 expression. In contrast, effector memory T cells resemble effector T cells and produce effector cytokines, however they lack CD62L and CCR7, thus do not enter LNs. It is T_{CM} cells that are thought to provide long-term antigen specific memory[124]. Upon exposure to the same antigen memory cells are able to respond through both effector function and proliferative capacity more rapidly than naïve T cells on a per cell basis.

Clonal expansion is required to rapidly increase helper T cell numbers. This results in a pool of effector cells to directly fight the infection, however also a pool of cells required for the activation of other lymphocytes. T follicular helper cells are characterised by expression of high levels of CXCR5, permitting migration into B cell follicles where they are required for

activation of B cells. Cytotoxic $CD8^+$ T cells also require T cell help for activation[123]. Activation of $CD8^+$ T cells by DCs is similar to $CD4^+$ T cell activation, requiring 3 signals, however DC 'licensing' by $CD4^+$ T cells is also needed for effective CD8 activation through CD40 - CD40L signalling[125]. $CD4^+$ T cells also provide help directly to the $CD8^+$ cells through IL-2 and IFNγ, enabling their full differentiation into cytotoxic T lymphocytes (CTL)[125]. Upon activation $CD8^+$ T cells also undergo clonal expansion, differentiating into CTLs and memory $CD8^+$ T cells, with a key role in intracellular pathogen, virus and tumor clearance[126].

1.13.2 B cell activation

Naïve B cells are located in organized follicle structures beneath the SCS. In response to antigen binding to the BCR, they migrate to the interface of the follicle and T cell zone, there they present antigen to $CD4^+$ T cells. If the T cell recognizes the antigen through its TCR, then it provides the B cell with a survival and proliferation signal from CD40L, binding CD40 on the B cell. Proliferating B cells remain at the follicle edge and continue presenting antigens to $CD4^+$ T cells for 2-3 days. The isotype of immunoglobulin the B cell will produce is guided by cytokine produced by T_H1 and T_H2 cells. T_H1 IFNγ stimulates IgG2a, whereas T_H2 IL-4 induces IgE production. Approximately 2-4 days after antigen exposure, the B cells then differentiate into GC B cells, memory B cells or short-lived plasma cells[127]. Germinal center B cells migrate into the follicle, guided by FDCs, and the GC forms. Germinal centers can last for many weeks depending on antigen availability and adjuvant. Germinal center B cells rapidly proliferate, undergo somatic hypermutation of their BCR variable region and Ig class switch recombination in a T_{FH} cell dependent process. T follicular helper cells produce IL-21 and IL-4, and provide CD40L, which are essential signals for GC B cell survival, proliferation and persistence. Germinal center B cells either survive or undergo apoptosis depending on the strength of their BCR for foreign and self-antigens. Thus self-reactive antibodies generated by somatic hypermutation are eliminated by negative affinity selection in a FAS dependent process[127].

Germinal center B cells can differentiate into long-lived memory B cells or long-lived plasma cells. Plasma cells can survive and produce protective antibodies for years. Plasma cells migrate to lymphoid tissues including the LN medullary cords, red pulp of the spleen and the bone marrow. They reside in niches where BAFF and a proliferation-inducing ligand (APRIL) are provided by a number of cell types including medullary cord macrophages, $CD11c^{hi}$ DCs, stromal cells in the spleen and bone marrow macrophages and stromal cells[110]. Plasma cell homing is mediated by CXCR4 expressed by plasma cells and CXCL12 by stromal cells[127].

Classically B cell activation occurs in response to thymus-dependent (TD) antigens, relying on T cells for help. However B cells can also activate in response to thymus-independent (TI)

antigens. This occurs in the splenic marginal zone and the intestinal lamina propria[128]. Thymus-independent antigens are divided into type 1 and type 2 antigens. Thymus-independent type 1 antigens, for example LPS, activate the BCR, but also B cell TLRs (in mice but not humans), thus inducing polyclonal B cell activation. Thymus-independent type 2 antigens are multivalent, for example *S. pneumoniae* capsular polysaccharide, or antigens with repeating epitope units. Thus multiple BCRs on one B cell bind the antigen resulting in receptor cross-linking, and inducing antigen-specific B cell activation[129]. Thymus-independent type 2 antigens can induce GCs and effector plasma cells, but not memory B cells or long lived plasma cells[130]. Thymus independent antigens generate low affinity IgM response that are highly potent at inducing complement mediated lysis of bacteria and have an important role in early protection to bacterial infection.

1.14 Lymph node function during inflammation

During the induction of adaptive immune responses in the LN there is an increased rate of lymphocyte migration into the LN. T cell clonal expansion and the proliferation of B cells in the GC reaction also helps drive the large net increase in the number of cells in the LN. Thus the LN needs to increase in size to accommodate an up to a tenfold increase in cellularity, a process termed LN hypertrophy.

1.14.1 HEV network expansion

To enable increased lymphocyte ingress into the LN rapid vasculature remodeling must occur. The HEV network expands, thus allowing entry of more lymphocytes, and vasodilation of capillaries permits entry of nutrients and oxygen into the LN. Inflammation can induce expansion of the HEV networks in LNs in a multi-step process. The initiation phase happens during the first two days post immunisation and involves rapid proliferation of blood endothelial cells resulting in a selective increase in the number and thus length of the HEV network. This proliferation is independent of B and T cells but reliant on vascular endothelial growth factor (VEGF) produced by FRCs. Fibroblastic reticular cell VEGF is produced upon LTβ receptor (LTβR) stimulation[131] and resident $CD11c^{hi}$ cells have a critical role in its upregulation[132]. The next phase is an expansion phase lasting 2-7 days, where continued HEV cell proliferation is dependent on B and T cell proliferation. After this phase the HEVs become quiescent with reduced proliferation and trafficking of lymphocytes through the HEVs. During the resolution of LN hypertrophy, FRCs tightly ensheath the HEVs leading to a reduced rate of lymphocyte entry into the LN, a process dependent on $CD11c^{hi}$ cells. The depletion of these cells results in HEV proliferation, FRC disorganization and increased vascular permeability[133].

The FRC network can also expand in response to inflammation, upon immunization with OVA in Complete Freund's Adjuvant (CFA) the FRC network dramatically expands and remodels[134]. Expansion of the FRC network follows the same kinetics as HEV expansion[132]. However, these processes are entirely stimulation dependent and LN remodeling and HEV dynamics do not occur by these mechanisms in *S. pneumoniae* infection. This process is dependent on mast cell mediated secretion of histamine and TNFα that drives NO production by SSM, inducing rapid vasodilation of HEVs and FRCs. This permits rapid changes in LN size without stimulating proliferation of either HEVs or FRCs (Coles laboratory, unpublished data).

1.14.2 Lymphangiogenesis in the draining lymph node

During an inflammatory immune response lymphangiogenesis can lead to the growth of new lymphatic vessels throughout the LN changing its structural organization. This process enables increased numbers of DC and activated myeloid cells to enter the lymph node[135]. It also enlarges the size of the medulla to accommodate the increased numbers of plasma cells generated during an immune response[136]. Lymph node lymphangiogenesis in response to some inflammatory signals has been shown to be dependent on B cells[135,136]. In mice lacking B cells, or B cells that can't home to the LN, lymphatic remodeling does not occur in these model systems, however in the absence of T cells or myeloid cells this process is intact. Blocking vascular endothelial growth factor receptor 2 (VEGFR-2) or VEGFR-3 or both reduces LN lymphatic growth, however does not block it. In another study, it was found that blockade of LTβR also decreased lymphatic remodeling, however does not block it. Thus it is likely that there is redundancy and that both VEGFR and LTBR signalling are involved in LN lymphangiogenesis, possibly other molecules could be involved too which makes interpretation of these results difficult. In these models there is an absolute role for B cells, possibly through the production of VEGF-A and LTα1β2, acting indirectly or directly on lymphatic endothelial cells[135,136]. However, these processes are very model dependent, in contrast to the published results we observe significant lymphangiogenesis in RAG deficient mice (no T or B cells) when mice are injected subcutaneously with adjuvants containing TLR4 adjuvants (monophosphoryl lipid A and glucopyranosyl lipid adjuvant; MPL and GLA). Thus the molecular mechanisms likely depend on the pathogen or adjuvant working by distinctly different mechanisms, consistent with multiple different mechanisms being involved depending on the type, duration and location of inflammation (Coles laboratory, unpublished data).

During the initiation of an immune response a reduction in lymphocyte egress can accompany the increased influx of immune cells. A transient block in T cell egress is important to allow full activation of responding T cells and the expansion of the effector T cell pool, in a process termed lymph node 'shut down'[137]. This works by an IFNα/β and S1P dependent process. Upon

T cell activation CD69 is transiently expressed at high levels on lymphocytes by both TCR stimulation and by type I interferons, CD69 binds to S1PR1 on the surface of the same cell, inducing receptor internalization of S1PR1. Thus the T cell is unresponsive to S1P and cannot exit the lymph node[137,138]. This block in lymphocyte egress lasts for several days, allowing time for clonal expansion of an effector T cell pool. Once CD69 expression is lost S1PR1 is then re-expressed on the cell surface allowing T cells to respond to lymphatic S1P gradients and exit the lymph node.

The stromal cell compartment must also remodel to accommodate the large numbers of accumulating lymphocytes. It has been proposed that the FRC cells proliferate, however in other model systems the FRCs stretch. In *S. pneumoniae* infection the FRCs stretch, rather than proliferate (Coles lab, unpublished data). This is likely a result of distal lung mast cell degranulation in regulating this process rather than being DC driven due to the early timing of this event. Collectively lymph node hypertrophy is a result of rapid changes to HEVs, stromal cells and the lymphatic network; however the mechanisms that drive this process are situation dependent.

1.15 Innate immune defenses in the lymph node

Lymph node macrophages form an important line of defense in the LN, removing pathogens and antigen entering the LN in the lymph. However these are not the only innate cells functioning to protect the LN. Natural killer cells, NKT cells, γδ T cells and innate-like $CD8^+$ T cells can be found in LNs in steady state, positioned in the medulla and interfollicular regions. During skin infection with *P. aeruginosa* and *Salmonella typhimuurium*, tissue dLN macrophages stimulate these cells to produce IFNγ, which boosts macrophage antimicrobial resistance. If this axis is disrupted then systemic pathogen spread can occur[139]. Innate cells not only function to clear lymph pathogens, they are also involved in regulating immune responses. Certain adjuvants including AS01 (MPL/QS-21) induce tissue NK migration to the draining lymph node where they are an early source of IFNγ and thus involved in T_H1 polarization[140]. In *L. major* infection NK cells were also found to produce IFNγ, and migrated to the paracortex where $CD4^+$ T cell activation occurs[141]. During *Schistosoma japonicum* infection, NK and NKT cells migrate to the mesenteric lymph node where they activate and express IL-4 and IL-17 cytokines[115]. Thus NK cells have an important role in early LN cytokine production and modulation of T cell polarization. NK cells were also found to directly interact with B cells where they migrate to and patrol the LN, in particular the follicle periphery. They can also form stable contacts with and eliminate MHC mismatched target B cells[142]. Neutrophils are also recruited to the LN in response to distal bacterial, fungal and parasitic infections and in response to vaccine challenge; the role of neutrophils in lymph nodes is explored in Chapter three.

1.16 *In vivo* live cell imaging

Techniques such as flow cytometry, immunohistochemistry and quantitative polymerase chain reaction (Q PCR) provide us with lots of information about cells and how they respond in inflammation. However to gain a greater understanding of how cells function in their normal tissue environment live *in vivo* cell imaging is required. Since 2002, when pioneering works were published utilizing *in vivo* cell imaging to demonstrate live T cell dynamics and behavior in the thymus and LN[143-145], the use of this technique has revolutionized and enhanced our understanding of how immune cells function, and the importance of tissue structure to their function. This permitted the discovery that paracortical T cells utilize FRCs to migrate along in order to scan for cognate antigen presented by DCs that adhered to the FRC network[92,146]. The intricacies of the neutrophil recruitment cascade; rolling, crawling, adhesion and abluminal crawling, and also swarming were all revealed through high-resolution *in vivo* live cell imaging techniques utilizing spinning disk and one and two photon (multiphoton) microscopy.

1.16.1 Visualising cells

To enable high resolution imaging of cells, in real time, laser scanning microscopy is used, however cells need to be tagged with fluorochromes or fluorescent proteins to visualise them. Cells can be labeled *ex vivo* with dyes such as carboxyfluorescein succinimidyl ester (CFSE), and then transferred back into the animal for visualization. This allows specific labeling of cells of interest, however the removal and manipulation of cells can often cause their activation, maturation or death, indeed only low percentages of adoptively transferred cells are observed, therefore this method is not ideal[147]. Injection of fluorochrome tagged monoclonal antibodies (mAb) can be used to label cells *in situ*, for example blood vasculature endothelial cells can be visualized by injection of mAbs to CD31 (PECAM1)[24], however this approach requires large amounts of antibody that can drive immune responses to the antibody and inhibit protein function. Fluorescent reporter mice have been extensively used in *in vivo* imaging. The DNA encoding fluorescent proteins such as green fluorescent protein (GFP), DsRed fluorescent protein (RFP) is inserted into the gene of interest, when that gene is transcribed and translated, so is the fluorescent protein, thus the resulting protein of interest is labeled *in situ* with the fluorescent protein allowing its visualization. When investigating neutrophils, classically, LysM-GFP mice have been used. These are knock-in mice, where GFP is inserted into the lysozyme M (LysM) locus[148]. Lysozyme M is specifically expressed by myelomonocytic cells; macrophages and neutrophils with high levels in neutrophils. The drawback to fluorescent protein knock-in mice is that the target gene will likely be either knocked-out or miss-expressed potentially effecting cellular function. Thus the reporter mice can only be used as heterozygotes

to avoid impacting cell function. Alternatively tissue specific Cre reporter mice crossed with Rosa26, floxed fluorescent reporter mice can be utilised.

1.16.2 Live cell imaging techniques

Two techniques have commonly been used to image cells *in situ*; tissue explants and intravital imaging of live mice. Tissue explants involve the excision of the tissue of interest then imaging it whilst embedded in agarose or in culture medium. This allows access to the whole organ for imaging. This is a major advantage for tissues that are not easily accessible in a live animal, for example the thymus and certain LNs. Some tissue draining LNs can be difficult to image *in situ*, the hilum, where blood vasculature enters and lymphatics exit, is buried deep thus not easy to access without disrupting these vessels and other tissues[147]. However, in explant cultures there is no flow of blood, lymph, nutrients and oxygen or entry of cells in this system. This is a major limitation that may alter cell behavior. Intravital imaging has the major advantage in this respect. Tissues are imaged *in situ*, with intact blood and lymph flow, thus true *in vivo* cell behavior is observed. However movements of the animal as a result of breathing or muscle contractions can make it difficult to obtain high quality images. Additionally it is possible that anesthetics may impact on cell behavior, an effect that has been observed in sheep. Finally a drawback of surgery in intravital microscopy is the possibility of generation of inflammatory immune responses to the surgery, thus events observed may be responses specific to the surgery[147].

1.16.3 One and two-photon microscopy

In confocal, single-photon microscopy, lasers emit single photons of light to excite the fluorescent tags. Emitted light is then focused through a pin hole that restricts out of focus light from above and below the focal plane reaching the detector. Therefore only light from the focal plane is detected, this generates high-resolution images. However the short wavelength of light used means penetration into tissue is low due to scattering of the laser and emitted light in the sample, thus deep tissue imaging is not possible[147]. Tissues that are thin and easily exteriorized, such as the cremaster muscle and mesentery are well suited to this method of microscopy. To image deep into tissue two-photon microscopy is utilised. Two-photon lasers emit two-photons of longer wavelength infrared light that are near simultaneously absorbed by fluorochromes. Their combined energy results in fluorescent light emission in the visible range[149]. The longer wavelength allows deeper tissue penetration due to reduced light scattering, however also reduces the resolution[147]. Single-photon microscopy causes tissue damage and photo-bleaching due to excitation of the whole sample. In two-photon microscopy this is limited due to the infrared photons simultaneously exciting fluorochromes in the focal plane only, the rest of the

tissue is only exposed to infrared light which is not harmful[150]. A further advantage of two-photon microscopy is the ability to visualize fibrillar collagen without the need to label it due to secondary harmonic generation from the multiphoton laser. This provides a further layer of detail when investigating how cells move in 3D in the interstitial environment. It also highlights their impact on the collagen structure in tissue, for example neutrophils swarming in the dermis of the ear, in response to sterile laser-induced injury, move collagen fibers generating a collagen-free core at the swarm center[33].

Three-dimensional (3D) images are acquired by the laser scanning in x and y planes, followed by changing the focus to the microscope to image successive z planes, generating a z stack. The repetition of this process over time generates four-dimensional (4D) data to form a time-lapse movie. These movies can be analysed using software such as Imaris (Bitplane) and Velocity (PerkinElmer) to quantify cellular behavior, for example velocity, directionality and co-localisation with other cells or molecules.

1.17 Summary and aims

Neutrophils are key innate immune cells, through a range of powerful mechanisms including phagocytosis, degranulation, NETosis and cytokine production neutrophils are essential for protection against bacterial, fungal, viral and protozoan pathogens. However they function further than first-line innate defenses and are capable of modulating both innate and adaptive immune cells. Thus they are capable of regulating other responding immune cells and thus the host immune response. Neutrophils are known to be terminally differentiated cells, generated and stored in the bone marrow and released as a mature cell. However it is clear that they are capable of adapting to the environment and the stimulus they encounter to alter their transcriptional profile, and thus generate the correct, specific tailored functional response.

Using the model human pathogen, *S. pneumoniae,* this project aims to investigate neutrophil responses to pulmonary infection with this bacteria. Specifically, their recruitment to and function in the tissue draining, mediastinal LN, including differences in their phenotype and function in comparison to neutrophils in the blood and lung. Utilising fluorescent reporter mice and multiphoton laser scanning microscopy technology this project will also investigate neutrophil migration; their dynamics and the underlying mechanisms controlling their movement and migration in the lung draining LN. Much work has been done on neutrophil migration *in vitro*, and *in vivo* investigating their extravasation and interstitial migration, however little is known of their dynamics in secondary lymphoid organs.

1.18 Hypothesis

We hypothesise that in response to pulmonary *Streptococcus pneumoniae* infection, in addition to a robust influx into the lung, neutrophils will also traffic to the LdLN. Neutrophil phenotype, function and migration mechanisms will be environment dependent rather than cell-intrinsic. The LdLN location will require adjustment of neutrophil phenotype from the highly activated, pathogen killing, destructive phenotype required at the site of infection, in order to avoid damage to the LdLN architecture, which could severely disrupt the development of a productive immune response.

1.19 Specific aims

- Define neutrophil recruitment kinetics to the LdLN during pulmonary *Streptococcus pneumoniae* infection.
- Investigate neutrophil location within the LdLN.
- Characterise neutrophil phenotype and function in the LdLN, and compare to blood and lung neutrophil phenotype.
- Utilise an explant imaging system, in combination with multi-photon laser scanning microscopy, to investigate neutrophil dynamics in real time, in 3D.
- Use pharmacological interventions, including GPCR antagonists, small molecule inhibitors and blocking antibodies to uncover some of the molecular mechanisms governing neutrophil migration within the LN.

Chapter 2: Materials and Methods

2.1 Reagents

Table 2.1: General reagents.

Selected Reagents	Brief Description/Use	Supplier
AccuCheck counting beads	Absolute cell number quantification in flow cytometry.	Invitrogen
Agar	Used to make BHI agar plates for *S. pneumoniae* culture.	Fisher
BHI broth	*S. pneumoniae* culture medium.	Oxoid
BSA	Used as a protein source for cells.	Sigma-Aldrich
CampyGen sachets	Absorb oxygen, generate carbon dioxide, producing microaerobic conditions.	Oxoid
CellMask Deep Red	Plasma membrane stain.	Invitrogen
Chamber slides	8 wells, No 1.5 glass.	Fisher
Collagenase D	Enzyme used in tissue digestion to degrade collagen.	Roche
Columbia horse blood agar plates	*S. pneumoniae* culture.	Thermo Scientific
Cover slips	22 x 50 mm, No 1.5 glass.	Fisher
CTV	Plasma membrane stain.	Invitrogen
DAPI	Nuclear stain.	Fisher
DHR 123	ROS detection.	Invitrogen
DMEM medium	Cell culture medium.	Invitrogen
DMSO	Used to dissolve compounds.	Sigma-Aldrich
DNase1	Endonuclease that cleaves DNA, used in tissue digestion.	Sigma-Aldrich
DTx	Used *in vivo* to deplete DTR expressing cells.	Sigma-Aldrich
EDTA	Used in FACS buffers and tissue digestion to prevent cation dependent cell-cell bonding.	Fisher
FCS	Used as a protein source for cells.	Thermo Scientific
Fine bore polythene tubing	Used to perform BAL.	Smiths Medical
Giemsa stain	Used to visualise cell nuclear and cytoplasmic morpholgy.	VWR
Glass bottom dishes	35 mm dish diameter, No 1.5 glass, 10 mm glass diameter.	MatTek Corporation
Goat serum	Used to block non-specific Ab binding in IHC.	Sigma-Aldrich

GoTaq Flexi DNA Polymerase	Kit for PCR using GoTaq DNA polymerase and green GoTaq buffer.	Promega
Hematocrit capillary	Sodium heparinized, used to collect exactly 100 µl of blood.	Hirschmann Laborgeräte
Heparin	Used for blood collection to prevent clotting.	Sigma-Aldrich
High Capacity cDNA Reverse Transcription Kit	Kit containing reverse transcriptase for cDNA synthesis from RNA.	Applied Biosystems
ImmEdge Pen	Wax pen used in immunohistochemistry	Vector Laboratories
MicroAmp Optical 96-well reaction plate	96 well Q-PCR reaction plate.	Applied Biosystems
miRNeasy micro kit	miRNA and RNA extraction kit.	Qiagen
OCT	Tissue embedding material for tissue sectioning.	Agar Scientific
Optochin disks	Used for the optochin sensitivity test to identify *S. pneumoniae.*	Sigma-Aldrich
PBS	Sterile PBS used as vehicle for administering substances or bacteria to mice.	GE Healthcare
PHK26	Plasma membrane stain.	Sigma-Aldrich
Poly-L-lysine slides	Used for frozen sectioning.	VWR
Power SYBR Green	Master mix for Q-PCR containing AmpliTaq Gold DNA polymerase and SYBR Green.	Invitrogen
ProLong Gold	Anti-fade reagent in IHC.	Fisher
QIAshredders	Column for homogenising cell lysates before RNA extraction.	Qiagen
Rat IgG	Polyclonal antibody used for Fc receptor blocking in flow cytometry.	Sigma-Aldrich
RNeasy mini kit	RNA extraction kit.	Qiagen
RPMI medium	Cell culture medium.	Invitrogen
Titertube micro test tubes	Used as flow cytometry tubes.	Bio-Rad
TruStain fcX	anti-mouse CD16/32 Ab, Rat IgG2a, clone 93, used for Fc receptor blocking in flow cytometry.	Biolegend

Table 2.2: Primary antibodies.

Specificity	Fluorophore	Clone	Host	Isotype	Supplier	Use
CD11b	PE Cy7	M1/70	Rat	IgG2b	Biolegend	FC
CD11c	A647	N418	Armenian Hamster	IgG	eBioscience	FC, IHC
CD169	FITC	MCA884F	Rat	IgG2a	AbD Serotec	IHC
CD4	PB	RM4-5	Rat	IgG2a	eBioscience	FC
F4/80	A647	BM8	Rat	IgG2a	eBioscience	FC, IHC
F4/80	PB	BM8	Rat	IgG2a	Biolegend	FC, IHC
Gr1	PE	RB6-8C5	Rat	IgG2b	BD Pharmingen	FC
ICAM-1	PE	YN1/1.7.4	Rat	IgG2b	eBioscience	FC
Ly6C	PE	HK1.4	Rat	IgG2c	Biolegend	FC
Ly6C	PerCP Cy5.5	HK1.4	Rat	IgG2c	Biolegend	FC
Ly6G	A647	1A8	Rat	IgG2a	Biolegend	FC, IHC
Ly6G	FITC	1A8	Rat	IgG2a	Biolegend	FC, IHC
Lyve-1	purified	Poly	Rabbit	IgG	AngioBio Co.	IHC
MECA79	A488*	MECA79	Rat	IgM	Nanotools	IHC
MHC II	e450	M5/114.15.2	Rat	IgG2b	eBioscience	FC
MHC II	PE	M5/114.15.2	Rat	IgG2b	Biolegend	FC
SIGNR1	A647	eBio22D1	Armenian Hamster	IgG	eBioscience	IHC
TCRB	FITC	H57-597	Armenian Hamster	IgG	eBioscience	FC

* labelled in house by Lisa Newman using an Invitrogen Alexa488 labelling kit

Table 2.3: Secondary antibodies.

Specificity	Fluorophore	Clone	Host	Supplier	Use
Rabbit IgG (H+L)	A594	Polyclonal	Goat	Invitrogen	IHC
Rat IgG (H+L)	A647	Polyclonal	Goat	Invitrogen	FC

Table 2.4: *In vivo* and *ex vivo* use antibodies.

Specificity	Clone	Host	Isotype	Supplier
CD11b*	M1/70	Rat	IgG2b	eBioscience
Ly6G	1A8	Rat	IgG2a	Bioxcel
Isotype	2A3	Rat	IgG2a	Bioxcel
* Functional grade purified.				

Table 2.5: Primers for quantitative PCR.

Gene	Refseq	Direction	Sequence
Hprt	NM_013556.2	Forward	AGGAGTCCTGTTGATGTTGCCAGT
		Reverse	GGGACGCAGCAACTGACATTTCTA
Ifng	NM_008337.3	Forward	CGGCACAGTCATTGAAAGCCTA
		Reverse	GTTGCTGATGGCCTGATTGTC
Mmp9	NM_013599.3	Forward	GTCCAGACCAAGGGTACAGC
		Reverse	ATACAGCGGGTACATGAGCG
Nos2	NM_010927.3	Forward	TTCACAGCTCATCCGGTACG
		Reverse	CGATGCACAACTGGGTGAAC
Ptgs2	NM_011198.3	Forward	ACTCATAGGAGAGACTATCAAG
		Reverse	GAGTGTGTTGAATTCAGAGG
S100a8	NM_013650.2	Forward	GTCCTCAGTTTGTGCAGAATATAAA
		Reverse	TTTGTGAGATGCCACACCCA
S100a9	NM_001281852.1	Forward	TAGCCTTGAGCAAGAAGATGGC
		Reverse	TTATGCTGCGCTCCATCTGA
Tnf	NM_013693.3	Forward	CTGTAGCCCACGTCGTAGC
		Reverse	TTGAGATCCATGCCGTTG
Tnfsf13	NM_001159505.1	Forward	TGGAAGGATGGGGCGAAATC
		Reverse	TGTCACGTCAGAGTCCTTGG
Tnfsf13b	NM_033622.1	Forward	GCTGGAGTCAAACTCCTGACA
		Reverse	GCTGCAGACAGTCTTGAATGAT

2.2 Mice

C57BL/6, B6J.CD45.1, B6.CX3CR1$^{GFP/GFP}$[151], B6.IL-7 Cre[152], B6.Rosa26 eYFP[153], B6.hCD2-DsRed.B[154,155], B6.LysM Cre[156], B6.Rosa26 mT/mG[157], B6.CD11c Cre[158], B6.Rosa26 iDTR[159] mice were bred and housed in microisolator cages in the Biological Services Facility (BSF) at University of York, under specific pathogen-free conditions. All mice used were between 7-12 weeks of age, all strains were on a C57BL/6 background (Harlan, NIMR or Jackson) with a minimum of 6-8 backcrosses. B6.IL-7 Cre transgenic mice were crossed with B6.Rosa26 eYFP mice, Cre negative Rosa26 eYFP negative mice and B6.hCD2-DsRed.B mice were used as wild type control mice in experiments where tissue was taken for histology. B6.CD11c Cre mice

were crossed with B6.Rosa26 iDTR mice and also B6.Rosa26 mT/mG to generate B6.CD11c Cre x B6.Rosa26 iDTR F1 and B6.CD11c Cre x B6.Rosa26 mT/mG F1 progeny. B6.LysM Cre mice were crossed with B6.Rosa26 mT/mG mice to generate B6.LysM Cre x B6.Rosa26 mT/mG F1 progeny. B6.CX3CR1$^{GFP/GFP}$ mice were crossed with C57BL/6 mice to generated B6. CX3CR1$^{GFP/+}$ heterozygous mice with a functional CX3CR1 receptor. CX3CR1 heterozygous mice were used in experiments. All animal procedures were performed under UK Home Office license 60/4129 (Mark Coles) in compliance with the ARRIVE guidelines.

2.3 Bacteria

2.3.1 *Streptococcus pneumoniae* culture

Streptococcus pneumoniae Glasgow strain D39 was a gift from Dr. Andreas Wack (National Institute for Medical Research). *S. pneumoniae* was cultured in brain-heart infusion broth (BHI) (Oxoid). Forty microliters of *S. pneumoniae* frozen glycerol stock was inoculated into 5 ml of BHI broth and incubated overnight (approximately 16 hours) at 37°C under anaerobic conditions; in an anaerobic jar containing one CampyGen sachet (Oxoid) to scavenge oxygen. The next day 5 ml of fresh BHI broth was inoculated with 100 µl of the overnight culture and incubated for 3-4 hours at 37°C. One milliliter of culture broth was sampled and the optical density (OD) at 600 nm determined by spectroscopy. When the OD_{600} was 0.4-0.6 the cultures were considered to be in log phase growth, once they reach this OD the cultures were spun down for 10 min at 2000 g at 4°C. The bacteria pellets were resuspended in BHI broth containing 30% glycerol. One microliter was removed for colony forming unit (CFU) determination on BHI agar plates, cryovials containing the stock bacteria were then placed at -20°C until required for *in vivo* infections. Bacteria were stored for no more than 24 hours before use, with one exception where bacteria were stored for three days for a time course experiment.

To prepare the bacteria for infection, an aliquot of bacteria from the stock corresponding to approximately 10^8 CFU/mouse (based on CFU calculation) was resuspended in sterile phosphate-buffered saline (PBS) and washed twice (10 min at 2000 g, 4°C) to remove any remaining traces of broth. The bacterial pellet was then resuspended in sterile PBS at a density of 10^8 CFU in 50 µl. This working bacterial stock was used for intranasal infection. One microlitre of bacteria was taken to check the CFU. Due to the freezing step following culture, prior to infection, the CFU of *S. pneumoniae* that infects the lung was often lower than 10^8 and sometimes closer to 10^7. The lower CFU induced fewer neutrophils to migrate to the lung draining LN (LdLN). This could not be avoided due to the method used to culture the bacteria and short time points between infections required for the project; however this variability was captured and quantified for all experiments undertaken.

2.3.2 CFU calculation

To calculate CFU, a 1 µl aliquot of *S. pneumoniae* culture was diluted to 1 in 100,000 and 1 in 1,000,000 in BHI broth. Fifty microliters of the diluted culture was added to a BHI agar plate and spread using sterile glass beads. The plates were incubated overnight at 37°C in anaerobic conditions. Agar plates with approximately 30-300 colonies on were counted (Figure 2.1 A) and number of CFU calculated as follows:

$$\text{CFU/ml} = \text{No colonies}/0.05 * \text{dilution factor}$$

2.3.3 Heat-killed *S. pneumoniae*

In explant imaging experiments heat-killed (HK) *S. pneumoniae* was used. Once the *S. pneumoniae* culture had reached OD_{600} 0.4-0.6 it was spun down as described above, the pellet was resuspended in 1 ml of sterile PBS and incubated at 60°C for 20 min. The HK *S. pneumoniae* was subsequently spun down and resuspended in sterile PBS. HK *S. pneumoniae* was stored at 4°C for no longer than 5 days. To demonstrate that the *S. pneumoniae* was heat killed, 20 µl of HK *S. pneumoniae* was spread on Agar plates and cultured overnight. No colonies grew, demonstrating that incubation at 60°C for 20 min was sufficient to HK the bacterial culture (Figure 2.1 B).

2.3.4 *S. pneumoniae* validation

To ensure that the bacterial culture only contained *S. pneumoniae* and not closely related *Streptococcus or Staphylococcus* strains with similar morphologies two tests were carried out; the optochin sensitivity test, and culture on blood agar. *S. pneumoniae* are exclusively sensitive to optochin antibiotic. When cultured on blood agar *S. pneumoniae* form small grey colonies with a zone of alpha-hemolysis around them that is green. The alpha-hemolysis is caused by the pneumolysin they produce that lyses red blood cells. Figure 2.1 (C) shows that a zone of inhibition of 18 mm was observed around optochin disks (Sigma) after 24 hours of culture on a Columbia horse blood agar plate (Thermo Scientific). The colonies on Columbia horse blood agar were characteristic of *S. pneumoniae*; small and grey, with clear alpha-hemolysis around them (Figures 2.1 D-F). Thus the bacterial cultures could be verified to be *S. pneumoniae*.

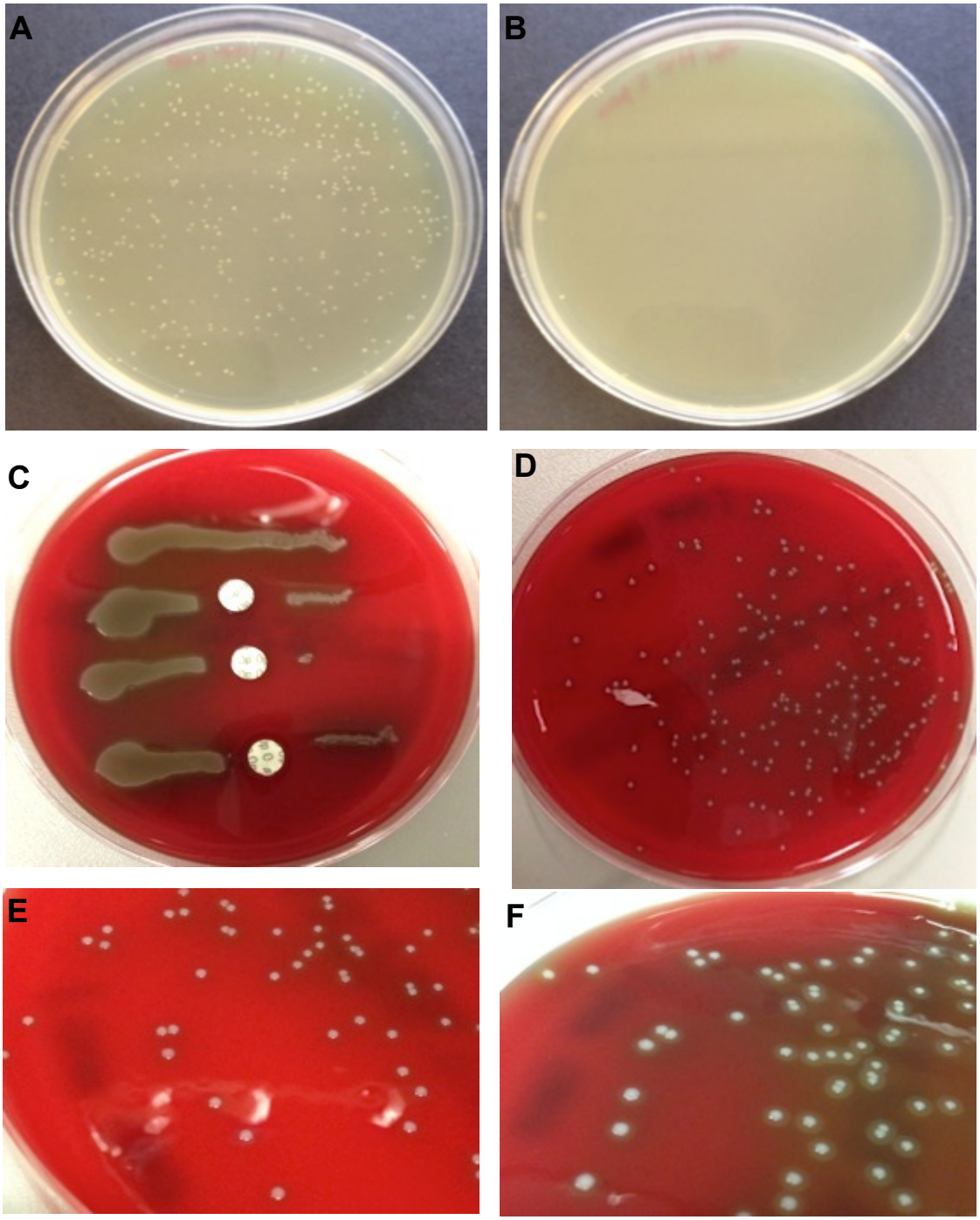

Figure 2.1: *Streptococcus pneumoniae* culture and verification.

(A) Representative image of 1:1,000,000 dilution of *S. pneumoniae* culture plated on BHI agar. (B) Confirmation of heat inactivation of *S. pneumoniae*. (A); before, (B); after heat inactivation at 60°C, 20 min. (C) Optochin sensitivity test. Validation of *S. pneumoniae* culture was demonstrated by zone of inhibition of 18 mm. (D) *S. pneumoniae* colonies on Columbia horse blood agar plates at 24 hours. (E) Close up of plate in (D), α haemolysis was visible around the colonies. (F) Plate in (D) at 48 hours, α haemolysis around *S. pneumoniae* colonies was clear.

2.3.5 Fluorescent labeling of *S. pneumoniae*

Heat killed *S. pneumoniae* were labeled with either PKH26, CellTracker Violet (CTV), or 4′, 6-Diamidino-2-phenylindole dihydrochloride (DAPI). *PKH26*: Heat killed *S. pneumoniae* were resuspended in 5 ml Diluent C from the PKH26 labeling kit (Sigma). In a separate tube 20 µl PKH26 was added to 5 ml Diluent C, this was added to the HK *S. pneumoniae* in Diluent C and incubated at room temperature for 5 min, whilst gently rocking. Ten milliliters of fetal calf serum (FCS) was added and incubated for a further 5 min, this time at 37°C. Next, 20 ml of Roswell Park Memorial Institute medium (RPMI) containing 5% FCS was added and bacteria spun down. The bacteria were washed a further two times in sterile PBS. The supernatant was collected each time and spun down again to reduce the amount of HK *S. pneumoniae* lost during the spins. *CTV*: Heat killed *S. pneumoniae* were resuspended in 5 ml of sterile PBS containing 1 in 2500 dilution of CTV (Invitrogen) and incubated at 37°C for 30 min. Bacteria were spun down then resuspended in 5 ml PBS 5% FCS, and incubated at 37°C for 30 min. The bacteria were then washed twice in sterile PBS. As with the PKH26 spin steps, supernatant was collected each time and spun down again. *DAPI:* During the PKH26 and CTV labeling many of the bacteria were lost during the labeling process. Thus DAPI (Fisher) was used as an alternative due to fewer incubations and wash steps required. Heat killed *S. pneumoniae* were resuspended in 5 ml sterile PBS containing 1 in 5000 dilution of DAPI and incubated at room temperature for 5 min. The bacteria were then washed twice in sterile PBS

2.3.6 Intranasal administration of *S. pneumoniae*

Mice were anaesthetised in an anesthetic chamber using isoflurane (3%) at a flow rate of 2 liter/min. Fifty microliters of *S. pneumoniae* (alive or HK) in PBS (or PBS alone as a vehicle control) was administered onto the nostrils of the mouse. The mouse was held horizontal until all the liquid was inhaled and the mouse had regained consciousness. The mouse was then returned to the cage and observed until it had fully recovered.

2.4 Tissue and Sample collection

Blood: Exactly 100 µl of blood was taken from tail vein using a sodium heparinized glass hematocrit capillary (Hirschmann Laborgeräte). The blood was placed in a 1.5 ml Eppendorf that had been coated in heparin and contained 100 µl of heparin. This was put on ice. The mouse was then sacrificed straight after using CO_2, death confirmed by exsanguination after cutting the vena cava. This is a schedule 1 kill methodology as approved by the UK Home Office.

Bronchiolar lavage (BAL) fluid: After the mouse was S1K the neck was exposed and muscle trimmed away to expose the windpipe. Using forceps approximately 10 cm of cotton was pulled through underneath the windpipe. A small hole was made in the windpipe using a scalpel blade, a BAL tube was then placed into the windpipe and secured using the cotton. The BAL tube was made of a 2 cm length of 0.58 mm diameter (inner diameter) fine bore polythene tubing (Smiths Medical) with a 23-gauge needle inserted at one end. A 1 ml syringe containing 500µl of PBS 0.25% bovine serum albumin (BSA) was attached to the BAL tube and then the lungs inflated with the liquid. The rib cage was massaged before the liquid was removed using the syringe. The BAL fluid was collected in a 15 ml flacon tube. The lavage was repeated a total of four times giving approximately 2 ml of BAL fluid. This was placed on ice.

Lungs and LdLN: The vena cava was cut (if not already done) and chest cavity was opened. Five milliliters of PBS was injected into the right ventricle. This inflated the lungs and flushed out blood in the vasculature. At this point the LdLN was excised and placed in 500µl RPMI 2% FCS on ice. The lungs were then removed and placed in 2ml RPMI 2% FCS on ice.

2.5 Flow Cytometry

2.5.1 Sample preparation

Buffers:

- Red blood cell (RBC) lysis buffer; 0.15 M NH_4Cl, 1 mM $NaHCO_3$ and 0.1 mM ethylenediaminetetraacetic acid (EDTA).
- Fluorescence-activated cell sorting (FACS) buffer/wash; PBS 0.5% BSA, 2 mM EDTA.
- Digestion buffer; RPMI 2% FCS, 2.5 mg/ml Collagenase D and 1.7 µg/ml DNase I.

A wash step refers to the resuspension of cells in FACS wash, centrifugation at 300 g for 5 min at 4°C, then removal of the supernatant.

Blood: To lyse the RBCs 1 ml of RBC lysis buffer was added directly to the blood and resuspended, then incubated for 5 min at room temperature. Three hundred microliters of FACS wash added to the tube, then spun at 1500 rpm in the microfuge for 5 min. The leukocyte pellet was washed and resuspended in FACS wash, the cells were then pipetted into a V-bottom 96 well plate ready for antibody staining.

BAL fluid: Samples were spun down in a centrifuge for 5 min, 4 °C at 300 g. The supernatant was removed, then if needed RBCs lysed using RBC lysis buffer. BAL fluid cells were then washed, resuspended in FACS wash, then pipetted into a V-bottom 96 well plate.

Lungs: Lungs were diced in a petri dish using a scalpel, then transferred to a 15 ml falcon tube containing 2 ml of digest buffer and incubated at 37°C in a water bath for 30 min, vortexing every 10 min. At the end of the incubation the lung homogenate was poured into a 70 µm cell strainer in a petri dish and crushed using the end of a 2.5 ml syringe plunger. The strainer was then placed in the top of a 50 ml falcon tube, the lung cell suspension was passed through the strainer a second time, into the falcon tube. The cell suspension was washed then RBC lysis performed. The cells were then washed, resuspended in FACS wash and pipetted into a V-bottom 96 well plate.

LdLN: In a petri dish, in 500 µl of digestion buffer LdLNs were teased apart using forceps. The pieces of LdLN and digest buffer were then transferred into a 1.5 ml Eppendorf tube and incubated at 37°C for 10 min, whilst shaking at 1400 rpm. Five microliters of 0.5 M EDTA was added and the LdLN suspension resuspended thoroughly to break up any remaining pieces of tissue. If there were large undigested pieces left then the sample was incubated for a further 5 min at 37°C, shaking. The suspension was passed through a 70 µm cell strainer into a 15 ml falcon tube. The cells were washed, resuspended in FACS wash, and pipetted into a V-bottom 96 well plate.

2.5.2 Reactive oxygen species detection

Reactive oxygen species production by neutrophils was investigated by flow cytometry using dihydrorhodamine 123 (DHR 123, Invitrogen). Dihydrorhodamine 123 is non-fluorescent and cell permeable. Inside the cell it is oxidized by ROS to rhodamine 123, which is fluorescent. Neither NO, superoxide or hydrogen peroxide are able to do this, thus the effect is specific to ROS. After single cell suspension preparation, cells in the 96 well plates were resuspended in RPMI 2% FCS containing 5 µM DHR 123 (Invitrogen) and incubated at 37°C for 30 min. Cells were then washed twice and stained for surface markers. Care was taken to keep samples in the dark.

2.5.3 Surface marker antibody staining for flow cytometry

Flow cytometry staining was performed in a V-bottom 96 well plate. Cells were first resuspended in 100 µl Fc block mix made up in FACS wash and incubated for 10 min on ice (or at 4°C). The Fc block mix included TruStain fcX (rat anti-mouse CD16/32 antibody) used at a dilution of 1:200 (BioLegend) and rat IgG, 10 µg/ml (Sigma). Following the incubation the plate was spun for 5 min, 4 °C, 300 g and supernatant discarded. Cells were then resuspended in 100 µl of antibody staining master mix containing fluorescent labeled monoclonal antibodies

(mAbs) in FACS wash and incubated for 25-30 min on ice (or at 4°C) in the dark. Single stain controls were also prepared; samples were stained with a single mAb used in the master mix, at the same concentration used in the master mix. A list of all antibodies used is detailed in Table 2.2. Cells were washed twice, resuspended in 200 µl FACS wash and transferred into micro tubes (Titertube micro test tubes, Bio-Rad) then put on ice. The samples were run on a Beckmann Coulter CyAn ADP flow cytometer using the software Summit (Beckmann Coulter). Flow cytometry data was analysed using FlowJo (Treestar) software.

2.5.4 Live cell/dead cell discrimination

Following the first wash after antibody staining cells were resuspended in 100 µl of PBS containing DAPI (a 1:5000 dilution), then incubated for 5 min at room temperature in the dark. Cells were then washed and resuspended in 200 µl FACS wash and transferred into micro tubes and kept on ice. The samples were run on a Beckmann Coulter CyAn ADP flow cytometer with the acquisition boost turned off.

2.5.5 Calculating total cellularity using flow cytometry

Accucheck counting (Invitrogen) beads were used to calculate accurately total cellularity of samples. Following antibody staining pellets were resuspended in 100 µl FACS wash and transferred into micro tubes. Counting beads were mixed for 1 min using a Pasteur pipette to ensure beads were evenly resuspended, then, 100 µl of beads was added to each tube. The cell and bead suspension was resuspended thoroughly before running on the flow cytometer. The counting beads have very low forward scatter so during acquisition there was very low threshold applied (0.5%). Figure 2.2 shows the counting beads on a flow cytometry plot. To ensure accuracy the beads are made up of two types of beads that differ in their fluorescent intensity in the FL2 channel. The beads should be at an approximate 50:50 ratio for the calculated cell number to be accurate (the exact ratio and accepted limits of difference vary between lots). The right hand plot in Figure 2.2 demonstrates this. To calculate cell number beads were gated on, the cell population of interest, for example neutrophils, was also gated on to obtain the number of events acquired. The following calculation was then made:

$$\text{Number of cells per µl} = \frac{\text{Number of events (beads)}}{\text{Number of events}} \times \text{Number of beads per µl}$$

The number of beads per µl was provided on the information with the counting beads. The total cellularity could be calculated using the value of cells per µl and final volume of FACS wash that containing the cells.

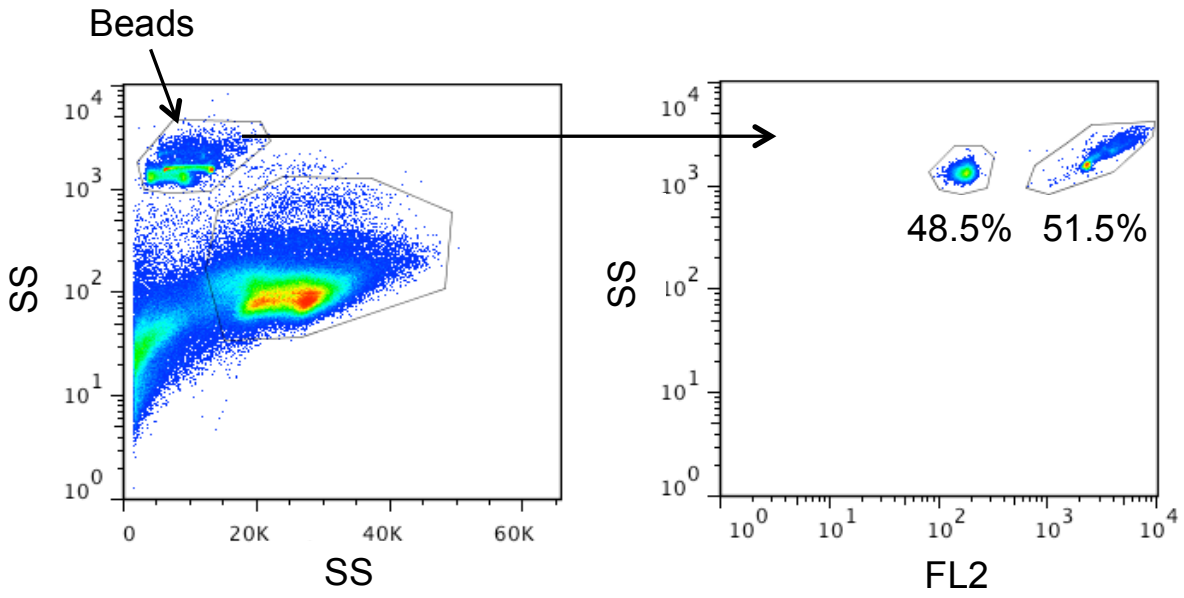

Figure 2.2: AccuCheck counting beads were used to calculate absolute cell number by flow cytometry.

Representative flow cytometry plots. AccuCheck counting beads were added to flow cytometry samples after staining. The beads had high side scatter (SS) and low forward scatter (FS), as shown in the plot on the left. The counting beads were made up of two sets of beads with different fluorescent intensities in the FL2 channel. The near 50:50 ratio of the beads indicated that they had been homogeneously mixed.

2.6 Cell sorting

Pure populations of neutrophils were obtained from blood, BAL fluid, lungs and LdLNs of *S. pneumoniae* infected mice using cell sorting. To ensure sufficient numbers of neutrophils were collected samples from 5-10 mice were pooled. Samples were processed and stained for flow cytometry as described in section 2.5; however the samples were not stained in a 96 well plate, but a 15 ml falcon tube. After staining the cells were resuspended at a density of 10^7 cells/ml in FACS wash and placed on ice. Cells were sorted into PBS 10% FCS using a Beckman Coulter MoFlo Astrios. A purity sort was performed, Figure 2.3 (A) shows the sorting strategy used. Following sorting an aliquot of sorted cells was run on the cell sorter to check the purity (Figure 2.3 B). Table 2.6 summarises the purity of each sample sorted.

Table 2.6: Purities of sorted neutrophils.

	Population purity (%)		
	Sample 1	Sample 2	Sample 3
Blood neutrophils	88	97	94
Lung neutrophils	96	Not done	96
BAL neutrophils	98	99	97
LdLN neutrophils	75	97	94

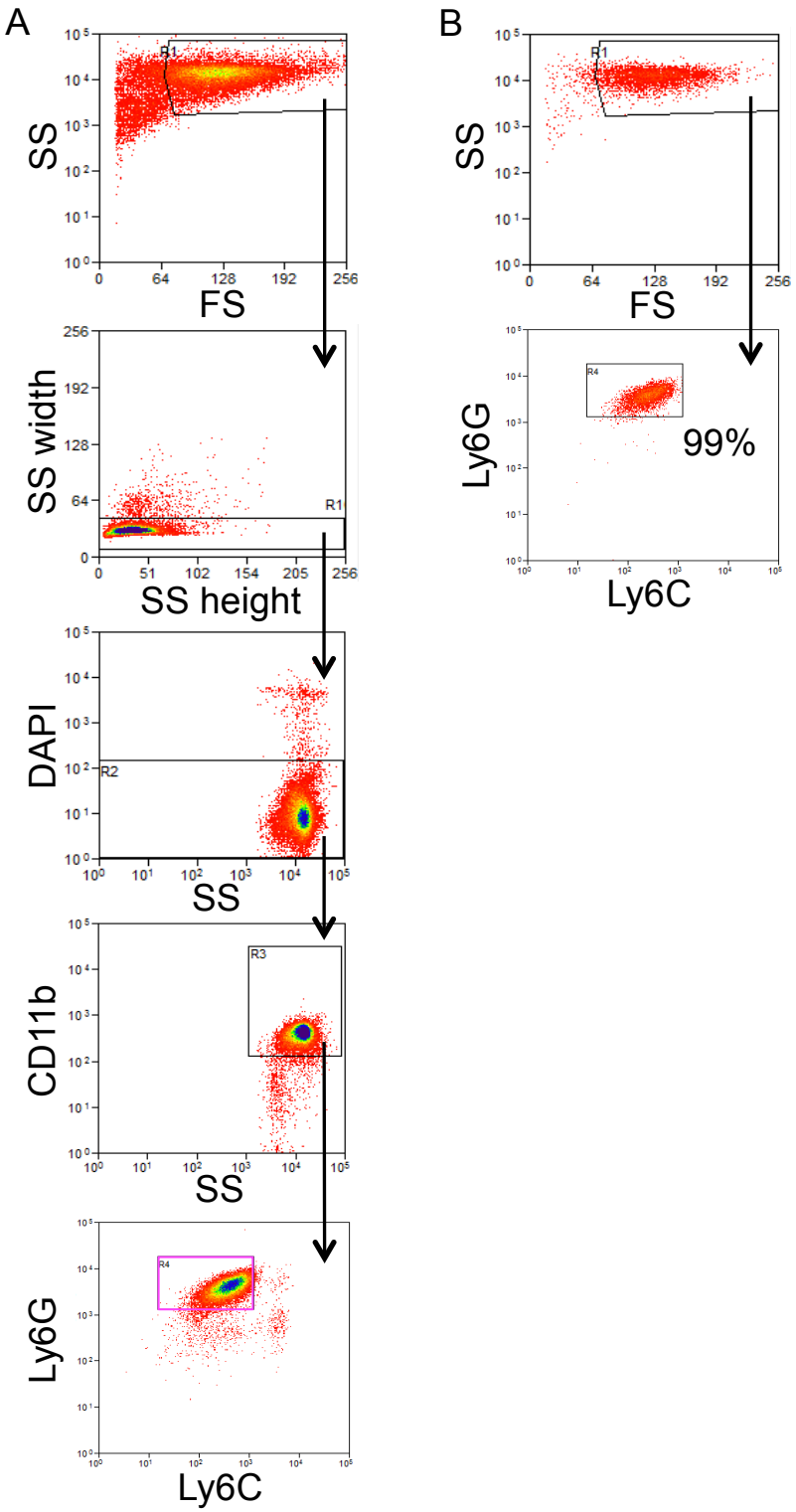

Figure 2.3: Cell sorting neutrophils using flow cytometry.

Representative flow cytometry sort plots. (A) Gating strategy used for cell sorting neutrophils, cells in the purple box were sorted. (B) Post-sort analysis of cells sorted in (A). A 99% pure neutrophil population had been sorted. Table 2.6 contains the purities of all populations sorted and used in Q-PCR experiments.

2.6.1 Giemsa staining

Sorted cells were spun down at 300 g for 10 min at 4 °C. The supernatant was removed and cells resuspended at a density of 10^5 cells in 30 µl. Thirty microlitre aliquots of each sample were placed on a poly-L-lysine coated microscope slide (VWR). The slide was then left to dry overnight. The cells were fixed using 100% methanol, methanol was dropped gently over the slides using a Pasteur pipette until the slide was covered. The methanol was then left to evaporate in the fume hood overnight. The slides were submerged in Giemsa stain (VWR), diluted 1 in 10 in dH_2O, and incubated at room temperature for 30 min. The Giemsa was washed off with water from a tap and slides left to dry before mounting coverslips using DPEX mounting medium (Sigma-Aldrich). The slides were imaged using a Zeiss light microscope. Images were processed using Volocity image analysis software (PerkinElmer).

2.7 Quantitative PCR

2.7.1 RNA extraction

Sorted cells were spun down at 300 g for 10 min at 4 °C. Supernatant was removed, taking care to remove as much as possible. The cells were then lysed using RLT buffer (Qiagen); the cells were resuspended in 350 µl RLT buffer, ensuring all the cells were resuspended. If the number of cells collected was less than 1×10^5 only 75 µl RLT buffer was used, however if 5×10^6 to 1×10^7 cells were collected 600 µl RLT buffer was used. The lysates were then stored at -20°C overnight. The next day RNA extraction was performed using an RNeasy mini kit (Qiagen) following the manufacturer's instructions. For the samples resuspended in 350 µl or more RLT buffer, lysates were first passed through a QIAshredder column (Qiagen). For the samples with low cell number ($< 1 \times 10^5$) the same RNA extraction protocol was followed, however spin columns from a miRNeasy micro kit (Qiagen) were used. This kit is designed for small cell numbers, with the final elution performed in a volume of 15 µl as opposed to 30 µl used for the RNeasy columns. Thus the RNA was less dilute. The quality and quantity of RNA was measured using a NanoDrop spectrophotometer, RNA samples were deemed suitable for use if the 260/230 nm ratio was above 1.8. Samples were then stored at -80°C

2.7.2 Complementary DNA synthesis

One microgram of RNA was diluted in nuclease free water to a final volume of 10 µl. In most samples the yield of RNA was low, less than 1 µg total, thus for these samples 10 µl of the RNA extract was used. The RNA was then mixed with 10 µl of a reverse transcriptase (RT) master mix made up of 4.2 µl H_20, 2 µl RT Buffer, 0.8 µl dNTP mix, 2 µl RT Random Primer and 1 µl

MultiScribe RT from a High Capacity cDNA Reverse Transcription Kit (Applied Biosystems). Samples were placed in a thermo cycler PCR machine for cDNA synthesis. The thermo cycling conditions were 10 min at 25°C, 120 min at 37°C, 5 min at 85°C, the machine then stayed at 4°C until samples were removed. At the end of the synthesis samples were made up to 100 µl with nuclease free water and stored at -20°C. Two batches of cDNA were made for each sample; these were pooled together for use in Q-PCR.

2.7.3 Primer design

Primers suitable for SYBR Green Q-PCR were designed using Primer BLAST software (NCBI) and ordered from Sigma. Primers were designed to span an exon-exon junction, in order to decrease the chance of genomic DNA amplification, have a melting temperature (T_m) of 60 °C ± 1, and have a resulting product length of 60-250 base pairs. Primers to *Ptgs2* were pre-designed by Sigma.

2.7.4 Primer testing

Primers were hydrated using nuclease free water to 100 nM concentration. A 10 nM aliquot of each primer was then made; this was the primer working stock. Primers were stored at -20°C. To test the optimum melting temperature (T_m) of the primers, and to check they were specific a gradient PCR was performed using GoTaq polymerase in green buffer (Promega). Following the PCR, products were run on a 2% agarose gel containing ethidium bromide. Single bands corresponding to the expected product length indicated that the primers were specific. Primers generating multiple PCR products were discarded. All primers worked optimally at T_m 60°C, except the *Ptgs2* primers, optimum T_m was 62°C. Table 2.5 lists the gene targets of the primers used and their sequences.

2.7.5 Q-PCR reaction

Power SYBR Green PCR Master Mix (Invitrogen) was used for Q-PCR. Each cDNA sample was run in triplicate. *Hprt* was used as the endogenous control gene, as all the Q-PCR reactions were completed over two days the plates were designed so that two genes were tested per plate, with *Hprt* only on one of the plates. The same machine, batch of nuclease-free water, primers and Power SYBR Green Master Mix was used to limit variation. Reactions using *Ptgs2* primers required a different T_m (62°C), thus were run on a separate plate with *Hprt* repeated, but at T_m 62°C. The Q-PCR mix was made up of 12.5 µl Power SYBR Green, 1 µl forward primer, 1 µl reverse primer, 6.5 µl nuclease free water and 3 µl cDNA and added to a MicroAmp Optical 96-well reaction plate (Applied Biosystems). Control samples of Q-PCR mix containing no cDNA,

or no RT samples were included in triplicate for each gene. The plate was loaded onto an Applied Biosystems 7300 real-time PCR machine and the Q-PCR reaction run. The reaction cycles were 2 min at 50°C, 10 min at 95°C, 15 sec at 95°C repeated 40 times, then 1 min at 60°C.

2.7.6 Q-PCR data analysis

Raw Ct values were used to calculate average Ct values and the standard deviation. Values for each gene tested were normalized to *Hprt* values for the same sample. This was done to try to avoid differences due to different quantities of cDNA in the samples. The values were then analysed to get the relative quantity (RQ) of mRNA transcripts for the genes of interest in BAL, lung and LdLN samples compared to blood neutrophil samples. To do this, the ΔΔCt values were calculated using one of the blood samples as a calibrator (sample 2 was used as it had most consistently the smallest standard deviation), then subtracting each samples ΔCt value from this. The fold change, or RQ was then calculated; $RQ= 2^{-\Delta\Delta Ct}$.

2.8 Immunohistochemistry

2.8.1 Tissue preparation and frozen sectioning

Lung draining lymph nodes were removed and placed in RPMI 2% FCS on ice. Using a dissecting microscope any pieces of fat or connective tissue were carefully removed, with care taken not to damage the LdLN. The tissue was then fixed by incubation in PBS 4% paraformaldehyde (PFA) at room temperature for 10 min, in the dark if the tissue contained fluorescent protein. Tissues were transferred to PBS 30% sucrose and incubated for at least 4 hours at 4°C, then in PBS 60% sucrose at 4°C overnight. The tissues were then embedded in optimal cutting temperature medium (OCT, Tissue-Tek, Sakura Finetek) on dry ice, wrapped in foil, then stored at -80°C. Optimal cutting temperature medium embedded tissue was sectioned using a cryostat. Six micrometer sections were cut and collected onto poly-L-lysine coated microscope slides. Sections were dried overnight, in the dark if necessary, then stored at -20°C.

2.8.2 Immunofluorescent staining of frozen tissue

Lung draining lymph node sections on poly-L-lysine coated microscope slides were removed from -20°C and brought to room temperature on the bench. If fluorescent protein was present the sections were kept in the dark thought the protocol. A circle was drawn around each section using a wax ImmEdge pen (Vector Laboratories), the sections were then hydrated and washed in PBS. Each wash step involved the slides being submerged in PBS for 15 min in total, with

changes of PBS ever 5 min. The sections were incubated in a blocking buffer of PBS 5% serum, at room temperature for 5 min. This was to prevent non-specific antibody staining. The serum of the host the secondary antibody was raised in was used; this was usually goat serum (Sigma). After blocking, sections were incubated in the primary antibody mix, made up in blocking buffer for 1 hour at room temperature. The slides were then washed. If needed, a further incubation with a secondary antibody was performed for 1 hour at room temperature. The slides were then washed and residual PBS removed using a tissue. A drop (approximately 10 µl per slide) of ProLong Gold (Invitrogen) was added to each section, then a No 1.5 glass coverslip (Fisher) mounted on top. The slides were incubated overnight at 4°C. The next day the slides were sealed using nail varnish. Stained slides were stored at 4°C. Images were processed using Volocity software (PerkinElmer). Tables 2.2 and 2.3 lists all antibodies used in frozen section staining.

2.8.3 Confocal microscopy

Immunofluorescent stained sections were imaged using the Zeiss LSM 710 confocal microscope on an Axio Observer.Z1 invert, and Zen software (Zeiss). The microscope had 5 lasers, 7 laser lines; 405, 458, 488, 514, 561, 594 and 633 nm. Positioning of the sample and area of interest was done using the 20x objective; image acquisition was performed using the 40x oil objective. In most experiments 4 laser lines were used and acquired individually, these were the 405, 488, 594 and 633 nm lines. Tile scans were performed to image the whole tissue. Images were processed using Volocity software.

2.9 Multiphoton explant imaging

2.9.1 Explant tissue preparation

The LdLN was removed and placed into warm (approximately 37°C) RPMI medium (medium contained no supplements). The fat and connective tissue was then removed from the LdLN using a dissecting microscope using ceramic coated forceps (Fine Scientific Tools), care was taken not to cause damage. The LdLN was placed in a No1.5 glass bottom petri dish (35 mm diameter, 10 mm glass diameter, MatTek) containing RPMI medium and a glass cover slip placed on top. The cover slip stopped the LdLN moving and helped reduce evaporation of the medium.

2.9.2 Multiphoton microscopy

The LdLN was imaged using the Chameleon pulsed Ti:Sa infrared multiphoton laser (Coherent) on a Zeiss 780 LSM, Axio Odserver.Z1 invert microscope, with 4 external non-descanned detectors (3 Gallium Arsenide (GsAs) PMTs) and Zen software (Zeiss). The microscope was fitted with a light tight incubation chamber set to 37°C. The 40x water dipping objective was used in every explant imaging experiment. The scan area imaged was 353.6 µm x 353.6 µm, frame size 512 x 512, averaging; 2, Z intervals of 3 µm, Z depth 18-30 µm. Images were acquired every 8-10 seconds, each imaging period was approximately 20-40 min, each LdLN was imaged for approximately 4 hours in total, until all of the LdLN had been covered. Table 2.7 lists all videos from explant imaging referred to in this thesis.

Table 2.7: List of explant imaging videos.

	Time Point (hours)	Intranasal treatment	Description	Scale (μm)
Video 1	6	HK unlabelled *S. pneumoniae*	Video shows all Z planes merged together.	9
Video 2	0	None		130
Video 3	19	PBS		25
Video 4	2	HK CTV labelled *S. pneumoniae*		28
Video 5	6	HK PKH26 labelled *S. pneumoniae*		25
Video 6	12	HK PKH26 labelled *S. pneumoniae*		27
Video 7	24	HK CTV labelled *S. pneumoniae*		27
Video 8	48	HK CTV labelled *S. pneumoniae*		31
Video 9	72	HK CTV labelled *S. pneumoniae*		31
Video 10	24	HK CTV labelled *S. pneumoniae*	Neutrophil interacting with macrophages.	18
Video 11	12	HK PKH26 labelled *S. pneumoniae*	Transient swarm.	14
Video 12	6	HK CTV labelled *S. pneumoniae*	Persistent swarm.	31
Video 13	6	HK PKH26 labelled *S. pneumoniae*	Persistent swarm.	16
Video 14	12	HK unlabelled *S. pneumoniae*	No inhibitor.	33
Video 15	12	HK unlabelled *S. pneumoniae*	10 μM Shionogi-12.	33
Video 16	6	10^8 CFU live *S. pneumoniae*	No inhibitor.	33
Video 17	6	10^8 CFU live *S. pneumoniae*	10 μM IC87114.	33
Video 18	15	HK unlabelled *S. pneumoniae*	No inhibitor.	33
Video 19	15	HK unlabelled *S. pneumoniae*	10 μM LY223982.	33
Video 20	13	HK PKH26 labelled *S. pneumoniae*	No inhibitor.	33
Video 21	13	HK PKH26 labelled *S. pneumoniae*	10 μM FTY720.	33
Video 22	6	HK unlabelled *S. pneumoniae*	No inhibitor.	33
Video 23	6	HK unlabelled *S. pneumoniae*	10 μM GSK143.	33
Video 24	12	HK unlabelled *S. pneumoniae*	No mAb.	33
Video 25	12	HK unlabelled *S. pneumoniae*	15 μg/ml M1/70.	33
Video 26	6	HK unlabelled *S. pneumoniae*	LdLN from B6.CD11c Cre x B6.Rosa26 mT/mG F1 mouse.	33

2.9.3 Investigating signalling pathways involved in neutrophil dynamics

Compounds and blocking antibodies to pathways involved in neutrophil migration were added to the explant culture medium. First the LdLN was imaged for 1 hour in RPMI medium, with images acquired from both medullary and subcapsular sinus regions of the LdLN. This provided a 'baseline' of neutrophil velocity and behaviors. The LN was then incubated at 37°C for 30 min in 1 ml of RPMI medium containing a compound or blocking antibody. The LdLN was then imaged in RPMI containing the compound of interest. The LdLN was imaged until the entire LN had been covered. Compounds used in explant imaging are found in Table 2.8.

Table 2.8: Chemical compounds.

Name	Description	MW	Supplier	Reference
FTY720	S1PR1,3-5 agonist	343.9	Caymen Chemical	Adachi *et al*[160]
Shionogi-12	PI3Kγ inhibitor	492.6	GSK	Patent WO2010/125799
GSK143	Syk inhibitor	342.4	GSK	Liddle *et al*[161]
IC87114	PI3Kδ inhibitor	397.4	Klaus Okkenhaug	Sadhu *et al*[162]
LY223982	BLT1 antagonist	502.6	Caymen Chemical	Gapinski *et al*[163]
S1P	Phospholipid	379.47	Sigma	

To test that compound was penetrating the LN samples were sent to GSK for liquid chromatography-tandem mass spectrometry analysis (LS-MS/MS). Lung draining lymph nodes were removed from mice that had received intranasal *S. pneumoniae*, 12 hour infection. The fat was trimmed off and the LdLN incubated in RPMI medium containing either 10 μM GSK G or IC87114, for 1 hour at 37°C. The LdLN was then removed from the medium, washed in PBS and weighed. Finally the LdLN was frozen at -20°C and sent to GSK (Stevenage) for LS-MS analysis. The media the LNs were incubated in was also frozen and sent for analysis. The results indicate that compounds could indeed penetrate the LN, both GSK143 and IC87114 were found in the LN tissue. Thus this methodology could be employed in *ex vivo* explant imaging.

Table 2.9: Liquid chromatography-tandem mass spectrometry (LC-MS/MS) results.

Compound	Nominal incubation concentration (μ M)	Measured media concentration (μ M)	LN concentration	Ratio (LN:Media)
IC87114	10	8.2	9.75*	1.15*
GSK143	10	5.86	81.7*	14*

*n=2

2.9.4 Image analysis

Videos were analysed using Volocity software. Individual neutrophils were manually tracked, for each neutrophil the centroid point was estimated and used for tracking. Neutrophils were

only tracked when they were distinguishable from other GFP^+ cells and other neutrophils. In each video as many neutrophils as possible were tracked, in videos with large numbers of neutrophils a minimum of 20 were tracked.

2.10 Cell culture

The human osteosarcoma cell line U2OS, expressing GFP-tagged S1PR1 was used to investigate S1PR1 internalisation in response to S1P and FTY720. The cell line was provided by GSK. Twenty thousand cells in 300 µl complete DMEM (containing 10% FCS, glutamine and penicillin and streptomycin) were added to each well of an 8 well, glass bottom (No 1.5) chamber slide (Fisher). The cells were then incubated for 48 hours at 37°C, 5% CO_2. The media was removed, cells washed with PBS, and 300 µl DMEM containing no FCS was added to each well. The cells were then incubated at 37°C, 5% CO_2 for a further 2 hours. This time allowed S1PR1 to be re-expressed at the cell surface. Foetal calf serum contains S1P; binding of S1P to S1PRs causes their internalisation. Thus to ensure S1PR1 was at the cell surface a period of serum starvation, that was not detrimental to the cell, was required. The media was then replaced with 300 µl DMEM (no FCS) containing 10 µM S1P (Sigma), 10 µM FTY720 (Caymen Chemical) or 1:100 dilution of acidified DMSO (5% 1M HCl; vehicle control). Cells were incubated for 1 hour, 37°C, 5% CO_2. The media was then removed and replaced with 20 µl of warm PBS containing 1:2000 dilution of CellMask Deep Red (Invitrogen) and incubated for 5 min at 37°C, 5% CO_2. The PBS was removed and replaced with warm PFA 4% and incubated for 10 min at 37°C, 5% CO_2. The cells were then washed three times with PBS and incubated with PBS containing 1:5000 dilution of DAPI (Invitrogen) for 5 min at room temperature. The DAPI was removed; cells washed three times, then 300 µl PBS left in the wells. The cells were imaged using the Zeiss LSM 710 confocal microscope.

2.11 $CD11c^+$ cell depletion using diphtheria toxin

In B6.CD11c Cre x B6.Rosa26 iDTR F1 mice, cells that express CD11c also express the primate diphtheria toxin receptor (DTR). Mice are insensitive to diphtheria toxin (DTx), however cells that express the primate receptor are highly sensitive and are thus depleted when DTx is administered[159]. One hundred nanograms of DTx (Sigma) in sterile PBS was administered intraperitoneal injections (i.p), control mice received sterile PBS only. In experiments using this model, mice received one dose of DTx, after 36 hours they were infected with *S. pneumoniae* (or PBS as a control), 12 hours later they were culled and tissues analysed by flow cytometry and immunohistochemistry.

2.12 Antibody mediated neutrophil depletion

In order to investigate neutrophil function antibody mediated depletion of neutrophils was performed using the Ly6G specific mAb, clone 1A8 (Bioxcel). Pilot experiments were completed to establish the correct does of antibody and time course of neutrophil depletion. Figure 2.4 shows an example of one pilot experiment. One mouse received 500 μg 1A8 i.p, another received 500 μg 1A8 i.p and 200 μg intranasal (i.n), and a control mouse received an isotype control mAb, 2A3, i.p. After 24 hours blood and lungs were removed and processed for flow cytometry as described in section 2.5. Figure 2.4 (A) shows that when analysing neutrophils using the surface marker Gr1 (neutrophils are Gr1 high), indeed after 1A8 mAb treatment neutrophils were depleted when compared to control 2A3 mAb treatment. However when looking at CD11b expression, neutrophils were visible by their distinct SS profile, Figure 2.4 (B). These neutrophils had reduced Gr1 expression. Gating on these cells revealed that indeed neutrophils weren't depleted; their percentage in 1A8 treated mice, in the blood and lungs, was not very different from 2A3 treated mice. In all pilot experiments neutrophil depletion was not achieved, thus experiments investigating neutrophil function by depletion of these cells were not conducted.

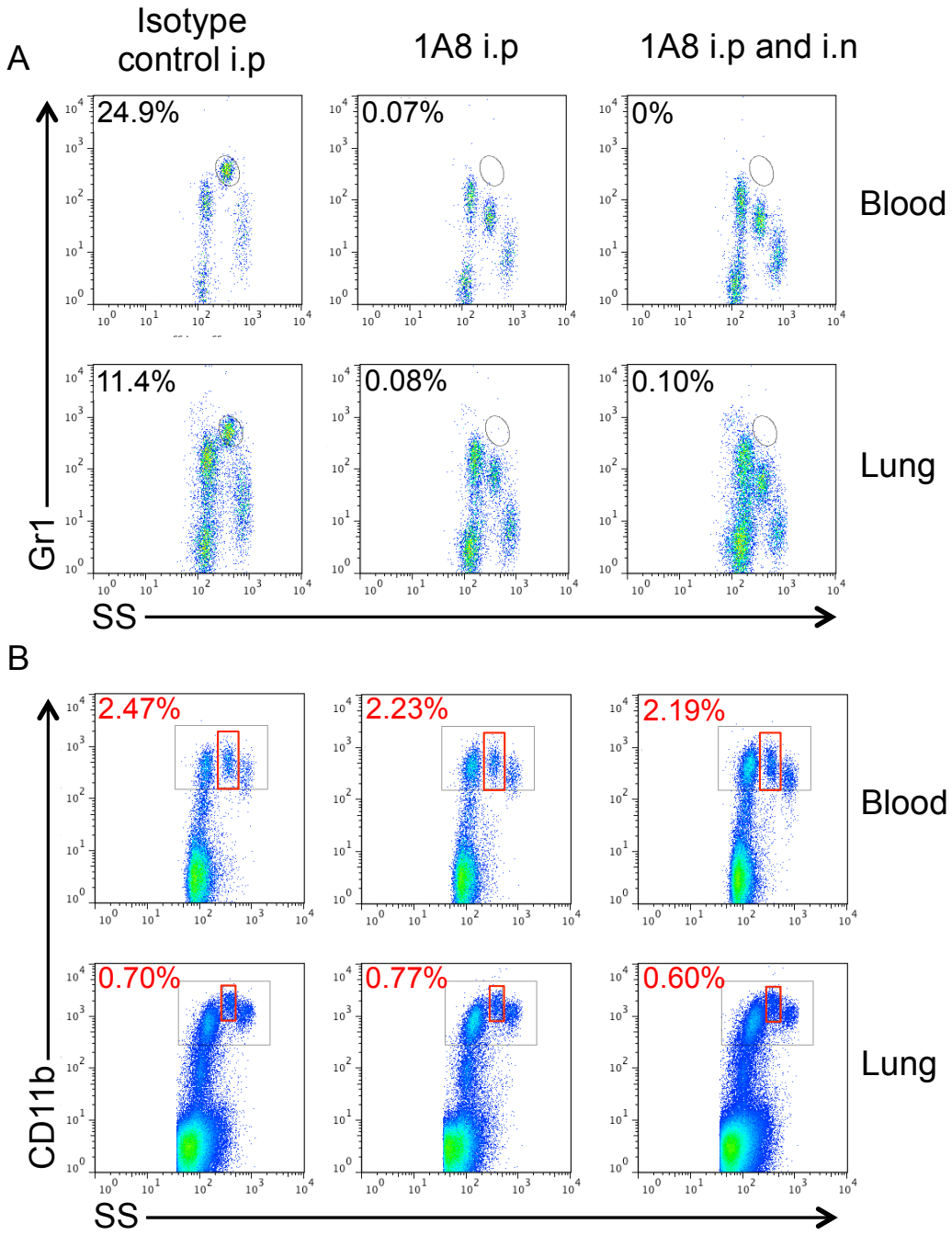

Figure 2.4: Neutrophil depletion was not achieved using the Ly6G specific 1A8 clone monoclonal antibody.

Mice received either 500 µg of isotype control (rat IgG2b) mAb i.p, or 500 µg anti-Ly6G (1A8) mAb i.p, or 500 µg of 1A8 mAb i.p and 200 µg 1A8 intranasal. After 24 hours blood and lungs were taken, processed and analysed by flow cytometry. (A) Flow plots gated on $CD11b^{+}$ cells. (B) Flow plots gated on all live cells, neutrophils could be identified by their expression of CD11b and SS (red boxes). 1A8 treatment did not deplete neutrophils but reduced their Gr1 expression. n=1, representative of 5 experiments.

2.13 Statistics

The software GraphPad Prism (GraphPad) was used for statistical analysis. The Kolmogorov-Smirnov test was used to test for a normal distribution. The Mann Whitney U test and Kruskal Wallis test, with Dunns post-hoc test were used to test for significance. No parametric tests were used due to either or a combination of; lack of normality, small sample size or uneven sample size. Data plotted on graphs have bars showing mean values and error bars showing standard error of the mean (SEM).

Chapter 3: Characterisation of neutrophils in the lung draining lymph node following acute pulmonary infection with *Streptococcus pneumoniae*

3.1 Neutrophils in secondary lymphoid organs

The role of neutrophils in modulating immune responses in secondary lymphoid organs is controversial. However, several recent publications provide evidence that neutrophils can traffic to the spleen and lymph nodes and contribute to adaptive immune responses.

3.1.1 B-helper neutrophils in the spleen

In the human, rhesus macaques and mouse, spleen B-helper (B_H) neutrophils have been described. Under homeostatic conditions neutrophils enter the spleen in response to microbial antigens that have been filtered from the blood after translocation from mucosal surfaces. This is not a classical inflammation driven process. Toll-like receptor signalling in splenic sinusoid endothelial cells (SEC) induces their production of IL-10 and neutrophil chemoattractants. When neutrophils cross the SEC wall this reprograms circulating neutrophils to become B_H neutrophils. Granulocyte macrophage colony-stimulating factor produced by splenic ILC3 cells is also involved in B_H neutrophil differentiation and activation[164]. These neutrophils localize to the splenic peri-marginal zone where they are close to marginal zone (MZ) B cells. B-helper neutrophils form NETs that interact with MZ B cells, they also produce BAFF, APRIL and IL-21 that induce MZ B cell somatic hypermutation, class-switch recombination, plasma cell differentiation and thus production of IgM, IgG and IgA. In addition to their MZ B cell activating capability they mediate T cell suppression in the spleen. Therefore B_H neutrophils potentiate extra-follicular B cell responses to TI antigens, and suppress follicular B cell TD responses thus minimizing inflammation[165].

3.1.2 Bacterial infection induced neutrophil recruitment to the tissue draining lymph node

Intradermal inoculation of *Mycobacterium bovis* bacille Calmette-Guérin (BCG) into the ear induces rapid migration of neutrophils to the dLN. Neutrophils are found as early as 4 hours, however after 24 hours they are no longer observed. Neutrophils localise in the SS and carry BCG. It is likely that the neutrophils migrate through the lymphatics, as neutrophils carrying BCG are observed in lymphatic vessels in the ear[166]. Similar neutrophil trafficking kinetics are found in other skin infections. Subcutaneous injection of *P. aeruginosa* in the footpad induces

rapid migration of neutrophils to the draining popliteal LN. Neutrophils are observed as early as 4 hours and intravital imaging reveals that they form dynamic swarms[33,139]. However, interestingly subcutaneous injection of *Salmonella typhimurium* in the footpad does not induce neutrophil migration to the dLN[139]. Thus some bacterial infections induce rapid migration of neutrophils to the dLN. Neutrophils are involved in early antigen transport to the dLN.

3.1.3 Parasitic infection induced neutrophil recruitment to the tissue draining lymph node

Parasitic infection induces similar LN neutrophil trafficking and behaviour as bacterial infections. Both skin (ear) and oral infection with *T. gondii* induces neutrophil recruitment to the dLNs where they localise in the SS. In the skin, dLN neutrophils are observed early; 1-5 hours after infection. Application of intravital microscopy shows that neutrophils form swarms. The swarms are either transient with less than 150 neutrophils rapidly migrating to the centre then dispersing, or persistent, involving more than 300 neutrophils recruited to the swarm, but not leaving it[36]. Skin (ear) inoculation with the nematode *N. brasiliensis* induces neutrophil migration to the dLN within 18 hours where neutrophils are located in the medulla, however no neutrophils are observed at 24 or 48 hours post infection. This migration is dependent on CCL2[167].

3.1.4 Chronic inflammation induced neutrophil recruitment to the tissue draining lymph node

In colitis, myeloid cells, including neutrophils accumulate in the gut where they contribute to tissue damage and disruption of the gut epithelia. In a model of bacterial driven T cell induced colitis, under non-colitic conditions; $CD4^{+}CD45RB^{low}$ T cells transferred into recombination-activating gene (RAG) deficient mice, there are very few neutrophils in the draining mesenteric LN. During colitis induced by transfer of $CD4^{+}CD45RB^{high}$ T cells into RAG deficient mice, there is a significant influx of neutrophils into mesenteric lymph nodes[168]. Interestingly these neutrophils, as well as colon neutrophils, express MHC II and ICAM-1, however blood and spleen neutrophils do not[168]. This disease model is thought to be driven by segmented filamentous bacteria in an IL-17 mediated process. IL-17 is a potent recruitment factor for neutrophils.

3.1.5 Vaccine and adjuvant induced neutrophil recruitment to the tissue draining lymph node

Multiple studies have demonstrated that immunisation results in neutrophil migration to the dLN. Immunisation with hen egg white lysozyme (HEL) in CFA into the footpad induces neutrophils to migrate to the dLN within 15 min, numbers peak after 2 hours and by 24 hours neutrophils are no longer found in the dLN. The neutrophils are found in the paracortical sinus and superficial cortex, similar to bacterial and parasitic infection[169]. In the same model, from the same group it was found that following this first acute influx of neutrophils, after 3 days of HEL/CFA immunisation a second wave of neutrophils arrive in the dLN. This second wave of neutrophils is more robust, greatly increased numbers are recruited and they persist until 18 days post-immunisation, they also localise to a different area; the cortex and medulla. The first wave of recruitment is dependent on prostaglandin-endoperoxide synthase (PTGS, also known as cyclooxygenase; COX-1 and -2) production of prostanoids, but not GPCR signalling, wave two depends on both prostanoids and GPCR signalling[170].

In a model of immunisation using an emulsion of OVA in CFA, one immunisation alone did not induce a robust recruitment of neutrophils, 3 doses of OVA/CFA over 30 days, followed by challenge with OVA labelled with fluorescein isothiocyanate (FITC) at day 40 was required to induce neutrophil influx into the dLN (popliteal). Like in the BCG infection, neutrophils carry antigen; OVA-FITC, to the dLN[171]. Complete Freund's adjuvant alone, during the priming immunisation can also induce neutrophil-dLN migration. As with bacterial infection, neutrophils accumulation is rapid, peaking at 6 hours post injection. In this model it was found that CCR7 is important for neutrophil-dLN migration; CCR7 knockout mice have reduced numbers of neutrophils infiltrating the dLN[172].

Other adjuvants aside from CFA also induce neutrophil migration to the tissue dLN. In combination with the adjuvant MF59 (oil-in-water emulsion) OVA induces rapid migration of neutrophils to the dLN, peaking at 3 hours and falling to near baseline levels at 17 hours. This is again an example of rapid neutrophil recruitment from tissues to LNs. Neutrophils are also found in the dLN carrying both the antigen and the adjuvant. However, interestingly this rapid recruitment is not observed using aluminium adjuvants (alum) in combination with OVA[173]. In unpublished data from our lab and others, it has also been found that alum does not induce neutrophil recruitment to tissue dLNs.

3.1.6 Neutrophil function in the tissue draining lymph node

Taken together, the studies outlined above all provide evidence that during inflammation neutrophils traffic to tissue dLNs and actively transport antigen to the dLN. This migration is often rapid, temporally and spatially separate from dendritic cells, with their localisation being in the LN sinuses rather than the paracortex of the lymph node. In cases where LN neutrophil influx is persistent, this might result from persistence of inflammation, in the case of colitis, or persistence of TLR stimulation in the case of HEL/CFA immunisation. There could be persistent antigen/adjuvant complex deposition in the injection site causing continued neutrophil recruitment, activation and subsequent trafficking to the dLN. However neutrophil-dLN migration is stimulus specific, *S. typhimurium* that induces systemic intracellular infection and the adjuvant alum do not induce their migration to the dLN. Alum, unlike CFA or MPL, does not activate TLRs[174]. Consistent with a role for TLRs in the process was the finding that in mice deficient of MyD88 adapter protein, a key component of TLR signalling and subsequent NF-κB activation, neutrophil recruitment to the dLN is significantly impaired[36].

Although there is some consensus across infection/inflammation models about recruitment kinetics, ability to transport antigen to the dLN, and their localisation in the LN, there has been no clear role found for neutrophils. Thus far only two studies have provided evidence for two potential functions of neutrophils in tissue dLNs. During immunisation with HEL/CFA neutrophils are proposed to be responsible for early T cell retention, in an S1P independent process. It is proposed that neutrophil derived thromboxane A2 limits the magnitude of the T cell response in the dLN, but also prevents T cell spread to distal LNs[170]. In a *P. aeruginosa* skin infection model, neutrophil depletion results in higher LN bacterial CFUs and also blood bacterial CFU. This indicates that neutrophils are involved in pathogen clearance in the dLN, thus preventing systemic spread[139]. However the neutrophil depletion would have also affected pathogen clearance from inflamed tissue by neutrophils, this effect was not investigated. Therefore the increased dLN and systemic bacterial spread could be partly due to failure to control the infection in the tissue, and not solely due to the absence of neutrophils in the dLN.[36]

3.1.7 Neutrophil heterogeneity

Various studies have identified neutrophils with different phenotypes in a range of settings, for example MHC II^+ ICAM-1^+ neutrophils in the colitic colon and ICAM-1^+ rTEM neutrophils in I-R injury. Other studies have detailed distinct neutrophil subsets; B-helper neutrophils in the spleen. There is some discussion as to whether bona fide subsets of neutrophils exist, or if they represent different activation profiles of neutrophils resulting from their specific tissue location and their surrounding cytokine milieu[175].

Infection of mice with *N. brasiliensis* third-stage larvae (L3) involves migration of the larvae from the skin to the lungs, then entry into the small intestine. The lung is an important site where the immune system interacts with the parasite larvae. Neutrophils recruited to the lung following L3 inoculation are found to polarize to a distinct, type 2 gene expression profile, characterized by increased gene expression of *IL13*, *IL33*, *Igf1*, *Retnla* and *Chi3l3*. These are termed 'N2' alternatively activated neutrophils, in line the with M2 macrophages. However inoculation through the same route with LPS polarized type 1 gene expression in lung neutrophils; *Il6* and *Il12b* are up-regulated in these 'N1' classically activated neutrophils. Compared to neutrophils from naïve mice, *N. brasiliensis* and LPS stimulated neutrophils similarly upregulate 153 genes, *Nos2* and *Tnf* being amongst the most upregulated genes. However, LPS stimulated neutrophils up-regulate 1,315 distinct genes, and *N. brasiliensis* neutrophils up-regulate 218 distinct genes. In addition to gene transcription differences, the neutrophils have different nuclear morphology; *N. brasiliensis* stimulated have band shaped nuclei, whereas LPS stimulated have classic lobed nuclei.

This phenotypic polarization is also observed in tumour models. Using two different tumor types and two different injection sites; flank and orthotopic, in three different mouse strains, tumor associated neutrophils polarise into N1 'anti-tumor' and N2 'pro-tumor' phenotypes. The cytokine transforming growth factor β (TGFβ) is responsible for this skew and favors N2 polarisation. As seen in the parasite infection, these different neutrophil phenotypes are also associated with distinct nuclear morphologies; N1 cells have hyper-segmented nuclei, however N2 cells have ring-shaped nuclei, similar, but not the same to band-shaped nuclei[176]. Thus, as seen in macrophage activation neutrophils can also polarize their response depending on the specific stimulus[63].

3.2 Summary

Neutrophils are capable of migrating to tissue draining secondary lymphoid organs. A clear function for them has yet to be found, however the current literature suggests that their role is stimulus and context dependent, rather than cell intrinsic. In various infection and inflammation models neutrophils have been found to have varying phenotypes including the expression of ICAM-1, MHC II and CD11c in some settings. Polarization to N1 or N2 phenotypes, characterised by distinct gene expression profiles and cytokine production has also been documented, however these phenotypes are highly stimulus and location dependent.

We hypothesised that in an acute pulmonary infection with the bacteria *S. pneumoniae* neutrophils would migrate to the LdLN where they have an important role in early events in the

initiation of immune responses. In addition to this neutrophils in the LdLN would be phenotypically different to lung and blood neutrophils, reflecting the change in their function; from pathogen clearance to a role in immune response modulation. The aim of this chapter was to investigate neutrophil recruitment to the LdLN following pulmonary infection with *S. pneumoniae.*

3.3 Aims

- Characterise the kinetics of neutrophil recruitment to the mediastinal LdLN.
- Establish the anatomical location of neutrophils within the LdLN.
- Compare LdLN neutrophils to circulating blood, lung and airway neutrophils using both surface phenotype and gene expression profile.

3.4 Results

3.4.1 Pulmonary infection with *S. pneumoniae* induced neutrophil recruitment to the LdLN

To investigate neutrophil recruitment to the LdLN in mice approximately 10^8 CFU *S. pneumoniae* or PBS (control) was delivered i.n. Exact CFU dose was determined using BHI agar plates, in all experiments between 10^7 - 10^8 CFU were administered. Lung dLN were then removed, digested and analysed by flow cytometry. To identify neutrophils a gating strategy was identified that permitted selective quantification of neutrophils but did not include other myeloid populations such as dendritic cells, macrophages and monocytes in the mediastinal LN (Figure 3.1). This grating strategy was then applied in all other tissues investigated in subsequent experiments. Following doublet exclusion live cells were gated on by excluding DAPI positive cells. The cells were then distinguished from cellular debris based on their FS and SS profiles. To identify myeloid lineages $CD11b^+$ (high) cells were gated on, then the Ly6C fluorescence intensity of these cells was plotted against the Ly6G fluorescence intensity. Neutrophils were identified as being $Ly6C^{int}$ and $Ly6G^+$ (Figure 3.1 A). In naïve, PBS treated mice only a small $Ly6C^-$ and $Ly6G^-$ population of cells was visible, with a few rare neutrophils observed. In the inflamed LdLN a population of neutrophils was clearly visible, as well as a population of $Ly6C^{hi}$ $Ly6G^-$ cells. Cell sorting of the $Ly6C^{int}$ $Ly6G^+$ population, followed by Giemsa staining confirmed that these cells were neutrophils, as demonstrated by the characteristic lobed nuclear morphology. The $Ly6C^{hi}$ $Ly6G^-$ cells resembled monocytes due to their expression of Ly6C, CX3CR1, F4/80, also low MHC II and CD11c expression[177-179], indicating they had not yet differentiated into dendritic cells. Thus using this gating strategy we could quantify and isolate different myeloid populations in tissue dLNs post infection with *S. pneumoniae*.

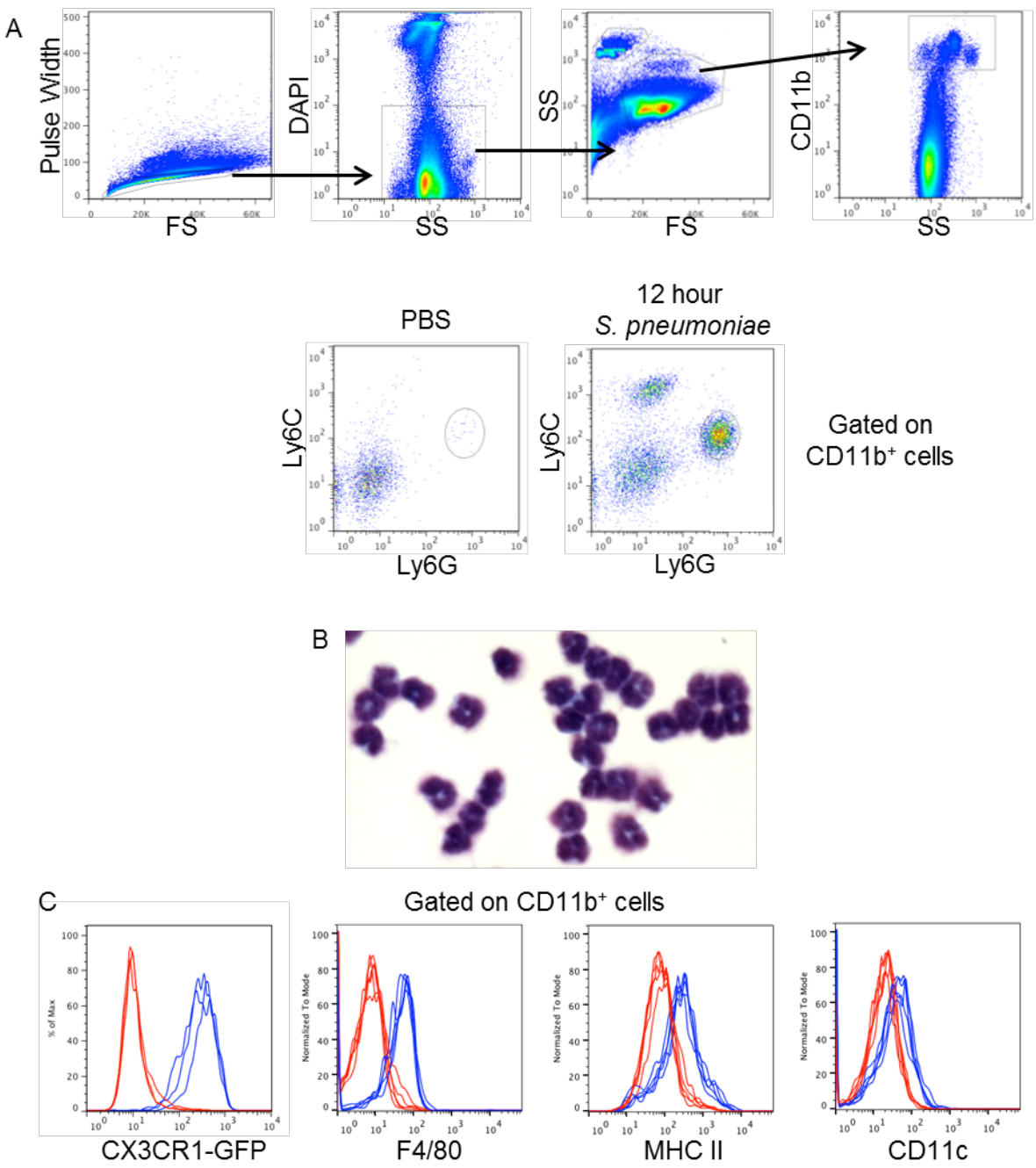

Figure 3.1: Pulmonary infection with *S. pneumoniae* induced neutrophil recruitment to the LdLN

(A) Representative plots showing the flow cytometry gating strategy. Neutrophils were identified as CD11b^{+} Ly6C^{int} Ly6G^{+} cells. Very few neutrophils were found in LdLN of mice that received PBS i.n. Neutrophils were found in the LdLN at 12 hours of pulmonary *S. pneumoniae* infection. (B) Sorted CD11b^{+} Ly6C^{int} Ly6G^{+} cells had lobed nuclear morphology. (C) Histogram overlays of Ly6C^{int} Ly6G^{+} neutrophils (red) and Ly6C^{+} Ly6G^{-} inflammatory monocytes (blue).

3.4.2 Formation of neutrophil:monocyte pairs

One surprising observation was the presence of very specific cell doublets as shown by doublet exclusion (Figure 3.2). In the top panel a very tight single pulse width gate is set leading to very clear $Ly6C^{hi}$ $Ly6G^{-}$ (monocyte) and $Ly6C^{int}$ $Ly6G^{+}$ (neutrophil) populations. However, if the gate set for doublet exclusion was not tight enough a population of $Ly6C^{hi}$ $Ly6G^{+}$ cells was observed. This was also seen in the lung, BAL fluid and to a lesser extent in the blood. These cells arose from the small population identified by an arrow in the bottom left plot in Figure 3.2. These cells were sorted, then an aliquot run on the flow cytometer for a post sort purity test (Figure 3.3 A). Two populations were observed when pulse width was plotted against FS; single cells and doublets. The single cells were a near 1:1 ratio of neutrophils to monocytes. No $Ly6C^{hi}$ $Ly6G^{+}$ cells were found. $Ly6C^{hi}$ $Ly6G^{+}$ events fell in the higher pulse width gate and were doublets. The sorted $Ly6C^{hi}$ $Ly6G^{+}$ cells were Giemsa stained and clear neutrophil monocyte pairs were observed (Figure 3.3 B). Approximately 50% of the pairs remained intact after cell sorting and therefore must have been tightly bound to each other.

As a result of this observation when investigating monocytes and neutrophils strict doublet exclusion was utilized in all experiments. It is however interesting that neutrophils and monocytes formed such tight interactions, interactions that survived tissue digestion, multiple rounds of cell resuspension and finally passing through a cell sorter. This could be simply down to cells attaching together during tissue processing. Alternatively these interactions could have been formed *in vivo*, for example as part of the process of efferocytosis by which apoptotic cells are phagocytosed. The images acquired from Giemsa staining are low quality so it is not clear, however in the synapse between the two cells *S. pneumoniae* was found in some of the pairs.

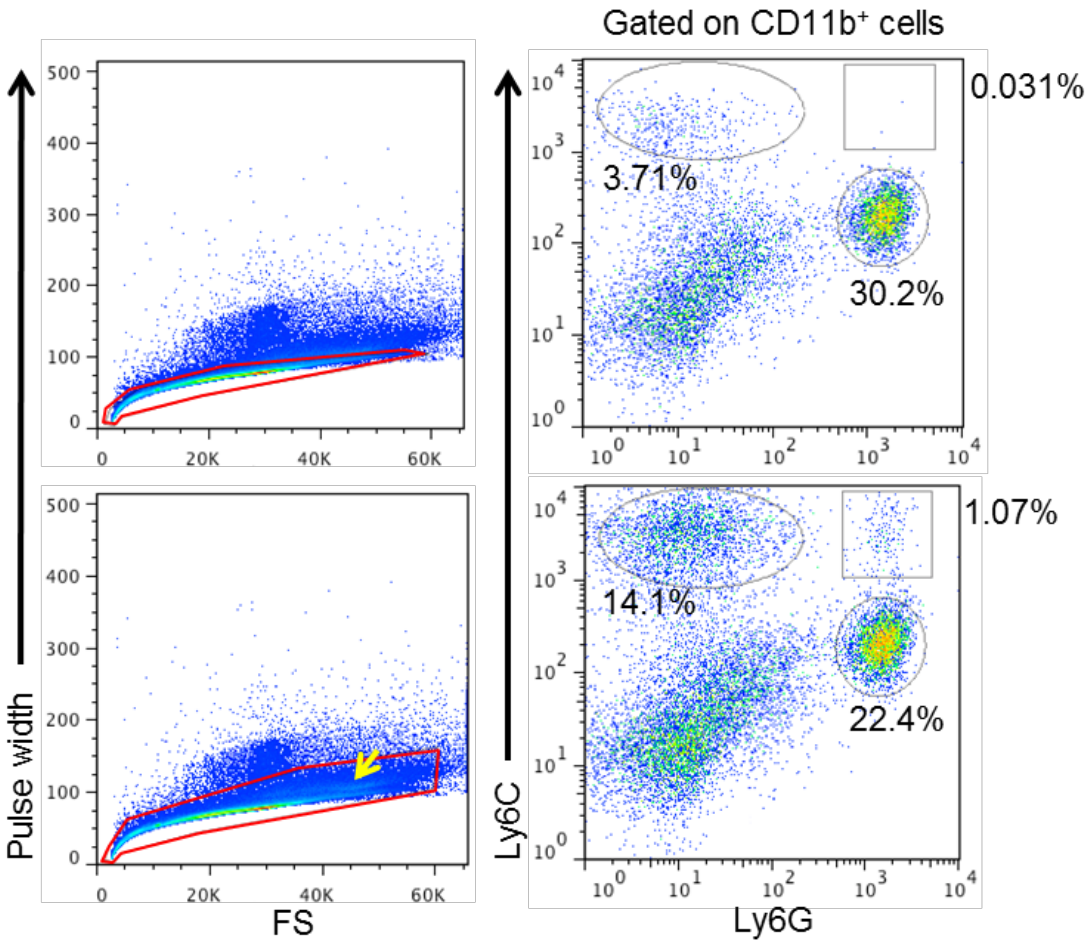

Figure 3.2: CD11b^{+} Ly6C^{hi} Ly6G^{+} cells in the LdLN following pulmonary *S. pneumoniae* infection.

Top row; tight pulse width gate (red). Bottom row; larger pulse width gate (red). Using the larger pulse width gate resulted in the appearance of a Ly6C^{hi} Ly6G^{+}cell population, arising from the population marked by the yellow arrow. 12 hour *S. pneumoniae* infection, representative plots of all flow cytometry experiments.

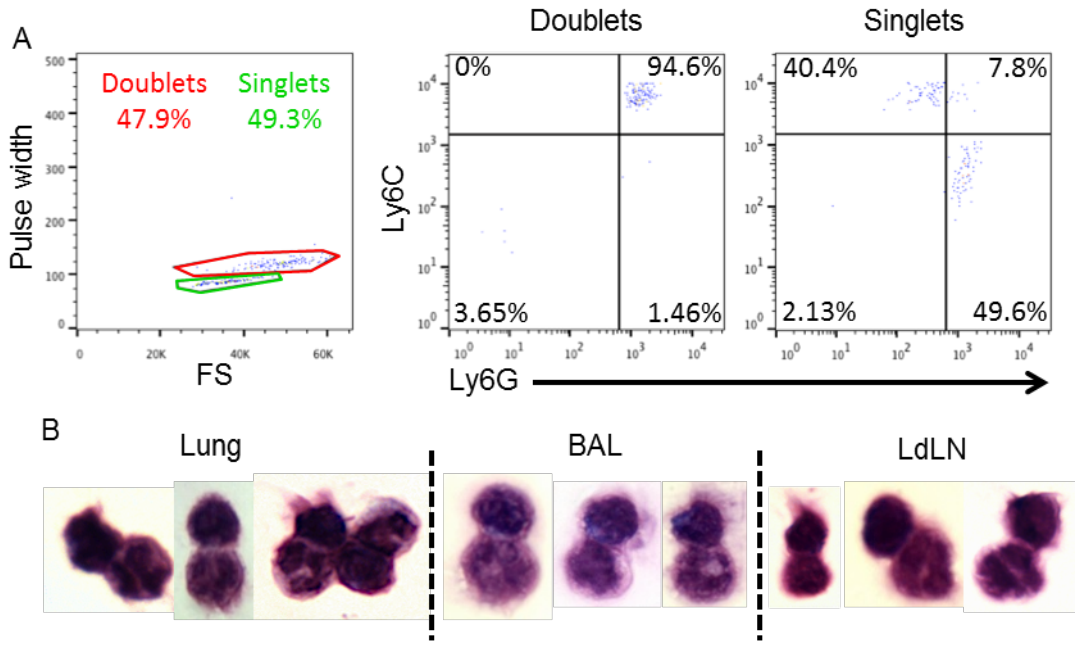

Figure 3.3: CD11b^{+} Ly6C^{hi} Ly6G^{+} cells were neutrophil-monocyte doublets.

(A) Post sort flow cytometric analysis of CD11b^{+} Ly6C^{+} Ly6G^{+} cells sorted from the lung at 12 hours of pulmonary *S. pneumoniae* infection. CD11b^{+} Ly6C^{+} Ly6G^{+} cells were doublets of Ly6C^{int} Ly6G^{+} neutrophils and Ly6C^{+} Ly6G^{-} monocytes. (B) Sorted CD11b^{+} Ly6C^{+} Ly6G^{+} doublets from the lung, BAL and LdLN stained with Giemsa. The doublets were pairs of neutrophils and monocytes.

3.4.3 Pulmonary infection with *S. pneumoniae* induced early neutrophil recruitment to the LdLN

Following identification of neutrophils in the LdLN during pulmonary *S. pneumoniae* infection the kinetics of neutrophil recruitment to the LdLN was investigated. Mice were infected at -72, -48, -24, -12, -6, and -2 hours with the same batch of *S. pneumoniae* culture. At time zero LdLNs were collected, digested and neutrophil numbers were analysed by flow cytometry using AccuCheck counting beads. Figure 3.4 (A) shows an early peak of neutrophil recruitment. Neutrophils were observed as early as 2 hours post infection, with numbers peaking at 6-12 hours. By 24 hours neutrophil numbers had reduced back down, they stayed low at 48 and 72 hours, however they didn't reduce back down to baseline levels seen in naïve mice (time zero). This early peak of neutrophil recruitment preceded the influx of other MHC II^{hi} cells. Figure 3.4 (B) shows that influx of MHC II^{+} $CD11c^{+}$ cells occurs at 24 hours, when the peak of neutrophil recruitment had fallen. Thus neutrophils were recruited early to the LdLN in pulmonary *S. pneumoniae* infection, preceding the influx of other responding immune cells.

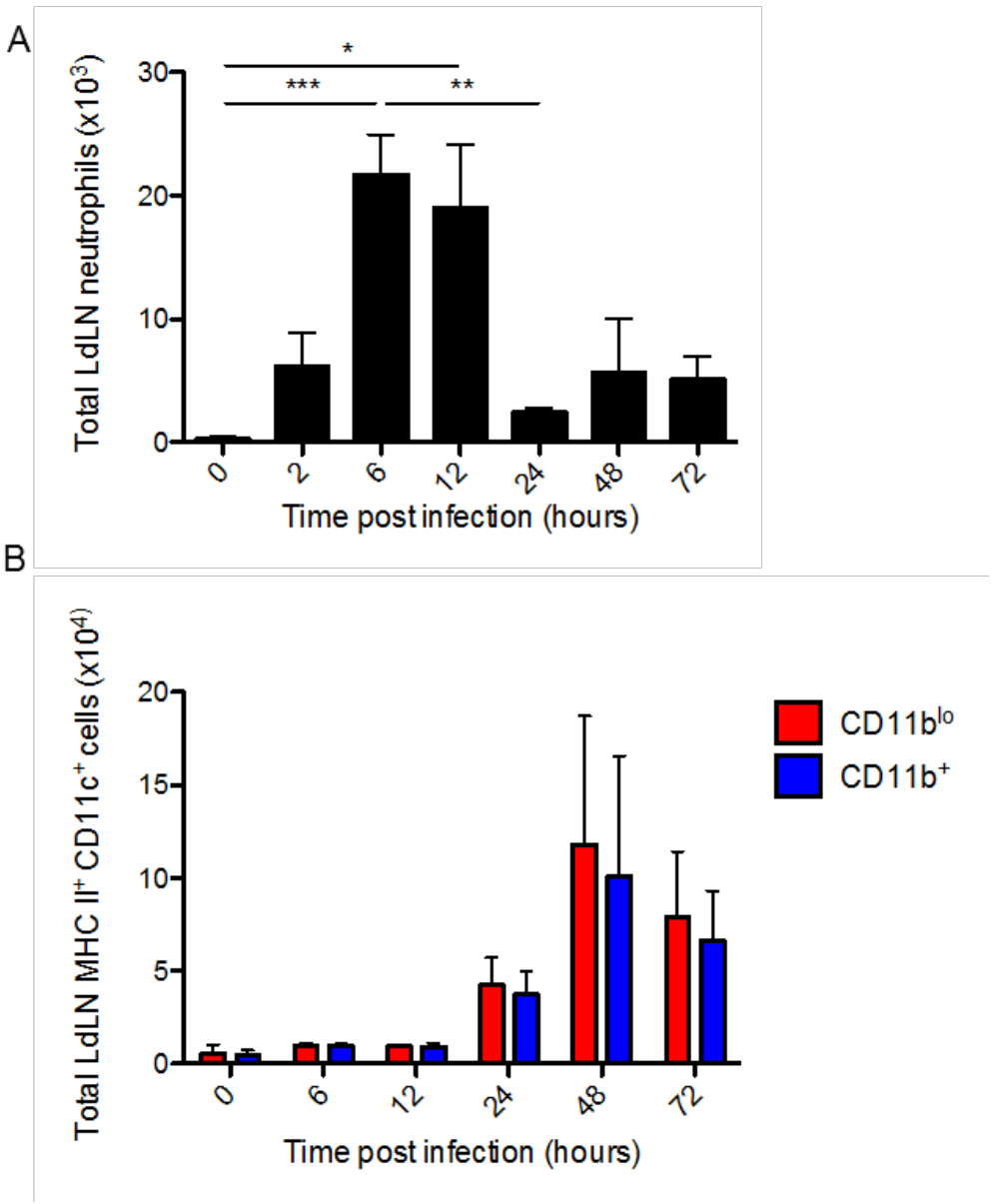

Figure 3.4: Pulmonary infection with *S. pneumonie* induced early neutrophil recruitment to the LdLN.

(A) Total neutrophil numbers in the LdLN at 0, 2, 6, 12, 24, 48 and 72 hours post pulmonary *S. pneumoniae* infection. Gated on $CD11b^{+}$ $Ly6C^{int}$ $Ly6G^{+}$ cells, pooled data from three experiments, n= 3-8. (B) Total $CD11c^{+}$ $CD11b^{+/lo}$ cell numbers in the LdLN. Gated on MHC II^{+} cells. Neutrophil numbers peaked early, preceding the influx of responding MHC II^{+} cells. Pooled data from two experiments, n= 3-5. Bars represent mean + SEM, * $P<0.05$, ** $P<0.01$ *** $P<0.001$ (Kruskal-Wallis test with Dunn's post hoc test).

3.4.4 Investigating neutrophil localisation within the LdLN following pulmonary infection with *S. pneumoniae*

In the highly organized structure of the LN, cellular location can in part determine function through localized cytokine and chemokine gradients, and other cell types sharing the niche. Thus frozen sections of LdLNs were stained to identify where neutrophils were situated. The surface markers Ly6G; neutrophils, lymphatic vessel endothelial hyaluronan receptor 1 (Lyve-1); lymphatic vessels and PNAd (MECA-79); HEVs, were used to identify these cell populations.

In the naïve LdLN (Figure 3.5 A), as observed in flow cytometry samples, very few neutrophils were observed. The few that were found were located within or near HEVs. This could indicate that these cells were not in the LdLN tissue, but rather in vessels, moving through the LN microvasculature. In LdLN from mice taken at 6 hours of pulmonary *S. pneumoniae* infection neutrophils were found mainly in lymphatic regions of the LdLN, with some in HEVs (Figure 3.5 B). The neutrophils were not in the cortex of the LN in the T cell zone, or in areas were the B cell follicles are located (Figure 3.6). This was representative of 12 and 24 hours of infection. Thus this area of the LN was further investigated.

Analysis of the sections from infected LdLN (Figure 3.7 A) showed that neutrophils were found to populate the lymphatic areas which contained $CD169^+$ macrophages with a round morphology. Staining on a serial section revealed that the $CD169^+$ macrophages were also SIGN-$R1^+$, neutrophils were closely located to these cells. Figure 3.7 (C) and (D) show that these round $CD169^+$ macrophages were indeed SIGN-$R1^+$ and $F4/80^+$ MSM. Thus neutrophils were found exclusively in lymphatic areas of the LdLN, densely populating the medullary sinus, in close proximity to MSMs.

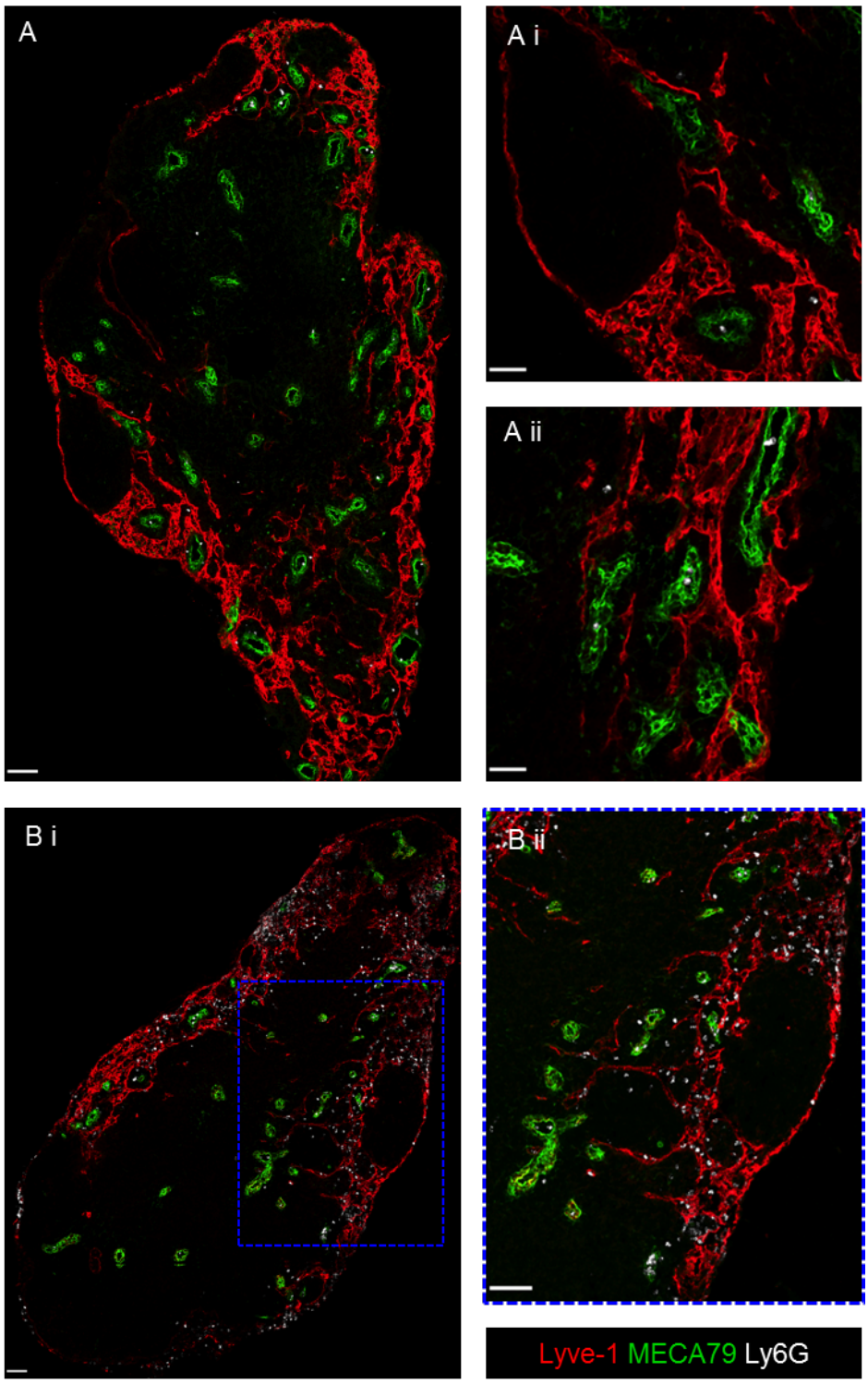

Figure 3.5: Neutrophils localised to the lymphatic sinus in the LdLN following pulmonary infection with *S. pneumoniae*.

Immunohistochemistry of frozen sections stained for lymphatics (lyve-1; red), HEVs (MECA79; green) and neutrophils (ly6G; white). (A) In naïve LdLN few neutrophils were found. Scale bars; A i= 70µm, A ii and iii= 35 µm. (B) At 6 hours of infection neutrophils in the LdLN were found in lymphatic areas. Scale bars; B i= 60 µm and B ii= 70 µm.

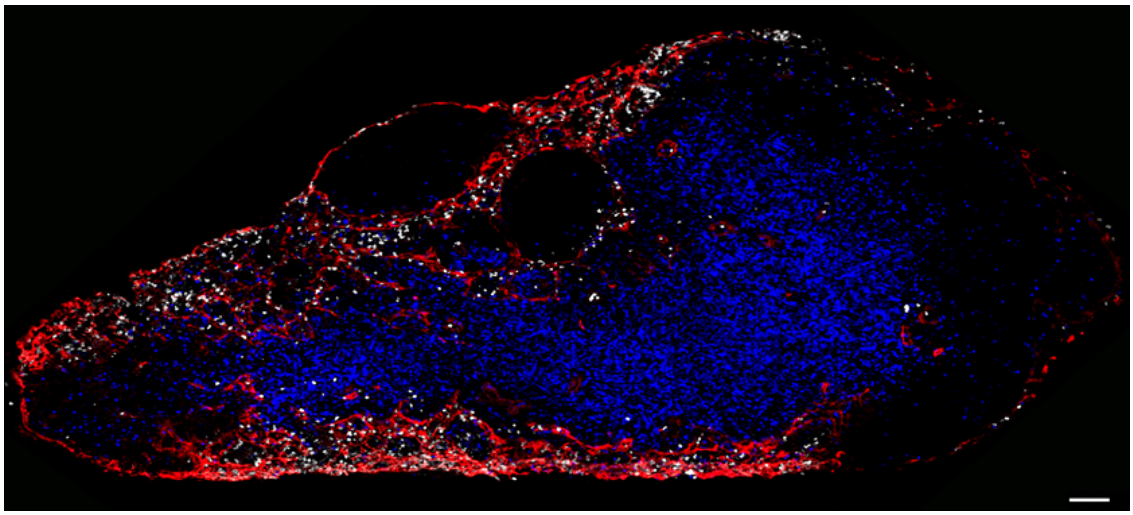

Figure 3.6: Neutrophils localised to the lymphatic sinus and not the T cell zone in the LdLN following pulmonary infection with *S. pneumoniae*.

Immunohistochemistry of a frozen section from the LdLN of a B6.hCD2-DsRed.B mouse. In this mouse strain T cells express the fluorescent protein DsRed (blue in the image). The section was stained for lymphatics (lyve-1; red) and neutrophils (Ly6G; white). At 6 hours of infection neutrophils in the LdLN were found in lymphatic areas, not in T cell areas or areas where B cell follicles are located. Scale bar= 70 μm.

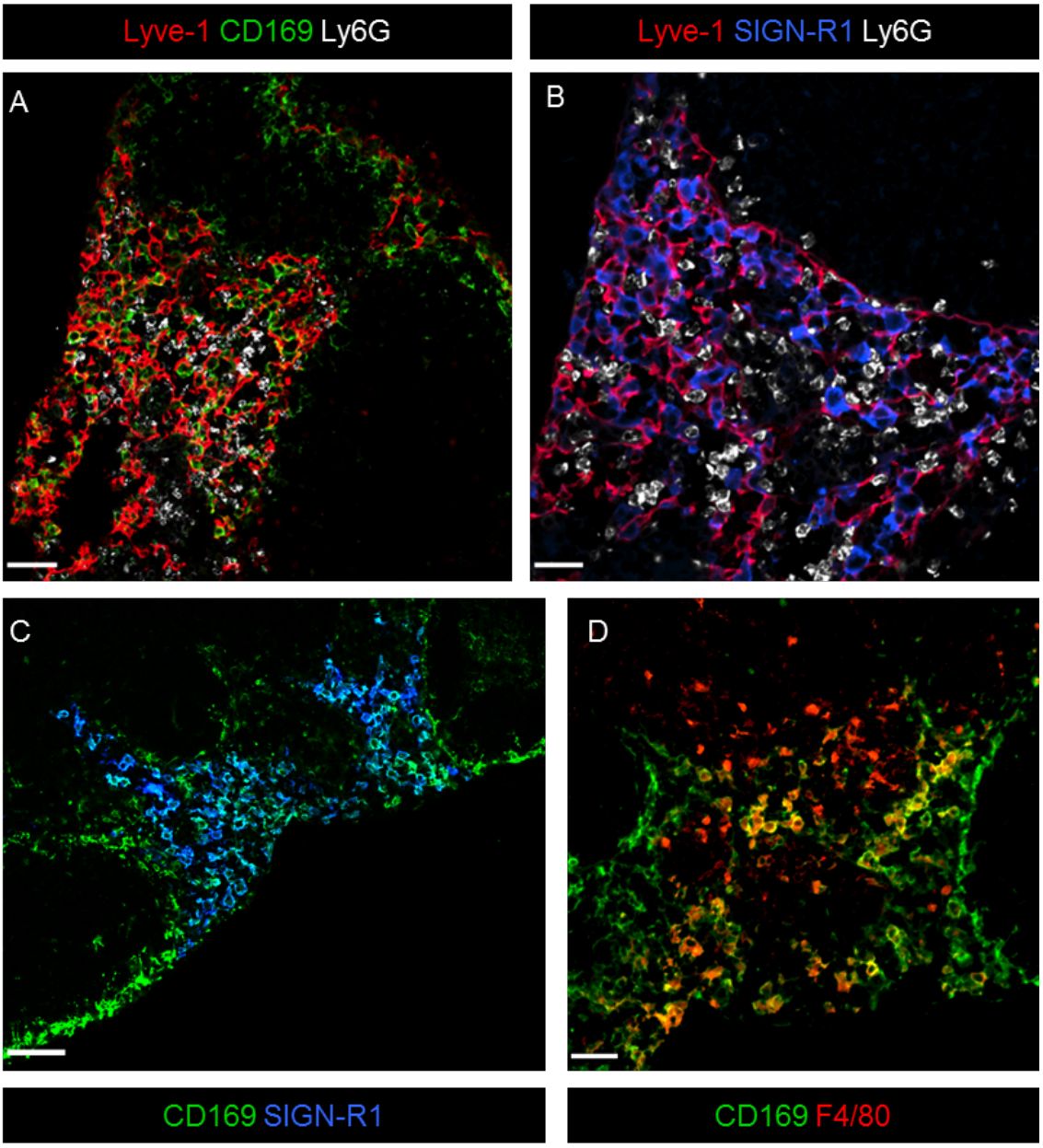

Figure 3.7: Neutrophils in the LdLN were located in close vicinity to medullary sinus macrophages following pulmonary infection with *S. pneumoniae*

Immunohistochemistry of frozen sections stained for lymphatics (Lyve-1; red), neutrophils (Ly6G; white) and LN macrophages (CD169; green). (A) At 12 hours of infection neutrophils were located in lymphatic areas close to $CD169^+$ macrophages. Scale bar= 42 µm. These macrophages were SIGN-$R1^+$ (B) and had a rounder morphology than other $CD169^+$ macrophages thus were MSMs. Scale bar= 24 µm. MSM were $CD169^+$ SIGN-$R1^+$ (C) and $F4/80^+$ (D), SSMs were SIGN-$R1^-$ $F4/80^-$ with dendrite-like structures. Scale bars C= 70 µm, D= 47 µm.

3.4.5 Neutrophils in the circulation, lung, alveolar space and LdLN had different activation states during pulmonary infection with *S. pneumoniae*

The phenotype and activation state of neutrophils in the LdLN was next investigated with the aim of identifying if these cells resembled neutrophils in the circulation or lung. Circulating blood, lung tissue, airway (from BAL fluid) and LdLN neutrophils were compared at 12 hours of *S. pneumoniae* infection. This time point was selected as it is when neutrophil numbers peaked in the LdLN. Flow cytometry and Q-PCR was used to investigate the following markers of neutrophil activation; CD11b, ICAM-1, ROS production, *Tnf* and *Ifng* gene expression. Lung dLN neutrophils had the highest mean (median) fluorescence intensity (MFI) for CD11b, almost 3.5 times higher than blood neutrophils, and over 1.5 times higher than lung and BAL fluid neutrophils (Figure 3.8 A). Few ICAM-1^+ neutrophils were found in the blood (5% ± 0.3 SEM were ICAM-1^+), however a high percentage of lung (90% ± 2), BAL (86% ± 2) and LdLN neutrophils (75% ± 2) were ICAM-1^+. When looking at ICAM-1 MFI, BAL fluid and Lung neutrophils had the highest MFI whereas LdLN neutrophils had an approximately 3 fold lower MFI (Figure 3.8 B). Reactive oxygen species production was assessed by flow cytometry using DHR 123. As compared to the blood (14% ± 1), a high percentage of lung (71% ± 2), BAL (84% ± 3) and LdLN (67% ± 4) neutrophils were positive for ROS. The highest percentage of ROS^+ neutrophils were found in the BAL fluid, these also had the highest MFI. Similar percentages of ROS^+ neutrophils were found in the Lung and LdLN, these cells also had similar ROS MFI (Figure 3.8 C).

Neutrophils were sorted from the blood, lung, BAL fluid and LdLN of mice at 12 hours of *S. pneumoniae* infection. Three separate experiments to sort neutrophils were performed, with 5-10 mice pooled for each experiment. The same gating strategy was employed as in flow cytometry experiments, RNA was extracted from these cells and Q-PCR performed. The relative quantity (RQ) of mRNA in blood, lung, BAL and LdLN neutrophils was calculated. One of the blood replicate samples was used as the calibrator, thus the RQ of all other samples was calculated relative to the mRNA in that sample.

Neutrophils in the BAL fluid had the highest amount of *Tnf* mRNA. Lung and LdLN showed similar levels of *Tnf* expression, higher than blood, however approximately half that of BAL neutrophils (Figure 3.8 D). *Ifng* mRNA was also most highly expressed in BAL neutrophils. Lung neutrophils had less *Ifng* mRNA than BAL neutrophils, but 2-fold more that LdLN neutrophils. Lung dLN neutrophils had 2-fold more *Ifng* mRNA than blood neutrophils (Figure 3.8 D). Thus, neutrophils in the circulation, lung tissue, airways and LdLN showed distinct activation states based on expression of known markers of neutrophil priming and activation.

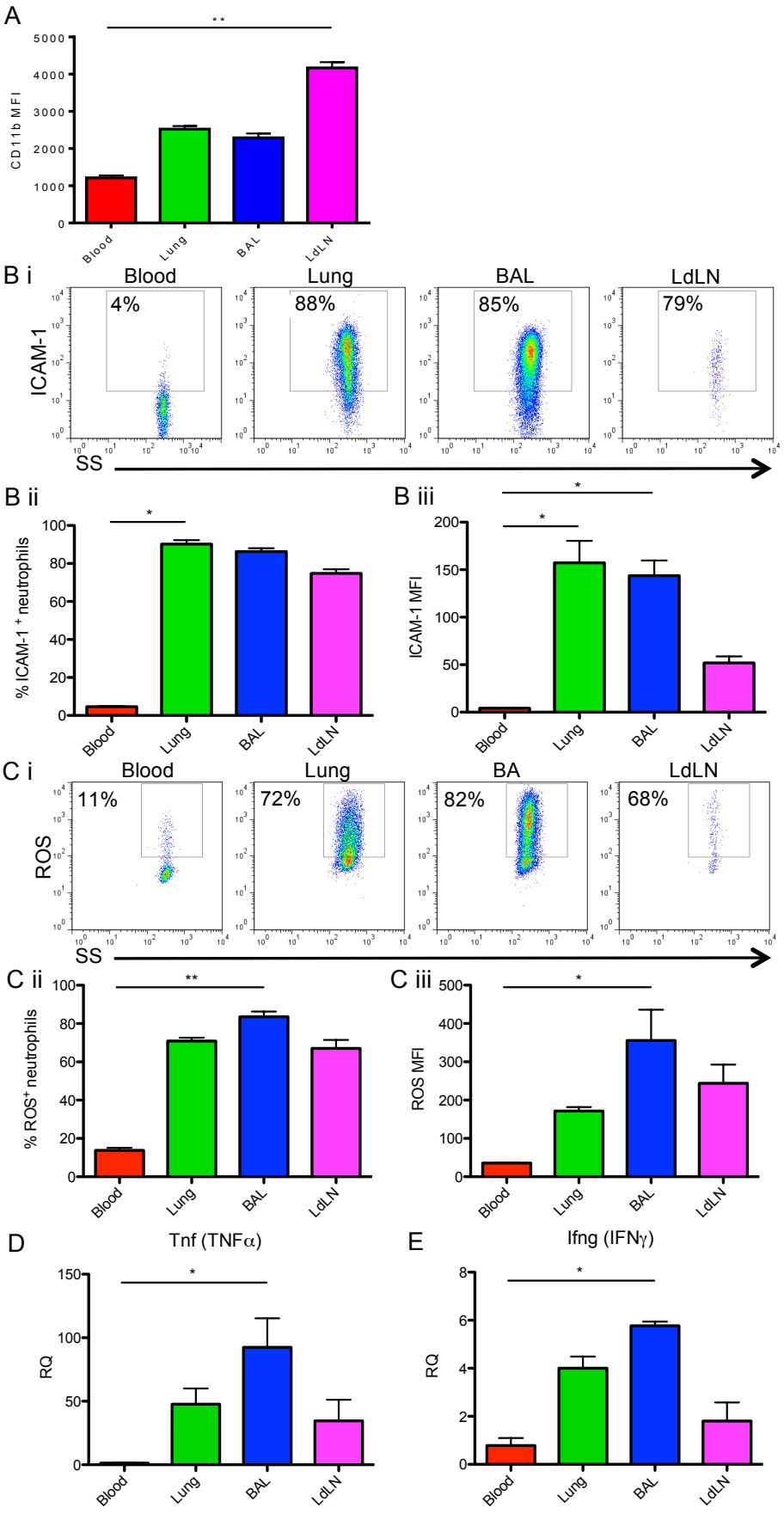

Figure 3.8: Neutrophils in the circulation, lung and LdLN had different activation states during pulmonary infection with *S. pneumoniae*.

Figure 3.8: Neutrophils in the circulation, lung and LdLN had different activation states during pulmonary infection with *S. pneumoniae*.

Quantification of flow cytometry plots gated on $Ly6C^{int}$ $Ly6G^{+}$ cells. (A) LdLN neutrophils had a higher MFI of CD11b. (B i) Gated on $CD11b^{+}$ $Ly6C^{int}$ $Ly6G^{+}$ cells, gating strategy to identify ICAM-1^{+} neutrophils. Quantification of flow cytometry plots; neutrophils in the Lung, BAL fluid and LdLN expressed ICAM-1 (B ii). (B iii) Total lung and BAL fluid neutrophils had a higher ICAM-1 MFI than LdLN neutrophils. (C i) Gated on $CD11b^{+}$ $Ly6C^{int}$ $Ly6G^{+}$ cells, gating strategy to identify ROS in neutrophils. (C ii) Fewer neutrophils in the blood, lung and LdLN made ROS as compared to BAL neutrophils. (C iii) Gated on total neutrophils. Q-PCR analysis of sorted $CD11b^{+}$ $Ly6C^{int}$ $Ly6G^{+}$ cells. Graphs show quantification of gene expression relative to blood neutrophils. BAL fluid neutrophils expressed more mRNA for *Tnf* (D) and *Ifng* (E). 12 hour *S. pneumoniae* infection. (A) and (B) n= 4. (C) n=3. (D) and (E) n=3. Bars represent mean + SEM, * $P<0.05$ and ** $P<0.01$ (Kruskal-Wallis test with Dunn's post hoc test).

3.4.6 Gene transcription analysis of neutrophils in the circulation, lung tissue, alveolar space and LdLN during infection with *S. pneumoniae*

In addition to *Tnf* and *Ifng* mRNA expression investigated in Figure 3.8, other genes involved in activation and neutrophil function were investigated by Q-PCR to further characterise the differences between neutrophils in the circulation, lung and LdLN. Quantitative PCR was performed to assess mRNA expression of *Nos2* to investigate the induction of iNOS synthesis. Figure 3.9 (A) shows that all populations of neutrophils expressed *Nos2* mRNA, however BAL neutrophils had the highest level.

In a HEL/CFA vaccine model LN neutrophils are found to produce high levels of prostanoids, in particular thromboxane A2, thus suppressing T cell responses. The enzymes COX-2 and COX-1 are responsible for prostanoid synthesis. In inflammation COX-2 is induced and is the dominant enzyme in prostanoid synthesis[180]. The gene *Ptgs2* encodes COX-2, thus *Ptgs2* transcription was investigated to see if neutrophils in this infection model were having a similar role. As observed in Figure 3.9 (B), lung and LdLN neutrophils had high *Ptgs2* mRNA expression as compared to blood, but also BAL neutrophils, with the highest level in lung tissue neutrophils.

Mmp9, *S100a8* and *S100a9* are three key, highly expressed neutrophil genes that encode abundant granular (MMP9) and cytoplasmic (S100A8 and S100A9) proteins. Their expression was analysed to see if there was variation at the different sites. Interestingly the blood neutrophils showed the highest expression of *Mmp9* mRNA (Figure 3.9 C). Blood neutrophils also showed the highest level of expression of both *S100a8* and *S100a9* mRNA. BAL and LdLN neutrophils showed slightly higher expression than lung neutrophils (Figure 3.9 D and E).

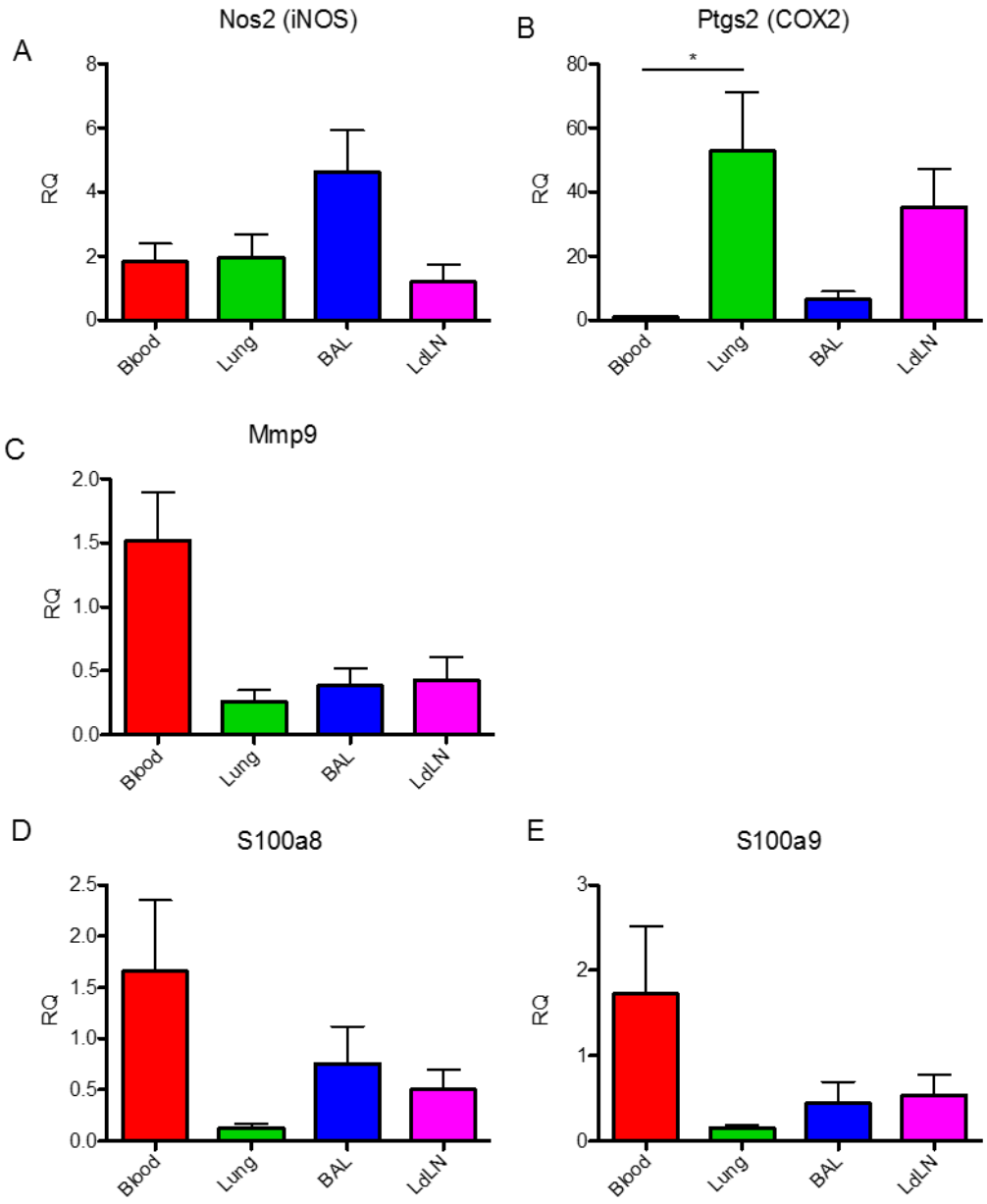

Figure 3.9: Gene transcription analysis of neutrophils in the circulation, lung tissue, alveolar space and LdLN during infection with *S. pneumoniae*.

Q-PCR analysis of sorted CD11b^{+} Ly6C^{int} Ly6G^{+} cells. Graphs show quantification of gene expression relative to blood neutrophils. BAL fluid neutrophils had more mRNA for *Nos2* (A). Lung tissue and LdLN neutrophils had high expression of *Ptgs2* mRNA (B). Blood neutrophils had more mRNA for *Mmp9* (C), *S100a8* (D) and *S100a9* (E). n=3. Bar represents mean + SEM, * P<0.05 and (Kruskal-Wallis test with Dunn's post hoc test).

3.4.7 Neutrophil antigen presenting cell marker expression in the LdLN during pulmonary infection with *S. pneumoniae*

The characterization of neutrophil activation state revealed that LdLN neutrophils resembled lung neutrophils and were in an intermediate activation state. However there had been no clear phenotypes that separated lung from LdLN neutrophils, therefore this was investigated further. In various *in vivo* and *in vitro* models it has been shown that neutrophils are capable of antigen presentation and T cell activation[67,168,181-183]. The high expression of ICAM-1 would aid stable T cell interactions with CD11a[184], thus neutrophil MHC II and CD11c expression was investigated to see if they had taken on an antigen presenting cell phenotype. In the blood (0.1% ± 0.03), lung (0.7% ± 0.1) and BAL (0.1% ± 0.02) there were few MHC II positive cells, however in the LdLN 10% (± 3) of neutrophils expressed MHC II (Figure 3.10 A ii). When looking at the neutrophil populations at each site, the LdLN population as a whole showed a shift to higher MHC II MFI (Figure 3.10 A iii). As with MHC II expression, a small population of neutrophils, 6% (± 1.3) expressed CD11c (Figure 3.10 B ii) and as a population LdLN neutrophils show a shift to higher CD11c MFI (Figure 3.10 B iii). Thus a subset of neutrophils had taken on antigen presenting cell phenotype.

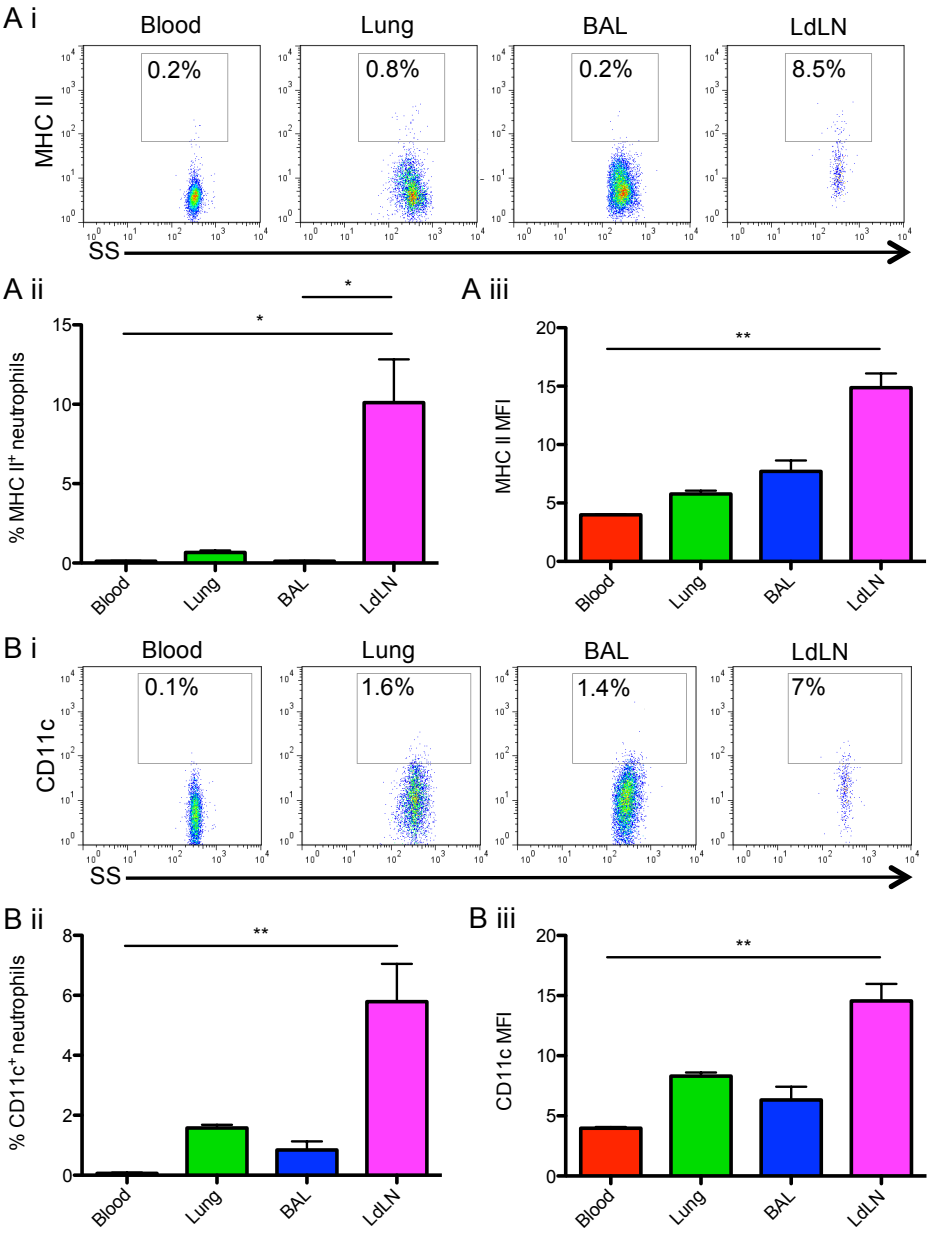

Figure 3.10: A subset of neutrophils in the LdLN express antigen presenting cell markers during pulmonary infection with *S. pneumoniae*.

Gated on CD11b^{+} Ly6C^{int} Ly6G^{+} cells, gating strategy to identify MHC II^{+} neutrophils (A i). (A ii) quantification of flow cytometry plots; a small population of neutrophils in the LdLN expressed MHC II. (A ii) Gated on total neutrophils. LdLN neutrophils had a higher MFI of MHC II. (B i) gated on CD11b^{+} Ly6C^{int} Ly6G^{+} cells, gating strategy to identify CD11c^{+} neutrophils. (B ii) quantification of flow cytometry plots; small population of neutrophils in the LdLN expressed CD11c. (B iii) Gated on total neutrophils. LdLN neutrophils had a higher MFI of CD11c. 12 hour *S. pneumoniae* infection. n=4. Bars represent mean + SEM, * P<0.05 and ** P<0.01 (Kruskal-Wallis test with Dunn's post hoc test).

3.4.8 Neutrophils in the LdLN were not specialised for B helper functions during infection with *S. pneumoniae*

B-helper neutrophils in the spleen have been described that make B cell survival and activation factors including BAFF and APRIL. They induce activation and antibody production by marginal zone B cells[165]. Figures 3.5-7 showed that neutrophils were located in the LN medulla after pulmonary *S. pneumoniae* infection, this location is a known niche for plasma B cells. Gene expression of *Tnfsf13*, encoding APRIL and *Tnfsf13b*, encoding BAFF was analysed to see if neutrophils in the LdLN had potential for a B cell helper function. Expression of *Tnfsf13* was lowest in LdLN neutrophils. The same was found for *Tnfsf13b*. Expression of mRNA for all these genes in lung, BAL and LdLN neutrophils was never above that detected in blood neutrophils (Figure 3.11). Thus LdLN neutrophils had not upregulated gene transcription of B cell activating factors.

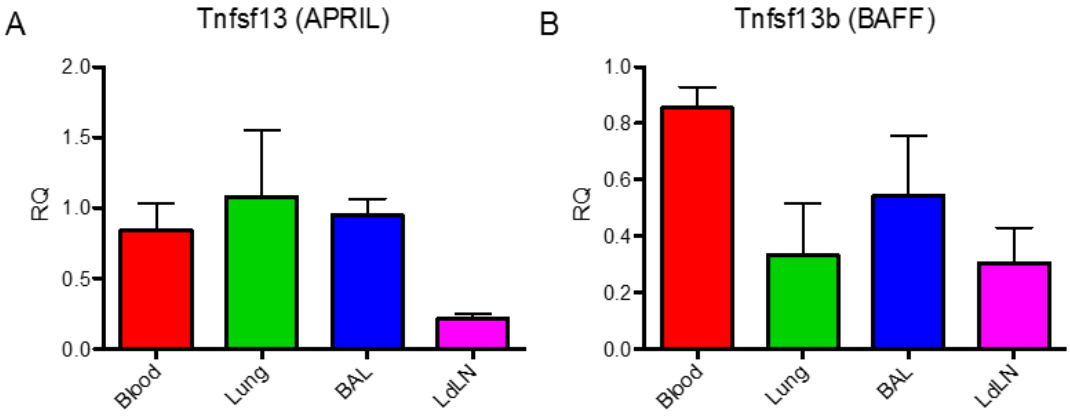

Figure 3.11: Neutrophils in the LdLN were not specialised for B helper function during infection with *S. pneumoniae*.

Q-PCR analysis of sorted CD11b^{+} Ly6C^{int} Ly6G^{+} cells. Graphs show quantification of gene expression relative to blood neutrophils for *Tnfsf13* (A) and *Tnfsf13b* (B). n=3, bars represent mean + SEM.

3.5 Summary of results

- Pulmonary *S. pneumoniae* infection induces neutrophil migration to the LdLN.
- Lung dLN neutrophil recruitment is rapid, peaking at 6-12 hours and falling at 24 hours.
- Neutrophils populate lymphatic areas of the LdLN.
- Neutrophils densely populate the medullary sinus in areas when MSM are found.
- Lung dLN neutrophils are in an intermediate activation state resembling lung tissue neutrophils. Blood neutrophils are in an inactivated state, BAL fluid neutrophils are highly activated.
- Lung dLN and lung neutrophils express high levels of *Ptgs2* mRNA, however no other clear marker was found to distinguish LdLN neutrophils from lung neutrophils.
- A small percentage of LdLN neutrophils express CD11c and MHC II.
- Neutrophils in the LdLN following acute pulmonary *S. pneumoniae* infection are not specialised for B helper activity.

3.6 Discussion

3.6.1 Neutrophil involvement in early immune response events in the lung draining lymph node following pulmonary *S. pneumoniae* infection

The rapid migration of neutrophils to the LdLN indicates they may have a role in very early immune response events in the lymph node. Lymphatic endothelial cells that line the medullary sinus are key in modulating lymphocyte egress[118]. The positioning of neutrophils within this area may indicate that they have a role in regulating early exit from the LN during inflammation. It has been proposed that neutrophil derived thromboxane A2 is a non-specific mechanism for early (less than 24 hour) T cell retention in the LN[170]. In this model *Ptgs2* is highly induced in these cells thus this data could support this, however neutrophil prostaglandin or thromboxane production was not confirmed. Alternatively neutrophils could be modulating early events in the expansion of the lymphatic endothelial cell network. Lymph node hypertrophy is an important process during an immune response, involving expansion of the HEV and lymphatic vessel network. Neutrophils have been reported to be involved in angiogenesis; neutrophil derived MMP9 aids vascularization in tissues during inflammations[185]. It also has a role in lymphangiogenesis through extracellular remodeling increasing VEGF-A bioavailability, additionally neutrophils are found to secrete VEGF-D[186]. We found that LdLN neutrophils also express MMP9, and thus it would be interesting to determine if neutrophils express VEGF-C and VEGF-D which are known to drive lymphangiogenesis[187], and if MMP9

expression by neutrophils has an important role in the rapid ECM remodeling that occurs in LNs during an immune response.

3.6.2 Neutrophils in the circulation, lung, airways and LdLN have different activation states

Phenotypic analysis finds that circulating blood neutrophils represent a 'quiescent' state. Few blood neutrophils were ICAM-1^{+} or ROS^{+} and they had the lowest CD11b expression. Gene transcription for *Tnf* and *Ifng* was not increased to the level of lung, BAL and LdLN neutrophils, however *Mmp9* and *S100a8/9* gene was the highest in these cells. Matrix metallopeptidase 9 is a gelatinase enzyme that cleaves collagen in the basement membrane[188] and has been shown to be an important proinflammatory mediator, produced by neutrophils to facilitate their migration to inflammatory sites including the bladder and lung. In the bladder MMP9 is essential for neutrophils get through the basement membrane in order to cross the uroepithelium[189]. In influenza infection MMP9 is produced in large amounts by lung tissue neutrophils, and is also important for neutrophil migration into the lung[188]. Thus it was expected that gene expression was going to be highest in lung neutrophils, in order to aid their interstitial migration and crossing of the pulmonary epithelia into the alveolar space. However this was not the case, circulating blood neutrophils had the highest MMP9 gene transcription. Although not to the levels expected, the gene was still expressed in lung neutrophils, thus it could indeed be having a role in neutrophil infiltration; however it is possible that MMP9 may not have such an important role in *S. pneumoniae* infection, as compared to influenza infection. Alternatively at 12 hours of infection, as investigated here, transcription may be turned down to favor transcription of other inflammatory genes in lung, airway and LdLN neutrophils. Matrix metallopeptidase 9 gene expression may be temporally regulated in neutrophils; alternatively pre-produced MMP9 is released without the need for new synthesis.

S100A8/9 have been reported to be important in neutrophil migration, it was not expected that blood neutrophils would have the highest gene expression for S100A8/9, it was expected that S100A8/9 may be involved in interstitial migration of lung neutrophils. In human neutrophils it is reported that S100A9 binding to pertussis toxin-sensitive receptors induces increased affinity of CD11b[190], and increases their adherence to fibrinogen[191]. Additionally it is found that both S100A8 and S100A9 induce activation of human endothelial cells; increased chemokine and adhesion molecule expression, and deceased junction molecule expression, thus loosening endothelial cell junctions[192]. Thus perhaps in this mouse bacterial infection model S100A8 and S100A9 are having the same effect and having a greater role in neutrophil TEM, acting on both the neutrophils and the endothelium, as opposed to interstitial migration in the lung or LdLN.

Once transmigrated these cells may down-regulate S100A8/9 expression to favor other inflammatory gene transcription, and use pre-made S100A8/9 cytoplasmic stores.

Lung tissue neutrophils were in an intermediate 'activation' state, between that of quiescent blood and highly activated BAL neutrophils. CD11b expression was high, 90% (± 2) of the neutrophils were ICAM-1^+, and 71% (± 2) were ROS^+. Gene expression of *Tnf* had increased 48 (± 12) fold as compared to blood neutrophils; *Ifng* mRNA expression has also increased. In contrast, *Nos2* transcription levels were not increased. Transcription of *Ptgs2* had been significantly induced in lung tissue neutrophils, with a 53 (± 18) fold induction over blood neutrophils. *Ptgs2* encodes COX-2 that is induced in inflammation. Cyclooxygenase 2 catalyses the first step in synthesis of five prostaglandins (PG); PGE_2, PGD_2, $PGF_{2\alpha}$, PGI_2 and thromboxane A2. Prostaglandin E_2 is the main PG active in the mouse lung, due to expression of PGE_2 receptors 2 and 4 (EP2 and EP4), and it has highly anti-inflammatory effects on lung myeloid cells. During efferocytosis (ingestion of apoptotic cells by macrophages) in the lung PGE_2 is generated, acting via EP2, it inhibits the recruitment of neutrophils to the lung. When combined with pulmonary *S. pneumoniae* infection this leads to impairment of clearance of the bacteria[193]. Prostaglandin E_2-EP2 signalling in neutrophils inhibits chemotaxis, ROS generation, LTB4 release and aggregation[194]. In the intestine, during acute *T. gondii* infection, inflammatory monocytes regulate neutrophil activation through PGE_2, preventing neutrophil mediated gut pathology[195]. Therefore in the lung tissue neutrophils, high *Ptgs2* expression could indicate that these intermediately activated neutrophils are also acting to prevent excessive neutrophil infiltration and activation that could drive lung pathology.

LdLN neutrophils showed a similar intermediate phenotype to lung neutrophils. CD11b expression was high, just 75% (± 2) were ICAM-1^+ and 67% (± 4) were ROS^+. As with lung neutrophils, *Tnf* gene expression had been increased to a comparable level, however *Ifng* transcription was not as high. *Nos2* expression had not been increased over blood neutrophil level. Similarly to lung neutrophils *Ptgs2* expression had been induced, however not to as high levels. The elevated expression of *Ptgs2* could indicate that these cells are also mediating anti-inflammatory effects. The intermediate state of LdLN neutrophils indicates that they may not be destructive in the LdLN; they are not activated to the level of airway neutrophils. Activation to that level could inhibit the adaptive immune response through inhibiting normal T cell - DC interactions by destruction of the collagen matrix secreted by FRCs in the paracortex of the LN.
Although not directly addressed or demonstrated, the similar phenotype of lung tissue and LdLN neutrophils, along with the positioning of LdLN neutrophils in mainly lymphatic areas indicates that these cells could have migrated from the lung through the lymphatics, similar to how DCs migrate to the LN. Prostaglandin E_2-EP2/EP4 signalling induces CCR7 expression on monocyte-derived DCs and is thought to be essential for the migratory capacity of human DC,

thus it would be interesting if the high *Ptgs2* in lung and LdLN neutrophils correlates with induced CCR7 on LdLN neutrophils, allowing their entry into lymphatics and subsequent migration to the LN[194].

Broncioalveolar lavage fluid (airway) neutrophils showed an activated phenotype. These cells had high ICAM-1 expression, and the highest expression of ROS. They also expressed significantly more *Tnf* mRNA that blood neutrophils, and nearly double the amount detected in lung and LdLN neutrophils. In addition to this they the highest level of *Ifng* mRNA and a two fold increase in *Nos2* mRNA expression, as compared to the other neutrophil populations. Reactive oxygen species are generated rapidly as an anti-microbial defense, however NO production is slower and requires iNOS transcription and translation[52], thus airway neutrophils were further along in the cascade of activation than lung and LdLN neutrophils. Nitric oxide has been shown to be pro-apoptotic in inflammatory cells including neutrophils[196]. The higher expression of iNOS (*Nos2*) mRNA could indicate that neutrophil apoptosis is being induced in the airway neutrophils. This is an important process to control inflammation and has been shown to have an essential role in macrophages during *S. pneumoniae* infection; high levels of NO induce macrophage apoptosis. Dysregulation of NO production causes a decrease in bacterial killing and induction of macrophage necrosis rather than apoptosis[197].

Tumor necrosis factor α stimulates endothelial cell activation, which in turn stimulates neutrophil transmigration and activation, including ROS production[52]. Both TNFα and IFNγ activate iNOS transcription[52]. Nitric Oxide produced by iNOS is thought to be important for pulmonary neutrophil infiltration, potentially by vasodilation of capillaries[198]. Thus the expression of TNFα, IFNγ and iNOS by BAL neutrophils indicates that, alongside bacterial killing, these cells were recruiting and activating more neutrophils. Neutrophils in the airways had not highly induced *Ptgs2* like lung and LdLN neutrophils. This could further indicate that these neutrophils are highly activated and solely polarized to generate inflammation to directly kill bacteria, not to promote anti-inflammatory responses.

Lung and LdLN neutrophils were in an intermediate state between that of 'quiescent' blood neutrophils and activated alveolar neutrophils. During transmigration of the endothelium neutrophils become primed, once in the tissue they fully activate. There is no clear definition of the process of neutrophil priming, or the phenotype of primed neutrophils, thus it is difficult to conclude if lung and LdLN neutrophils were 'primed' or 'activated'. However, due to the high percentage of ROS^+ cells observed without *ex vivo* stimulation of the neutrophils, perhaps the lung and LdLN neutrophils were beyond priming and were activated, with alveolar neutrophils in a highly activated state.

Using *in vivo* inflammation models it is challenging to capture 'primed' neutrophils. At an inflammatory site, many inflammatory mediators are released from a variety of hematopoietic and non-hematopoietic cells. Thus the neutrophils may experience "priming" agents within seconds, or even at the same time as binding the activation agent. The majority of the work characterising neutrophil priming has been performed *in vitro*. *In vitro* it is possible to sequentially add these mediators, for example TNFα followed by fMLP[44], however this is unlikely to occur *in vivo* during an inflammatory immune response.

3.6.3 ICAM-1 expression on neutrophils

In the lung, airways and LdLN neutrophils were found to express high levels of ICAM-1. Thus activated neutrophils expressed ICAM-1. This is consistent with what has been found in human lung neutrophils; BAL fluid neutrophils from both normal healthy individuals and sarcoidosis patients express ICAM1, however blood neutrophils from either patient groups do not express it[199]. The same is seen for neutrophils from the colitic colon[67]. ICAM-1 is expressed on many cell types, its up-regulation is a signature event in tissue inflammation. Tumor necrosis factor α, IL-1β and IFNγ, all neutrophil activating cytokines, all are known to up-regulate ICAM-1[200]. Thus it is perhaps not surprising that activated neutrophils were expressing ICAM-1. Clearance of neutrophils by tissue macrophages during an immune response is an important mechanism of controlling neutrophil release from the bone marrow and for inflammation resolution. ICAM-1 is a ligand for CD11b, thus perhaps ICAM-1 on neutrophils helps mediate macrophage uptake of neutrophils through CD11b.

Expression of ICAM-1 protein on neutrophil membrane may be modulated by many factors other than transcription. Neutrophil arrest, crawling and transendothelial migration is dependent on neutrophil CD11b-endothelial cell ICAM-1 interaction. Thus perhaps during the process of transendothelial migration neutrophils rip ICAM-1 off the surface of endothelial cells, leaving it bound to CD11b on their surface, and thus making them positive for ICAM-1 when analysed by flow cytometry. This process is known as trogocytosis, or trans-endocytosis. It occurs between APCs and lymphocytes at the immune synapse, the lymphocyte extracts APC surface molecules[201,202]. However this process involves endocytosis and degradation of acquired molecules. Thus with such high percentages of neutrophils positive for ICAM-1, at high MFI, it seems unlikely that neutrophils are ripping ICAM-1 from other cells. Q-PCR analysis of ICAM-1 gene transcription would demonstrate if neutrophils really are making ICAM-1, or acquiring it.

3.6.4 Clues to neutrophil function in the LdLN following acute pulmonary *S. pneumoniae* infection

The data presented in this chapter sheds light on neutrophil phenotype within LdLN and hints at their function. Neutrophils were activated, producing ROS, thus they could represent another line of defense in the LN, killing bacteria that enter the LN. This has been proposed as an essential step for preventing systemic spread of bacteria[139]. Indeed they were situated in close proximity to SIGN-R1$^+$ macrophages that are known to be important for uptake of *S. pneumoniae* in the spleen[203]. Thus neutrophils could be acting in addition to these macrophages to clear *S. pneumoniae* from the lymph fluid, or indeed modulating tissue resident macrophage function.

Neutrophils may also function further to bacterial clearance in the LdLN and be involved in early T cell activation. CD11c and MHC II expression was detected on small percentages of neutrophils; these molecules are hallmarks of APCs. Thus some LdLN neutrophils may be developing professional APC function. This has been demonstrated in other infection and inflammatory models. In chronic colitis MHC II is expressed highly on neutrophils in the colon, and to lower levels on neutrophils in the mesenteric LN. However in this model CD11c expression was not detected. *In vitro* these MHC II$^+$ neutrophils are indeed able to present antigens to T cells[67]. ICAM-1 was also expressed by neutrophils. This was also observed on neutrophils in the mesenteric LN and colon of a colitic mouse model, however not on blood neutrophils[168], similar to results seen in this project. On DCs ICAM-1 binds CD11a on T cells co-stimulating T cell activation and stabilizing the immune synapse[184]. DCs also skew the differentiation of T_H subsets through cytokine secretion. Lung dLN neutrophils were found to express *Ifng* mRNA, thus could have a role in T_H1 differentiation. It would be interesting to investigate if the MHC II$^+$ neutrophils were also producing IFNγ.

The location of LN neutrophils in the lymphatic sinus and that less than 10% of neutrophils were CD11c or MHC II positive however indicates that a T cell activation role may be unlikely as T cell activation occurs in the LN paracortex. Alternatively LdLN neutrophils could be having a contact-independent inhibitory effect on T cells; ROS production, *Nos2* and *Ptgs2* gene expression are consistent with this. Reactive oxygen species production by T cells themselves modulates T cell proliferation, however bystander neutrophils have also found to have the same effect[204]. Nitric oxide produced by iNOS in macrophages and mesenchymal stem cells also has a suppressive role on T cell proliferation[205,206]. Finally prostanoids are anti-inflammatory, significantly neutrophil thromboxane A2 is found to be suppressive of T cell activation[170].

Expression of APRIL and BAFF mRNA in LdLN neutrophils did not differ from expression in blood neutrophils, it was indeed lower. This suggests that, unlike in the spleen, LdLN neutrophils may not function as 'B-helper' cells. This could be due to the difference in the location. B-helper splenic neutrophils were involved in MZ B cell activation to TI antigens, however in the LN B cells predominantly respond to TD antigen. Alternatively the difference could be attributed to the fact that the mice had never previously been exposed to *S. pneumoniae*, so there were unlikely to be a pool of plasma cells in the medulla. Thus neutrophils in the LdLN medulla, early in infection, may not be functioning to provide B cell survival factors to plasma cells.

3.6.5 Investigating neutrophil function in the lymph node

The data presented in this chapter provides an in depth characterization of neutrophil recruitment, location and phenotype in the LdLN following pulmonary *S. pneumoniae* infection. It also starts to dissect whether LdLN neutrophils resemble circulating, lung tissue or alveolar neutrophils, or another phenotype entirely. This has not been done before in this infection model or, to date, in another model. Lacking in this work is the identification of a function for LdLN neutrophils. Hypotheses for neutrophil function can be drawn from gene expression analysis, however there has been no demonstration of protein production, for example cytokine detection by flow cytometry or enzyme-linked immunosorbant assay (ELISA), thus no direct conclusions on neutrophil function can been made.

Many studies investigating the function of neutrophils use the anti-Ly6G, clone 1A8, antibody to deplete neutrophils and then look for changes in immune responses in the absence of neutrophils, thus indicating neutrophil function. This was not done in this study. As described in Chapter 2.12, preliminary experiments were carried out to deplete neutrophils using the 1A8 antibody however neutrophil depletion was not achieved. Thus no functional experiments using neutrophil depletion were conducted, as neutrophil depletion could not be confirmed. The lack of depletion may be down to the antibody used being defective, or too low dose administered, however a comparable, if not higher dose to that in other studies was used; 500 μg. Antibody protein concentration of the stock was confirmed using a nano-drop spectrophotometer to ensure correct dosing. Alternatively the antibody may not actually cause neutrophil depletion, rather block neutrophil migration out of the blood[207,208]. However this phenomenon was observed using a 100-fold lower dose of 5 μg.

A study aimed to prove that neutrophils contribute to chronic oviduct pathology following chlamydial infection. To do this 1A8 depletion of neutrophils was utilized, using doses of 300 μg 1A8 given i.p. Depletion of $Ly6G^{hi}$ neutrophils from the circulation was confirmed, however

there was no effect on disease pathology, indeed there were comparable levels of TNFα, IL-6 and IL-1β in tissue homogenates. This was not expected due to previous results and other studies all pointing to neutrophils as having a major role in pathology. Further investigation revealed a robust infiltration of $Gr1^{low}$ immature neutrophils in the oviduct, taking the place of $Ly6G^{hi}$ neutrophils in their absence[209]. The same was observed in attempts to deplete neutrophils in this thesis. Treatment with 1A8 resulted in the disappearance of $Gr1^{hi}$ cells but the appearance of an equivalent percentage of $Gr1^{int}$ cells. Perhaps depleted mature neutrophils were rapidly replaced by immature neutrophils, as opposed to a down-regulation of Gr1 in response to 1A8 binding. Cell sorting, followed by Giemsa staining would answer this question. Mature and immature neutrophils can be distinguished by their nuclei; mature cells have segmented nuclei, whereas immature cells have ring-shaped, band nuclei[210].

It is very difficult with existing technologies to selectively target LdLN neutrophils without disturbing the balance of the immune response in the draining tissue. Any method would also affect lung neutrophils, with most methods likely affecting neutrophil trafficking to the lung. Neutrophils have been observed in the LN in several different types of infection (bacterial, viral and parasitic), but also immunization models, however no clear, agreed, function has been found for them. The difficulty in targeting LN neutrophils alone could be the reason for this.

3.7 Conclusion

In line with the hypothesis neutrophils were indeed found to migrate to the tissue dLN during acute pulmonary infection with *S. pneumoniae*. This was very rapid and neutrophils in the LdLN showed an altered, less activated phenotype to airway neutrophils in the BAL fluid. Interestingly lung tissue neutrophils shared this phenotype. However a role for neutrophils in the LdLN was not elucidated. The dense population of neutrophils found in the LN lymphatic sinus was very interesting. The lymphatics sit below the capsule of the LN, making this area easy to image by real-time microscopy. Thus to further the in-depth analysis of neutrophils in the LdLN, the dynamics and migration mechanisms of neutrophils was investigated using 4D multi-photon microscopy of LdLN explants.

Chapter 4: Investigating neutrophil dynamics and migration mechanisms in the lung draining lymph node

4.1 Molecular mechanisms of leukocyte migration

Neutrophils and indeed all leukocytes migrate as single cells using 'amoeboid' cell migration. This form of migration is similar to that used by the amoeba *Dictyostelium discoideum*. Cells can assume many different shapes, immobile leukocytes are rounded (Figure 4.1 a), however during migration they polarise and develop a leading edge (lamellipod), mid-body and uropod; the trailing edge of the cell (Figure 4.1 b). Amoeboid cell migration is very fast, with neutrophils found to move up to 30 µm/min; this enables rapid scanning of the extracellular environment. It is also weakly adhesive, strong focal adhesions to the tissue are not required, thus avoiding tissue destruction[211].

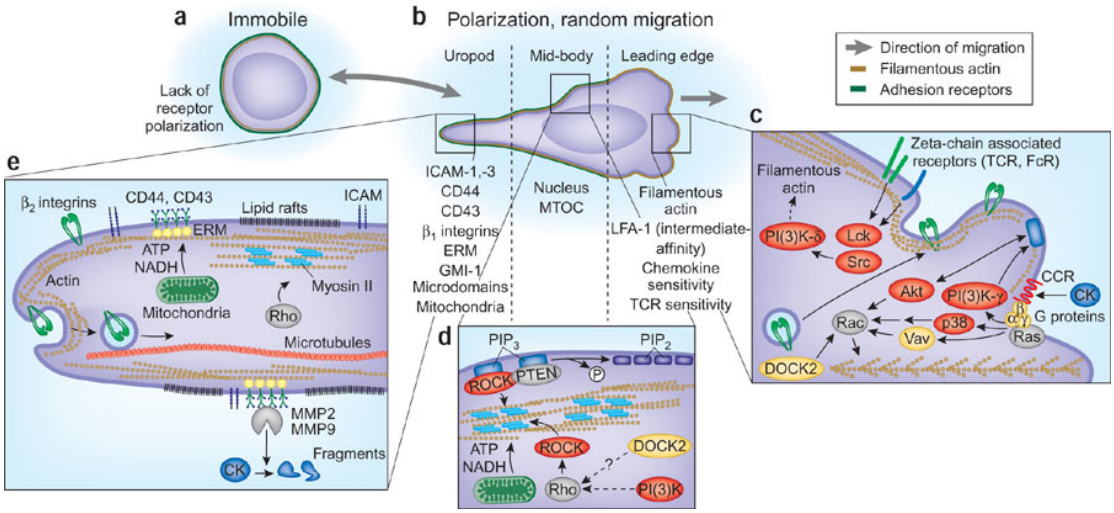

Figure 4.1: Amoeboid cell polarisation and migration.
Diagrams of the molecular components and processes involved in amoeboid cell polarisation and subsequent migration. Diagram (a) depicts the shape change from an immobile, rounded cell, to a highly polarised migrating cell (b) with a leading edge, mid-body and uropod. Diagrams (c), (d) and (e) show the subcellular molecular machinery involved in maintaining cell polarisation and driving forward migration. From Friedl and Weigelin, 2008[211].

At the leading edge dynamic ruffling of the cell membrane and short-lived protrusions, pseudopodia, are generated by rapid generation of networks of actin filaments. Various receptors at the leading edge include Fc receptors (FcR), chemokine receptors and β_2 integrins. These make the leading edge of the cell highly sensitive to receptor engagement and thus signal transduction and phagocytosis. The mid-body is immobile and contains the cell nucleus. This region is essential in maintaining the front-rear axis by creating a stiff core through actinmyosin

filaments, preventing lateral protrusion formation. The uropod contains microtubules and mitochondria; it has various adhesion molecules at the surface and forms the adhesive and contractive rear of the cell. The uropod forms cell-ECM and cell-cell interactions[211]. The underlying mechanism of amoeboid cell migration involves actin polymerisation at the leading edge, pushing the cell forwards, followed by actinmyosin contraction at the rear, releasing the cell.

Cell polarisation is induced in response to a wide range of extracellular signals including; cytokines, chemokines, lipids, alarmins, formyl peptides and complement factors. Leukocytes integrate these signals into intracellular signalling cascades and as a result shape change, cell polarisation and cell migration occurs. Cell polarisation, followed by directed migration towards a soluble gradient of chemokine is termed chemotaxis. However cells can also polarise and migrate in homogenous fields of soluble chemokines, without a gradient, this is called chemokinesis. Directed migration along a surface in response to a surface-bound chemokine gradient is called haptotaxis, whereas non-directed migration is haptokinesis[212].

G-protein coupled receptors, coupling to $G_{\alpha i}$ G proteins signal through PI3K to mediate cell migration and polarisation. Class I PI3Ks are heterodimeric proteins that consist of a catalytic and a regulatory subunit. Class IA PI3Ks are PI3Kα, β and δ, they are characterised by having a p85 regulatory subunit that binds the p110α, β and δ catalytic subunit. There is only one member of class IB PI3K; PI3Kγ. This is also a heterodimer, and consists of a regulatory subunit p101 or p84 that binds the catalytic subunit p110γ. Class I PI3Ks are mainly involved in receptor tyrosine kinase signalling, however class IB PI3Kγ is mainly activated by GPCRs. Thus PI3Kγ, that is mainly restricted to hematopoietic cells, is involved in cell migration. However there is evidence that the hematopoietic restricted class IA PI3Kδ also has a role in immune cell migration[213]. The $G_{\beta\gamma}$ subunit of $G_{\alpha i}$ coupled GPCRs directly binds to the catalytic p110γ domain of PI3Kγ, recruiting it to the cell membrane where it becomes activated. The p110γ domain of the active kinase binds the membrane lipid phosphatidylinositol-3,4-bisphosphate (PIP2) and also adenosine triphosphate (ATP). A phosphate is transferred from ATP to PIP2, phosphorylating it to generate phosphatidylinositol 3,4,5-triphosphate (PIP3) at the leading edge of the neutrophil. The serine-threonine kinase Akt (also known as protein kinase B) binds PIP3 inducing Akt activation; Akt is then able to activate Rac, a member of the Rho family of small GTPases[211]. Rac, and also the small GTPase Cdc42 activate WASP family verprolin-homologous protein (WAVE/Scar) and the actin-related protein 2/3 (ARP2/3) complex. WAVE is an actin binding protein that generates actin filaments (F-actin) and ARP2/3 causes the sideways branching of F-actin. Rac is important for membrane protrusion and cell movement; in contrast Cdc42 is important in directional sensing. Without Rac cells do not move, however without Cdc42 cells are still able to move, but their migration is random and

they are no longer able to sense chemotactic gradients[214,215]. Other pathways, independent of PI3Kγ, also induce Rac dependent actin filament generation. Accumulation of PIP3 at the leading edge ultimately leads to local Rac activation, F-actin generation and pushing forward of the plasma membrane (Figure 1.2 c)[211].

In the mid-body, and also the uropod the GTPase RhoA works to generate stiffness to limit lateral protrusion formation. RhoA activates Rho-associated protein kinase (ROCK) that phosphorylates the cytoskeletal motor protein myosin II, increasing its activity[214]. Myosin II cross-links and contracts F-actin. This generates a rigid core to the cell and pushes the nucleus forwards. Alongside actinmyosin stiffness controlling the mid-body and uropod, the phosphatase and tensin homolog (PTEN) works to dephosphorylate PIP3 and the kinases PI3Kγ and Akt, thus preventing protrusion formation[211].

Integrins are also involved in amoeboid cell migration, however they are not always essential, in non-adhesive environments leukocytes can migrate in an integrin-independent manner. Integrins form dynamic, weakly-adhesive nascent adhesions and focal contacts with the ECM. The actin-binding proteins talin and vinculin link the cytoplasmic domain of integrins to intracellular actinmyosin fliaments[216]. Contraction of the actin filaments by myosin II causes retrograde pulling on the integrins, pushing the cell forward[217]. These nascent adhesions rapidly turn over at the leading edge and allow the fast traction of these cells across the ECM. Integrins activate the spleen tyrosine kinase (Syk), which is found to associate with CD18 at the leading edge; Syk is involved in maintaining the leading edge and thus cell polarity during chemotaxis. *In vitro*, Syk deficient neutrophils form multiple lamellipodia and when migrating on immobilised fibrinogen show defective migration towards fMLP in comparison to wild type neutrophils[218,219].

4.2 Leukocyte migration is environment dependent

Since the early use of *D. discoideum,* DCs have been used as a model of amoeboid cell migration *in vitro, ex vivo* and *in vivo*. Work has found that these cells can rapidly adapt to the extracellular environment and switch migration mechanisms. When moving from adhesive to non-adhesive surfaces *in vitro* they switch from integrin-dependent to integrin-independent migration allowing maintenance of cell speed and amoeboid migration[220]. *In vitro* assays using 3D collagen (type I) gels or 2D assays where cells migrate on surfaces coated with integrin ligands for example, reveal that leukocyte migration is context dependent. In 3D collagen gels migration is integrin-independent, relying only on actin polymerisation driving the cell through the collagen network. This has been demonstrated using T cells with blocked integrin function, or B cells, neutrophils and DCs depleted of all integrins[217]. However in 2D leukocytes migration

is integrin-dependent. Integrin mediated adhesion is required for migration; macrophages and DCs depleted of integrins can't adhere to ligand-coated 2D tissue culture dishes and thus can't migrate[212,217].

In vitro assays however do not reflect the true physiological environments leukocytes migrate in *in vivo*. Explant imaging and intravital microscopy studies have been essential in providing insight into immune cell migration *in vivo*. The interstitial space of mouse skin is dense with extracellular matrix, type I collagen is the major constituent of this. Collagen I forms a thick mesh with other extracellular matrix components, as well as blood vessels, lymphatics, fat cells, nerves and muscle fibres. In this environment neutrophil and DC migration is integrin independent; DCs depleted of all integrins and neutrophils lacking β_2 integrins migrate at similar speeds and directionality as wild-type neutrophils in the same tissue[33,217].

The process of TEM in extravasation from the circulation can be seen as a 2D process. Neutrophils must firmly adhere to the vessel wall to resist the sheer flow of the blood. They must then crawl along the lumen to find a suitable exit point to cross the endothelial cell layer. In this context neutrophil migration is integrin-dependent, neutrophils depleted of all integrins, or deficient in β_2 integrins only can't perform TEM, and thus can't infiltrate tissues[28,217]. Unlike the interstitial space of non-lymphoid organs, lymphoid organs are densely packed with lymphocytes and stromal cells, with little accessible ECM. In this setting DC migration within the LN was integrin-independent; DCs lacking all integrins migrate with comparable speed and dynamics to wild-type DCs[217]. Dendritic cell migration to LNs is also shown be integrin-independent, but dependent on the chemokine receptor CCR7[217]. T cell migration within the LN is also highly dependent on chemokine receptor signalling and actin-myosin dynamics[221]. However, integrins do have a role in their migration; blocking T cell CD11a reduces their velocity in the paracortex[222]. Interestingly in the medulla integrins have a key role in T cell migration and dynamics, T cell CD11a mediates adhesion dependent migration on the lymphatic endothelium, preventing their early exit from the LN, allowing them to re-enter and scan the para-cortex[223].

4.3 Investigating leukocyte migration

To investigate live cellular migration, in real time, *ex vivo* or *in vivo,* microscopy has been used in combination with fluorescent reporter mice where DNA encoding fluorescent proteins is inserted into the genome of animals including zebrafish and mice, allowing visualisation of particular cell types, often depending on the expression of a gene of interest, or a gene unique to that cell type. In order to investigate neutrophils in tissues, lineage specific fluorescent reporter mice have been used. The work in this thesis has utilized B6.LysM Cre mice that have the Cre

recombinase gene inserted into the translational start site of the lysozyme M gene. Lysozyme M is expressed by monocytes, macrophages and neutrophils[156]. B6.Rosa26 mT/mG mice are double fluorescent reporter mice. The mT/mG cassette consists of the membrane targeted tdTomato (mT) gene and a transcriptional stop sequence in between two loxP sites and downstream of the Rosa26 promoter. Distal to the last loxP site is the membrane targeted EGFP (mG) gene. The cassette is in the Rosa26 locus on chromosome 6, this locus is a ubiquitously expressed, thus all cells contain the mT/mG cassette. B6.Rosa26 mT/mG mice express tdTomato fluorescent protein in all cells, however upon Cre excision, Cre^+ cells express GFP. Thus crossing B6.LysM Cre mice with B6.Rosa26 mT/mG mice generates B6.LysM Cre x B6.Rosa26 mT/mG F1 progeny that have GFP^+ monocytes, macrophages and neutrophils[157]. This approach has been used in a number of studies to understand myeloid lineage cellular dynamics.

To understand what receptors, molecules and signalling pathways are involved in driving cellular migration blocking antibodies, receptor agonist and antagonist compounds, as well as small molecule inhibitor compounds can be utilized. Thus to investigate what receptors and pathways could be involved in neutrophil migration within the LdLN this strategy was utilized, focusing on key chemotactic effectors such as PI3Kγ and δ, LTB4 and the role of integrins and Syk signalling in cellular behaviour.

4.4 Summary

Leukocytes are capable of rapidly adapting their migratory mechanisms to their environment, allowing their efficient migration. Neutrophil extravasation can be seen as a 2D process that is highly dependent upon integrins. However in the ECM-rich environment of the non-lymphoid interstitium their migration is integrin independent. The LN is a 3D structure, tightly packed with cells and no ECM to negotiate, thus we hypothesis that the mechanisms driving neutrophil migration will be tissue specific rather than cell intrinsic; migration mechanisms of neutrophils in the LN will differ from those required for peripheral tissue infiltration and migration. Thus we aim to determine the molecular mechanisms regulating neutrophil dynamics in tissue dLNs.

4.5 Aims

- Investigate *ex vivo*, in real time, neutrophil dynamics and behavior in the LdLN in an explant system.
- Understand the molecular mechanisms controlling neutrophil migration within the LdLN.

4.6 Results

4.6.1 Tracking neutrophils using GFP B6.LysM Cre x B6.Rosa26 mT/mG F1 mice

Flow cytometry experiments revealed that at the peak of neutrophil recruitment inflammatory monocytes were also found in the LdLN (Figure 3.1). Thus neutrophils and inflammatory monocytes were analysed in B6.LysM Cre x B6.Rosa26 mT/mG F1 mice to determine if the different cell types could be distinguished. In these mice, in the blood 89.5% (± 1.38) of neutrophils were GFP^+, similarly in the spleen 87.7% (± 1.18) were GFP^+ (Figure 4.2). There were significantly fewer GFP^+ monocytes; in the spleen 28.2% (± 2.53) were GFP^+, whilst in the blood only 16.1% (± 2.0) were GFP^+. Analysis of the GFP^+ cells revealed that neutrophils had a significantly higher MFI for GFP. Thus neutrophils could be distinguished from monocytes based on GFP expression and fluorescence intensity in B6.LysM Cre x B6.Rosa26mT/mG F1 mice. In addition to GFP expression, when imaging the cells *ex vivo* in the LdLN explant, the characteristic neutrophil lobed nuclear morphology was visible, thus neutrophils were distinguished on this basis (Chapter 4.6.2). These fluorescent reporter mice were therefore suitable for use to image neutrophil dynamics in LNs using multiphoton microscopy.

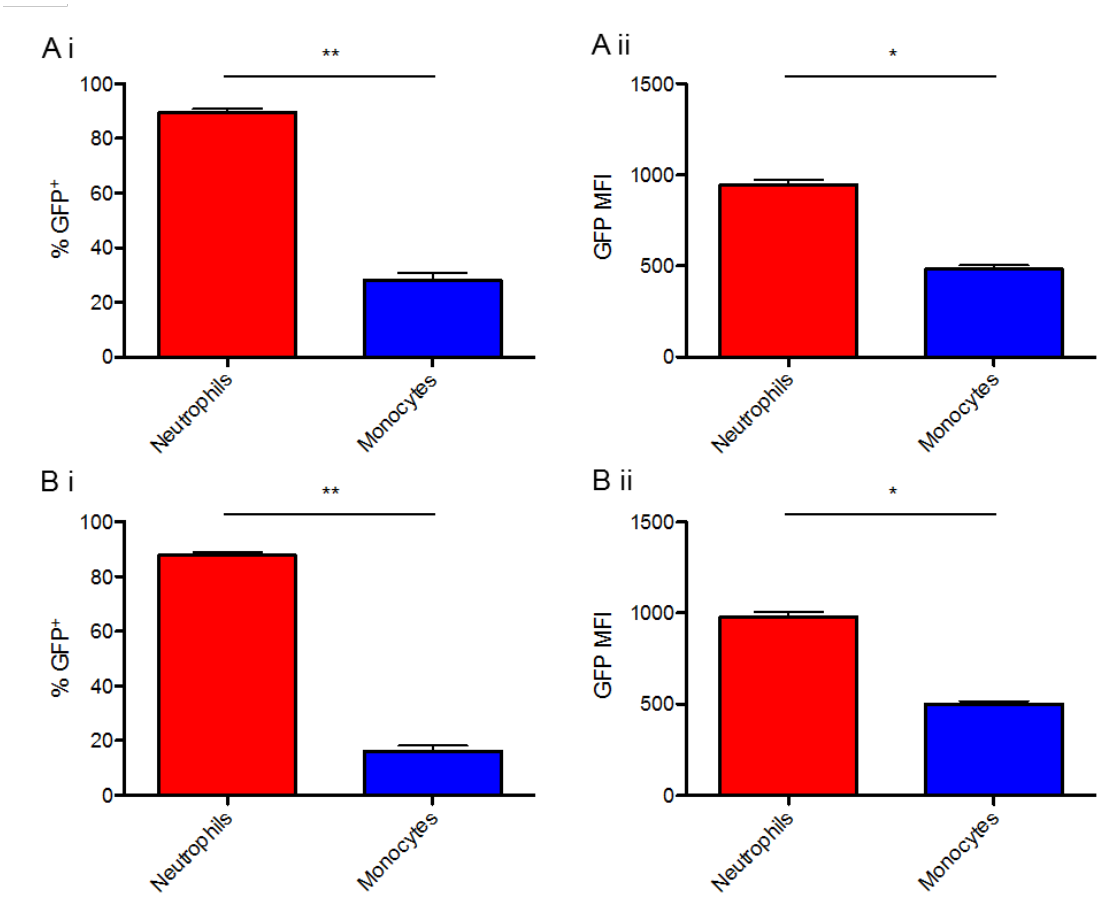

Figure 4.2: Neutrophils were distinguished from monocytes in B6.LysM Cre x B6.Rosa26 mT/mG F1 mice by GFP expression.

Quantification of flow cytometry plots gated on $CD11b^+$ cells. Percentage of GFP^+ neutrophils ($Ly6C^{int}$ $Ly6G^+$) and inflammatory monocytes ($Ly6C^+$ $Ly6G^-$) in the blood (A i) and spleen (B i) of B6.LysM Cre x B6.Rosa26 mT/mG F1 mice after 24 hour *S. pneumoniae* infection. GFP MFI of GFP^+ neutrophils and inflammatory monocytes in the blood (A ii) and spleen (B ii). Compared to monocytes, more neutrophils were GFP^+, of the GFP^+ neutrophils and monocytes, neutrophils had a higher GFP MFI and thus were distinguishable from monocytes. n=5, bars represent mean + SEM, * $P<0.05$ and ** $P<0.01$ (Mann-Whitney U test).

4.6.2 Visualising neutrophil dynamics in the lung draining lymph node using *ex vivo* explant imaging

To visualize neutrophil dynamics in the LdLN explant imaging was used, in combination with multiphoton laser scanning microscopy. Mice received intranasal administered heat inactivated *S. pneumoniae*, were sacrificed then the LdLN removed and placed into warmed RPMI culture medium that contained no supplements. Under a dissecting microscope any fat or connective tissue was removed from around the LdLN. This was done as quickly as possible, and as carefully as possible to cause as little damage or stress to the LdLN as possible. The LdLN was then placed in a glass bottom dish (No 1.5 glass, MatTek) containing approximately 75 µl of RPMI (supplement free) that was warmed to 37°C. A glass cover slip was then placed over the LdLN, this was done to ensure the LdLN stayed in place and to limit evaporation of the RPMI around the LdLN. Extra RPMI was then added at the edges of the dish as an extra measure to limit evaporation of media surrounding the LdLN. The dish was then placed on the microscope stage, the microscope had a light tight incubator fitted that kept the chamber at 37°C, thus the LdLN was kept at 37°C. The LdLN was then imaged using the multiphoton laser. A summary of the explant culture system used is shown in Figure 4.3 (A). A typical single image from a 4D time lapse sequence is shown in Figure 4.3 (B i). The collagen of the LdLN capsule was visualized by second-harmonic generation. $LysM^-$ cells were identified by tdTomato expression. Vasculature in the LdLN had high tdTomato expression; however other cells, particularly haematopoietic cells, had lower expression. $LysM^+$ GFP^+ cells, of various morphologies, were clearly visible. Large immotile GFP^+ cells had morphologies similar to SSM and MSM. The only highly motile GFP^+ cells were bright for GFP and had visible lobed nuclear morphology (Figure 4.3 B ii), thus these cells were classified as neutrophils and in quantification were tracked specifically on these criteria. The software Volocity was used to track these cells; arrows in Figure 4.3 (B i) indicate three representative neutrophils that were tracked using this software. Figure 4.3 (B iii) shows a graph of the tracks of these neutrophils. The tracks were plotted from an arbitrary starting position of zero. Cell tracking showed that neutrophils were highly dynamic in X, Y and Z planes. Serial stills of a GFP^+ neutrophil found in Video 1 demonstrates how dynamic the shape of neutrophils was, enabling them to rapidly navigate the tightly packed LN microenvironment (Figure 4.4, Video 1). Neutrophils showed classic amoeboid cell morphology with a distinct leading edge (lamellipod) and tail (uropod) when migrating in the LdLN.

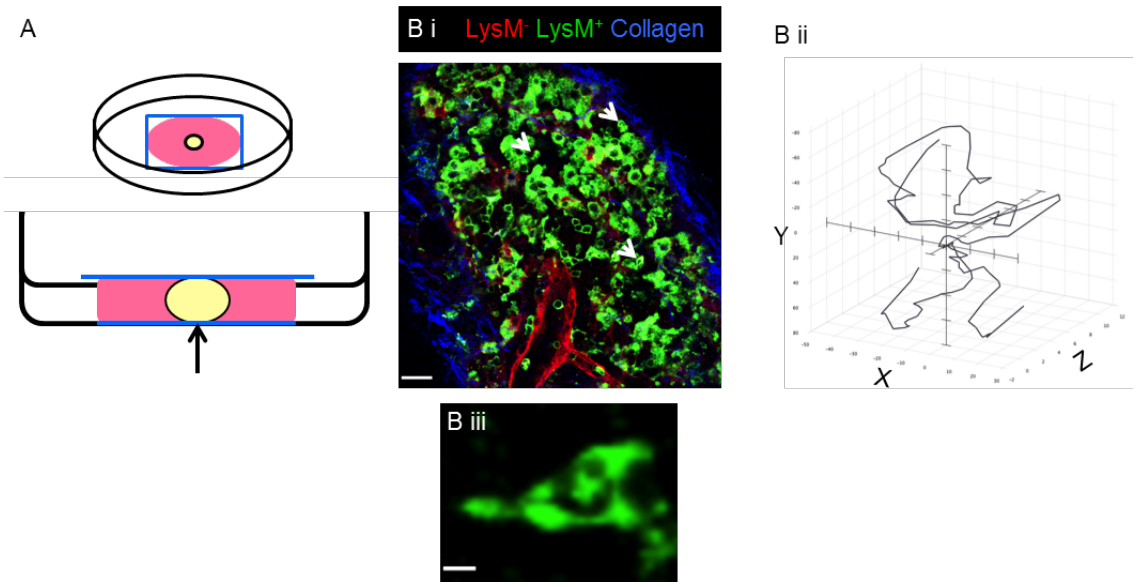

Figure 4.3: Explant imaging was used to visualise neutrophil dynamics in the LdLN in 3D, in real time.

(A) Diagram of explant imaging set up. Arrow indicates direction of multiphoton laser. (B i) B6.LysM Cre x B6.Rosa26 mT/mG F1 mice were used to visualise neutrophils in the LdLN. Collagen LdLN capsule (blue) was visualised by second-harmonic generation. LysM$^-$ tdTomato$^+$ cells (red), LysM$^+$ GFP$^+$ cells (green). Large immotile GFP$^+$ cells had morphologies similar to SSM and MSM. Motile GFP$^+$ cells were neutrophils. Scale bar= 25 µm. (B ii) Neutrophil migration was quantified by cell tracking using Volocity software (PerkinElmer). Cell tracks from neutrophils identified by arrows in (B i). (B iii) The characteristic lobed nuclei of neutrophils is easily identified in motile GFP$^+$ cells. Scale bar= 4.2 µm.

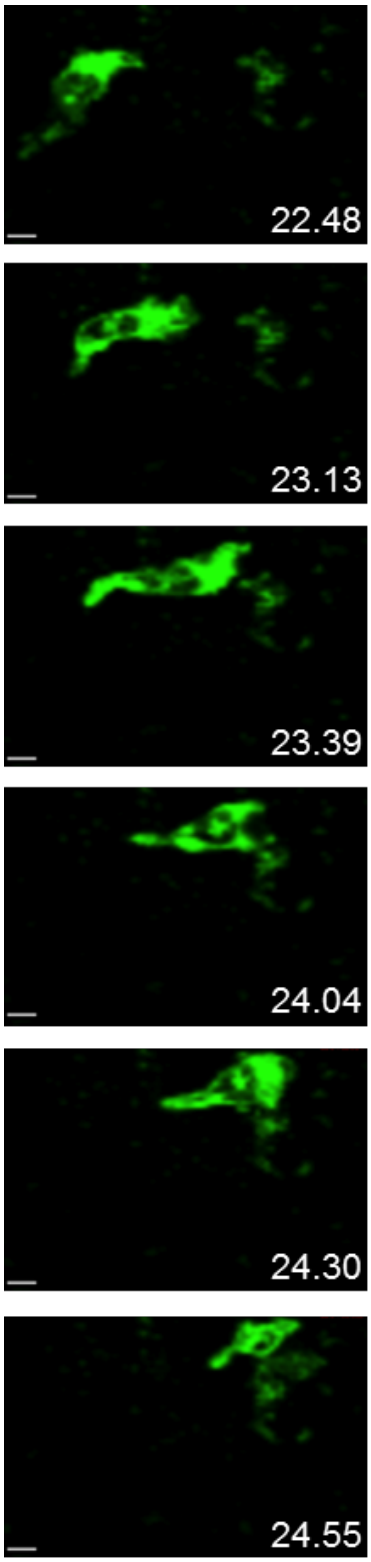

Figure 4.4: Neutrophil cell shape was highly dynamic during migration in the LdLN. Sequential stills from video 1 showing the migration of one GFP^+ neutrophil. Explant imaging of the LdLN from a B6.LysM Cre x B6.Rosa26 mT/mG F1 mouse after 6 hours of pulmonary *S. pneumonia*e infection. Scale bar= 4.2 μm.

4.6.3 Dynamic neutrophil migration in the lung draining lymph node following pulmonary *S. pneumoniae* infection

Very few migrating GFP^+ neutrophils were found in naïve mice (Figure 4.5 stills from videos 2-9). Video 2 shows a LdLN from a naïve mouse, and video 3 shows a LdLN from a mouse that received intranasal PBS and was sacrificed after 19 hours. The videos are representative of the whole LdLN. In contrast after 2, 6, 12, 24, 48 and 72 (videos 4-9) of pulmonary *S. pneumoniae* infection highly motile neutrophils were observed below the capsule of the LdLN. Videos 6 and 10 show the close interactions of neutrophils and large sessile GFP^+ cells, likely to be MSMs. In each experiment Z stack videos were collected covering all areas of the LdLN that were imageable. The LdLN was turned over in the dish after one side was imaged to image the other side. Each area was imaged for 30-40 min, covering a Z depth of 21-33 μm, photobleaching of the tdTomato occurred during imaging; however this was useful to identify areas that had already been imaged so as not to image an area twice. There was no observed effect of imaging on neutrophil dynamics or behavior. Each video was analysed using Volocity software and neutrophil migration quantified. Figure 4.6 shows the quantification of neutrophil velocity. Neutrophils were highly dynamic, moving at an average velocity of 15.5 (± 0.16) μm/min. At 6 and 12 hours neutrophils had a greater velocity than at other time points investigated; average neutrophil velocity was 16.6 (± 0.38) μm/min at 6 and 16.6 (± 0.28) μm/min at 12 hours. Interestingly this corresponded to the time when neutrophil numbers peaked in the LdLN (Figure 4.6 B).

It has previously been found that neutrophils form swarms in LNs during parasite and bacterial infection[33,36]. In the LdLN following *S. pneumoniae* infection, neutrophils were also observed to form swarms. Neutrophils formed transient swarms, involving small numbers of cells coming together for a few minutes, but dispersing. They were also observed forming persistent swarms, where neutrophils where continuously recruited to the swarm. These swarms did not disperse during the length of imaging, and were still there when the same area was reimaged later in the experiment (Figure 4.7, videos 11-13). It was likely that cell death was occurring in the persistent swarms, bubbling of the membrane GFP was observed which could have been neutrophils undergoing apoptosis, or perhaps NETosis. Neutrophils were tracked moving towards swarms, from the same LdLN in areas were swarms were not present these cells were also tracked. The presence of a swarm altered the migration of neutrophils, in the presence of a swarm there was a mild, but significant increase in neutrophil velocity, however there was a profound increase in meandering index (Figure 4.8). Meandering index is a measure of directionality and thus swarming alters the directionality of the cells, causing them to travel in straighter tracks, towards the swarm.

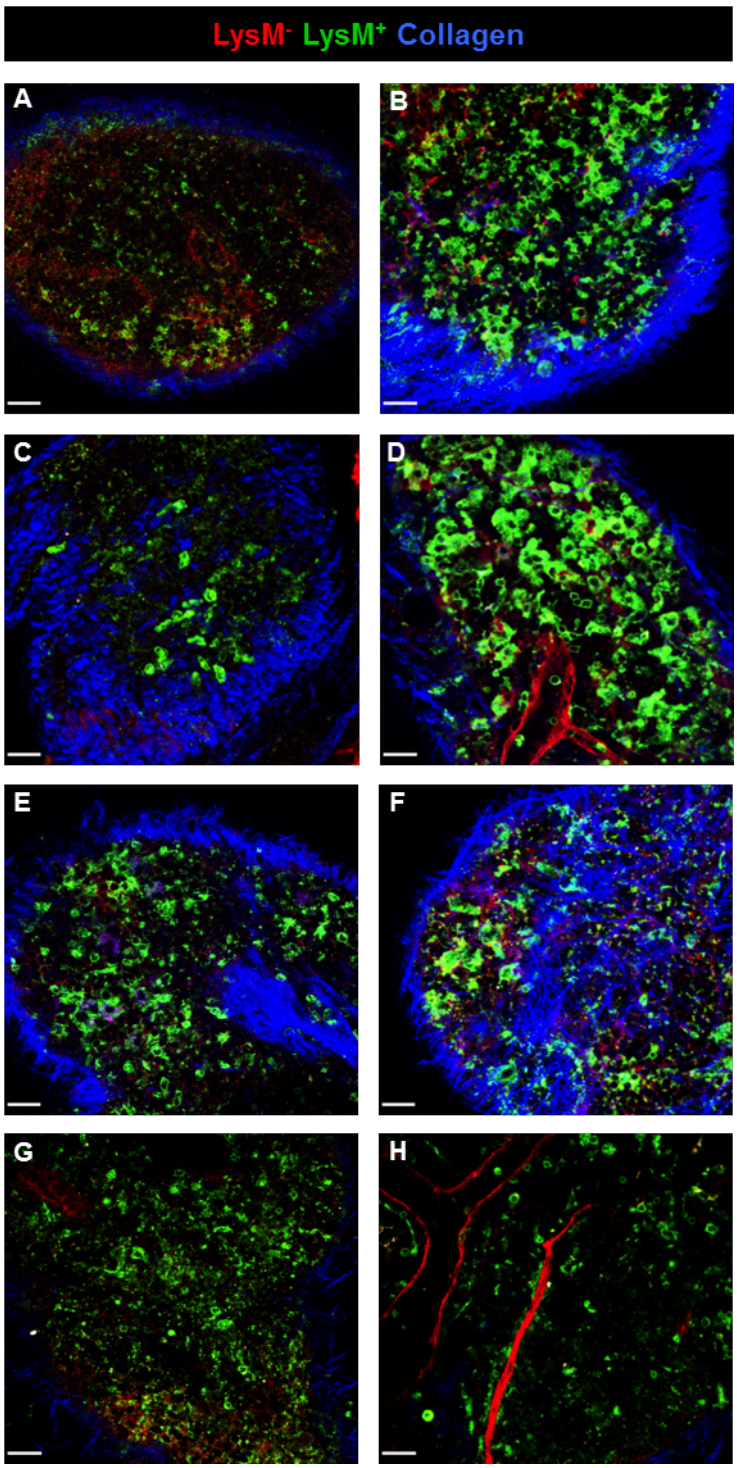

Figure 4.5: Neutrophil migration was dynamic in the LdLN following pulmonary *S. pneumoniae* infection.

Representative stills from explant imaging videos of the LdLN from B6.LysM Cre x B6.Rosa26 mT/mG F1 mice; (A) naïve, (B) PBS control, (C) 2 hour, (D) 6 hour, (E) 12 hour, (F) 24 hour, (G) 48 hour and (H) 72 hour pulmonary *S. pneumoniae* infection. Scale bars; A= 130 µm, B and D= 25 µm, C and F= 27 µm, E= 28 µm, G and H= 32µm. The corresponding videos are 2-9. *S. pneumoniae* was heat inactivated and labeled with either CTV or PKH26. In the stills both the GFP^+ sessile macrophages and motile neutrophils are shown. In the videos the distincion betweent he two populations is clear due to the motility of the neutrophils.

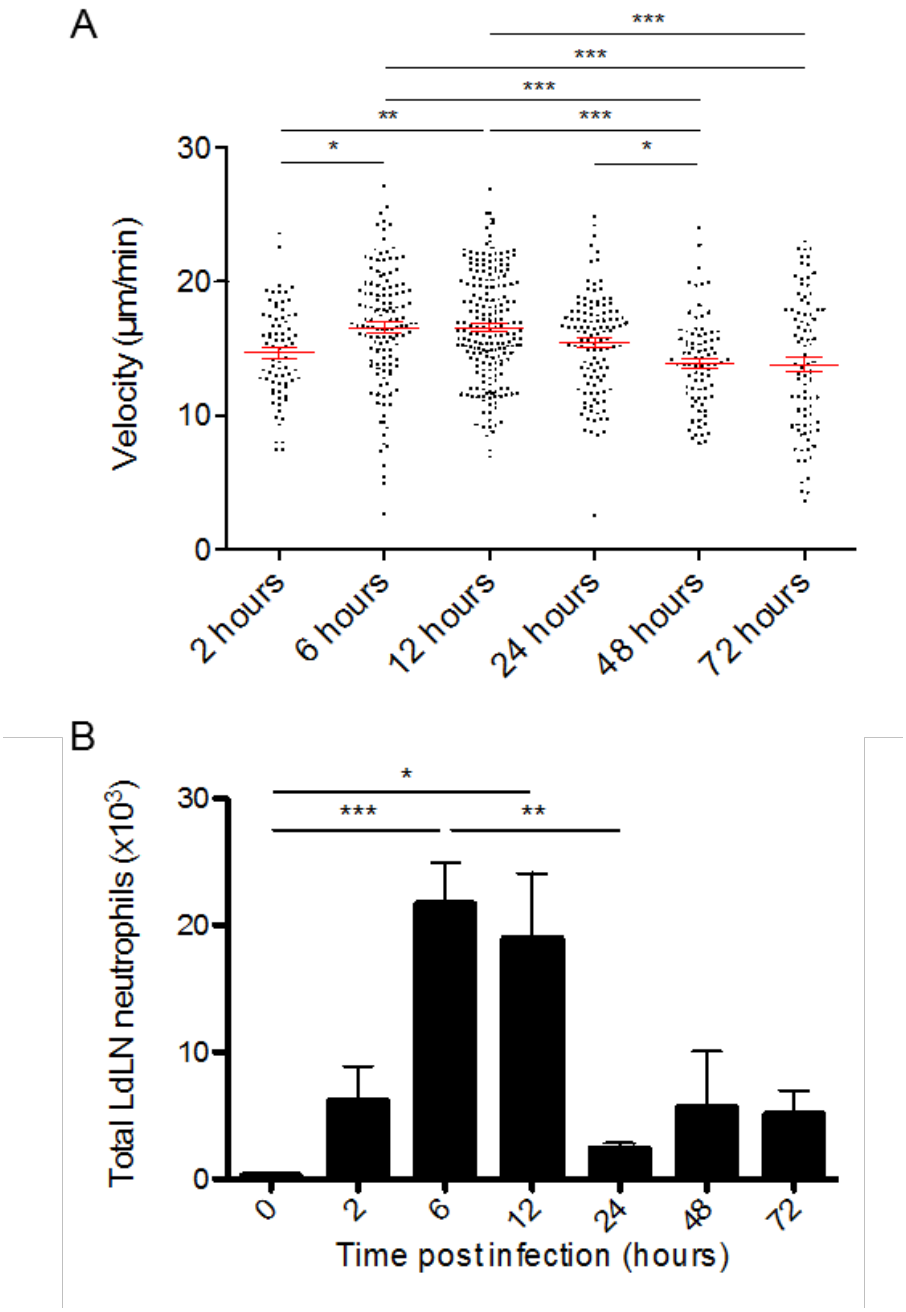

Figure 4.6: Neutrophils in the LdLN were highly dynamic following pulmonary *S. pneumoniae* infection.

Quantification of neutrophil velocity (A) in the LdLN at 2-72 hours of pulmonary *S. pneumoniae* infection. n=3, red bars represent mean ± SEM, * P<0.05, ** P<0.01 *** P<0.001 (Kruskal-Wallis test with Dunn's post hoc test). Neutrophils had the highest velocity when their numbers were highest in the LdLN. (B) Is Figure 3.4 (A); total neutrophil numbers in the LdLN following pulmonary *S. pneumoniae* infection.

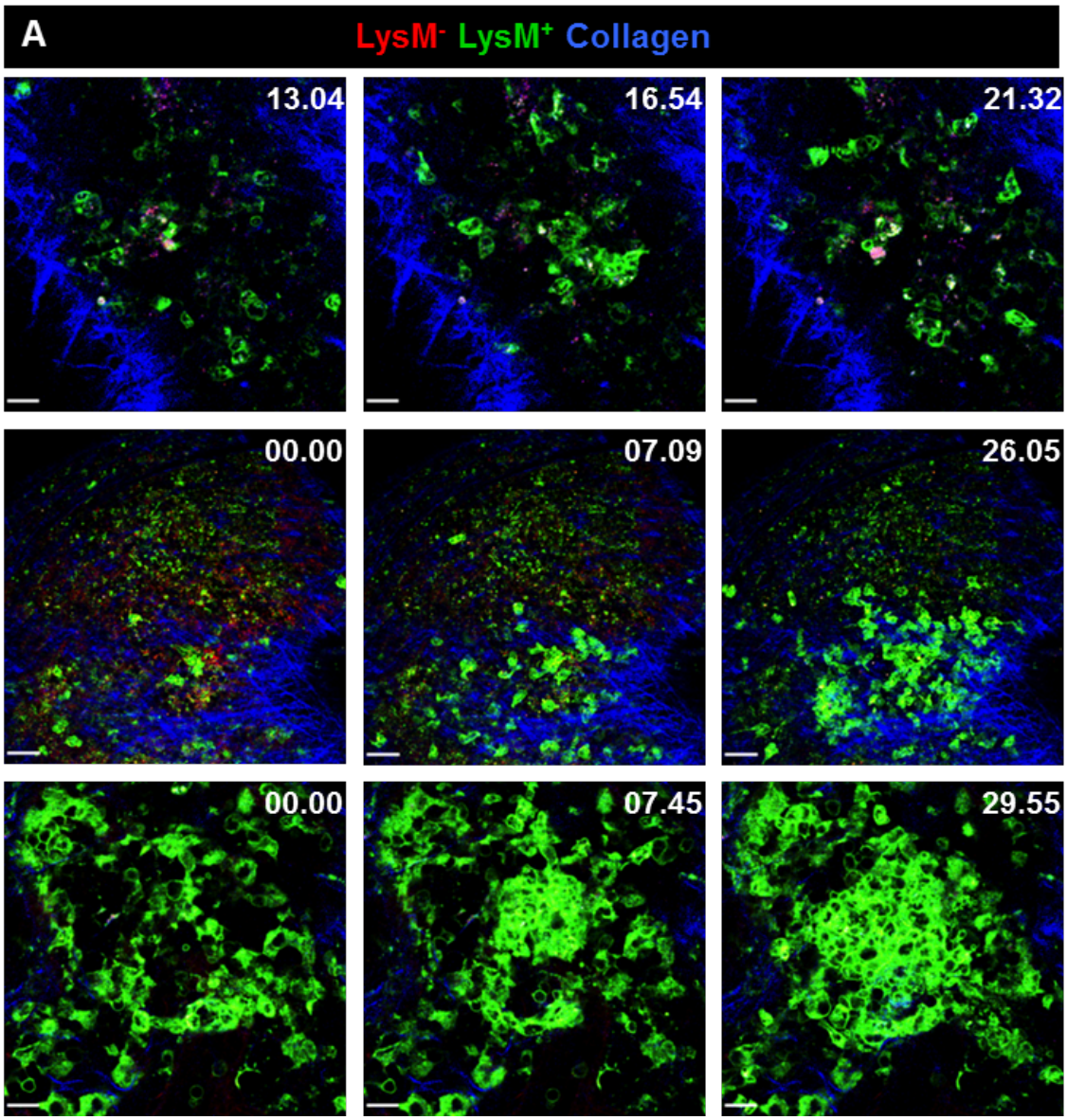

Figure 4.7: Neutrophils formed swarms in the LdLN following pulmonary *S. pneumoniae* infection.

Sequential stills from explant imaging videos of the LdLN from B6.LysM Cre x B6.Rosa26 mT/mG F1 mice. Top; a transient swarm at 12 hours of infection. Scale bar= 14 µm. Middle and bottom; persistent swarms at 6 hours of infection. Scale bars, middle= 31 µm, bottom= 16 µm. The corresponding videos are 11-13.

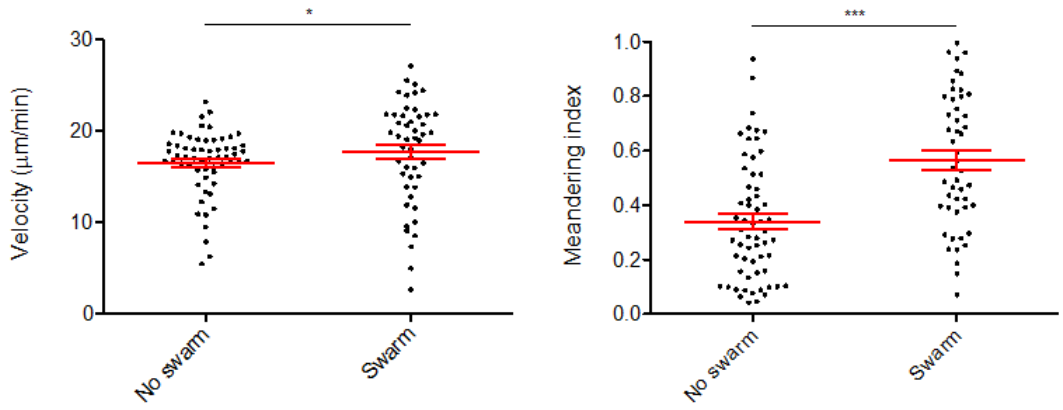

Figure 4.8: The effect of swarming on neutrophil migration.

Quantification of neutrophil velocity and meandering index in the LdLN at 6 hours of pulmonary *S. pneumoniae* infection in the presence and absence of swarms. Neutrophils migrating in the presence of a swarm had increased velocity and meandering index. n=3, red bars represent mean ± SEM, * P<0.05 and *** P<0.001 (Mann-Whitney U test).

4.6.4 Role of phosphoinositide 3-kinase γ in neutrophil migration in the lung draining lymph node

The explant culture set-up allowed addition of compounds and antibodies to the culture to directly target cells in the LdLN. Thus blocking agents of signalling pathways known to be important in regulating neutrophil migration were added to evaluate if these pathways were involved in neutrophil migration within the complex 3D structure of the LdLN. G-protein coupled receptor signalling through PI3Kγ is a major signalling pathway driving neutrophil migration[211]. Thus a selective inhibitor of PI3Kγ; Shionogi-12, was used to assess the contribution GPCR and PI3Kγ signalling in neutrophil migration within the LdLN following pulmonary *S. pneumoniae* infection. The inhibitor works by binding to the p110γ catalytic subunit of PI3Kγ in the ATP binding pocket, thus inhibiting binding of ATP and the accumulation of PIP3 at the leading edge. This mechanism is not unique to this inhibitor, all kinase inhibitors work in this way. The compound was made by, and provided by GSK (Stevenage), it was originally designed and synthesised by Shionogi & Co, Ltd, in Japan, example number 12 in patent WO2010/125799. The IC_{50} of an inhibitor compound is the concentration that inhibits the response by 50%. This value is used to determine potency or selectivity for a target. The IC_{50} of Shionogi-12 for PI3Kγ inhibition is 0.003 μM, whereas the IC_{50} values for PI3Kα, PI3Kβ and PI3Kδ are 15.9, 1 and 1.26 μM (unpublished data from GSK). Thus Shionogi-12 is highly selective for PI3Kγ.

The LdLN was first explant imaged as described in Chapter 2.9 and Figure 4.3, images were collected for approximately one hour. Two videos were acquired, one from each side of the LdLN corresponding to the medullary sinus and the subcapsular sinus. This gave a 'baseline' for neutrophil migration in the absence of the inhibitor. The LdLN was then placed in 1ml of warmed RPMI containing 10 μM Shionogi-12 and incubated at 37 °C, in the dark, for 30 minutes. Following the incubation period the LdLN was explant imaged in RPMI containing 10 μM Shionogi-12. As with previous explant imaging experiments, Z stack videos were collected covering all areas of the LdLN that were imageable. Neutrophil migration was quantified using Volocity software. This methodology was employed for all compounds tested. Neutrophil tracks in X and Y dimensions were plotted from a starting position of zero, the corresponding videos are 14 and 15 (Figure 4.9 A). PI3Kγ inhibition clearly inhibited neutrophil migration, with most neutrophils not moving far from their original starting position. PI3Kγ inhibition had a profound effect on neutrophil velocity, reducing it by 47.8% (Figure 4.9 B). The same effect was observed on neutrophil meandering index, with a reduction of 48% (Figure 4.9 C). Thus PI3Kγ inhibition severely impaired both the velocity of neutrophils but also their random directionality.

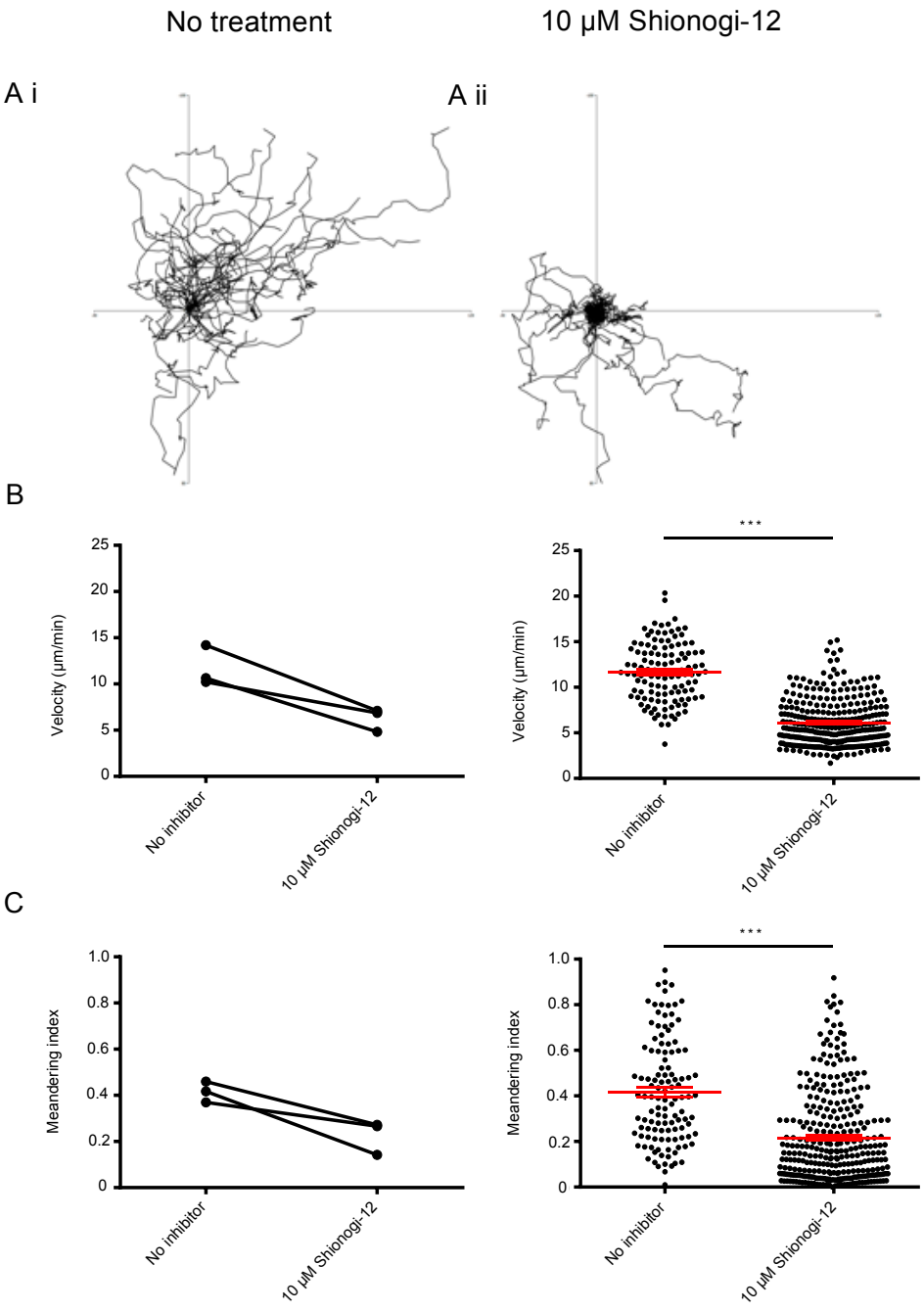

Figure 4.9: Investigating the effect of PI3 Kinase γ inhibition on neutrophil migration in the LdLN following pulmonary *S. pneumoniae* infection.

Explant imaging of the LdLN from B6.LysM Cre x B6.Rosa26 mT/mG F1 mice after 6-12 hours of pulmonary *S. pneumoniae* infection. Neutrophil tracks in X and Y planes, starting position set to zero, before (A i) and after (A ii) addition of 10 µM PI3Kγ inhibitor Shionogi-12. Quantification of neutrophil velocity (B) and meandering index (C) before and after the addition of 10 µM Shionogi-12. PI3Kγ inhibition impaired neutrophil migration in the LdLN. Pooled data from three experiments, n=3, red bars represent mean ± SEM, *** P<0.001 (Mann-Whitney U test).

4.6.5 Role of phosphoinositide 3-kinase δ in neutrophil migration in the lung draining lymph node

The *in vivo* role of PI3Kδ signalling in cell migration is not as clear as it is for PI3Kγ. PI3Kδ does not couple to GPCRs like PI3Kγ, but binds tyrosine-kinase linked receptors. In NK cells and B cells, PI3Kδ signalling has been shown to be involved in chemotaxis and activated downstream of selected chemokine receptors[224,225]. Production of ROS in response to stimulation of human neutrophils with fMLP, is inhibited by PI3Kδ inhibition[44]. The fMLP receptor FPR is a GPCR. Thus PI3Kδ may be involved in chemokine receptor signalling, however how it fits in the signalling cascade is not clear. To investigate the role of PI3Kδ signalling in neutrophil migration in the LdLN the specific inhibitor IC87114[162] was utilized. IC87114 binds the p110δ catalytic domain binding pocket, inhibiting ATP binding. The IC_{50} of IC87114 for PI3Kδ inhibition is 0.5 μM, whereas the IC_{50} values for PI3Kα, PI3Kβ and PI3Kγ are >100, 75 and 29 μM. Thus IC87114 is highly selective to PI3Kδ. *In vitro* it is selective at a concentration range of 0.3-10 μM[162]. Like PI3Kγ, PI3Kδ inhibition impairs neutrophil migration (Figure 4.10 A). The corresponding videos are 16 and 17. The velocity (Figure 4.10 B) and meandering index (Figure 4.10 C) of neutrophils was significantly impaired by PI3Kδ inhibition, with a 37.8% and 39% reduction in velocity and meandering index respectively. This was significantly less than that observed for PI3Kγ.

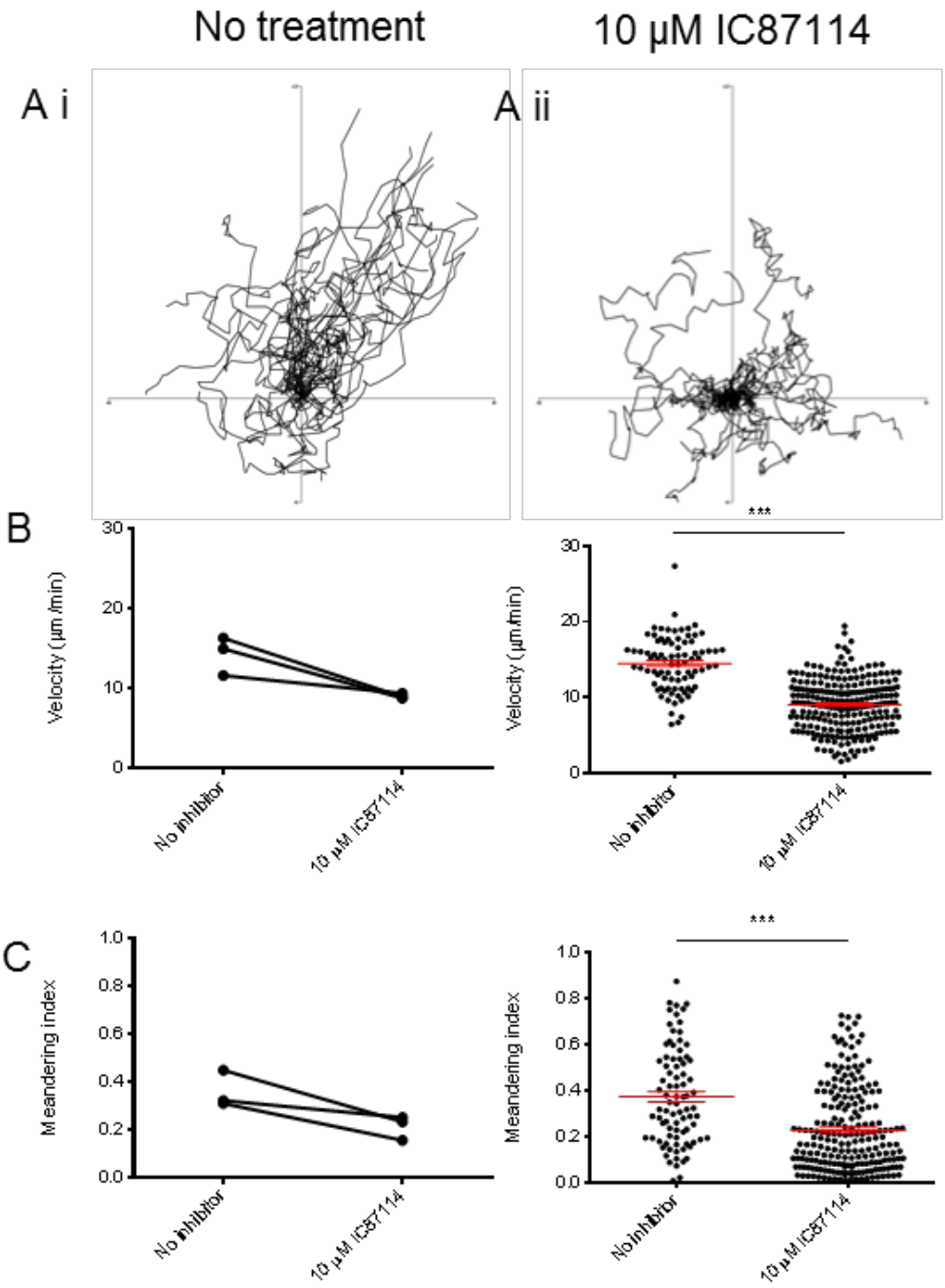

Figure 4.10: Investigating the effect of PI3 Kinase δ inhibition on neutrophil migration in the LdLN following pulmonary *S. pneumoniae* infection.

Explant imaging of the LdLN from B6.LysM Cre x B6.Rosa26 mT/mG F1 mice after 6 hours of pulmonary *S. pneumoniae* infection. Neutrophil tracks in X and Y planes, starting position set to zero, before (A i) and after (A ii) addition of 10 µM PI3Kδ inhibitor IC87114. Quantification of neutrophil velocity (B) and meandering index (C) before and after the addition of 10 µM IC87114. PI3Kδ inhibition impaired neutrophil migration in the LdLN. Pooled data from three experiments, n=3, red bars represent mean ± SEM, *** P<0.001 (Mann-Whitney U test).

4.6.6 Role of leukotriene B4 in neutrophil migration in the lung draining lymph node

Leukotriene B4 is a potent chemoattractant of neutrophils, acting on the GPCR BLT1. It has been described as a 'relay signal', produced by neutrophils themselves, stimulating their own migration in an autocrine and paracrine mannor[34] *in vitro*. *In vivo* LTB4 is involved in initial neutrophil recruitment to inflammatory sites[226,227]. It was also demonstrated to be involved in neutrophil swarm formation[33] recruiting neutrophils to the swarm. Thus the BLT1 antagonist LY223982[163] was used to inhibit LTB4 signalling and investigate the role of LTB4 in neutrophil migration in the LdLN. Similar to PI3Kγ inhibition, BLT1 antagonism impaired neutrophil migration (Figure 4.11 A). The corresponding videos are 18 and 19. The velocity (Figure 4.11 B) and meandering index (Figure 4.11 C) of neutrophils was significantly impaired by BLT1 antagonism, velocity was reduced by 35.5% and meandering index by 36.7%. Thus the inhibition observed using the PI3Kγ inhibitor may be in part due to inhibition of LTB4 signalling through BLT1.

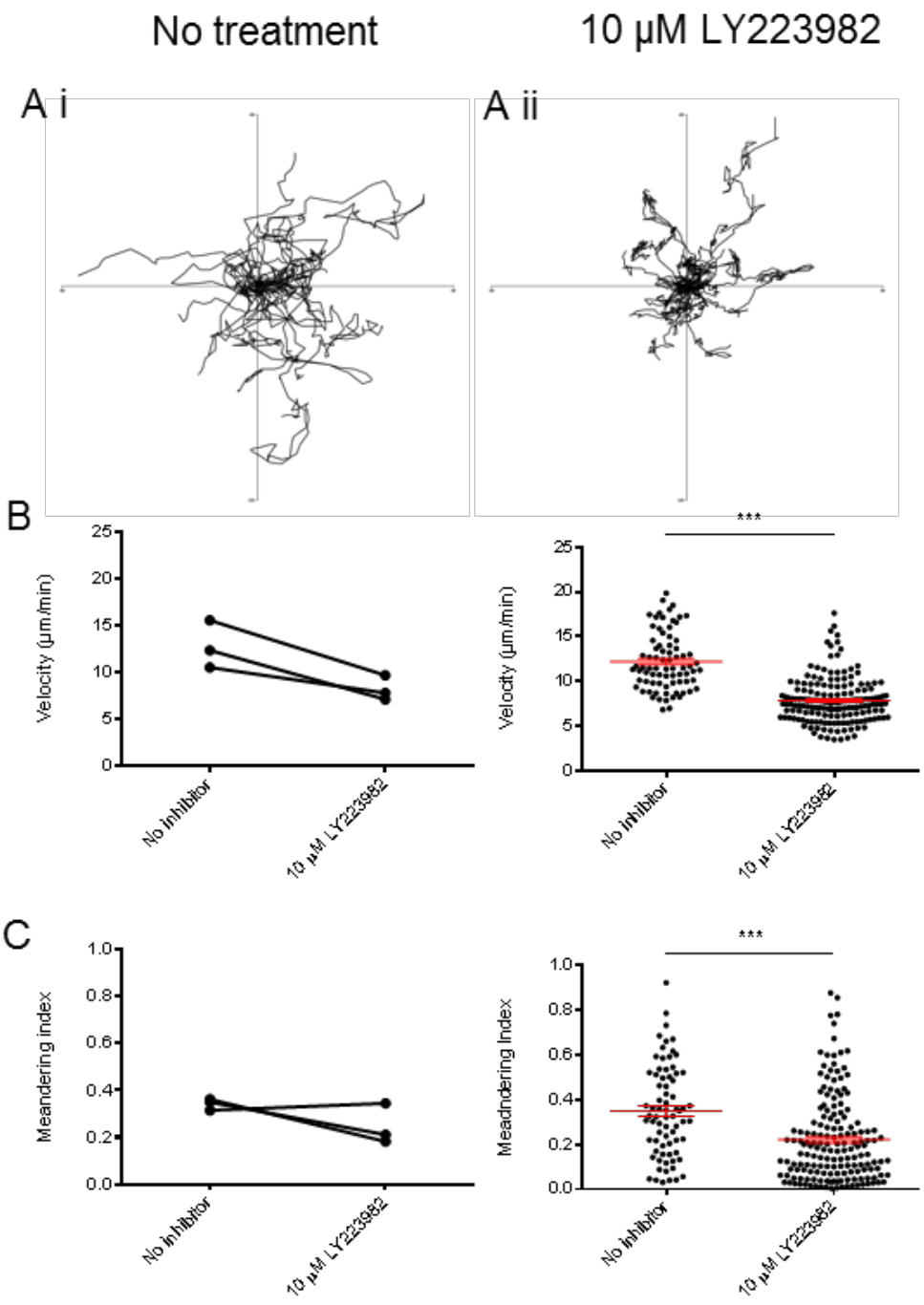

Figure 4.11: Investigating the effect of LTB4 receptor BLT1 inhibition on neutrophil migration in the LdLN following pulmonary *S. pneumoniae* infection.

Explant imaging of the LdLN from B6.LysM Cre x B6.Rosa26 mT/mG F1 mice after 6-12 hours of pulmonary *S. pneumoniae* infection. Neutrophil tracks in X and Y planes, starting position set to zero, before (A i) and after (A ii) addition of 10 µM BLT1 antagonist LY223982. Quantification of neutrophil velocity (B) and meandering index (C) before and after the addition of 10µM LY223982. BLT1 antagonism impaired neutrophil migration in the LdLN. Pooled data from three experiments, n=3, red bars represent mean ± SEM, *** P<0.001 (Mann-Whitney U test).

4.6.7 Role of sphingosine-1-phosphate in neutrophil migration in the lung draining lymph node

Sphingosine-1-phosphate signalling through S1PR1 has an essential role in controlling T cell egress from the LN. S1P receptors are GPCRs, neutrophils express S1PR4, which couples to $G_{\alpha i}$[228]. Neutrophils were located in the LdLN in the lymphatic sinus, densely populating the medulla (Figure 3.5-7). This region has the highest concentration of S1P, produced by lymphatic endothelial cells[117]. The effect of S1P signalling directly on neutrophils and how it affects their migration is not known. However, due to the location of these cells and the effect of PI3Kγ inhibition on neutrophil migration, the effect of S1PR inhibition on neutrophil migration was investigated. The S1PR1,3-5 agonist FTY720 was used. FTY720 binding induces internalization of S1PRs and thus the cells are unresponsive to S1P. Incubation of a cell line expressing GFP-tagged S1PR1 with 10 μM FTY720 showed that receptor internalization was induced, this was comparable to receptor internalization induced by the receptor ligand S1P (Figure 4.12). FTY720 has a high affinity for S1PR4, thus this dose was deemed sufficient to induce internalization of S1PR4. Incubation of the LdLN in 10 μM FTY720 impaired neutrophil migration (Figure 4.13 A). The corresponding videos are videos 20 and 21. The velocity and meandering index of LdLN neutrophils was impaired (Figure 4.13 B and C), however not to the extent of PI3K inhibition. Velocity was reduced by 16.5% as compared to 47.8% by PI3Kγ, meandering index was reduced by 25.1%, but PI3Kγ inhibition caused a 48% reduction.

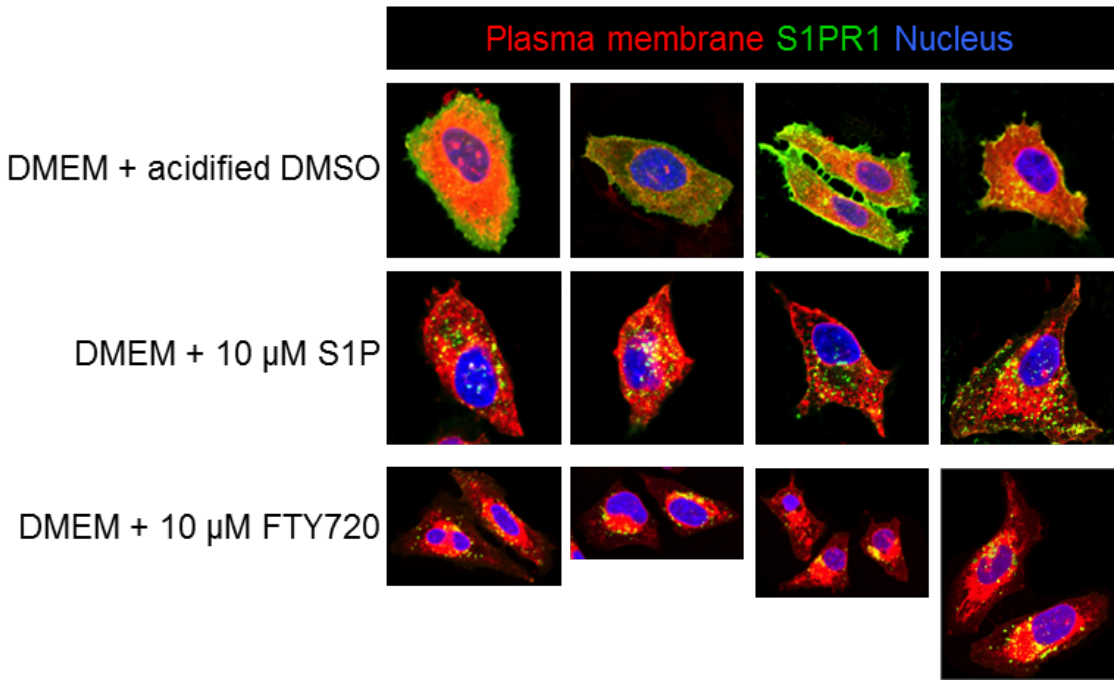

Figure 4.12: 10 µM FTY720 induced S1P receptor internalisation.

The U20S S1PR1-GFP cell line was cultured with serum free DMEM, with either acidified DMSO, 1:100, as a vehicle control (top panel), 10µM S1P (middle) or 10 µM FTY720 (bottom) added for 1 hour. The cells had GFP tagged S1PR1 receptors (green), the plasma membrane was stained with CellMask DeepRed and the nuclei with DAPI (blue). 10 µM FTY720 was sufficient to induce receptor internalisation, and thus insensitivity to S1P.

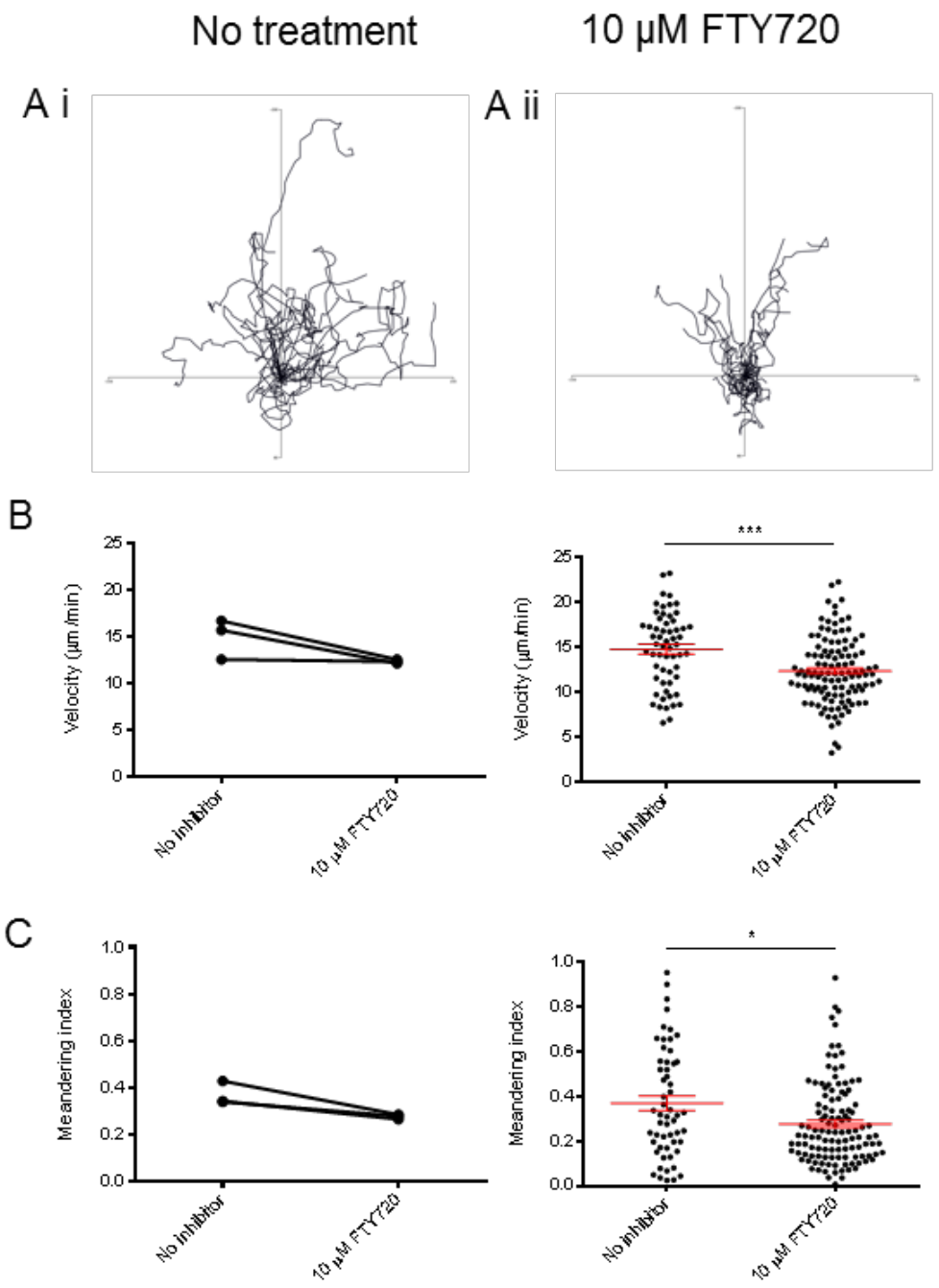

Figure 4.13: Investigating the effect of S1P receptor inhibition on neutrophil migration in the LdLN following pulmonary *S. pneumoniae* infection.

Explant imaging of the LdLN from B6.LysM Cre x B6.Rosa26 mT/mG F1 mice after 6-12 hours of pulmonary *S. pneumoniae* infection. Neutrophil tracks in X and Y planes, starting position set to zero, before (A i) and after (A ii) addition of 10 µM S1PR1,3-5 agonist FTY720. Quantification of neutrophil velocity (B) and meandering index (C) before and after the addition of 10 µM FTY720. FTY720 inhibition impaired neutrophil migration within the LdLN. Pooled data from 3 experiments, n=3, red bars represent mean ± SEM, * P<0.05 and *** P<0.001 (Mann-Whitney U test).

4.6.8 Role of spleen tyrosine kinase in neutrophil migration in the lung draining lymph node

Analysis of mechanisms involved in neutrophil migration in the LdLN found that migration was largely chemotactic, mediated by GPCR and PI3K signalling (Figures 4.9-11,13). However integrin mediated migration is also known to be a key mechanism for neutrophil migration, particularly on 2D surfaces such as vessel walls. Dendritic cell migration in a 3D interstitial environment and LNs is reliant on chemokines, however not integrins. T cells utilize both integrin dependent and independent migratory mechanisms in the LN, depending on their location; in the medulla they utilize integrin mediated migration. Thus it was investigated if neutrophil migration in the LdLN was independent or dependent on integrin signalling.

One the signalling molecule required for integrin mediated signalling is Syk which is activated by multiple integrins in neutrophils, including the β_1, β_2 and β_3 families. Thus GSK provided a highly selective Syk specific inhibitor[161] (referred to as GSK143) to assess the contribution of Syk signalling in neutrophil LdLN migration. This inhibitor works by binding to the ATP binding pocket, preventing access to ATP. GSK143 is highly selective for Syk over other protein kinases, of note the IC50 value of GSK143 for Syk is 30 nM, but 18.9 μM for Zeta-chain-associated protein kinase 70 (ZAP-70), the other member of the Syk kinase family[161]. Syk inhibition did inhibit neutrophil migration (Figure 4.14 A, videos 22 and 23); there was a significant reduction in neutrophil velocity (Figure 4.14 B) and meandering index (Figure 4.14 C), however this impairment was not as marked as the effect observed during PI3Kγ, PI3Kδ or LTB4 inhibition. Velocity was only decreased by 15% and meandering index by 14.4%, consistent with a role for integrins in neutrophil migration in the LdLN.

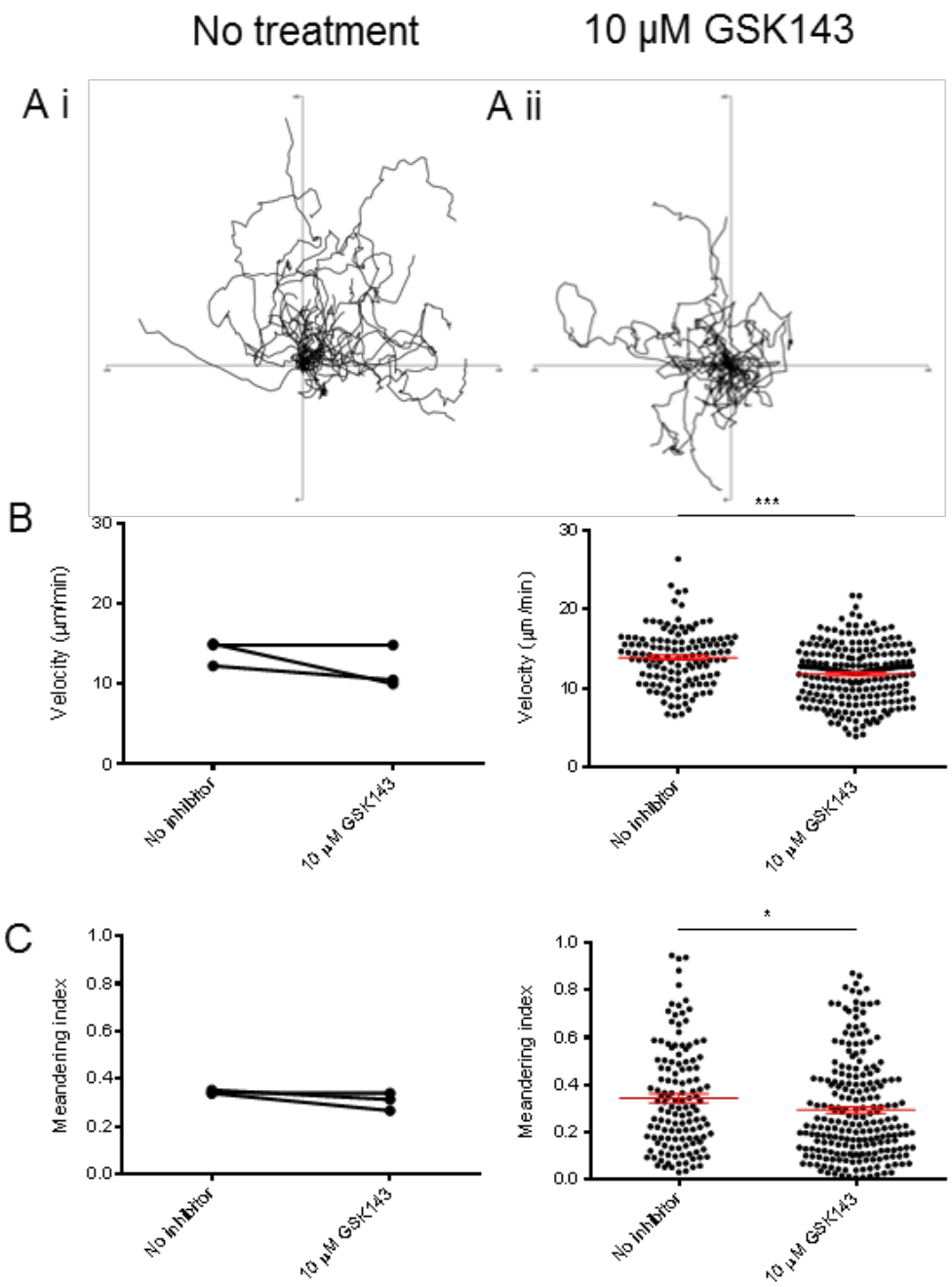

Figure 4.14: Investigating the effect of Syk inhibition on neutrophil migration in the LdLN following pulmonary *S. pneumoniae* infection.

Explant imaging of the LdLN from B6.LysM Cre x B6.Rosa26 mT/mG F1 mice after 6-12 hours of pulmonary *S. pneumoniae* infection. Neutrophil tracks in X and Y planes, starting position set to zero, before (A i) and after (A ii) addition of 10 µM Syk inhibitor GSK143. Quantification of neutrophil velocity (B) and meandering index (C) before and after the addition of 10 µM GSK143. Syk inhibition had a minor negative effect on neutrophil migration in the LdLN Pooled data from three experiments, n=3, red bars represent mean ± SEM, * $P<0.05$ and *** $P<0.001$ (Mann-Whitney U test).

4.6.9 Role of CD11b in neutrophil migration in the lung draining lymph node

Based on the analysis of Syk inhibition, the role of integrin-mediated neutrophil migration was investigated by blocking CD11b on the cell surface, using a known inhibitory antibody clone M1/70. CD11b is known to be key in neutrophil migration *in vitro* and *in vivo* during extravasation, however not in 3D environments. To ensure sufficient antibody was being used to target neutrophils, and that the antibody could penetrate the LdLN explant and bind neutrophil CD11b; the experiment in Figure 4.15 was performed. LdLN were incubated in the same way as they would be for explant imaging; placed in warmed RPMI containing 15 μg/ml purified anti-CD11b M1/70 (a rat antibody) and incubated at 37 °C for 45 min. The LdLN were then digested and single cell suspension prepared. The cell suspension was first incubated with a goat anti-rat secondary antibody to detect the rat anti-CD11b mAb. This incubation was in the presence of 5% goat serum to block non-specific binding of the secondary antibody. The cells were then washed three times to remove the secondary antibody. Finally the cells were stained for neutrophil markers using anti-Gr1 and Ly6C rat antibodies. To ensure no residual secondary antibody was binding the anti-Gr1 and Ly6C antibodies an excess of rat IgG was added to the staining mix, also an anti-CD4 rat antibody was included. CD4 T cells are not known to express CD11b, thus if $CD4^+$ T cells co-stained with the secondary antibody this would be an indication of residual secondary antibody binding to the rat antibodies in the second staining step. Analysis of LdLN neutrophils showed that 15 μg/ml CD11b was sufficient to bind 98.4% (± 0.7) of the neutrophils in the LdLN (Figure 4.15). A low percentage of CD4 T cells co-stained for the secondary antibody (4% ± 0.19), thus residual secondary antibody binding was not a problem. Incubation of an explanted LdLN with anti-CD11b antibody successfully bound neutrophil CD11b, thus blocking neutrophil CD11b. In explant imaging experiments, blockade of CD11b reduced both the velocity and meandering index of neutrophils in the LdLN (Figure 4.16 A-C, videos 24 and 25), effects were strongest on the meandering index.

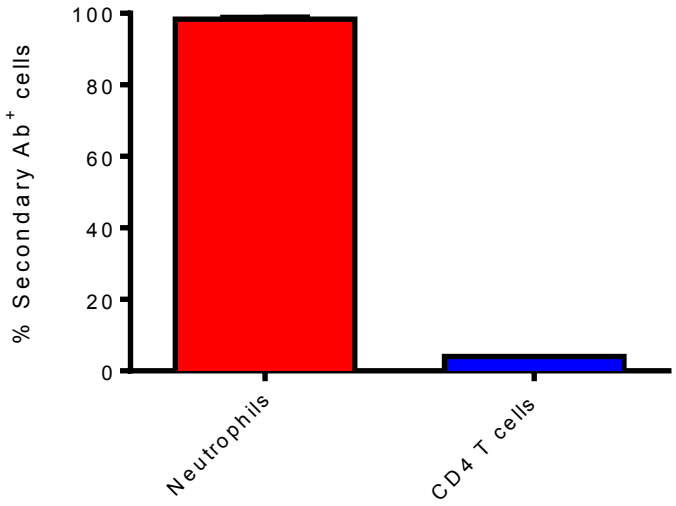

Figure 4.15: Confirmation of *ex vivo* anti-CD11b monoclonal antibody clone M1/70 binding.

A whole LdLN was incubated with 15 µg/ml purified anti-CD11b mAb M1/70 in RPMI medium for 45 mins at 37 °C. The percentage of neutrophils labeled with anti-CD11b was assessed by flow cytometry using a goat anti-rat secondary Ab. CD4 T cells were also stained as a control for non-specific binding on the anti-rat secondary antibody. Nearly all neutrophils were labeled with goat anti-rat secondary Ab. 12 hour, heat inactivated *S. pneumoniae*, representative of one experiment, n=3, bars represent mean + SEM.

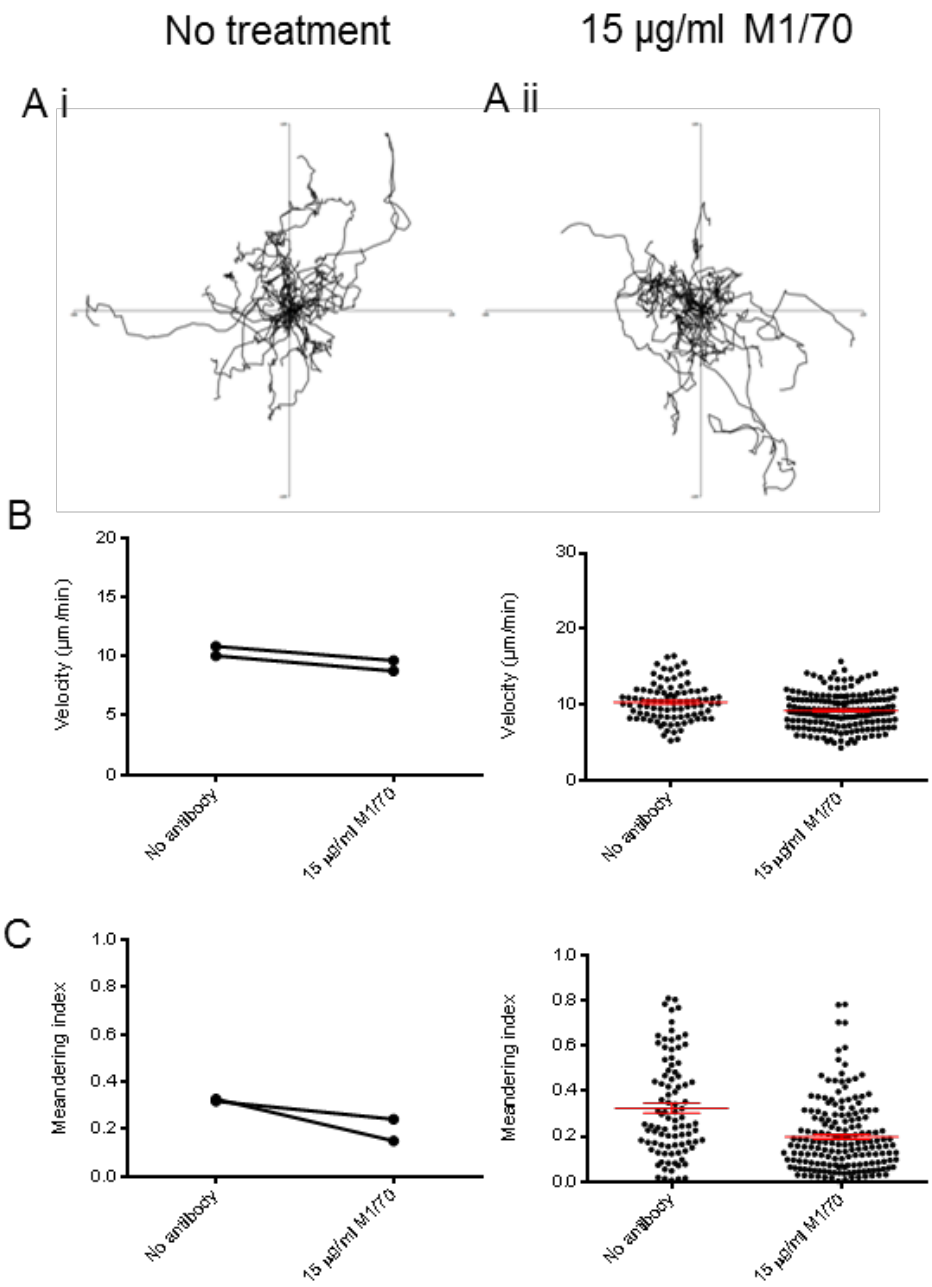

Figure 4.16: Investigating the effect of CD11b blockade on neutrophil migration in the LdLN following pulmonary *S. pneumoniae* infection.

Explant imaging of the LdLN from B6.LysM Cre x B6.Rosa26 mT/mG F1 mice after 12 hours of pulmonary *S. pneumoniae* infection. Neutrophil tracks in X and Y planes, starting position set to zero, before (A i) and after (A ii) addition of 15 µg/ml purified anti-CD11b mAb M1/70. Quantification of neutrophil velocity (B) and meandering index (C) before and after the addition of 15 µg/ml M1/70. CD11b blockade had a minor effect on neutrophil velocity, but a bigger negative effect on neutrophil directionality in the LdLN. Pooled data from two experiments, n=2, red bars represent mean ± SEM.

4.7 Summary of results

- Explant imaging the LdLN was used successfully to investigate neutrophil dynamics in the LdLN *ex vivo*.
- Neutrophils are highly motile in the LdLN following pulmonary *S. pneumoniae* infection, moving at an average velocity of 15.5 ± 0.16 μm/min.
- Neutrophils for dynamic swarms.
- Addition of compounds or blocking antibodies to the explant culture medium can be used to investigate pathways involved in neutrophil migration in the LdLN.
- Neutrophil migration in the LdLN is mainly integrin independent involving PI3K signalling, with a minor role for integrin signalling.

Table 4.1 Analysis of mechanisms involved in neutrophil migration within the LdLN

		Effect on neutrophil migration	
Compound	**Mechanism**	**Velocity**	**Meandering index**
Shionogi-12	PI3Kγ inhibition	↓48%	↓48%
IC87114	PI3Kδ inhibition	↓38%	↓39%
LY223982	BLT1 antagonist	↓35%	↓37%
FTY720	S1PR1,3-5 agonist	↓17%	↓25%
GSK143	Syk inhibition	↓15%	↓14%
M1/70 mAb	CD11b blockade	↓11%	↓39%

4.8 Discussion

4.8.1 Dynamic neutrophil migration in the lung draining lymph node

Neutrophil location and phenotype within the LdLN was described in Chapter 3. Using an explant imaging system, in combination with fluorescent reporter mice and multiphoton laser scanning microscopy, neutrophil dynamics and migration in the LdLN has been investigated in this chapter. Neutrophils were found to be highly dynamic in the sinus region of the LN, moving below the collagen capsule. Neutrophils were only observed shallow in the LdLN, no neutrophils were found deeper in the cortex of the LdLN. This was in line with immunohistochemistry results in Chapter three using frozen section staining. Neutrophils showed classic amoeboid cell morphology with a distinct lamellipod and uropod when migrating in the LdLN. The lobed nucleus was also clear. This was important as in B6.LysM Cre x B6.Rosa26 mT/mG F1 mice monocytes and macrophages are also GFP^+. Thus being able to identify the nuclear morphology reinforces that it was neutrophils that were the highly motile GFP^+ cells. In the literature it is accepted that during inflammation in the lung 'stiffening' of

neutrophils is a part of neutrophil activation. This aids in sequestering these cells in the fine capillary beds within the lung. In this chapter neutrophils seen in the LdLN did not have a 'rigid' shape. The neutrophil cell shape was highly dynamic, allowing it to move through the densely packed LN microenvironment and sense local chemokine gradients. Thus, in agreement with the phenotypic analysis in Chapter three, LdLN neutrophil may not be fully activated, allowing them to move freely within the LdLN.

Neutrophils were observed to be highly dynamic, moving at an average speed of 15.5 μm/min. Neutrophils were moving at a greater velocity at 6 and 12 hours post pulmonary *S. pneumoniae* infection. This was in line with when their numbers peaked in the lymph node. Thus perhaps this enhancement in speed was due to factors made by the neutrophils themselves; more neutrophils, lead to more released factors, resulting in increased neutrophil velocity. These factors could have been chemoattractants, for example LTB4, this is known to be produced by neutrophils to enhance recruitment of other neutrophils. This data supports the hypothesis that how cells move is location dependent rather than cell type specific.

4.8.2 *Ex vivo* explant imaging

A caveat must be considered when analyzing neutrophil speed and behavior in this explant system. Great care was taken to excise the LdLN, and remove fat, causing as little damage or disturbance to the LdLN as possible. However, this process would have undoubtedly caused sterile injury. The multiphoton laser may have added to this effect. However no tissue damage or cell was observed during 4-5 hours of imaging. Sterile injury can induce DAMP production and subsequent inflammatory mediator release, which may activate the neutrophils further causing them to migrate faster. Intravital microscopy could have been a better method, however the surgery required would have also generated sterile injury, also the LdLN is not easily assessable without disturbing the heart and lungs. In addition, to examine neutrophil migration in the LdLN *in vivo* using the compounds used here would have been impossible. Blocking PI3K, LTB4 or Syk would have prevented neutrophil extravasation and recruitment to the lung and LdLN. For this same reason using mice with gene deficient neutrophils, for example neutrophils lacking integrins, would not have been possible. In the explant system neutrophils were already in the LdLN, thus by adding the compound or blocking antibody to the explant culture medium, pathways involved in neutrophil migration could be investigated. Despite the caveats to this system it provides meaningful methodology to understand molecular mechanisms driving neutrophil migration and behaviors in lymph nodes.

4.8.3 Molecular mechanisms involved in neutrophil dynamics in the lung draining lymph node: Phosphoinositide 3-kinase γ

The PI3Kγ signalling pathway was key for neutrophil migration within the LdLN, inhibition of this pathway impaired both the velocity and directional migration of neutrophils. Phosphoinositide 3-kinase γ is activated by GPCR signalling; therefore neutrophil migration was highly dependent on GPCR signalling. In the brain it was found that CXCL10 aids CD8 T cells to locate *T. gondii* parasites by aiding a generalised Levy walk strategy as opposed to Brownian walks[229]. The generalized Levy walk involves short spurts of movement followed by scanning of the environment for a target, then another spurt of movement. Brownian migration is random cell migration. Thus perhaps in the LN chemokine signalling supports more directed neutrophil migration similar to a levy walk, however inhibition of this signalling causes neutrophil migration to become more random, like Brownian walking. Mathematical analysis of the raw data would address this question; however that was not done in this project.

Phosphoinositide 3-kinase γ inhibition did not fully inhibit neutrophil migration; it reduced neutrophil velocity by 48%. This indicates that neutrophil migration in the LdLN is not entirely dependent on PI3Kγ and other signalling pathways are also being utilised. The total reduction in neutrophil velocity/meandering index was an average of all the neutrophils tracked, however neutrophils did not respond homogeneously to PI3Kγ inhibition; some cells did not move at all and were stuck to one position, however others were still able to migrate, all be it at a reduced velocity, with more meandering tracks taken, whilst other cells looked uninhibited and moved as normal. This could reflect differences in chemokine receptor levels and/or chemokine receptor types on individual cells. Different cells may be responding to varying local chemokine gradients, or 'prioritising' different chemokines. Indeed PI3Kγ signalling is dispensable in chemotaxis to the 'end-point' chemoattractant fMLP, which instead relies on p38 MAPK[29,30]. Thus some cells in the LdLN may be migrating in a p38 MAPK dependent as opposed to PI3Kγ dependent manner. Additionally it is possible that neutrophils have an inherent migratory capacity that is independent of exogenous cues, and does not require integrin interactions in order to undergo amoeboid type migration.

4.8.4 Molecular mechanisms involved in neutrophil dynamics in the lung draining lymph node: Phosphoinositide 3-kinase δ

Phosphoinositide 3-kinase δ inhibition using IC87114 also resulted in inhibition of neutrophil chemotaxis. This result is both interesting and puzzling. The role of PI3Kδ signalling in neutrophil migration is not clear from the literature, additionally the signalling pathways it is downstream of are unclear. It has been reported to be involved in integrin signalling,

downstream of Syk, and is important for neutrophil TEM. However it has also been demonstrated to have a role in chemokine signalling and chemotaxis. Due to the minor effect of Syk inhibition and major effect of PI3Kγ inhibition, the effect of PI3Kδ inhibition on neutrophil migration in the LdLN would indicate that PI3Kδ is involved in GPCR signalling and not integrin signalling. PI3Kγ is also involved in integrin outside-in signalling for activation of integrins, however, as with PI3Kδ, the minor effect of Syk inhibition and major effect of PI3Kγ indicates that it is GPCR signalling that PI3Kγ is involved in in LdLN neutrophil migration.

It is important to note that whilst interpretating the results from experiments using IC87114 there may have been an additional partial inhibition of PI3Kγ due to a narrow window of selectivity for PI3Kδ over PI3Kγ. The IC87114 IC_{50} value for PI3Kγ is 29 μM, thus at the concentration used; 10 μM, there may have been some inhibition of PI3Kγ. However the calculation of IC87115 IC_{50} values was performed using purified PI3Ks in a kinase assay. This assay involves incubating recombinant PI3K proteins with PIP2, ATP and IC87114, and measuring the amount of PIP3 produced compared to samples without any inhibitor. This assay is very different to the *ex vivo* tissue explant system used here. Thus an off target effect on PI3Kγ may not be great.

4.8.5 Molecular mechanisms involved in neutrophil dynamics in the lung draining lymph node: Leukotriene B4

Leukotriene B4 receptor BLT1 inhibition resulted in an impairment of neutrophil chemotaxis. Thus in the LN neutrophils are moving towards LTB4, which is produced by neutrophils themselves[227]. The inhibition of neutrophil migration was not as great as PI3Kγ inhibition, thus neutrophils must be responding to other chemokines as well as LTB4, demonstrating the redundancy of neutrophil chemoattractants. However, a titration of the BLT1 antagonist was not performed although the levels of inhibitor used in these experiments was the same as that used historically in the literature. Thus it is possible that a higher concentration of the antagonist could produce a larger effect on neutrophil migration. Experiments blocking other major neutrophil chemokine receptors, for example CXCR2 could provide evidence as to which other chemokines the neutrophils are responding to in the LdLN.

4.8.6 Molecular mechanisms involved in neutrophil dynamics in the lung draining lymph node: Sphingosine-1-phosphate

Sphingosine-1-phosphate signalling is crucial for T cell egress from the LN, desensitization of S1PR1 by FTY720 blocks T cell egress. This occurs in areas of the LN where neutrophils populate. Neutrophils express S1PR4, a S1P receptor, thus due to the effect of PI3Kγ inhibition and that neutrophils are located in areas of high LN S1P concentration; the role of S1PR4 was

investigated. Indeed, FTY720, which binds S1PR4, caused inhibition of neutrophil migration, however not to the level of PI3Kγ, PI3Kδ or LTB4 inhibition. Thus S1P signalling has a role in neutrophil migration, but secondary to that of PI3Kγ, PI3Kδ and LTB4.

Little is known of the role of S1P and S1PR4 on neutrophils. In mice that lack S1P lyase, the enzyme that is responsible for breaking down S1P, there is neutrophilia in the blood. This is attributed to a disruption in the IL-23/IL-17/G-CSF neutrophil homeostasis feedback loop due to the inability of neutrophils to infiltrate tissues in these mice, and thus elevated IL-23 mRNA, and serum IL-17 and G-CSF. Mice deficient in both S1P lyase and S1PR4 showed a partial reduction in neutrophilia, however this could not be attributed to a direct effect on neutrophils or restoration of the ability of neutrophil to infiltrate tissues[230]. The effect of S1P on neutrophil migration could be indirect, involving an intermediate cell type, for example lymphatic endothelial cells, that in turn release factors effecting neutrophils. Indeed studies have found that S1P acting on other cell types, for example airway smooth muscle cells[231] and lung endothelial cells[232] induces the production of chemokines by these cells that induce neutrophil migration.[233]

4.8.7 Molecular mechanisms involved in neutrophil dynamics in the lung draining lymph node: Spleen tyrosine kinase and CD11b

Spleen tyrosine kinase signalling was found to have a role in neutrophil migration, however blocking Syk did not cause as great impairment on neutrophil migration as seen with PI3Kγ blockage; a 14% decrease in velocity and meandering index as compared to a 47% decrease. This result indicated integrin signalling may have been having an effect on neutrophil migration. Thus to investigate further antibody mediated blockage of the $\alpha_M\beta_2$ integrin (CD11b) was investigated. CD11b blockade produced a larger inhibitory effect on neutrophil migration than Syk inhibition. This might indicate that Syk is not heavily involved in integrin-mediated migration where-by integrins form adhesions with extracellular ligands, linking the intracellular actin filaments to the extracellular environment to generate force and forwards locomotion. However the result with CD11b blockade may be flawed. In areas where large GFP^+ macrophages were observed, neutrophil migration did not look as previously observed. Neutrophils appeared to be stuck to the macrophages, the interaction did not look similar to interactions between neutrophils and macrophages in the absence of the M1/70 antibody. Macrophages in the LdLN could be binding the Fc region of the M1/70 antibody, thus hindering neutrophil migration. This possibility could be eliminated through using Fab or Fab2 fragments, however this was not done. Alternatively, the presence of the antibody alone could hinder neutrophil migration. Neutrophils express high levels of CD11b, thus large amounts of the M1/70 antibody would bind the surface of the neutrophils. This coating of large protein molecules could modify the migratory capacity of these cells.

4.8.8 Neutrophil migration within the lung draining lymph node is dependent on chemokines and integrins

In summary, explant imaging experiments combined with inhibitor compounds reveal that neutrophil migration in the LdLN is mainly chemokine-GPCR driven, with a small role for integrins. Chemokines and integrins may work in synergy, driving optimum neutrophil migration. This could be explained by the medulla microenvironment where neutrophils were found to densly populate. Neutrophil migration within the ECM rich environment of the skin is integrin independent, migration is dependent on chemokines and 'squeezing' of cells through the dense collagen meshwork found in tissue[33,217]. Whilst migration of neutrophils within the LN was mainly chemokine driven, the lack of dense collagen fibers may mean that neutrophils also need help from integrins to move through the medullary sinus, this could involve binding integrin ligands on stromal cells or lymphatic endothelial cells. Indeed this is true for T cells; their migration in the paracortex is mainly chemotactic, however is not integrin independent. However their adhesive migration on lymphatic endothelial cells in the medulla is dependent on CD11a-ICAM-1 interaction, and is important for their retention in the LN[223]. Although the underlying stromal networks and ECM of the cortex and B cell follicles has been studied in detail, far less is known about the networks and ECM composition of the medullary sinus.

4.9 Conclusion

In conclusion, neutrophils are highly dynamic and motile in the LdLN, form swarms and closely interacting with macrophages. Neutrophil migration is mainly chemokine driven involving PI3K signalling, with LTB4 having an important role. Integrin signalling through Syk has a minor role in neutrophil migration within the LdLN. Chapters 3 and 4 have characterized neutrophils within the LdLN, however the factors driving their recruitment to the LdLN has not been addressed. Chapter 5 investigates the recruitment of neutrophils to the LdLN following pulmonary *S. pneumoniae* infection.

Chapter 5: Investigating neutrophil recruitment to the lung draining lymph node

5.1 Neutrophil recruitment to tissue draining lymph nodes

The factors involved in driving trafficking of neutrophils from an infection site to the dLN have not been well investigated. In a model of footpad inoculation with *P. aeroguinosa*, neutrophil recruitment to the dLN (popliteal LN) is mediated by SSMs through their production of IL-1β. In mice depleted of macrophages by clodronate liposomes, and also IL-1R deficient mice, neutrophil recruitment to the dLN during *P. aeroguinosa* infection is greatly reduced[139]. The most detailed study of neutrophil LN homing has found that following OVA challenge in the footpad of mice immunized with OVA/CFA, neutrophils enter the dLN from both the blood, through HEVs, and the lymph through lymphatic vessels[234]. This occurs rapidly, large numbers of neutrophils are found in the dLN at 6 hours post-OVA challenge. Entry through HEVs requires the selectins L-selectin and PSGL1 and integrins CD11b and CD11a. These integrins, but not the selectins are also required for neutrophil dLN entry through lymphatics. The chemokine receptor CXCR4 and S1P receptor S1PR4 are required for entry through both the HEVs and lymphatics. Indeed treatment of OVA/CFA immunised mice with FTY720 before CFA challenge markedly inhibited neutrophil migration to the dLN[234].

5.2 Summary

Little is known of the exact mechanisms by which neutrophils are recruited to dLNs. Previous studies have found a role for SSMs through production of IL-1β[139]. In Chapter 3.4.4 neutrophils were found to be located in the LdLN strictly in lymphatic areas, thus it is plausible that SSM could also be having a role in neutrophil recruitment to the LdLN during pulmonary *S. pneumoniae* infection. Lymphatic endothelial cells are known to be a key source of S1P in the LN, in Chapter 4.6.7 it was found that FTY720 desensitisation of S1PR1,3-5 inhibited neutrophil motility in the LdLN. Thus the finding that FTY720 inhibited neutrophil migration to the dLN[234] supports the hypothesis that S1P may have a role in neutrophil recruitment to and retention in the LdLN.

5.3 Aims

- Investigate the role of LN SSM in recruitment of neutrophils to the LdLN.
- Investigate the role of S1P signalling in neutrophil recruitment to and retention in the LdLN.

5.4 Results

5.4.1 Investigating the role of subcapsular macrophages on neutrophil recruitment to the lung draining lymph node following pulmonary *S. pneumoniae* infection

The role of SSM in recruitment of neutrophils to the LdLN during pulmonary *S. pneumoniae* was investigated by depleting this macrophage population. In order to deplete SSM DTx mediated depletion was used. Subcapsular sinus macrophages express CD11c, thus B6.CD11c Cre x B6.Rosa26 iDTR F1 mice were used, this is a methodology that has been employed in other studies[108]. In these mice once CD11c expression is turned on Cre recombinase is expressed and made. Cre recognizes loxP sites either side of a 'stop' site upstream of the gene for the DTR, thus $CD11c^+$ cells express the DTR and are susceptible to DTx. This excision is irreversible. If the cell stops expressing CD11c it will still express the DTR. Figure 5.1 shows that, compared to PBS treated mice, 48 hours after i.p injection with 100 ng of DTx CD11c cells were absent from the LdLN and $CD169^+$ SSM were depleted, however $CD169^+$ MSM were not. Thus SSM could be depleted using DTx mediated depletion.

To investigate neutrophil recruitment in these mice one group received PBS as a control, and another group received 100 ng DTx i.p. After 36 hours half of each grouped received i.n PBS and the other i.n *S. pneumoniae*. Following 12 hours of infection the mice were culled and neutrophil recruitment to the LdLN analysed by flow cytometry. Figure 5.2 shows that in i.p PBS treated mice, upon infection there was a significant recruitment of neutrophils to the LdLN. However, in DTx treated mice the number of neutrophils recruited during infection was much lower. Thus $CD11c^+$ cell depletion reduced the number of neutrophils recruited to the LdLN. The BAL fluid and lungs of these mice were also investigated. It was found that, like in the LdLN, DTx mediated CD11c cell depletion caused a reduction in the number of neutrophils recruited following infection (Figure 5.3). Thus $CD11c^+$ cells were important for neutrophil recruitment to the lungs during pulmonary *S. pneumoniae* infection.

In Chapter 3.4.7 (Figure 3.10) it was shown that a small percentage of neutrophils in the LdLN express CD11c, thus this was further investigated using B6.Rosa26 mT/mG mice crossed with B6.CD11c Cre mice to generate B6.CD11c Cre x B6.Rosa26 mT/mG F1 mice. In these mice, any cell that was $CD11c^+$, or importantly had ever expressed CD11c, was GFP^+. The blood and LdLN of these mice were analysed by flow cytometry. Figure 5.4 shows that, surprisingly on average 44% (± 12) of blood neutrophils were GFP^+. Interestingly three distinct populations were observed; GFP^-, GFP^{int} and a distinct population of GFP^{hi} neutrophils. Six hour pulmonary

S. pneumoniae infection did not significantly alter the percentage of GFP^+ neutrophils. In the LdLN similar percentages were also observed. In control LdLN from mice receiving i.n PBS, of the small numbers of neutrophils found, indeed 46% (± 9) were GFP^+, similar to blood neutrophils. Following infection this percentage increased to 66% (± 1.6) in the LdLN. Interestingly in the LdLN only the GFP^- and GFP^{hi} populations of neutrophils were observed.

In chapter 3.4.7 (Figure 3.10); it was also found that a small percentage of neutrophils express MHC II in the LdLN. Thus MHC expression on the GFP^- and GFP^+ neutrophils was investigated. There was a clear cut difference found, GFP^- had very low expression of MHC II, GFP^+ also had low expression of MHC II, however this was three fold higher than the expression on GFP^- cells (Figure 5.5). Thus CD11c expression on neutrophils correlated with expression of MHC II.

These mice were also investigated by explant imaging, 6 hours after pulmonary *S. pneumoniae* infection. Figure 5.6 (A) shows a still from video 26, (B) and (C) are Z stack, 3D images taken at higher resolution. Motile GFP^+ cells were observed that had the same dynamics as neutrophils in Chapter 4 explant imaging experiments. These GFP^+ cells had distinct lobed nuclear morphology, thus were neutrophils. Most interestingly in the LdLN there were many different populations of GFP^+ cells with various morphologies. Many of the vessels, as highlighted by high TdTomato expression, were lined with long, thin GFP^+ cells. Thus CD11c was expressed by a wide range of cells in the LdLN, including neutrophils.

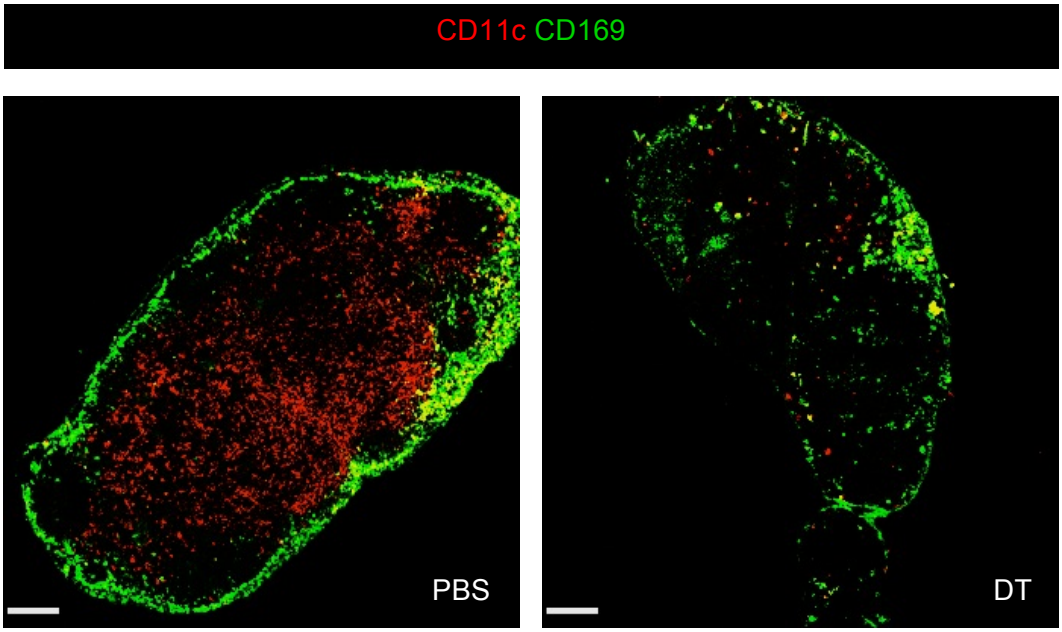

Figure 5.1: Subcapsular macrophage depletion following DT treatment of B6.CD11c Cre x B6.Rosa26 iDTR F1 mice.

Immunohistochemistry of frozen sections of LdLN from B6.CD11c Cre x B6.Rosa26 iDTR F1 mice. Sections were stained for CD169 (green) and CD11c (red). Mice received 100 ng DTx or 100 µl PBS i.p, after 48 hours LdLN removed. Scale bars = 130 µm. DTx treatment depleted $CD11c^{+}$ cells and also SSM, but not MSMs.

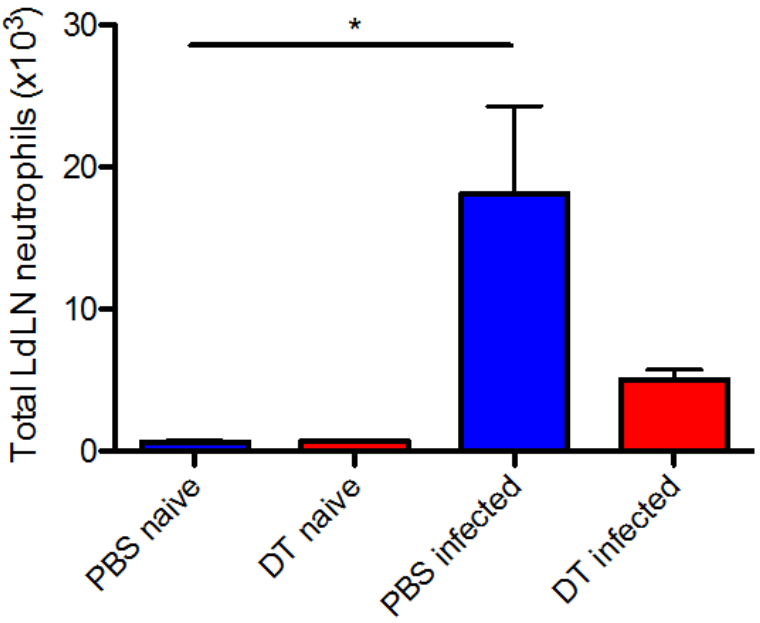

Figure 5.2: CD11c depletion resulted in a reduction of the number of neutrophils migrating to the LdLN.

B6.CD11c Cre x B6.Rosa26 iDTR F1 mice received 100 ng DT or 100 µl PBS i.p, after 48 hours half of each treatment group received intranasal *S. pneumoniae* and the other half intranasal PBS. At 12 hours of infection LdLN were removed and neutrophil numbers analysed by flow cytometry. CD11c depleted mice had fewer neutrophils recruited to the LdLN. n= 3-4, bars represent mean + SEM, * $P<0.05$ (Kruskal-Wallis test with Dunn's post hoc test).

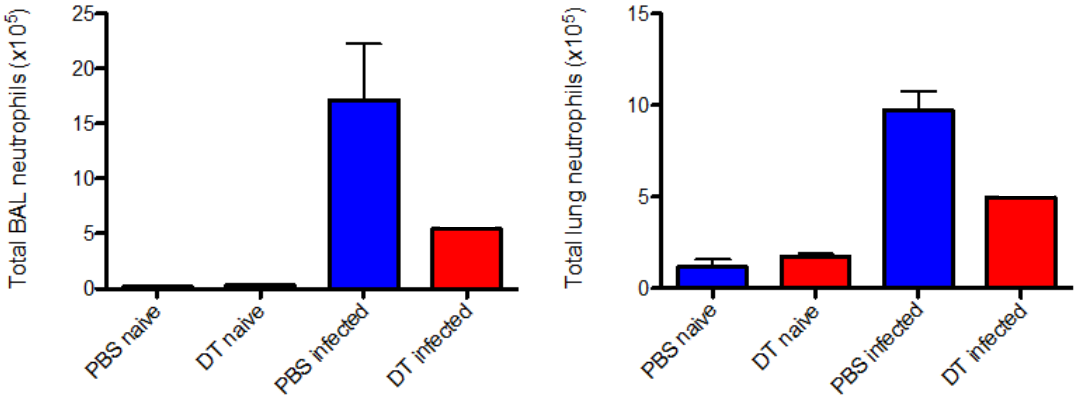

Figure 5.3: CD11c depletion resulted in a reduction in the number of neutrophils recruited to the lung.

B6.CD11c Cre x B6.Rosa26 iDTR F1 mice received 100 ng DT or 100 µl PBS i.p, after 36 hours half of each treatment group received intranasal *S. pneumoniae* and the other half intranasal PBS. At 12 hours of infection BAL was performed and lungs removed, neutrophil numbers were analysed by flow cytometry. CD11c depleted mice had fewer neutrophils in the BAL fluid and lung tissue. n=2-3, bars represent mean + SEM.

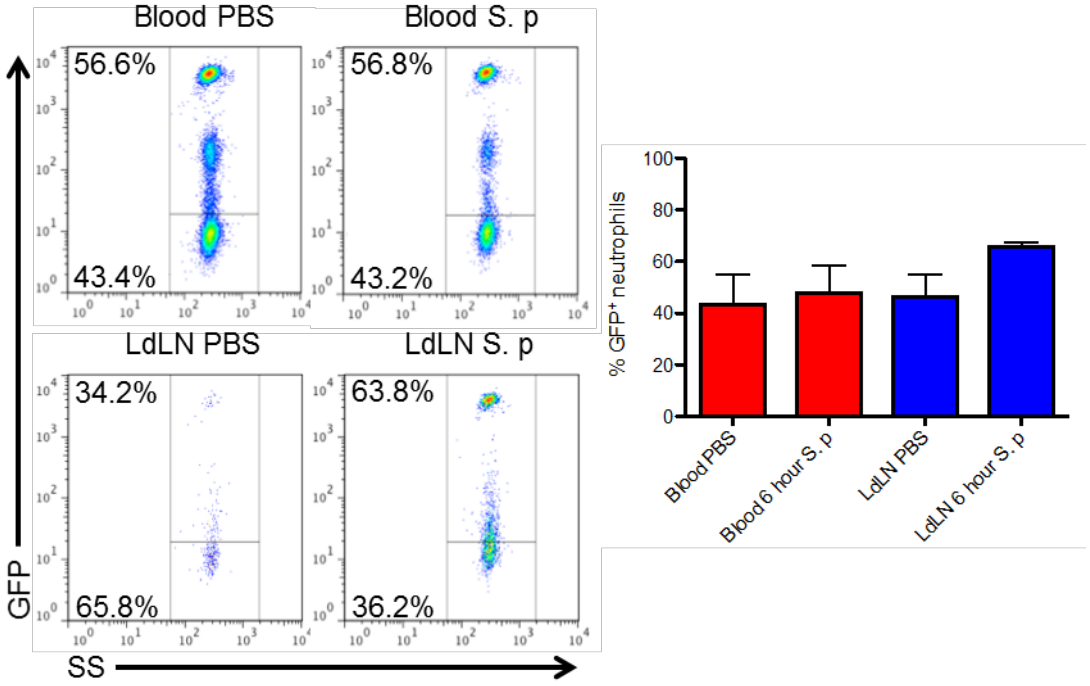

Figure 5.4: GFP expression on neutrophils in B6.CD11c Cre x B6.Rosa26 mT/mG F1 **mice.** (A) Representative flow plots from B6.CD11c Cre x B6.Rosa26 mT/mG F1 mice following intranasal PBS or 6 hour *S. pneumoniae* infection. Gated on $CD11b^{+}$ $Ly6C^{int}$ $Ly6G^{+}$ cells. (B) Quantification of the number of GFP^{+} neutrophils in the blood and LdLN. A high percentage of neutrophils in the blood and LdLN are GFP^{+}. n= 3, bars represent mean + SEM, representative.

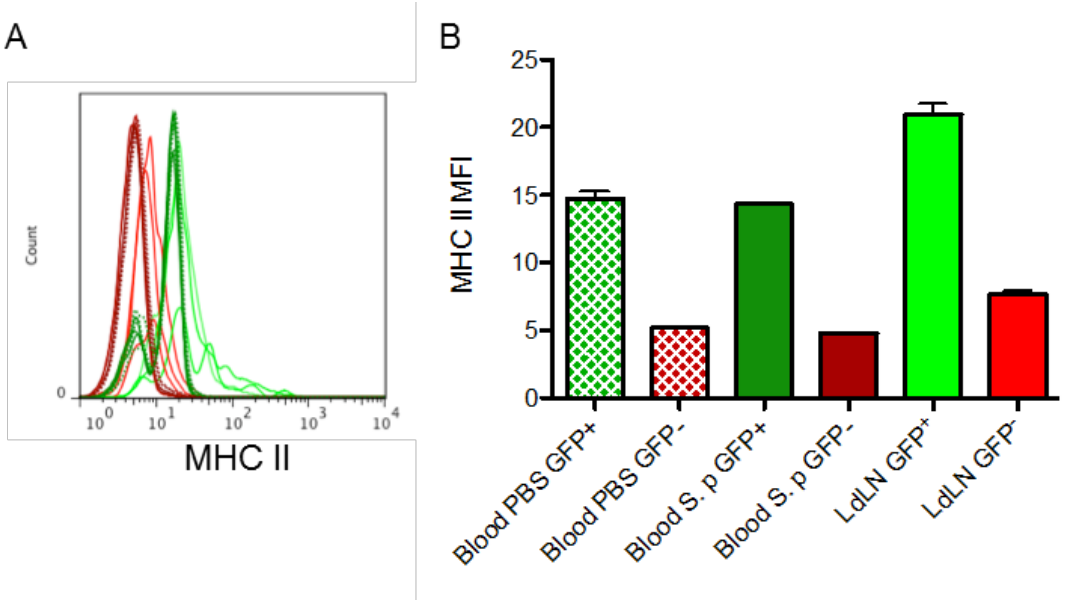

Figure 5.5: MHC II expression on neutrophils from B6.CD11c Cre x B6.Rosa26 mT/mG F1 **mice.**

(A) Histogram overlays showing MHC II expression on GFP^+ and GFP^- neutrophils in B6.CD11c Cre x B6.Rosa26 mT/mG F1 mice following intranasal PBS or 6 hour *S. pneumoniae* infection. Blood GFP^+ neutrophils (PBS treated); dark green dotted line, blood GFP^- neutrophils (PBS treated); dark red dotted line, blood GFP^+ neutrophils (*S. pneumoniae* infected); dark green solid line, blood GFP^- neutrophils (*S. pneumoniae* infected); dark red solid line, LdLN GFP^+ neutrophils (*S. pneumoniae* infected); bright green solid line and LdLN GFP^- neutrophils (*S. pneumoniae* infected); bright solid red line. LdLN neutrophils from PBS treated mice not shown due to low numbers. (B) Quantification of MHC II MFI. The GFP^+ neutrophils had the highest MHC II MFI, in both the blood and LdLN. n= 3, bars represent mean + SEM.

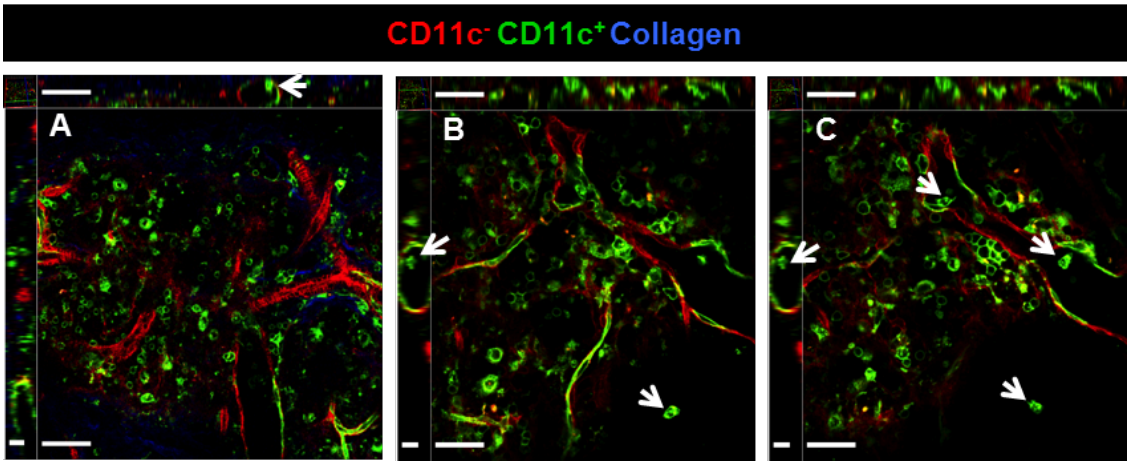

Figure 5.6: CD11c expression in the LdLN following pulmonary infection with *S. pneumoniae.*

(A) Still from explant imaging video of a LdLN from a B6.CD11c Cre x B6.Rosa26 mT/mG F1 mouse at 6 hours of infection. (B) and (C), Z stack image of the same LdLN at two different Z depths. Arrows identify motile GFP^+ cells with neutrophil cell morphology and nuclear morphology. Many cell types of various morphology were GFP^+. Scale bars; left= 51 µm X, 16 µm Z, middle and right= 33 µm X, 11 µm Y.

5.4.2 Investigating the role of S1P signalling in neutrophil recruitment to, and retention in the lung draining lymph node

In Chapter 4.6.7 (Figure 4.13) it was found that FTY720 inhibited neutrophil migration within the LdLN. The exact mechanism of this inhibition was not clear; neutrophils only express S1PR4 highly[234], however there is sparse literature on the effect of S1P-S1PR4 signalling on neutrophils themselves. Additionally, there is very little literature on S1PR4 signalling in general, the studies that have been done do not present clear functions specifically of S1PR4 signalling. The bulk of the literature on S1P signalling is on S1P-S1PR1 signalling and its function in regulating cell migration, in particular T cell egress from the LN. Due to the results in chapter 4.6.7 it was investigated if S1P signalling had an effect on neutrophil migration to, or retention in the LdLN by using FTY720.

Mice were treated with either 1 mg/kg FTY720 i.p, or PBS only as a vehicle control. After 12 hours all mice received i.n inoculation with *S. pneumoniae*. At 12 hours post infection (24 hours post FTY720 dose) blood, lungs and LdLN were removed and analysed by flow cytometry. Figure 5.7 (A) confirms that FTY720 was effective and induced lymphopenia in the blood, also a mild reduction in neutrophil numbers (Figure 5.7 B). In the lungs there was a small, but not significant reduction in neutrophil numbers in the lung (Figure 5.7 C), whereas in the LdLN there was a small, but not significant, increase in neutrophils (Figure 5.7 D). Thus FTY720 (S1PR1,3-5 agonist) treatment had no significant effect in neutrophil migration to or retention in the lung and LdLN during 12 hour pulmonary *S. pneumoniae* infection.

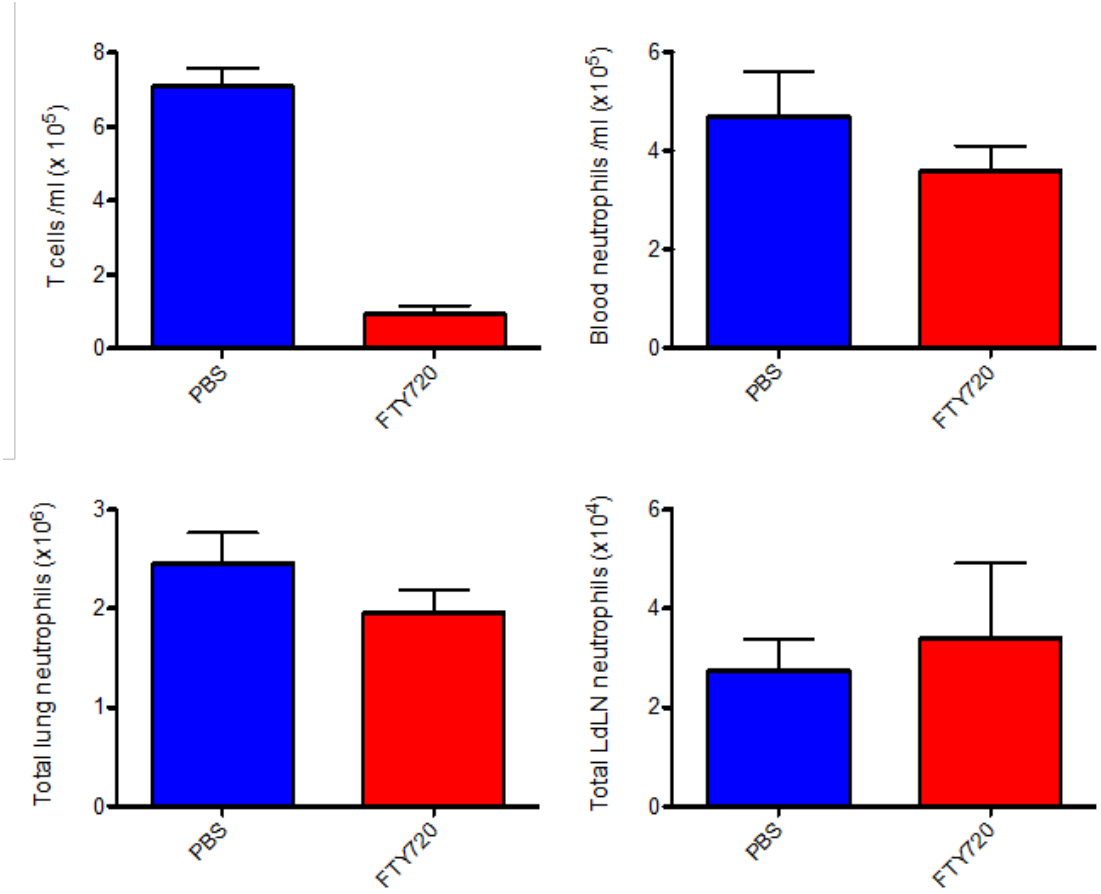

Figure 5.7: FTY720 treatment had no effect on neutrophil recruitment to the LdLN following pulmonary infection with *S. pneumoniae.*

Mice were treated with either PBS or 1 mg/kg FTY720 i.p, after 12 hours both groups were infected intranasal with *S. pneumoniae.* At 12 hours of infection blood, lungs and LdLNs removed and neutrophil numbers analysed by flow cytometry. (A) Number of T cells (gated on TCR β^+ cells) and (B) neutrophils per ml of blood. (C) Total number of neutrophils in the lung, and (D) LdLN. A reduction of T cells in the blood confirmed that FTY720 was effective, however it had little effect on neutrophil numbers in the blood, or their recruitment to the lung or LdLN. (A) n= 3, (B-D) n= 4, bars represent mean $\pm$ SEM.

5.4.3 Summary of results:

- CD11c cells are involved in neutrophil recruitment to the lungs during pulmonary *S. pneumoniae* infection.
- A large percentage of neutrophils (44%) expressed CD11c during their life time.
- CD11c expression on neutrophils correlated with MHC II expression.
- S1P signalling had no role in neutrophil recruitment to or retention in the LdLN.

5.5 Discussion

5.5.1 CD11c cell mediated recruitment of neutrophils to the lung *during S. pneumoniae* infection

CD11c cells were found to be key in neutrophil recruitment to the lungs. This was perhaps mainly due to alveolar macrophage and lung DC depletion, these cells are known to recruit neutrophils to the lung during infection and inflammation[86,88]. These cells are CD11c positive[235] and thus would have been depleted, however this was not assessed. Interestingly alveolar macrophage depletion during *S. pneumoniae* infection was found to result in increased neutrophil influx into the lung, the opposite of what was observed here[236,237]. Thus perhaps more complex processes were going on in the lungs, or mouse as a whole, in response to the DTx treatment.

The experiments did not address neutrophil recruitment to the LdLN. Neutrophil migration to the lung was inhibited and thus it is difficult to draw conclusions about recruitment to the LdLN. However when looking at DTx treated mice alone, there was indeed neutrophil recruitment to the LdLN when compared to uninfected mice. Thus it is possible that recruitment of neutrophils to the LdLN was intact, however there were fewer neutrophils in the lung to migrate there. To address if SSM have a role in neutrophil recruitment to the LdLN without affecting alveolar macrophages or DC populations CD169-DTR mice could be used. This however would also deplete MSM.

The use of B6.CD11c Cre x B6.Rosa26 mT/mG F1 demonstrated that many cells in the LdLN express CD11c, including neutrophils. CD11c expression was not limited to DCs. Indeed during *S. pneumoniae* infection there was an increase in GFP^+ $CD11c^+$ neutrophils. This supports phenotypic analysis performed in Chapter 3.4.7 using antibody staining, and links MHC II and CD11c co-expression by neutrophils. It also shows that these surface molecules are upregulated by neutrophils in response to infection.

This reporter mouse also demonstrated an issue with the B6.CD11c Cre x B6.Rosa26 iDTR F1 mouse strain. In the LdLN of these mice (also the blood) there were many GFP positive cells of different morphologies, suggesting various cell populations express CD11c at some point. In the B6.CD11c Cre x B6.Rosa26 iDTR F1 these cells would be depleted. This could cause a significant disturbance to the structure and homeostasis of the LdLN. Thus in experiments comparing DTx treated mice to PBS treated mice a like-for-like comparison was not being made. The disturbance to LN structure due to DTx treatment could alter immune cell entry and exit. Indeed large thin GFP^+ cells were observed lining LN vessels, thus their depletion could damage vessel integrity. In addition the DTx induced cell death would have caused DAMP release and sterile inflammation. Thus when comparing PBS treated mice to DTx treated mice, the DTx treated mice are already in an inflamed state and not at homeostasis.

5.5.2 Sphingosine-1-phosphate receptor signalling and neutrophil recruitment to the LdLN

In the LdLN it was found that FTY720 treatment had a minor effect on neutrophil migration within the LN, however no effect on neutrophil recruitment to the LdLN, thus S1PR signalling didn't have a role in neutrophil recruitment to the LdLN during acute pulmonary *S. pneumoniae* infection. This is contrary to recent results that found that the same dose of FTY720 inhibited neutrophil recruitment to the tissue draining, popliteal LN[234]. However this work was performed using a very different model to that used in this thesis. In that study an immunization model was used; mice received OVA/CFA immunization, 3 doses over 30 days, followed by OVA challenge in the footpad. Popliteal LNs were analysed for neutrophil recruitment 6 hours after the OVA challenge. FTY720 was administered i.p. 2 hours before the OVA. In the majority of experiments neutrophils in the dLN analysed in the study were adoptively transferred bone marrow neutrophils. Bone marrow neutrophils were first stimulated *in vitro* with OVA/anti-OVA ICs, then differentially labeled depending on the injection route. The differently labeled cells were injected either in the footpad or intravenously. The dLN were then analysed 90 min later for these transferred populations to assess trafficking of neutrophils through the lymphatics (footpad injected neutrophils) versus HEVs (intravenous injected neutrophils). It is likely that bone marrow neutrophils are phenotypically different to peripheral neutrophils. In addition to this, in this study the neutrophils trafficking through HEVs were pre-activated, whereas work in chapter 3 of this thesis has demonstrated that circulating neutrophils are in a quiescent state during a localized tissue infection. Further to this BALB/c mice were used, work in this thesis has been entirely performed on the B6 background. Thus the differences in results are likely to be due to differences in the experimental models, with perhaps a difference due to the BALB/c versus B6 background. Differences in neutrophil function have been observed in models of *L. major* infection[238], however the differences seen here are more likely to be due to the different inflammatory models.

5.6 Conclusion

In summary, the role of SSM in neutrophil recruitment to the LdLN is not clear, however S1P signalling does not have a role in neutrophil recruitment to the LdLN, thus the mechanisms involved in neutrophil recruitment to the LdLN during pulmonary *S. pneumonaie* infection remain elusive.

The involvement of the chemokine receptor CCR7 and its ligands CCL19 and CCL21 was not investigated. One previous study had found that in CCR7 deficient mice, following footpad injection of CFA neutrophils failed to migrate to the dLN unlike in wild type mice[172]. Preliminary experiments using mice homozygous for a naturally occurring paucity of lymph node T cell (*plt/plt*) mutation[239] that results in a deficiency in CCL19 and CCL21 in secondary lymphoid organs[240], were performed to investigate if neutrophil migration to the LdLN was inhibited during *S. pneumoniae* infection. However these results did not provide consistent results. These mice have major defects in DC and T cell recruitment to, and positioning in LNs[241], thus as with the CD11c depletion experiments in section 5.4.1, any defect in neutrophil recruitment to the LdLN could not be concluded to be directly due to the neutrophils themselves. Thus experiments using these mice were not pursued further.

The technical problems involved in dissecting mechanisms involved in neutrophil recruitment to the LdLN are the same as those identified in Chapter 3 when investigating the function of neutrophils in the LdLN. It is not possible to specifically target neutrophils in the LdLN or migration to the LdLN without impacting lung neutrophils or neutrophil recruitment to the lung. Thus any conclusions drawn cannot be solely related to LdLN neutrophils.

Chapter 6: Discussion

Neutrophils are potent first-line effector cells for the immune system, rapidly infiltrating tissues from the blood and killing pathogens through powerful mechanisms including phagocytosis, degranulation, NETosis and release of inflammatory factors. However more recently neutrophils have been shown to have many other roles including helping B cells through the production of survival factors, containing pathogens within the draining LN, modulating lymphocyte recirculation, macrophage polarisation, DC activation and NK cell function.

In this thesis we aimed to test the hypothesis that neutrophil behaviors, gene expression profiles and migration mechanisms are dictated by the localized microenvironment rather than being cell type intrinsic. By investigating neutrophils in the LdLN following acute pulmonary *S. pneumoniae* infection we aimed to test this hypothesis using flow cytometry, immunohistochemistry, Q-PCR and 4D multiphoton explant imaging. The use of these techniques together allowed a deep analysis of neutrophil phenotype, both on the transcriptional and surface protein expression level, recruitment kinetics, location and migration mechanisms within the LdLN.

6.1 Summary of findings

6.1.1 Early recruitment to the lung draining lymph node following pulmonary *S. pneumoniae* infection

The model organism *S. pneumoniae* was used to investigate neutrophil dynamics in an acute inflammatory response, specifically determining the dynamics of neutrophil trafficking to the tissue dLN. Following pulmonary infection with *S. pneumoniae* neutrophils were found in the mediastinal LdLN as early as 2 hours following infection, with numbers peaking at 6 to 12 hours. This early recruitment preceded the recruitment of other migratory antigen presenting cells including dendritic cells, macrophages and infiltrating monocytes. Neutrophil numbers in the LdLN were rapidly reduced 24 hours post infection and stayed at a low level at 48 and 72 hours, however the absolute numbers of neutrophils did not completely reduce back to levels seen in naïve mice during this time period. Neutrophils were located shallow in the LdLN, below the collagen-rich capsule in lymphatic areas, but not in the cortex or paracortex of the LN. They densely populated areas containing MSM which have a key role in control of pathogen and antigen uptake in the medullary region of the lymph node.

6.1.2 Lung draining lymph node neutrophils resembled lung tissue neutrophils

The phenotype of neutrophils in the LdLN was investigated using gene expression and flow cytometry to determine if they differed from blood, lung tissue or airway neutrophils, and also to gain information on their possible function. Surface protein expression and gene expression revealed that blood neutrophils were in a quiescent state, with low expression of markers that indicate neutrophil activation; ICAM-1, ROS, *Tnfa*, *Ifng* and *Nos2*. Airway neutrophils collected in BAL fluid were highly activated, with high expression of CD11b, ICAM-1, ROS and up regulation of *Tnfa*, *Ifng* and *Nos2*. Lung tissue neutrophils had high expression of CD11b, ICAM-1, ROS, and had up regulated *Tnfa*, *Ifng*, however not to the level of BAL neutrophils. They had not up regulated *Nos2*. Interestingly they had high up regulation of *Ptgs2*. Lung dLN neutrophils had a similar phenotype to lung tissue neutrophils; high expression of CD11b, ICAM-1, ROS and had up regulation of *Tnfa* and *Ifng*, but not *Nos2*. Like lung tissue neutrophils, LdLN also had a high induction of *Ptgs2*. Lung and LdLN neutrophils were not in a quiescent state like blood neutrophils and had high expression of activation markers, thus were activated, however not to the level of BAL neutrophils as indicated by *Tnfa*, *Ifng* and *Nos2* relative expression. Cell surface antibody staining and CD11c Cre reporter mice revealed that a small population of LdLN neutrophils expressed MHC II and CD11c on their surface. Using the CD11c gene expression fluorescent reporter mouse it was found that CD11c expression correlated with MHC II expression.

6.1.3 Both phosphoinositide 3-kinase and integrin signalling control neutrophil migration in the lung draining lymph node

An *ex vivo* explant system was set up using fluorescent reporter mice and multiphoton laser scanning microscopy to visualise and thus investigate neutrophil dynamics within the LdLN following pulmonary *S. pneumoniae* infection. Neutrophils were found to be highly motile, moving in a classic 'amoeboid' manner. Swarms of neutrophils were observed, both persistent and transient swarms. Neutrophil migration to a swarm was highly directional as compared to neutrophil migration in areas without swarms. Small molecule inhibitors, and blocking antibody were used to investigate mechanisms involved in neutrophil migration within the LdLN. Inhibiting PI3Kγ, PI3Kδ and Syk function, blocking LTB4 and S1P receptor binding and blocking the integrin CD11b all had an inhibitory effect of neutrophil migration; both the velocity and the directionality of the cells. However PI3Kγ and LTB4 inhibition had the most profound inhibitory effect indicating that PI3Kγ signalling is highly utilised by migrating neutrophils, possibly largely by activation of the LTB4 receptor BLT1. It was of interest that PI3Kδ, a molecule that does not directly couple to chemokine receptors, also appeared to have a role in regulating migration. Integrin signalling did not have as large a role as PI3Kγ signalling

in controlling neutrophil migration, however neutrophil migration within the LdLN was not entirely integrin-independent. Thus neutrophils utilise a number of mechanisms including both chemokine and integrin signalling to navigate the LdLN, specifically the medullary sinus niche.

6.1.4 Mechanism of neutrophil trafficking to the lung draining lymph node following pulmonary *S. pneumoniae* infection

In order to investigate neutrophil recruitment to the LdLN, and the role of SSMs in this process these cells were depleted using DTx mediated deletion of $CD11c^+$ cells. Deletion of SSM was successful and it was found that neutrophil recruitment to the LdLN was reduced following this treatment. However the role of other $CD11c^+$ cells, for example DCs and alveolar macrophages, in this process cannot be ignored as they would have also been depleted. Neutrophil recruitment to the lung and airways was also acutely inhibited, thus it can't be concluded that SSM or indeed $CD11c^+$ cells are involved in the specific recruitment of neutrophils to the LdLN.

In the explant imaging studies it was found that inhibition of S1P receptors 1, 3, 4 and 5 by FTY720 had a negative effect on neutrophil migration. Due this result, and the location of neutrophils in areas of lymphatic vasculature; a source of S1P, it was investigated if FTY720 treatment had any effect on neutrophil trafficking to, or retention in the LdLN. Results showed no significant difference in neutrophil numbers in the LdLN following FTY720 treatment, thus in this setting of acute pulmonary *S. pneumoniae* infection, S1P is not involved in the recruitment or retention of neutrophils in the LdLN.

Collectively this work has found that in response to pulmonary *S. pneumoniae* infection, within 6-12 hours neutrophils are capable of migrating to the tissue dLN, the site of the adaptive immune response to the infection. Due to the phenotype of these cells it is likely that they have come from the lung, via the lymphatics, however this has not been directly demonstrated. This indicates that neutrophils do not respond in a homogeneous manner, for example, fully activate, locate and destroy the invading pathogen. Some are capable of resisting the chemotactic draw to the infection site and are able to traffic away from the lung to the dLN. Those that do are not fully activated to the levels of cells at the infection site and have turned up transcription and expression of other effector molecules that are associated with modulation of other immune cells, rather than pathogen killing mechanisms.

Neutrophil recruitment to the LN is transient, and their location is highly restricted to lymphatic areas. This indicates that neutrophils are acting in a specific manner, potentially in the initiation of immune responses in the LN, however unfortunately their function was not uncovered in this work. Through *ex vivo* live imaging, it has been found though that in the dense cellular 3D

environment of a secondary lymphoid organ neutrophils migrate in a largely chemokine driven manner with a small role for integrins. This is different to the entirely integrin-dependent migration seen at the 2D post-capillary vessel wall during TEM, or to integrin-independent migration of neutrophils in the 3D, collagen rich ECM of the interstitial space.

6.2 Conclusion

The results presented in this thesis support the evolving view of the neutrophil as a complex cell type that has multiple functional profiles and mechanisms of migration. Lung dLN neutrophils showed an intermediate activation state, rather than a highly activated phenotype as found in the alveolar space, the location of the infection. Intermediately activated alveolar neutrophils may fail to fully fight the infection, and highly activated neutrophils in the LdLN may cause destruction of the tissue architecture, resulting in disruption of functional immune response generation. Thus to avoid this neutrophils have tuned their activation state and phenotype to their location and function at that site. Unfortunately the function of neutrophils in the LdLN remains to be found.

In addition to phenotype and functional tuning neutrophils adapt their migrational mechanisms according to their location. In the vasculature migration and adherence to the endothelial cell surface is absolutely integrin dependent, however in the ECM rich interstitial space migration is integrin independent, rather driven by chemokines and actin polarization, pushing the cell through the mesh of collagen fibres in the ECM. However in the cell dense LdLN, in the medullary sinus that is lined by lymphatic endothelial cells, neutrophils employ both integrin independent and dependent migrational mechanisms. They are likely to utilise ICAM-1 on lymphatic endothelial cells and LN macrophages, and respond to cytokines and chemoattractants produced by these cells and other neutrophils.

In conclusion, collectively results in this thesis support the hypothesis that neutrophil phenotype and function is not wholly cell intrinsic, it is dictated by the local microenvironment.

6.3 Outstanding questions and future directions

6.3.1 Neutrophils in the lung draining lymph node at 24 to 72 hours following pulmonary *S. pneumoniae* infection

As discussed, neutrophils showed a transient wave of early recruitment to the LdLN. However it was not clear if the neutrophils stayed and died in the LdLN, or egressed through the lymphatics. Were the low numbers seen at 24-72 hours residual neutrophils from the early wave

of recruitment, or were they fresh neutrophils that had been recruited at later time points? A way to address this could be to do more in-depth analysis of apoptosis in these cells using Annexin V and Propidium Iodide (PI) staining. If there is a difference in the percentage of cells that are apoptotic between early and later time points, for example more apoptotic cells at later time points, this could indicate that the neutrophils are not freshly recruited. The phenotype of neutrophils in the LdLN at later time points was not investigated, mainly due to the small numbers found. However it would be interesting to see if at these time points a larger percentage of these cells are $CD11c^+$ and MHC II^+. Are the persistent, or later recruited neutrophils polarised to an immune-modulatory phenotype involved in promoting or inhibiting immune response generation in the dLN?

6.3.2 Neutrophil function in the lung draining lymph node following pulmonary *S. pneumoniae*

The technical difficulties identified in targeting LdLN neutrophils specifically meant that a function for neutrophils at this site was not found, however phenotypic analysis did provide clues, for example the acquisition of APC markers by some LdLN neutrophils. The markers and genes investigated in chapter 3 were selected based on the literature of studies investigating neutrophil function, and also analysis of microarray data from the Immunological Genome Project[242] data base, identifying neutrophil specific genes. However the list of markers and genes to investigate was restricted by the availability of antibodies and quantity of mRNA obtained. Thus it is likely that there are indeed markers that define LdLN neutrophils, however they were not identified in this work. Ideally a gene expression analysis using a microarray would have been used in this project. This would have demonstrated any highly up-regulated or down-regulated genes specifically in LdLN neutrophils. Follow up of these markers to confirm protein expression could have given the answer to neutrophil function in the LdLN. This method was employed recently to find that in the lung, neutrophils can polarize their activation and response depending on the activating agent, for example LPS versus *N. brasiliensis* larvae[63].

Definitions

3D	three-dimensions
4D	four-dimensions
Ab	antibody
alum	aluminium salts
AM	alveolar macrophage
APC	antigen presenting cell
APRIL	a proliferation-inducing ligand
ARP2/3	actin-related protein 2/3
ATP	adenosine triphosphate
BAFF	B cell activating factor
BAL	bronchiolar lavage
BCG	Bacillus Calmette-Guérin
BCR	B cell receptor
BH	B helper neutrophil
BHI	brain-heart infusion
BLT1	leukotriene B4 receptor 1
BM	basement membrane
BSA	bovine serum albumin
C5a	complement component 5a fragment
CCL	CC chemokine ligand
CCR	CC chemokine recepor
CD	cluster of differentiation
CFA	Complete Freund's Adjuvant
CFSE	carboxyfluorescein succinimidyl ester
CFU	colony forming unit
CLEC2	C-type lectin domain family 2
CLR	C-type lectin receptor
CO_2	carbon dioxide
COX	cyclooxygenase
CR	complement receptor
CTL	cytotoxic lymphocyte
CTV	CellTracker Violet
CXCL	CXC chemokine ligand
CXCR	CXC chemokine receptor
DAMP	danger-associated molecular pattern

DAPI	4′,6-Diamidino-2-phenylindole dihydrochloride
DARC	Duffy antigen/chemokine receptor
DC	dendritic cell
DC-SIGN	dendritic cell-specific intercellular adhesion molecule
DHR 123	dihydrorhodamine 123
dLN	draining lymph node
DMSO	dimethyl sulphoxide
DTR	diphtheria toxin receptor
DTx	diphtheria toxin
ECM	extracellular matrix
EDTA	ethylenediaminetetraacetic acid
EP	PGE_2 receptor
ESAM	endothelial cell specific adhesion molecule
F-actin	filamentous actin
FACS	fluorescence-activated cell sorting
FcR	Fc receptor
FCS	fetal calf serum
FDC	fibroblastic dendritic cell
FITC	flourescein isothiocyanate
fMLP	N-Formylmethionyl-leucyl-phenylalanine
FPR	formul peptide receptor
FRC	fibroblastic reticular cell
FS	forward scatter
G-CSF	granulocyte-colony stimulating factor
GC	germinal center
Gfi-1	growth factor independent-1
GFP	green fluorescent protein
GLA	glucopyranosyl lipid adjuvant
GPCR	G-protein coupled receptor
GSK	GlaxoSmithKline
HEL	hen egg white lysozyme
HEV	high endothelial venule
HIV	human immunodeficiency virus
HK	heat-killed
HSPC	hematopoietic stem and progenitor cell
I-R	ischemia-reperfusion injury
i.n	intranasal
i.t	intratracheal

IC	immune complex
IC_{50}	half maximal inhibitory concentration
ICAM	intercellular adhesion molecule
IFNγ	interferon γ
Ig	immunoglobulin
IL	interleukin
ILC	innate lymphoid cell
iNOS	inducible nitric oxide synthase
IPD	invasive pneumococcal disease
JAM	junctional adhesion molecule
LCMV	lymphatic choriomeningitis virus
LdLN	lung draining lymph node
LFA-1	lymphocyte function-associated antigen 1
LN	lymph node
LPS	lipopolysaccharide
LS-MS/MS	liquid chromatography-tandem mass spectrometry
LT	lympotoxin
LTA	lipoteichoic
LTB4	leukotriene B4
LTβR	lympotoxin β receptor
LXR	liver X receptor
LysM	lysozyme M
Lyve-1	lymphatic vessel endothelial hyaluronan receptor 1
M2	alternatively activated macrophage
mAb	monocolonal antibodies
MAC-1	macrophage-1 antigen
MAdCAM-1	mucosal vascular addressin cell adhesion molecule 1
MAPK	mitogen-acivated protein kinase
MARCO	macrophage receptor with collagenous structure
MFI	mean fluoresecence intensity
mG	membrane targeted green fluorescent protein
MHC	major histocompatibility
MIF	macrophage inhibitory factor
MMP	matrix metalloproteinase
MPL	monophosphoryl lipid A
MPO	myeloperoxidase
MRC	marginal zone reticular cell
MS	medullary sinus

MSM	medullary sinus macrophage
mT	membrane targeted tdTomato
MZ	marginal zone
NE	neutrophil elastase
NET	neutrophil extracellular trap
NK	natural killer cell
NKT	natural killer T cell
NLR	NOD-like receptor
NO	nitric oxide
NOD	nucleotide-binding oligomerisation domain
OCT	optimal cutting temperature medium
OD	optical density
OVA	ovalbumin
PAMP	pathogen-associated molecular pattern
PBS	phosphate-buffered saline
PECAM	platelet endothelial cell adhesion molecule
PFA	paraformaldehyde
PG	prostaglandin
PI3K	phosphoinositide 3-kinase
PIP2	phosphatidylinositol-3,4-bisphosphate
PIP3	phosphatidylinositol-3,4,5-triphosphate
PNAd	peripheral node addressins
PRR	pattern recognition receptor
PSGL1	P-selectin glycoprotein ligand-1
PTEN	phosphatase and tensin homolog
PTGS	prostaglandin-endoperoxide synthase
Q-PCR	quantitative PCR
RAG	recomnination-activating gene
RBC	red blood cell
RFP	red fluorescent protein
RNS	reactive nitrogen species
ROCK	Rho-associated protein kinase
ROS	reactive oxygen species
RPMI	Roswell Park Memorial Institute medium
rTEM	reverse transendothelial migration
S1P	Sphingosine-1-phosphate
S1PR	Sphingosine-1-phosphate receptor
SCS	subcapsular sinus

SEC	sinusoid endohelial cell
SEM	standard error of the mean
SP	surfactant protein
SS	side scatter
SSM	subcapsular sinus macrophage
Syk	spleen tyrosine kinase
T_{CM}	central memory T cell
TCR	T cell receptor
TD	thymus-dependent
TEM	transendothelial migration
T_{EM}	effector memory T cell
T_{FH}	follicular T helper cell
T_{FR}	regulatory follicular T helper cell
TGFβ	transforming growth factor β
T_H	T helper cell
TI	thymus-independent
TLR	toll-like receptor
TNFα	tumor necrosis factor α
T_{reg}	regulatory T cell
TREM-1	triggering receptor expressed on myeloid cells 1
VCAM-1	vascular cell adhesion protein 1
VEGF	vascular endothelial growth factor
VEGFR	vascular endothelial growth factor receptor
VLA-4	very late antigen-4
VSV	vesicular stomatitis virus
WAVE	WASP family verprolin-homologous protein
WHIM	warts, hypogammaglobulinemia, infections and myelokathexis syndrome
YFP	yellow fluorescent protein
ZAP-70	zeta-chain-associated protein kinase 70

Bibliography

1 Amulic, B., Cazalet, C., Hayes, G. L., Metzler, K. D. & Zychlinsky, A. Neutrophil function: from mechanisms to disease. *Annual review of immunology* **30**, 459-489, (2012).

2 Mayadas, T. N., Cullere, X. & Lowell, C. A. The multifaceted functions of neutrophils. *Annual review of pathology* **9**, 181-218, (2014).

3 Borregaard, N. Neutrophils, from marrow to microbes. *Immunity* **33**, 657-670, (2010).

4 Day, R. B. & Link, D. C. Regulation of neutrophil trafficking from the bone marrow. *Cellular and molecular life sciences : CMLS* **69**, 1415-1423, (2012).

5 Summers, C. *et al.* Neutrophil kinetics in health and disease. *Trends Immunol* **31**, 318-324, (2010).

6 Balabanian, K. *et al.* WHIM syndromes with different genetic anomalies are accounted for by impaired CXCR4 desensitization to CXCL12. *Blood* **105**, 2449-2457, (2005).

7 Devi, S. *et al.* Neutrophil mobilization via plerixafor-mediated CXCR4 inhibition arises from lung demargination and blockade of neutrophil homing to the bone marrow. *J Exp Med* **210**, 2321-2336, (2013).

8 Stark, M. A. *et al.* Phagocytosis of apoptotic neutrophils regulates granulopoiesis via IL-23 and IL-17. *Immunity* **22**, 285-294, (2005).

9 Moutsopoulos, N. M. *et al.* Defective neutrophil recruitment in leukocyte adhesion deficiency type I disease causes local IL-17-driven inflammatory bone loss. *Science translational medicine* **6**, 229ra240, (2014).

10 Hong, C. *et al.* Coordinate regulation of neutrophil homeostasis by liver X receptors in mice. *J Clin Invest* **122**, 337-347, (2012).

11 Wirths, S., Bugl, S. & Kopp, H. G. Neutrophil homeostasis and its regulation by danger signalling. *Blood* **123**, 3563-3566, (2014).

12 Kessenbrock, K. *et al.* Netting neutrophils in autoimmune small-vessel vasculitis. *Nature medicine* **15**, 623-625, (2009).

13 Casanova-Acebes, M. *et al.* Rhythmic modulation of the hematopoietic niche through neutrophil clearance. *Cell* **153**, 1025-1035, (2013).

14 Manz, M. G. & Boettcher, S. Emergency granulopoiesis. *Nat Rev Immunol* **14**, 302-314, (2014).

15 Mei, J. *et al.* Cxcr2 and Cxcl5 regulate the IL-17/G-CSF axis and neutrophil homeostasis in mice. *J Clin Invest* **122**, 974-986, (2012).

16 Bugl, S. *et al.* Steady-state neutrophil homeostasis is dependent on TLR4/TRIF signalling. *Blood* **121**, 723-733, (2013).

17 Sadik, C. D., Kim, N. D. & Luster, A. D. Neutrophils cascading their way to inflammation. *Trends Immunol* **32**, 452-460, (2011).

18 Ley, K., Laudanna, C., Cybulsky, M. I. & Nourshargh, S. Getting to the site of inflammation: the leukocyte adhesion cascade updated. *Nat Rev Immunol* **7**, 678-689, (2007).

19 Kolaczkowska, E. & Kubes, P. Neutrophil recruitment and function in health and inflammation. *Nat Rev Immunol* **13**, 159-175, (2013).

20 Alon, R. & Ley, K. Cells on the run: shear-regulated integrin activation in leukocyte rolling and arrest on endothelial cells. *Current opinion in cell biology* **20**, 525-532, (2008).

21 Pruenster, M. *et al.* The Duffy antigen receptor for chemokines transports chemokines and supports their promigratory activity. *Nat Immunol* **10**, 101-108, (2009).

22 Phillipson, M. *et al.* Intraluminal crawling of neutrophils to emigration sites: a molecularly distinct process from adhesion in the recruitment cascade. *J Exp Med* **203**, 2569-2575, (2006).

23 Woodfin, A., Voisin, M. B. & Nourshargh, S. Recent developments and complexities in neutrophil transmigration. *Current opinion in hematology* **17**, 9-17, (2010).

24 Woodfin, A. *et al.* The junctional adhesion molecule JAM-C regulates polarized transendothelial migration of neutrophils in vivo. *Nat Immunol* **12**, 761-769, (2011).

25 Proebstl, D. *et al.* Pericytes support neutrophil subendothelial cell crawling and breaching of venular walls in vivo. *The Journal of experimental medicine* **209**, 1219-1234, (2012).

26 Wang, S. *et al.* Venular basement membranes contain specific matrix protein low expression regions that act as exit points for emigrating neutrophils. *J Exp Med* **203**, 1519-1532, (2006).

27 Weninger, W., Biro, M. & Jain, R. Leukocyte migration in the interstitial space of non-lymphoid organs. *Nat Rev Immunol* **14**, 232-246, (2014).

28 Phillipson, M. & Kubes, P. The neutrophil in vascular inflammation. *Nature medicine* **17**, 1381-1390, (2011).

29 Heit, B., Liu, L., Colarusso, P., Puri, K. D. & Kubes, P. PI3K accelerates, but is not required for, neutrophil chemotaxis to fMLP. *J Cell Sci* **121**, 205-214, (2008).

30 Heit, B., Tavener, S., Raharjo, E. & Kubes, P. An intracellular signalling hierarchy determines direction of migration in opposing chemotactic gradients. *J Cell Biol* **159**, 91-102, (2002).

31 Peters, N. C. *et al.* In vivo imaging reveals an essential role for neutrophils in leishmaniasis transmitted by sand flies. *Science* **321**, 970-974, (2008).

32 Ng, L. G. *et al.* Visualizing the neutrophil response to sterile tissue injury in mouse dermis reveals a three-phase cascade of events. *J Invest Dermatol* **131**, 2058-2068, (2011).

33 Lammermann, T. *et al.* Neutrophil swarms require LTB4 and integrins at sites of cell death in vivo. *Nature* **498**, 371-375, (2013).

34 Afonso, P. V. *et al.* LTB4 is a signal-relay molecule during neutrophil chemotaxis. *Developmental cell* **22**, 1079-1091, (2012).

35 Stark, K. *et al.* Capillary and arteriolar pericytes attract innate leukocytes exiting through venules and 'instruct' them with pattern-recognition and motility programs. *Nat Immunol* **14**, 41-51, (2013).

36 Chtanova, T. *et al.* Dynamics of neutrophil migration in lymph nodes during infection. *Immunity* **29**, 487-496, (2008).

37 Kreisel, D. *et al.* In vivo two-photon imaging reveals monocyte-dependent neutrophil extravasation during pulmonary inflammation. *Proc Natl Acad Sci U S A* **107**, 18073-18078, (2010).

38 McDonald, B. *et al.* Interaction of CD44 and hyaluronan is the dominant mechanism for neutrophil sequestration in inflamed liver sinusoids. *J Exp Med* **205**, 915-927, (2008).

39 Rossaint, J. & Zarbock, A. Tissue-specific neutrophil recruitment into the lung, liver, and kidney. *J Innate Immun* **5**, 348-357, (2013).

40 Worthen, G. S., Schwab, B., 3rd, Elson, E. L. & Downey, G. P. Mechanics of stimulated neutrophils: cell stiffening induces retention in capillaries. *Science* **245**, 183-186, (1989).

41 Mizgerd, J. P. *et al.* Selectins and neutrophil traffic: margination and Streptococcus pneumoniae-induced emigration in murine lungs. *J Exp Med* **184**, 639-645, (1996).

42 Mizgerd, J. P., Horwitz, B. H., Quillen, H. C., Scott, M. L. & Doerschuk, C. M. Effects of CD18 deficiency on the emigration of murine neutrophils during pneumonia. *J Immunol* **163**, 995-999, (1999).

43 Mizgerd, J. P. Molecular mechanisms of neutrophil recruitment elicited by bacteria in the lungs. *Semin Immunol* **14**, 123-132, (2002).

44 Condliffe, A. M. *et al.* Sequential activation of class IB and class IA PI3K is important for the primed respiratory burst of human but not murine neutrophils. *Blood* **106**, 1432-1440, (2005).

45 Thomas, C. J. & Schroder, K. Pattern recognition receptor function in neutrophils. *Trends Immunol* **34**, 317-328, (2013).

46 Sabroe, I. *et al.* Selective roles for Toll-like receptor (TLR)2 and TLR4 in the regulation of neutrophil activation and life span. *J Immunol* **170**, 5268-5275, (2003).

47 Li, X. *et al.* The beta-glucan receptor Dectin-1 activates the integrin Mac-1 in neutrophils via Vav protein signalling to promote Candida albicans clearance. *Cell Host Microbe* **10**, 603-615, (2011).

48 Nordenfelt, P. & Tapper, H. Phagosome dynamics during phagocytosis by neutrophils. *J Leukoc Biol* **90**, 271-284, (2011).

49 Faurschou, M. & Borregaard, N. Neutrophil granules and secretory vesicles in inflammation. *Microbes Infect* **5**, 1317-1327, (2003).

50 Lau, D. *et al.* Myeloperoxidase mediates neutrophil activation by association with CD11b/CD18 integrins. *Proc Natl Acad Sci U S A* **102**, 431-436, (2005).

51 Dupre-Crochet, S., Erard, M. & Nubetae, O. ROS production in phagocytes: why, when, and where? *J Leukoc Biol* **94**, 657-670, (2013).

52 Fang, F. C. Antimicrobial reactive oxygen and nitrogen species: concepts and controversies. *Nature reviews. Microbiology* **2**, 820-832, (2004).

53 Brinkmann, V. *et al.* Neutrophil extracellular traps kill bacteria. *Science* **303**, 1532-1535, (2004).

54 Saitoh, T. *et al.* Neutrophil extracellular traps mediate a host defense response to human immunodeficiency virus-1. *Cell Host Microbe* **12**, 109-116, (2012).

55 Papayannopoulos, V., Metzler, K. D., Hakkim, A. & Zychlinsky, A. Neutrophil elastase and myeloperoxidase regulate the formation of neutrophil extracellular traps. *J Cell Biol* **191**, 677-691, (2010).

56 Metzler, K. D., Goosmann, C., Lubojemska, A., Zychlinsky, A. & Papayannopoulos, V. A Myeloperoxidase-Containing Complex Regulates Neutrophil Elastase Release and Actin Dynamics during NETosis. *Cell reports* **8**, 883-896, (2014).

57 Fuchs, T. A. *et al.* Novel cell death program leads to neutrophil extracellular traps. *J Cell Biol* **176**, 231-241, (2007).

58 Brinkmann, V. & Zychlinsky, A. Neutrophil extracellular traps: is immunity the second function of chromatin? *J Cell Biol* **198**, 773-783, (2012).

59 Sumby, P. *et al.* Extracellular deoxyribonuclease made by group A Streptococcus assists pathogenesis by enhancing evasion of the innate immune response. *Proc Natl Acad Sci U S A* **102**, 1679-1684, (2005).

60 Beiter, K. *et al.* An endonuclease allows Streptococcus pneumoniae to escape from neutrophil extracellular traps. *Curr Biol* **16**, 401-407, (2006).

61 Savill, J. & Fadok, V. Corpse clearance defines the meaning of cell death. *Nature* **407**, 784-788, (2000).

62 Esmann, L. *et al.* Phagocytosis of apoptotic cells by neutrophil granulocytes: diminished proinflammatory neutrophil functions in the presence of apoptotic cells. *J Immunol* **184**, 391-400, (2010).

63 Chen, F. *et al.* Neutrophils prime a long-lived effector macrophage phenotype that mediates accelerated helminth expulsion. *Nat Immunol*, (2014).

64 Blomgran, R. & Ernst, J. D. Lung neutrophils facilitate activation of naive antigen-specific CD4+ T cells during Mycobacterium tuberculosis infection. *Journal of immunology* **186**, 7110-7119, (2011).

65 Blomgran, R., Desvignes, L., Briken, V. & Ernst, J. D. Mycobacterium tuberculosis inhibits neutrophil apoptosis, leading to delayed activation of naive CD4 T cells. *Cell Host Microbe* **11**, 81-90, (2012).

66 Park, S. J., Burdick, M. D. & Mehrad, B. Neutrophils mediate maturation and efflux of lung dendritic cells in response to Aspergillus fumigatus germ tubes. *Infection and immunity* **80**, 1759-1765, (2012).

67 Ostanin, D. V. *et al.* Acquisition of antigen-presenting functions by neutrophils isolated from mice with chronic colitis. *Journal of immunology* **188**, 1491-1502, (2012).

68 Abi Abdallah, D. S., Egan, C. E., Butcher, B. A. & Denkers, E. Y. Mouse neutrophils are professional antigen-presenting cells programmed to instruct Th1 and Th17 T-cell differentiation. *Int Immunol* **23**, 317-326, (2011).

69 Beauvillain, C. *et al.* Neutrophils efficiently cross-prime naive T cells in vivo. *Blood* **110**, 2965-2973, (2007).

70 Muller, I., Munder, M., Kropf, P. & Hansch, G. M. Polymorphonuclear neutrophils and T lymphocytes: strange bedfellows or brothers in arms? *Trends Immunol* **30**, 522-530, (2009).

71 Sporri, R., Joller, N., Hilbi, H. & Oxenius, A. A novel role for neutrophils as critical activators of NK cells. *J Immunol* **181**, 7121-7130, (2008).

72 Jaeger, B. N. *et al.* Neutrophil depletion impairs natural killer cell maturation, function, and homeostasis. *The Journal of experimental medicine* **209**, 565-580, (2012).

73 England, P. H. *Pneumococcal Disease*, <http://www.hpa.org.uk/Topics/InfectiousDiseases/InfectionsAZ/Pneumococcal/GeneralInformationPneumococcal/pneumoBackground/> (2014).

74 Organisation, W. H. *Pneumonia*, <http://www.who.int/mediacentre/factsheets/fs331/en/> (2013).

75 Brito, D. A., Ramirez, M. & de Lencastre, H. Serotyping Streptococcus pneumoniae by multiplex PCR. *Journal of clinical microbiology* **41**, 2378-2384, (2003).

76 AlonsoDeVelasco, E., Verheul, A. F., Verhoef, J. & Snippe, H. Streptococcus pneumoniae: virulence factors, pathogenesis, and vaccines. *Microbiological reviews* **59**, 591-603, (1995).

77 Chiavolini, D., Pozzi, G. & Ricci, S. Animal models of Streptococcus pneumoniae disease. *Clinical microbiology reviews* **21**, 666-685, (2008).

78 Bhowmick, R. *et al.* Systemic disease during Streptococcus pneumoniae acute lung infection requires 12-lipoxygenase-dependent inflammation. *J Immunol* **191**, 5115-5123, (2013).

79 Koppe, U., Suttorp, N. & Opitz, B. Recognition of Streptococcus pneumoniae by the innate immune system. *Cell Microbiol* **14**, 460-466, (2012).

80 Marchisio, P. *et al.* Nasopharyngeal carriage of Streptococcus pneumoniae in healthy children: implications for the use of heptavalent pneumococcal conjugate vaccine. *Emerg Infect Dis* **8**, 479-484, (2002).

81 Kadioglu, A., Weiser, J. N., Paton, J. C. & Andrew, P. W. The role of Streptococcus pneumoniae virulence factors in host respiratory colonization and disease. *Nature reviews. Microbiology* **6**, 288-301, (2008).

82 Andrews, N. J. *et al.* Serotype-specific effectiveness and correlates of protection for the 13-valent pneumococcal conjugate vaccine: a postlicensure indirect cohort study. *The Lancet. Infectious diseases* **14**, 839-846, (2014).

83 Jiang, Y., Gauthier, A., Keeping, S. & Carroll, S. Cost-effectiveness of vaccinating the elderly and at-risk adults with the 23-valent pneumococcal polysaccharide vaccine or 13-valent pneumococcal conjugate vaccine in the UK. *Expert review of pharmacoeconomics & outcomes research*, 1-15, (2014).

84 Pilishvili, T. *et al.* Sustained reductions in invasive pneumococcal disease in the era of conjugate vaccine. *J Infect Dis* **201**, 32-41, (2010).

85 Currie, A. J. *et al.* Primary immunodeficiency to pneumococcal infection due to a defect in Toll-like receptor signalling. *The Journal of pediatrics* **144**, 512-518, (2004).

86 Hasenberg, M., Stegemann-Koniszewski, S. & Gunzer, M. Cellular immune reactions in the lung. *Immunol Rev* **251**, 189-214, (2013).

87 Kishore, U. *et al.* Surfactant proteins SP-A and SP-D: structure, function and receptors. *Mol Immunol* **43**, 1293-1315, (2006).

88 Lelkes, E., Headley, M. B., Thornton, E. E., Looney, M. R. & Krummel, M. F. The spatiotemporal cellular dynamics of lung immunity. *Trends Immunol* **35**, 379-386, (2014).

89 Teijeira, A., Russo, E. & Halin, C. Taking the lymphatic route: dendritic cell migration to draining lymph nodes. *Seminars in immunopathology* **36**, 261-274, (2014).

90 Cyster, J. G. B cell follicles and antigen encounters of the third kind. *Nat Immunol* **11**, 989-996, (2010).

91 Girard, J. P., Moussion, C. & Forster, R. HEVs, lymphatics and homeostatic immune cell trafficking in lymph nodes. *Nat Rev Immunol* **12**, 762-773, (2012).

92 Bajenoff, M. *et al.* Stromal cell networks regulate lymphocyte entry, migration, and territoriality in lymph nodes. *Immunity* **25**, 989-1001, (2006).

93 Weber, M. *et al.* Interstitial dendritic cell guidance by haptotactic chemokine gradients. *Science* **339**, 328-332, (2013).

94 Acton, S. E. *et al.* Podoplanin-rich stromal networks induce dendritic cell motility via activation of the C-type lectin receptor CLEC-2. *Immunity* **37**, 276-289, (2012).

95 Malhotra, D., Fletcher, A. L. & Turley, S. J. Stromal and hematopoietic cells in secondary lymphoid organs: partners in immunity. *Immunol Rev* **251**, 160-176, (2013).

96 Malhotra, D. *et al.* Transcriptional profiling of stroma from inflamed and resting lymph nodes defines immunological hallmarks. *Nat Immunol* **13**, 499-510, (2012).

97 Scandella, E. *et al.* Restoration of lymphoid organ integrity through the interaction of lymphoid tissue-inducer cells with stroma of the T cell zone. *Nat Immunol* **9**, 667-675, (2008).

98 Cremasco, V. *et al.* B cell homeostasis and follicle confines are governed by fibroblastic reticular cells. *Nat Immunol*, (2014).

99 Bajenoff, M. Stromal cells control soluble material and cellular transport in lymph nodes. *Frontiers in immunology* **3**, 304, (2012).

100 Sixt, M. *et al.* The conduit system transports soluble antigens from the afferent lymph to resident dendritic cells in the T cell area of the lymph node. *Immunity* **22**, 19-29, (2005).

101 Wang, X. *et al.* Follicular dendritic cells help establish follicle identity and promote B cell retention in germinal centers. *J Exp Med* **208**, 2497-2510, (2011).

102 Phan, T. G., Green, J. A., Gray, E. E., Xu, Y. & Cyster, J. G. Immune complex relay by subcapsular sinus macrophages and noncognate B cells drives antibody affinity maturation. *Nat Immunol* **10**, 786-793, (2009).

103 Green, J. A. *et al.* The sphingosine 1-phosphate receptor S1P(2) maintains the homeostasis of germinal center B cells and promotes niche confinement. *Nat Immunol* **12**, 672-680, (2011).

104 Katakai, T. Marginal reticular cells: a stromal subset directly descended from the lymphoid tissue organizer. *Frontiers in immunology* **3**, 200, (2012).

105 Jarjour, M. *et al.* Fate mapping reveals origin and dynamics of lymph node follicular dendritic cells. *J Exp Med* **211**, 1109-1122, (2014).

106 Gray, E. E. & Cyster, J. G. Lymph node macrophages. *J Innate Immun* **4**, 424-436, (2012).

107 Moseman, E. A. *et al.* B cell maintenance of subcapsular sinus macrophages protects against a fatal viral infection independent of adaptive immunity. *Immunity* **36**, 415-426, (2012).

108 Iannacone, M. *et al.* Subcapsular sinus macrophages prevent CNS invasion on peripheral infection with a neurotropic virus. *Nature* **465**, 1079-1083, (2010).

109 Hargreaves, D. C. *et al.* A coordinated change in chemokine responsiveness guides plasma cell movements. *J Exp Med* **194**, 45-56, (2001).

110 Fooksman, D. R. *et al.* Development and migration of plasma cells in the mouse lymph node. *Immunity* **33**, 118-127, (2010).

111 Miyasaka, M. & Tanaka, T. Lymphocyte trafficking across high endothelial venules: dogmas and enigmas. *Nat Rev Immunol* **4**, 360-370, (2004).

112 Majumdar, R., Sixt, M. & Parent, C. A. New paradigms in the establishment and maintenance of gradients during directed cell migration. *Current opinion in cell biology* **30C**, 33-40, (2014).

113 Mionnet, C. *et al.* High endothelial venules as traffic control points maintaining lymphocyte population homeostasis in lymph nodes. *Blood* **118**, 6115-6122, (2011).

114 Tal, O. *et al.* DC mobilization from the skin requires docking to immobilized CCL21 on lymphatic endothelium and intralymphatic crawling. *The Journal of experimental medicine* **208**, 2141-2153, (2011).

115 Luo, X. *et al.* Changes in NK and NKT cells in mesenteric lymph nodes after a Schistosoma japonicum infection. *Parasitology research* **113**, 1001-1009, (2014).

116 Ulvmar, M. H. *et al.* The atypical chemokine receptor CCRL1 shapes functional CCL21 gradients in lymph nodes. *Nat Immunol* **15**, 623-630, (2014).

117 Pham, T. H. *et al.* Lymphatic endothelial cell sphingosine kinase activity is required for lymphocyte egress and lymphatic patterning. *J Exp Med* **207**, 17-27, (2010).

118 Grigorova, I. L. *et al.* Cortical sinus probing, S1P1-dependent entry and flow-based capture of egressing T cells. *Nat Immunol* **10**, 58-65, (2009).

119 Kabashima, K. *et al.* Plasma cell S1P1 expression determines secondary lymphoid organ retention versus bone marrow tropism. *J Exp Med* **203**, 2683-2690, (2006).

120 Tan, J. K. & O'Neill, H. C. Maturation requirements for dendritic cells in T cell stimulation leading to tolerance versus immunity. *J Leukoc Biol* **78**, 319-324, (2005).

121 Chakraborty, A. K. & Weiss, A. Insights into the initiation of TCR signalling. *Nat Immunol* **15**, 798-807, (2014).

122 Kapsenberg, M. L. Dendritic-cell control of pathogen-driven T-cell polarization. *Nat Rev Immunol* **3**, 984-993, (2003).

123 MacLeod, M. K., Kappler, J. W. & Marrack, P. Memory CD4 T cells: generation, reactivation and re-assignment. *Immunology* **130**, 10-15, (2010).

124 MacLeod, M. K., Clambey, E. T., Kappler, J. W. & Marrack, P. CD4 memory T cells: what are they and what can they do? *Semin Immunol* **21**, 53-61, (2009).

125 Zhang, S., Zhang, H. & Zhao, J. The role of CD4 T cell help for CD8 CTL activation. *Biochem Biophys Res Commun* **384**, 405-408, (2009).

126 Ito, H. & Seishima, M. Regulation of the induction and function of cytotoxic T lymphocytes by natural killer T cell. *J Biomed Biotechnol* **2010**, 641757, (2010).

127 Goodnow, C. C., Vinuesa, C. G., Randall, K. L., Mackay, F. & Brink, R. Control systems and decision making for antibody production. *Nat Immunol* **11**, 681-688, (2010).

128 Litinskiy, M. B. *et al.* DCs induce CD40-independent immunoglobulin class switching through BLyS and APRIL. *Nat Immunol* **3**, 822-829, (2002).

129 Mond, J. J., Lees, A. & Snapper, C. M. T cell-independent antigens type 2. *Annu Rev Immunol* **13**, 655-692, (1995).

130 Vinuesa, C. G. & Chang, P. P. Innate B cell helpers reveal novel types of antibody responses. *Nat Immunol* **14**, 119-126, (2013).

131 Chyou, S. *et al.* Fibroblast-type reticular stromal cells regulate the lymph node vasculature. *J Immunol* **181**, 3887-3896, (2008).

132 Chyou, S. *et al.* Coordinated regulation of lymph node vascular-stromal growth first by CD11c+ cells and then by T and B cells. *J Immunol* **187**, 5558-5567, (2011).

133 Kumar, V., Chyou, S., Stein, J. V. & Lu, T. T. Optical projection tomography reveals dynamics of HEV growth after immunization with protein plus CFA and features shared with HEVs in acute autoinflammatory lymphadenopathy. *Frontiers in immunology* **3**, 282, (2012).

134 Katakai, T., Hara, T., Sugai, M., Gonda, H. & Shimizu, A. Lymph node fibroblastic reticular cells construct the stromal reticulum via contact with lymphocytes. *J Exp Med* **200**, 783-795, (2004).

135 Angeli, V. *et al.* B cell-driven lymphangiogenesis in inflamed lymph nodes enhances dendritic cell mobilization. *Immunity* **24**, 203-215, (2006).

136 Abe, J. *et al.* B cells regulate antibody responses through the medullary remodeling of inflamed lymph nodes. *Int Immunol* **24**, 17-27, (2012).

137 Shiow, L. R. *et al.* CD69 acts downstream of interferon-alpha/beta to inhibit S1P1 and lymphocyte egress from lymphoid organs. *Nature* **440**, 540-544, (2006).

138 Bankovich, A. J., Shiow, L. R. & Cyster, J. G. CD69 suppresses sphingosine 1-phosophate receptor-1 (S1P1) function through interaction with membrane helix 4. *J Biol Chem* **285**, 22328-22337, (2010).

139 Kastenmuller, W., Torabi-Parizi, P., Subramanian, N., Lammermann, T. & Germain, R. N. A spatially-organized multicellular innate immune response in lymph nodes limits systemic pathogen spread. *Cell* **150**, 1235-1248, (2012).

140 Martin-Fontecha, A. *et al.* Induced recruitment of NK cells to lymph nodes provides IFN-gamma for T(H)1 priming. *Nat Immunol* **5**, 1260-1265, (2004).

141 Bajenoff, M. *et al.* Natural killer cell behavior in lymph nodes revealed by static and real-time imaging. *J Exp Med* **203**, 619-631, (2006).

142 Garrod, K. R., Wei, S. H., Parker, I. & Cahalan, M. D. Natural killer cells actively patrol peripheral lymph nodes forming stable conjugates to eliminate MHC-mismatched targets. *Proc Natl Acad Sci U S A* **104**, 12081-12086, (2007).

143 Bousso, P., Bhakta, N. R., Lewis, R. S. & Robey, E. Dynamics of thymocyte-stromal cell interactions visualized by two-photon microscopy. *Science* **296**, 1876-1880, (2002).

144 Miller, M. J., Wei, S. H., Parker, I. & Cahalan, M. D. Two-photon imaging of lymphocyte motility and antigen response in intact lymph node. *Science* **296**, 1869-1873, (2002).

145 Stoll, S., Delon, J., Brotz, T. M. & Germain, R. N. Dynamic imaging of T cell-dendritic cell interactions in lymph nodes. *Science* **296**, 1873-1876, (2002).

146 Katakai, T. *et al.* A novel reticular stromal structure in lymph node cortex: an immuno-platform for interactions among dendritic cells, T cells and B cells. *Int Immunol* **16**, 1133-1142, (2004).

147 Germain, R. N., Miller, M. J., Dustin, M. L. & Nussenzweig, M. C. Dynamic imaging of the immune system: progress, pitfalls and promise. *Nat Rev Immunol* **6**, 497-507, (2006).

148 Faust, N., Varas, F., Kelly, L. M., Heck, S. & Graf, T. Insertion of enhanced green fluorescent protein into the lysozyme gene creates mice with green fluorescent granulocytes and macrophages. *Blood* **96**, 719-726, (2000).

149 Ellenbroek, S. I. & van Rheenen, J. Imaging hallmarks of cancer in living mice. *Nature reviews. Cancer* **14**, 406-418, (2014).

150 Cahalan, M. D., Parker, I., Wei, S. H. & Miller, M. J. Two-photon tissue imaging: seeing the immune system in a fresh light. *Nat Rev Immunol* **2**, 872-880, (2002).

151 Jung, S. *et al.* Analysis of fractalkine receptor CX(3)CR1 function by targeted deletion and green fluorescent protein reporter gene insertion. *Molecular and cellular biology* **20**, 4106-4114, (2000).

152 Repass, J. F. *et al.* IL7-hCD25 and IL7-Cre BAC transgenic mouse lines: new tools for analysis of IL-7 expressing cells. *Genesis* **47**, 281-287, (2009).

153 Srinivas, S. *et al.* Cre reporter strains produced by targeted insertion of EYFP and ECFP into the ROSA26 locus. *BMC Dev Biol* **1**, 4, (2001).

154 de Boer, J. *et al.* Transgenic mice with hematopoietic and lymphoid specific expression of Cre. *Eur J Immunol* **33**, 314-325, (2003).

155 Veiga-Fernandes, H. *et al.* Tyrosine kinase receptor RET is a key regulator of Peyer's patch organogenesis. *Nature* **446**, 547-551, (2007).

156 Clausen, B. E., Burkhardt, C., Reith, W., Renkawitz, R. & Forster, I. Conditional gene targeting in macrophages and granulocytes using LysMcre mice. *Transgenic Res* **8**, 265-277, (1999).

157 Muzumdar, M. D., Tasic, B., Miyamichi, K., Li, L. & Luo, L. A global double-fluorescent Cre reporter mouse. *Genesis* **45**, 593-605, (2007).

158 Stranges, P. B. *et al.* Elimination of antigen-presenting cells and autoreactive T cells by Fas contributes to prevention of autoimmunity. *Immunity* **26**, 629-641, (2007).

159 Buch, T. *et al.* A Cre-inducible diphtheria toxin receptor mediates cell lineage ablation after toxin administration. *Nat Methods* **2**, 419-426, (2005).

160 Adachi, K. *et al.* Design, Synthesis, and Structure-Activity-Relationships of 2-Substituted-2-Amino-1,3-Propanediols - Discovery of a Novel Immunosuppressant, Fty720. *Bioorganic & Medicinal Chemistry Letters* **5**, 853-856, (1995).

161 Liddle, J. *et al.* Discovery of GSK143, a highly potent, selective and orally efficacious spleen tyrosine kinase inhibitor. *Bioorg Med Chem Lett* **21**, 6188-6194, (2011).

162 Sadhu, C., Masinovsky, B., Dick, K., Sowell, C. G. & Staunton, D. E. Essential role of phosphoinositide 3-kinase delta in neutrophil directional movement. *J Immunol* **170**, 2647-2654, (2003).

163 Gapinski, D. M., Mallett, B. E., Froelich, L. L. & Jackson, W. T. Benzophenone dicarboxylic acid antagonists of leukotriene B4. 2. Structure-activity relationships of the lipophilic side chain. *J Med Chem* **33**, 2807-2813, (1990).

164 Magri, G. *et al.* Innate lymphoid cells integrate stromal and immunological signals to enhance antibody production by splenic marginal zone B cells. *Nat Immunol* **15**, 354-364, (2014).

165 Puga, I. *et al.* B cell-helper neutrophils stimulate the diversification and production of immunoglobulin in the marginal zone of the spleen. *Nature immunology* **13**, 170-180, (2012).

166 Abadie, V. *et al.* Neutrophils rapidly migrate via lymphatics after Mycobacterium bovis BCG intradermal vaccination and shuttle live bacilli to the draining lymph nodes. *Blood* **106**, 1843-1850, (2005).

167 Pesce, J. T. *et al.* Neutrophils clear bacteria associated with parasitic nematodes augmenting the development of an effective Th2-type response. *J Immunol* **180**, 464-474, (2008).

168 Ostanin, D. V. *et al.* Acquisition of antigen-presenting functions by neutrophils isolated from mice with chronic colitis. *J Immunol* **188**, 1491-1502, (2012).

169 Yang, C. W., Strong, B. S., Miller, M. J. & Unanue, E. R. Neutrophils influence the level of antigen presentation during the immune response to protein antigens in adjuvants. *Journal of immunology* **185**, 2927-2934, (2010).

170 Yang, C. W. & Unanue, E. R. Neutrophils control the magnitude and spread of the immune response in a thromboxane A2-mediated process. *The Journal of experimental medicine* **210**, 375-387, (2013).

171 Maletto, B. A. *et al.* Presence of neutrophil-bearing antigen in lymphoid organs of immune mice. *Blood* **108**, 3094-3102, (2006).

172 Beauvillain, C. *et al.* CCR7 is involved in the migration of neutrophils to lymph nodes. *Blood* **117**, 1196-1204, (2011).

173 Calabro, S. *et al.* Vaccine adjuvants alum and MF59 induce rapid recruitment of neutrophils and monocytes that participate in antigen transport to draining lymph nodes. *Vaccine* **29**, 1812-1823, (2011).

174 De Gregorio, E., Tritto, E. & Rappuoli, R. Alum adjuvanticity: unraveling a century old mystery. *Eur J Immunol* **38**, 2068-2071, (2008).

175 Beyrau, M., Bodkin, J. V. & Nourshargh, S. Neutrophil heterogeneity in health and disease: a revitalized avenue in inflammation and immunity. *Open biology* **2**, 120134, (2012).

176 Fridlender, Z. G. *et al.* Polarization of tumor-associated neutrophil phenotype by TGF-beta: "N1" versus "N2" TAN. *Cancer cell* **16**, 183-194, (2009).

177 Geissmann, F., Jung, S. & Littman, D. R. Blood monocytes consist of two principal subsets with distinct migratory properties. *Immunity* **19**, 71-82, (2003).

178 Henderson, R. B., Hobbs, J. A., Mathies, M. & Hogg, N. Rapid recruitment of inflammatory monocytes is independent of neutrophil migration. *Blood* **102**, 328-335, (2003).

179 Jakubzick, C. *et al.* Minimal differentiation of classical monocytes as they survey steady-state tissues and transport antigen to lymph nodes. *Immunity* **39**, 599-610, (2013).

180 Ricciotti, E. & FitzGerald, G. A. Prostaglandins and inflammation. *Arterioscler Thromb Vasc Biol* **31**, 986-1000, (2011).

181 Mantovani, A., Cassatella, M. A., Costantini, C. & Jaillon, S. Neutrophils in the activation and regulation of innate and adaptive immunity. *Nat Rev Immunol* **11**, 519-531, (2011).

182 Geng, S. *et al.* Emergence, origin, and function of neutrophil-dendritic cell hybrids in experimentally induced inflammatory lesions in mice. *Blood*, (2013).

183 Matsushima, H. *et al.* Neutrophil differentiation into a unique hybrid population exhibiting dual phenotype and functionality of neutrophils and dendritic cells. *Blood*, (2013).

184 Lebedeva, T., Dustin, M. L. & Sykulev, Y. ICAM-1 co-stimulates target cells to facilitate antigen presentation. *Curr Opin Immunol* **17**, 251-258, (2005).

185 Christoffersson, G. *et al.* VEGF-A recruits a proangiogenic MMP-9-delivering neutrophil subset that induces angiogenesis in transplanted hypoxic tissue. *Blood* **120**, 4653-4662, (2012).

186 Tan, K. W. *et al.* Neutrophils contribute to inflammatory lymphangiogenesis by increasing VEGF-A bioavailability and secreting VEGF-D. *Blood* **122**, 3666-3677, (2013).

187 Stacker, S. A. *et al.* Lymphangiogenesis and lymphatic vessel remodelling in cancer. *Nature reviews. Cancer* **14**, 159-172, (2014).

188 Bradley, L. M., Douglass, M. F., Chatterjee, D., Akira, S. & Baaten, B. J. Matrix metalloprotease 9 mediates neutrophil migration into the airways in response to influenza virus-induced toll-like receptor signalling. *PLoS Pathog* **8**, e1002641, (2012).

189 Schiwon, M. *et al.* Crosstalk between sentinel and helper macrophages permits neutrophil migration into infected uroepithelium. *Cell* **156**, 456-468, (2014).

190 Newton, R. A. & Hogg, N. The human S100 protein MRP-14 is a novel activator of the beta 2 integrin Mac-1 on neutrophils. *J Immunol* **160**, 1427-1435, (1998).

191 Ryckman, C., Vandal, K., Rouleau, P., Talbot, M. & Tessier, P. A. Proinflammatory activities of S100: proteins S100A8, S100A9, and S100A8/A9 induce neutrophil chemotaxis and adhesion. *J Immunol* **170**, 3233-3242, (2003).

192 Viemann, D. *et al.* Myeloid-related proteins 8 and 14 induce a specific inflammatory response in human microvascular endothelial cells. *Blood* **105**, 2955-2962, (2005).

193 Medeiros, A. I., Serezani, C. H., Lee, S. P. & Peters-Golden, M. Efferocytosis impairs pulmonary macrophage and lung antibacterial function via PGE2/EP2 signalling. *J Exp Med* **206**, 61-68, (2009).

194 Woodward, D. F., Jones, R. L. & Narumiya, S. International Union of Basic and Clinical Pharmacology. LXXXIII: classification of prostanoid receptors, updating 15 years of progress. *Pharmacological reviews* **63**, 471-538, (2011).

195 Grainger, J. R. *et al.* Inflammatory monocytes regulate pathologic responses to commensals during acute gastrointestinal infection. *Nature medicine* **19**, 713-721, (2013).

196 Taylor, E. L., Megson, I. L., Haslett, C. & Rossi, A. G. Nitric oxide: a key regulator of myeloid inflammatory cell apoptosis. *Cell death and differentiation* **10**, 418-430, (2003).

197 Marriott, H. M. *et al.* Nitric oxide levels regulate macrophage commitment to apoptosis or necrosis during pneumococcal infection. *FASEB J* **18**, 1126-1128, (2004).

198 Wang, L. *et al.* Specific role of neutrophil inducible nitric oxide synthase in murine sepsis-induced lung injury in vivo. *Shock* **37**, 539-547, (2012).

199 Fortunati, E., Kazemier, K. M., Grutters, J. C., Koenderman, L. & Van den Bosch v, J. Human neutrophils switch to an activated phenotype after homing to the lung irrespective of inflammatory disease. *Clin Exp Immunol* **155**, 559-566, (2009).

200 Ramos, T. N., Bullard, D. C. & Barnum, S. R. ICAM-1: isoforms and phenotypes. *J Immunol* **192**, 4469-4474, (2014).

201 Joly, E. & Hudrisier, D. What is trogocytosis and what is its purpose? *Nat Immunol* **4**, 815, (2003).

202 Qureshi, O. S. *et al.* Trans-endocytosis of CD80 and CD86: a molecular basis for the cell-extrinsic function of CTLA-4. *Science* **332**, 600-603, (2011).

203 Kang, Y. S. *et al.* The C-type lectin SIGN-R1 mediates uptake of the capsular polysaccharide of Streptococcus pneumoniae in the marginal zone of mouse spleen. *Proceedings of the National Academy of Sciences of the United States of America* **101**, 215-220, (2004).

204 Cauley, L. S., Miller, E. E., Yen, M. & Swain, S. L. Superantigen-induced CD4 T cell tolerance mediated by myeloid cells and IFN-gamma. *J Immunol* **165**, 6056-6066, (2000).

205 Bingisser, R. M., Tilbrook, P. A., Holt, P. G. & Kees, U. R. Macrophage-derived nitric oxide regulates T cell activation via reversible disruption of the Jak3/STAT5 signalling pathway. *J Immunol* **160**, 5729-5734, (1998).

206 Sato, K. *et al.* Nitric oxide plays a critical role in suppression of T-cell proliferation by mesenchymal stem cells. *Blood* **109**, 228-234, (2007).

207 Wang, J. X. *et al.* Ly6G ligation blocks recruitment of neutrophils via a beta 2 integrin-dependent mechanism. *Blood*, (2012).

208 Daley, J. M., Thomay, A. A., Connolly, M. D., Reichner, J. S. & Albina, J. E. Use of Ly6G-specific monoclonal antibody to deplete neutrophils in mice. *J Leukoc Biol* **83**, 64-70, (2008).

209 Frazer, L. C., O'Connell, C. M., Andrews, C. W., Jr., Zurenski, M. A. & Darville, T. Enhanced neutrophil longevity and recruitment contribute to the severity of oviduct pathology during Chlamydia muridarum infection. *Infect Immun* **79**, 4029-4041, (2011).

210 Ueda, Y., Kondo, M. & Kelsoe, G. Inflammation and the reciprocal production of granulocytes and lymphocytes in bone marrow. *J Exp Med* **201**, 1771-1780, (2005).

211 Friedl, P. & Weigelin, B. Interstitial leukocyte migration and immune function. *Nat Immunol* **9**, 960-969, (2008).

212 Lammermann, T. & Germain, R. N. The multiple faces of leukocyte interstitial migration. *Seminars in immunopathology* **36**, 227-251, (2014).

213 Ruckle, T., Schwarz, M. K. & Rommel, C. PI3Kgamma inhibition: towards an 'aspirin of the 21st century'? *Nat Rev Drug Discov* **5**, 903-918, (2006).

214 Etienne-Manneville, S. & Hall, A. Rho GTPases in cell biology. *Nature* **420**, 629-635, (2002).

215 Szczur, K., Xu, H., Atkinson, S., Zheng, Y. & Filippi, M. D. Rho GTPase CDC42 regulates directionality and random movement via distinct MAPK pathways in neutrophils. *Blood* **108**, 4205-4213, (2006).

216 Plotnikov, S. V. & Waterman, C. M. Guiding cell migration by tugging. *Current opinion in cell biology* **25**, 619-626, (2013).

217 Lammermann, T. *et al.* Rapid leukocyte migration by integrin-independent flowing and squeezing. *Nature* **453**, 51-55, (2008).

218 Schymeinsky, J., Then, C. & Walzog, B. The non-receptor tyrosine kinase Syk regulates lamellipodium formation and site-directed migration of human leukocytes. *J Cell Physiol* **204**, 614-622, (2005).

219 Schymeinsky, J. *et al.* The Vav binding site of the non-receptor tyrosine kinase Syk at Tyr 348 is critical for beta2 integrin (CD11/CD18)-mediated neutrophil migration. *Blood* **108**, 3919-3927, (2006).

220 Renkawitz, J. *et al.* Adaptive force transmission in amoeboid cell migration. *Nature cell biology* **11**, 1438-1443, (2009).

221 Munoz, M. A., Biro, M. & Weninger, W. T cell migration in intact lymph nodes in vivo. *Current opinion in cell biology* **30C**, 17-24, (2014).

222 Katakai, T., Habiro, K. & Kinashi, T. Dendritic cells regulate high-speed interstitial T cell migration in the lymph node via LFA-1/ICAM-1. *J Immunol* **191**, 1188-1199, (2013).

223 Reichardt, P. *et al.* A role for LFA-1 in delaying T-lymphocyte egress from lymph nodes. *The EMBO journal* **32**, 829-843, (2013).

224 Saudemont, A. *et al.* p110gamma and p110delta isoforms of phosphoinositide 3-kinase differentially regulate natural killer cell migration in health and disease. *Proc Natl Acad Sci U S A* **106**, 5795-5800, (2009).

225 Reif, K. *et al.* Cutting edge: differential roles for phosphoinositide 3-kinases, p110gamma and p110delta, in lymphocyte chemotaxis and homing. *J Immunol* **173**, 2236-2240, (2004).

226 Chou, R. C. *et al.* Lipid-cytokine-chemokine cascade drives neutrophil recruitment in a murine model of inflammatory arthritis. *Immunity* **33**, 266-278, (2010).

227 Chen, M. *et al.* Neutrophil-derived leukotriene B4 is required for inflammatory arthritis. *J Exp Med* **203**, 837-842, (2006).

228 Graler, M. H. *et al.* The sphingosine 1-phosphate receptor S1P4 regulates cell shape and motility via coupling to Gi and G12/13. *J Cell Biochem* **89**, 507-519, (2003).

229 Harris, T. H. *et al.* Generalized Levy walks and the role of chemokines in migration of effector CD8+ T cells. *Nature* **486**, 545-548, (2012).

230 Allende, M. L. *et al.* Sphingosine-1-phosphate lyase deficiency produces a pro-inflammatory response while impairing neutrophil trafficking. *J Biol Chem* **286**, 7348-7358, (2011).

231 Rahman, M. M. *et al.* Sphingosine 1-phosphate induces neutrophil chemoattractant CXCL8: repression by steroids. *PLoS One* **9**, e92466, (2014).

232 Teijaro, J. R. *et al.* Endothelial cells are central orchestrators of cytokine amplification during influenza virus infection. *Cell* **146**, 980-991, (2011).

233 Brinkmann, V. *et al.* The immune modulator FTY720 targets sphingosine 1-phosphate receptors. *J Biol Chem* **277**, 21453-21457, (2002).

234 Gorlino, C. V. *et al.* Neutrophils exhibit differential requirements for homing molecules in their lymphatic and blood trafficking into draining lymph nodes. *J Immunol* **193**, 1966-1974, (2014).

235 Kirby, A. C., Raynes, J. G. & Kaye, P. M. CD11b regulates recruitment of alveolar macrophages but not pulmonary dendritic cells after pneumococcal challenge. *J Infect Dis* **193**, 205-213, (2006).

236 Knapp, S. *et al.* Alveolar macrophages have a protective antiinflammatory role during murine pneumococcal pneumonia. *Am J Respir Crit Care Med* **167**, 171-179, (2003).

237 Thepen, T., Van Rooijen, N. & Kraal, G. Alveolar macrophage elimination in vivo is associated with an increase in pulmonary immune response in mice. *J Exp Med* **170**, 499-509, (1989).

238 Ribeiro-Gomes, F. L. *et al.* Neutrophils activate macrophages for intracellular killing of Leishmania major through recruitment of TLR4 by neutrophil elastase. *J Immunol* **179**, 3988-3994, (2007).

239 Nakano, H. *et al.* A novel mutant gene involved in T-lymphocyte-specific homing into peripheral lymphoid organs on mouse chromosome 4. *Blood* **91**, 2886-2895, (1998).

240 Mori, S. *et al.* Mice lacking expression of the chemokines CCL21-ser and CCL19 (plt mice) demonstrate delayed but enhanced T cell immune responses. *J Exp Med* **193**, 207-218, (2001).

241 Gunn, M. D. *et al.* Mice lacking expression of secondary lymphoid organ chemokine have defects in lymphocyte homing and dendritic cell localization. *J Exp Med* **189**, 451-460, (1999).

242 Consortium, I. G. P. *Immunological Genome Project*, <http://www.immgen.org> (2014).